ISSN: 1813-1786 (Print)
ISSN: 2313-7770 (Online)
Volume No. 20
Indexed & Abstract in:
- PASTIC SCIENCE ABSTRACTS
- AGRIS DATABASE
- ProQuest Products
- EBSCO DATABASES
- Library of Congress, USA
- OCLC World Cat
- Aluminum Industry Abstracts
- ANTE: Abstracts in New Technology & Engineering
- Ceramic Abstracts
- Civil Engineering Abstracts
- Computer and Information Systems Abstracts (Module)
- Copper Technical Reference Library
- Corrosion Abstracts
- Earthquake Engineering Abstracts
- Electronics & Communications Abstracts
- Engineering Research Database
- Engineered Materials
- Environmental Engineering Abstracts
- Environmental Science and Pollution Management
- Materials Research Database
- Mechanical & Transportation Engineering Abstracts
- Solid State and Superconductivity Abstracts
- Metadex

TECHNICAL JOURNAL

(Quarterly)

for online access please visit http://web.uettaxila.edu.pk/techjournal/index.html

2016

University of Engineering and Technology
Taxila, Pakistan

Vol: 21 **No. I (Jan - Mar)**

TECHNICAL JOURNAL *University of Engineering and Technology (UET) Taxila, Pakistan* **Vol. 21, No. I**

AIM & SCOPE

"Technical journal is a multidisciplinary journal in the field of engineering science and technology that offers platform for researchers, engineers and scientists to publish their original and to date research of high scientific value. It is a double blind peer-reviewed open access academic journal, published quarterly by University of Engineering & Technology, Taxila, Pakistan. Articles published in the Journal illustrate innovations, developments and achievements in the field of engineering and technology. The journal is being published electronically as well as in print form."

Technical Journal

A Quarterly Journal of University of Engineering & Technology (UET) Taxila, Pakistan
Recognized by Higher Education Commission (HEC)
Y Category

ISSN: 1813-1786 (Print) ISSN: 2313-7770 (Online)
Volume No. 21 (Quarterly)
No. I (Jan - Mar)
2016

Phone: 92 - 51 - 9047298 **Fax: 92 - 51 - 9047420** **E-Mail: technical.journal@uettaxila.edu.pk**

EDITORIAL OFFICE:
General Editor Technical Journal
Central Library, University of Engineering and Technology (UET) Taxila, Pakistan

EDITORIAL BOARD

CONTENTS

Section A

CIVIL/ENVIRONMENTAL/ ARCHITECTURE/ TRANSPORTATION ENGG./ CITY AND REGIONAL PLANNING

Estimation of Trap Efficiency and Life of Large Reservoirs by using Empirical Equations

Z. Fida[1], M.Ashiq[2]

[1,2]Civil Engineering Department, University of Engineering and Technology, Lahore
[1]zulqarnain.uetian@gmail.com

***Abstract*—**This paper explores the rate of sedimentation and trap efficiency empirical methods which are important regarding the performance of reservoirs. There are various empirical relations that may be usedfordetermining trap efficiency of reservoirs. Among them, Brown (1943), Churchill (1948), Brune (1953), Dendy (1974), Gill(1979), USDA-SCS (1983) and Siyam (2000) relationshipshave been used for determination of trap efficiency of Tarbela & Mangla reservoirs. The results were compared with the observed trap efficiencies. Trap efficiency (TE) equations were also developed both for Tarbela & Mangla reservoirs along with a combine equation for both of the reservoirs. Performance of the developed equations was evaluated using reservoir data. Further, by using capacity / inflow (C/I) ratio, TE and density of sediments, useful life of Tarbela reservoirwas estimated as of 51 years (up to year 2065) and of Mangla reservoir as 154 years (up to year 2168).

***Keywords*—**Trap Efficiency, Sediment, Empirical relations, Life of Reservoir.

I. Introduction

With the construction of a dam the velocity of incoming sediment reduces and the sedimentstart to settle down in the reservoir. The major factors which result in reservoir sedimentation are (a) capacity/inflow, (b) capacity/watershed area, (c) sedimentation index (S.I.) (period of retention/velocity). Based upon these factors, empirical relations have been developed by different researchers. Among the methods commonly used to estimate the trap efficiency of reservoir are Brune (1953) Method & Churchill (1948) Methods.Brown (1943) used capacity/watershed area (C/W), Churchill (1948) used sedimentation index, while Brune (1953) Dendy (1974), Gill (1979), USDA-SDC (1983) used capacity/inflow (C/I) and Siyam (2000) used inflow/capacity (I/C) ratio in estimation of Trap Efficiency of reservoirs.

II. Study Objectives

This study mainly focuses on investigation of sediment related parameters of Tarbela and Mangla reservoirs. Trap Efficiency is a very important parameter; it can be predicted using several empirical equations as stated earlier. This study has been conducted to determine the applicability of various existing empirical approaches for the estimation of trap efficiency of Tarbela and Mangla Reservoirs. The objective of this study is to investigate the best method which predicts the trap efficiency and to make comparison with actual trap efficiency computed by Hydrographic Surveys. The other objective of the study is to predict life of the reservoir from the best method which predicts trap efficiency closer to the actual trap efficiency. The other objective of this study is to develop equations for the trap efficiency of large reservoirs using the data of Mangla and Tarbela reservoirs.

III. Description of Study Area

Mangla and Tarbela reservoirs are located in the northern region of Pakistan near to capital city of Islamabad. The location of both of the dams may be seen in Fig. 1.

Mangla dam was completed in 1967 on the river Jhelum. The gross reservoir capacity at completion time was 7.26 Bm^3 (Billion cubic meter) and live storage of 6.59 Bm^3 which reduced to 5.67 Bm^3 and 4.50 Bm^3 in 2010receptively i.e. 21.92 %reduction in gross storage and 15.84% in live storage. Jhelum, Poonch and Kanshi rivers, contribute sediment to Mangla Reservoir.

For Mangla reservoir, Average Annual flow series from 1967 to 2010 is shown in Fig. 2. Average Annual Inflow of Mangla reservoir is 819 cumecs and maximum inflow came in years 1996. Computation of total sediment inflow to Mangla reservoir is calculated considering the sediment inflow of Jhelum, Poonch andKanshi River. Maximum sediment load came as 135.06 MST in year 2006 as represented in Fig. 4.

Tarbela dam was built on the river Indus and have catchment area of 169,600 km^2. It is an earth and rock fill dam which was completed in year 1974 to regulate the seasonal flows of the upper Indus both for irrigation and hydropower generation and receives average annual inflow of 2324 cumecs. The gross reservoir capacity at completion in 1974 was 14.34 Bm^3 (Billion

cubic meter) and live storage of 11.94 Bm³ which reduced to 9.54 Bm³ and 8.17 Bm³ in 2010receptively i.e. 33.5% reduction in gross storage and 31.5 % in live storage [i]. Location of Tarbela dam is shown in Fig. 1.

The annual inflow of Tarbela reservoir for 1974-2014 (40 years) is shown in Fig. 3. Average Annual inflow of Tarbela reservoir is 2324 cumecs and maximum inflow came in year 1994.Maximum sediment load came in year 2010.

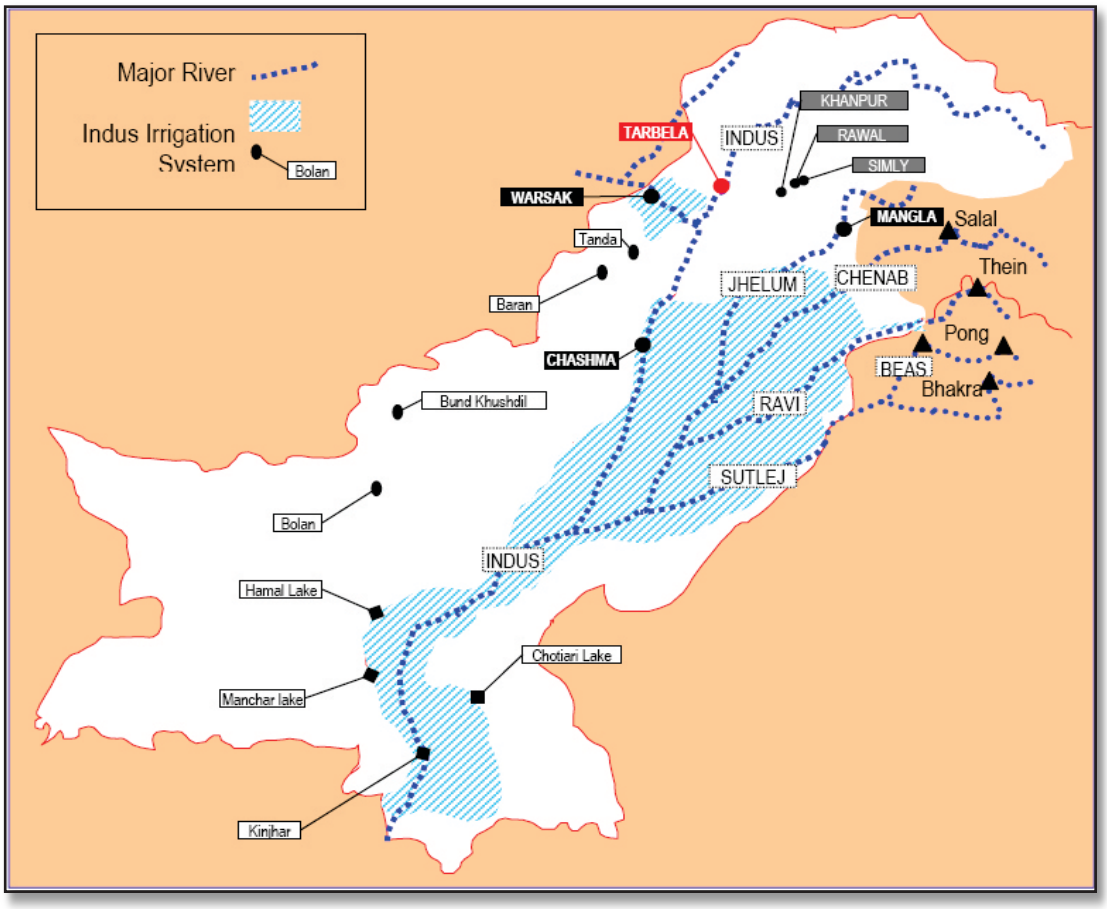

Fig. 1. Location of Tarbela and Mangla dams.

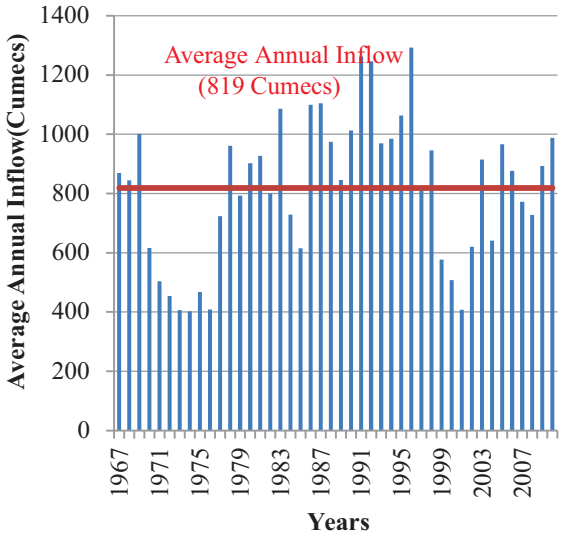

Fig. 2. Average annual inflows of Mangla reservoir.

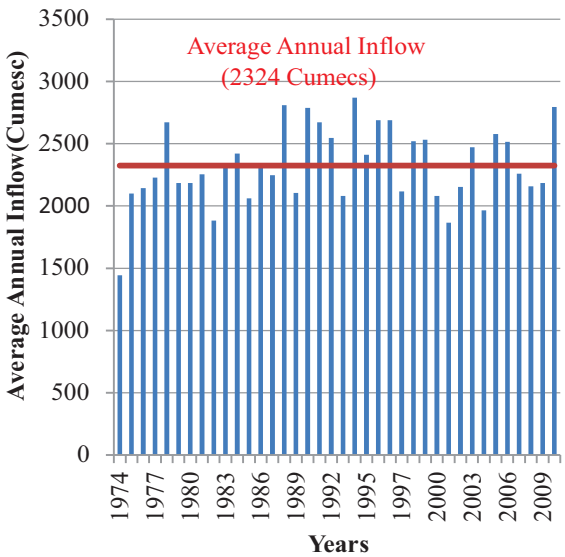

Fig. 3. Average annual inflows of Tarbelareservoir.

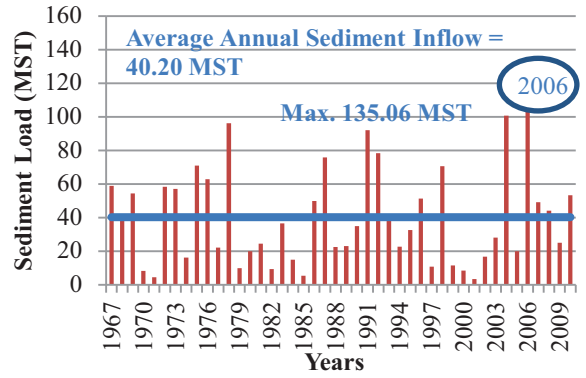

Fig. 4. Sediment load series of Mangla reservoir.

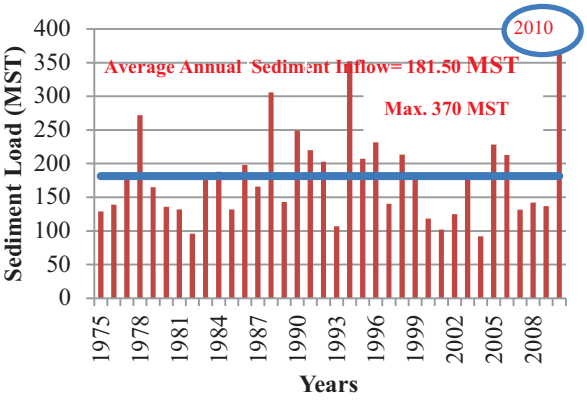

Fig. 5. Sediment load series of Tarbela reservoir.

Total sediment inflow to Mangla reservoir in year 2006 was 135.06 MST (Million Short Ton) as shown in Fig. 4, whereas, Total sediment inflow to Tarbela reservoir was estimated using the data from Besham Qila Gauging Station. Maximum sediment inflow in Year 2010 was 370 MST (Million Short Ton) as shown in Fig. 5.

IV. Sediment Trap Efficiency

Reservoir sediment trap efficiency is the ratio of the sediment deposited to the totalsediment inflowtoa reservoir.SedimentTrapEfficiencyiscalculatedbyequation (1):

$$E=\frac{[Y_s(in)-Y_s(out)]}{Y_s(in)} \quad (1)$$

where, E is the Trap efficiency, Y_s(in) is the sediment inflow in the reservoir and Y_s(out) is the sediment outflow from the reservoir.

Trap Efficiency decreases due to sedimentation. Knowledge of Trap Efficiency is needed to control the sediment accumulation and thereby the life of the reservoir, and to assure its proper operation.

There are various empirical methods for trap efficiency with some limitations. Overview of these empirical methods is discussed below.

V. Trap Efficiency Determination Methods

A. Capacity-Watershed Area Method

Brown (1943) developed a curve that shows relation of trap efficiency to capacity/watershed area, where capacity (C, in acre-ft.) and watershed area (W, in mi^2) [ii]. This curve is shown in Fig. 6 and its mathematical expression is given in equation (2):

$$E=100\ [1-\frac{1}{1+\frac{KC}{W}}] \quad (2)$$

K is the coefficient with value ranging from 0.046 to 1.0 having 0.1 value for median curve.

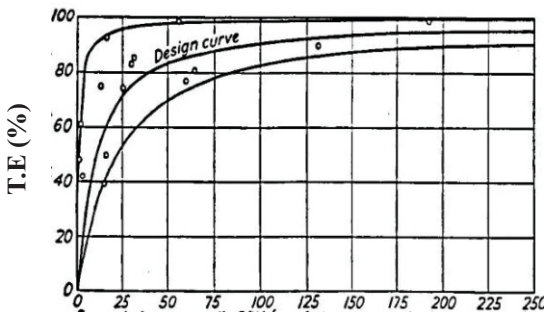

Fig. 6. Trap Efficiency curve by Brown (1943).

B. Capacity-Inflow Method (Brune Curve)

Brune (1953) used a capacity–annual inflow ratio (C/I) to predict Trap Efficiency. Brune's curves are not recommended for dry reservoirs. Trap Efficiency equation proposed by Brune is given in Equation (3):.

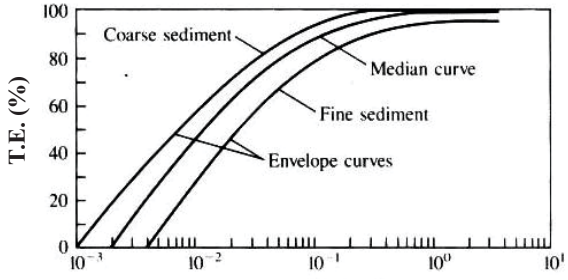

Fig. 7. Trap Efficiency curve by Brune (1953).

C. Sedimentation Index Method (Churchill's Curve)

Churchill (1948) proposed a relation between sedimentation index and percentage of silt passing through the reservoir.

The sedimentation index is defined as ratio of period

of retention and mean velocity. This can be mathematically expressed as given in Equation (4):

$$S.I. = \frac{R}{V} \quad (4)$$

In this method percentage of silt passing through reservoir is obtained by subtracting Trap Efficiency from 100, which is on ordinate axis and sedimentation index is on X-axis as shown in Fig. 8. This method is used for small reservoirs [iv]. Trap Efficiency is calculated using the equation (5):

$$(1- T.E.) = (800)\cdot (S.I.)^{0.2} - 12 \quad (5)$$

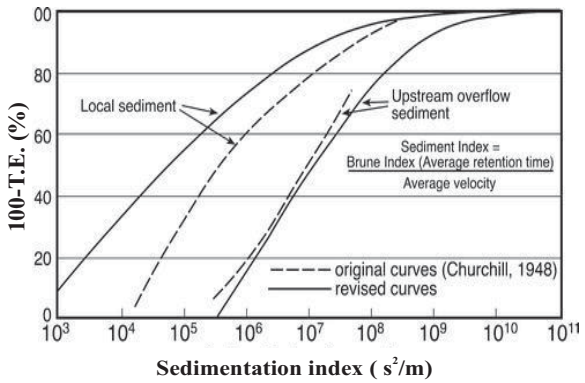

Fig. 8. Trap Efficiency curve by Churchill.

D. USDA-SCS Curves

USDA-SCS (1983) developed Trap Efficiency equations using Capacity / Inflow ratios for different textures. Trap efficiency be lowered for sandy and fine sediments [xxiv]. USDA-SCS curves are shown in Fig. 9 and Equations are shown in Table I.

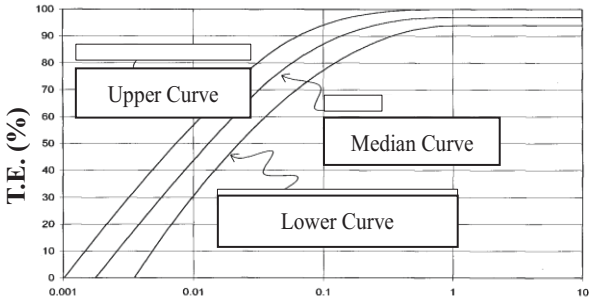

Fig. 9. Trap Efficiency curves by USDA-SCS.

TABLE I
USDA-SCS PREDICTION EQUATIONS

	C/I>1	1>C/I>0.02	C/I<0.02
Upper curve	100	$100-(0.485)\lvert\ln(C/I)\rvert^{2.99}$	$124-(6.59)\lvert\ln(C/I)\rvert^{1.52}$
Median curve	97	$97-(1.275)\lvert\ln(C/I)\rvert^{2.47}$	$128-(11.51)\lvert\ln(C/I)\rvert^{1.304}$
Lowerc urve	94	$94-3.38\lvert\ln(C/I)\rvert^{1.92}$	$94-3.38\lvert\ln(C/I)\rvert^{1.92}$

E. Dendy (1974) Method

Dendy (1974) developed a Trap Efficiency equation (6) for the median curve:

$$E = (100)(0.97)^{[0.19*LOG(C/I)]} \quad (6)$$

This equation was developed by Dendy by adding more data to Brune method [v].

F. Gill (1979) Method

Gill (1979) developed equations (Eqs.7-9) which provide close results to Brune's curves [viii].

Lower Curve:

$$T_e = \frac{(C/I)^2}{\left[0.994701(C/I)^2 + 0.006297(C/I) + 0.3\cdot 10^{-5}\right]} \quad (7)$$

Median Curve:

$$T_e = \frac{(C/I)}{\left[0.012 + (1.02C/I)\right]} \quad (8)$$

Upper Curve:

$$T_e = \frac{(C/I)^3}{\left[1.02655(C/I)^3 + 0.02621(C/I)^2 - 0.133\cdot 10^3\cdot (C/I) + 0.1\cdot 10^{-5}\right]} \quad (9)$$

where, T_e is trap efficiency of the reservoir in decimal, C is capacity of reservoir in volume units and I is mean annual inflow in volume units.

F. Siyam (2000) Method

Siyam (2000) developed a new relationship for the trap efficiency of reservoirs showing that Brune curves are a case of trap efficiency in exponential function as shown in Equation(10):

$$T.E.(\%) = 100[e]^{-\beta(I/C)} \quad (10)$$

where I/C is the ratio between average annual inflow (I) and reservoir capacity (C), β is a sedimentation parameter which have valuesequalto0.0055,0.0079and0.015for upper, lower and median curves respectively [xix].

VI. Useful Life Estimation

Useful life of reservoir is defined as the period up to which reservoir can serve the defined purpose;while, economic life is defined as the period after which the cost of operating the reservoir exceeds the additional benefits expected from it; whereas, design life is generally the useful life; likewise; full life period is that when no capacity is available in the reservoir for useful

purpose. In most of the developed countries full life is said to be arrived, when half of the total capacity of reservoir is depleted [vii].

In the present study, trap efficiency calculated using Dendy method, Brune Method, Gill Method, Churchill Method and Hydrographic survey methods have been adopted to estimate the life of Tarbela and Mangla reservoirs. Life of reservoirs is determined considering the sedimentation rate will remain constant and 80% of reservoir useful capacity will deplete.

VII . METHODOLOGY

To investigate sediment related parameters data mentioned below was assembled from Besham Qila stream gauging station for Tarbela reservoir and Mangla Cableway gauging station for Mangla reservoir. The data obtained was analyzed and Trap efficiencies were calculated using the Trap Efficiency equations considering the parameters of Capacity, Average Annual Inflow, Sedimentation Index, Watershed area. Suspended Sediment data was collected through Hydrographic surveys. Life of reservoirs was calculated considering the sedimentation rate and predicting trend equations, considering useful life of reservoir as 80%.

A. Data Collection for Mangla reservoir and Trap Efficiency Estimation

Suspended sediment inflow data was assembled for Jhelum River at Kohala, Poonch River at Kotli and Kanshi River near Palote for years (1967-2010) from SWHP (Surface Water Hydrology Project), WAPDA.

Average daily inflow data from Mangla cableway gauging station was collected, which is upstream of Mangla reservoir, for years (1967-2010) from SWHP (Surface Water Hydrology Project), WAPDA.Bed load was calculated using the Modified Einstein Method, according to which 10 to 20 % of suspended sediment load is considered as bed load.

Actual Trap Efficiency of Tarbela reservoir was calculated as ratio of Suspended Sediment inflow to Total Sediment inflow

After analyzing data, Trap Efficiency of Mangla reservoir was estimated using the equations of Brown (1943), Churchill (1948), Brune (1953), Dendy (1974), Gill (1979), USDA-SDC (1983) and Siyam (2000).

B. Data Collection for Tarbela reservoir and Trap Efficiency Estimation

Suspended sediment inflow data from Besham Qila [which is upstream of Tarbela reservoir] stream gauging station were assembled, for years (1974-2010) from SWHP (Surface Water Hydrology Project), WAPDA,along with sediment data, mean daily inflow data were also assembled for this site.

Bed load was calculated using the Modified Einstein Method, according to which 10 to 20 % of suspended sediment load is considered as bed load. Actual Trap Efficiency of Tarbela reservoir was calculated as ratio of Suspended Sediment inflow to Total Sediment inflow.

After analyzing data, Trap efficiency of Tarbela was estimated using the equations of Brown (1943), Churchill (1948), Brune (1953), Dendy (1974), Gill (1979), USDA-SDC (1983) and Siyam (2000).

C. Comparison of Trap Efficiencies

After trap efficiency calculation by empirical methods for both reservoirs, a comparison of computed trap efficiencies was made with the trap efficiencies calculated using Hydrographic Survey data to analyze which method gives close fit value to the observed trap efficiency, so that a method for future use may be proposed.

D. Development of Equations for Trap Efficiency

To develop correlation for trap efficiency, factors of capacity/inflow (C/I), capacity/watershed (C/W) and sedimentation index (S.I.) were analyzed for both reservoirs, which predicted that C/I has more influence on trap efficiency. Hence 3 equations between C/I and T.E. were developed, one using the data of Mangla reservoir, one using the data of Tarbela reservoir, one combined equation using the data of Tarbela & Mangla reservoirs. Performance of these equations was evaluated using the data of Simly reservoir.

VIII. RESULTS & DISCUSSIONS

A. Tarbela Reservoir Trap Efficiency Results

Comparison of trap efficiency using Hydrographic Survey data and estimated trap efficiencies by different empirical methods of Tarbela reservoir is shown in Table II and Fig. 10.

Trap Efficiency curve calculated through Hydrographic Survey shows that data is so scattered. Comparison of Tarbela reservoir trap efficiency calculated by different methods shows that new developed curve has close relation with the Hydrographic Survey curve as shown in Fig. 10.

TABLE II
TRAP EFFICIENCY OF TARBELA RESERVOIR (1974-2010) USING EMPIRICAL METHODS

Year	Brown	Brune	Churchill	Gill	Dendy	USDA SCS	Siyam	New Developed Equation	Hydrographic Survey
1974	94.88	90.07	92.48	90.78	90.60	95.93	96.05	92.34	94
1975	94.84	90.02	92.44	87.25	90.54	95.94	96.38	89.05	94
1976	94.79	89.98	92.39	86.96	90.48	95.95	96.27	89.05	94
1977	94.74	89.94	92.34	86.47	90.42	95.96	96.09	89.05	94
1978	94.70	89.90	92.29	84.44	90.36	95.98	95.28	89.05	94
1979	94.60	89.81	92.18	86.39	90.23	96.00	96.06	89.05	94
1980	94.60	89.81	92.18	86.38	90.23	96.00	96.05	89.05	92
1981	94.48	89.70	92.05	85.80	90.07	96.03	95.83	85.58	97
1982	94.44	89.67	92.01	87.55	90.02	96.04	96.48	85.58	84
1983	94.40	89.63	91.96	85.24	89.97	96.05	95.61	85.58	73
1984	94.32	89.56	91.88	84.72	89.86	96.07	95.40	85.58	86
1985	94.27	89.53	91.83	86.34	89.81	96.08	96.04	81.90	99
1986	94.23	89.49	91.78	85.04	89.75	96.09	95.53	81.90	72
1987	94.19	89.46	91.74	85.27	89.70	96.10	95.62	81.90	58
1988	94.13	89.41	91.68	82.66	89.63	96.11	94.51	81.90	54
1989	94.09	89.37	91.64	85.77	89.57	96.12	95.82	81.90	84
1990	94.02	89.31	91.55	82.51	89.48	96.14	94.43	81.90	84
1991	93.95	89.26	91.49	82.87	89.40	96.15	94.60	78.01	72
1992	93.91	89.23	91.44	83.33	89.34	96.16	94.81	78.01	59
1993	93.87	89.20	91.40	85.49	89.29	96.17	95.71	78.01	91
1994	93.75	89.10	91.26	81.58	89.14	96.20	94.00	78.01	90
1995	93.69	89.05	91.20	83.52	89.06	96.21	94.89	78.01	72
1996	93.62	89.00	91.13	82.12	88.98	96.23	94.26	78.01	87
1997	93.55	88.95	91.06	84.72	88.89	96.24	95.40	73.87	87
1998	93.50	88.91	90.99	82.64	88.82	96.25	94.50	73.87	87
1999	93.40	88.84	90.89	82.40	88.70	96.27	94.39	73.87	87
2000	93.40	88.83	90.89	84.64	88.70	96.27	95.36	73.87	86
2001	93.26	88.74	90.74	85.58	88.53	96.30	95.74	73.87	86
2002	93.19	88.69	90.67	83.89	88.45	96.32	95.05	69.44	87
2003	93.13	88.64	90.60	82.17	88.36	96.33	94.28	69.44	67
2004	93.07	88.59	90.53	84.68	88.29	96.34	95.38	69.44	61
2005	93.01	88.55	90.47	81.44	88.22	96.35	93.94	69.44	48
2006	92.89	88.47	90.34	81.52	88.07	96.38	93.97	69.44	84
2007	92.79	88.40	90.23	82.62	87.95	96.39	94.49	69.44	80
2008	92.72	88.36	90.16	83.04	87.87	96.41	94.68	64.68	70
2009	92.69	88.33	90.12	82.84	87.82	96.41	94.59	64.68	64
2010	92.50	88.21	89.92	79.46	87.60	96.45	92.94	64.68	85
	93.83	89.19	91.35	84.33	89.25	96.17	95.15	78.61	81

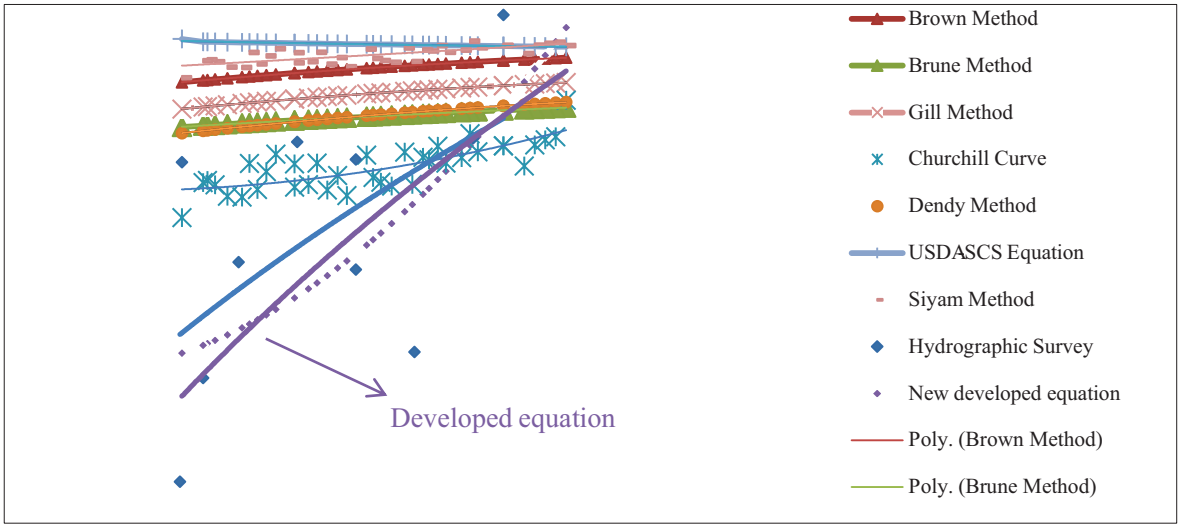

Fig. 10: Comparison of Trap Efficiencies of Tarbela reservoir using empirical methods.

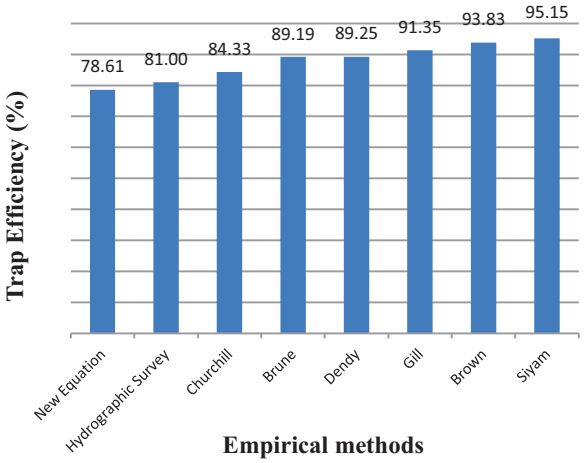

Fig. 11. Comparison of trapefficiencies of Tarbela reservoir.

Whereas, trap efficiency computed by Empirical methods in comparison with observed one is given in the following chronological order:

i. New Equation, 2.9% less than observed T.E.
ii. Churchill Method, 2.9% more than observed T.E.
iii. Brune Method, 10.11% more than observed T.E.
iv. Dendy Method, 10.19% more than observed T.E.

A. Life of Tarbela Reservoir Results

Comparison of life of Tarbela reservoir by different empirical methods is shown in Fig. 12. According to Hydrographic Survey Life of Tarbela reservoir is up to year 2064 and as per New developed equation Life of Tarbela reservoir is up to year 2065 as shown in Fig.12.

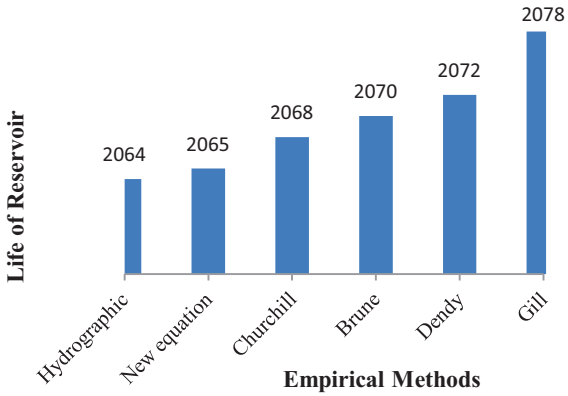

Fig. 12. Comparison of Life of Tarbela reservoir

B. Mangla Reservoir Trap Efficiency Results

Comparison of trap efficiency using Hydrographic Survey data and estimated trap efficiencies by different empirical methods of Mangla reservoir is shown in Table III and Fig. 13.

Comparison of Mangla reservoir Trap Efficiency calculated by different methods shows that new developed curve has close relation with the Trap Efficiency calculated through Hydrographic survey as shown in Fig. 13.

TABLE III
TRAP EFFICIENCY OF MANGLA RESERVOIR USING EMPIRICAL METHODS

Years	Brown	Brune	Churchill	Gill	Dendy	USDA-SCS	Siyam	New Developed Equation	Hydrographic Survey
1967	97.85	91.41	88.63	93.85	92.33	95.55	97.04	90.00	90.91
1968	97.85	91.41	88.89	93.85	92.33	95.55	97.04	90.00	90.91
1969	97.85	91.41	87.26	93.85	92.33	95.55	97.04	90.00	90.91
1970	97.81	91.32	91.46	93.76	92.22	95.58	96.98	90.00	90.91
1971	97.81	91.32	93.06	93.76	92.22	95.58	96.98	90.00	90.09
1972	97.81	91.32	93.83	93.76	92.22	95.58	96.98	90.00	90.09
1973	97.77	91.23	94.47	93.68	92.12	95.60	96.93	89.43	90.09
1974	97.77	91.23	94.54	93.68	92.12	95.60	96.93	89.43	89.29
1975	97.77	91.23	93.46	93.68	92.12	95.60	96.93	89.43	89.29
1976	97.77	91.23	94.43	93.68	92.12	95.60	96.93	89.43	89.29
1977	97.77	91.23	89.93	93.68	92.12	95.60	96.93	89.43	89.29
1978	97.67	91.03	86.83	93.50	91.88	95.66	96.79	88.84	89.29
1979	97.67	91.03	88.70	93.50	91.88	95.66	96.79	88.84	88.34
1980	97.67	91.03	87.47	93.50	91.88	95.66	96.79	88.84	88.34
1981	97.67	91.03	87.20	93.50	91.88	95.66	96.79	88.84	88.34
1982	97.67	91.03	88.62	93.50	91.88	95.66	96.79	88.84	88.34
1983	97.62	90.94	85.36	93.41	91.76	95.68	96.73	88.84	88.34
1984	97.62	90.94	89.29	93.41	91.76	95.68	96.73	88.84	88.89
1985	97.62	90.94	90.78	93.41	91.76	95.68	96.73	88.84	88.89
1986	97.62	90.94	85.23	93.41	91.76	95.68	96.73	88.84	88.89
1987	97.62	90.94	85.18	93.41	91.76	95.68	96.73	88.84	88.89
1988	97.57	90.83	86.24	93.30	91.62	95.72	96.65	88.22	88.89

1989	97.57	90.83	87.66	93.30	91.62	95.72	96.65	88.22	87.72
1990	97.57	90.83	85.84	93.30	91.62	95.72	96.65	88.22	87.72
1991	97.57	90.83	83.43	93.30	91.62	95.72	96.65	88.22	87.72
1992	97.57	90.83	83.57	93.30	91.62	95.72	96.65	88.22	87.72
1993	97.46	90.63	85.84	93.10	91.37	95.77	96.50	87.57	87.72
1994	97.46	90.63	85.68	93.10	91.37	95.77	96.50	87.57	87.57
1995	97.46	90.63	84.86	93.10	91.37	95.77	96.50	87.57	87.57
1996	97.46	90.63	82.65	93.10	91.37	95.77	96.50	87.57	87.57
1997	97.39	90.51	87.36	92.97	91.21	95.81	96.41	87.57	87.57
1998	97.39	90.51	85.82	92.97	91.21	95.81	96.41	87.57	87.64
1999	97.39	90.51	90.51	92.97	91.21	95.81	96.41	87.57	87.64
2000	97.36	90.44	91.47	92.90	91.12	95.82	96.35	86.89	87.64
2001	97.36	90.44	93.19	92.90	91.12	95.82	96.35	86.89	87.34
2002	97.34	90.42	89.72	92.88	91.09	95.83	96.34	86.89	87.34
2003	97.34	90.42	85.96	92.88	91.09	95.83	96.34	86.89	87.18
2004	97.34	90.42	89.42	92.88	91.09	95.83	96.34	86.89	87.18
2005	97.31	90.37	85.26	92.82	91.02	95.85	96.29	86.89	87.18
2006	97.31	90.37	86.28	92.82	91.02	95.85	96.29	86.89	86.88
2007	97.31	90.37	87.56	92.82	91.02	95.85	96.29	86.89	86.88
2008	97.31	90.37	88.12	92.82	91.02	95.85	96.29	86.89	86.88
2009	97.31	90.37	86.10	92.82	91.02	95.85	96.29	86.89	86.88
2010	97.27	90.29	84.83	92.73	90.91	95.87	96.23	86.89	86.88
Average	97.56	90.83	93.29	88.23	91.62	95.71	96.64	88.31	88.38

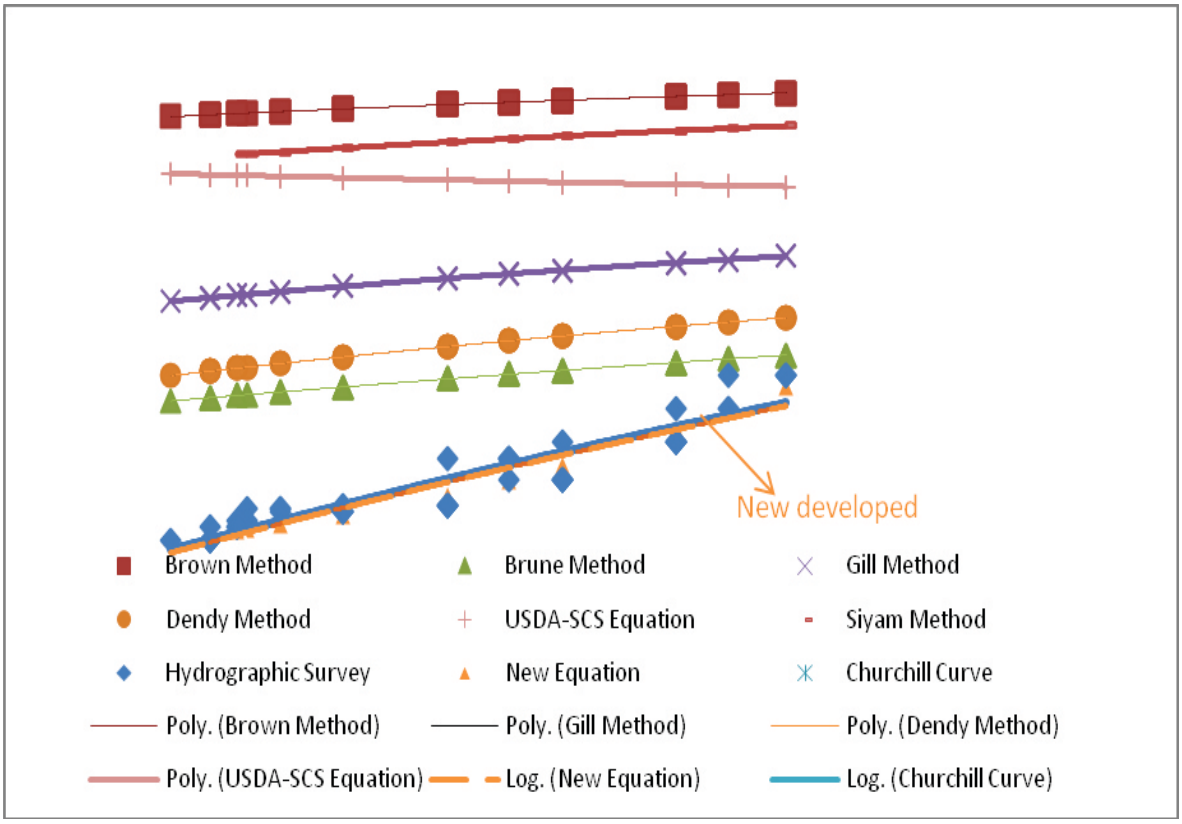

Fig. 13. Comparison of Trap Efficiencies of Mangla reservoir using empirical methods.

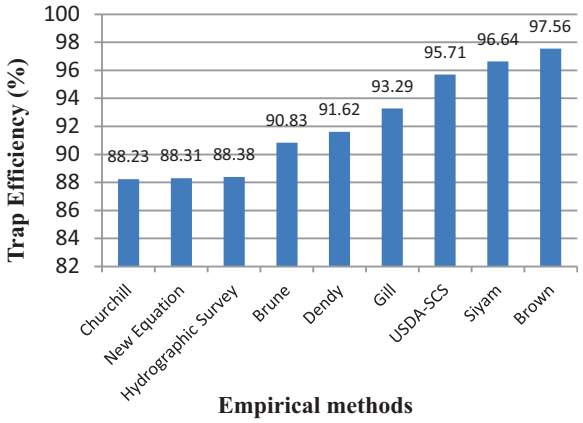

Fig. 14. Comparison of trap efficiencies of Mangla reservoir.

Figure 14 depicts such a comparison of trap efficiencies by different empirical methods for average value of all years. Comparison of Trap Efficiencies of Mangla reservoir for 1967-2010 by different empirical methods is represented in Table III.
Whereas, trap efficiency computed by Empirical methods in comparison with observed one is given in the following chronological order:

i. New developed equation, 0.08% less than observed T.E.
ii. Churchill Method, 0.17% less than observed T.E.
iii. Brune Method, 2.7% more than observed T.E.
iv. Dendy Method, 3.6% more than observed T.E.
v. Gill Method, 5.5% more than observed T.E.

C. Life of Mangla Reservoir Results

According to Bruneand Hydrographic Survey Method life of Mangla reservoir is up to year 2140 and as per new developed equation life of reservoir is up to year 2168 (154 years) as shown in Fig. 15.

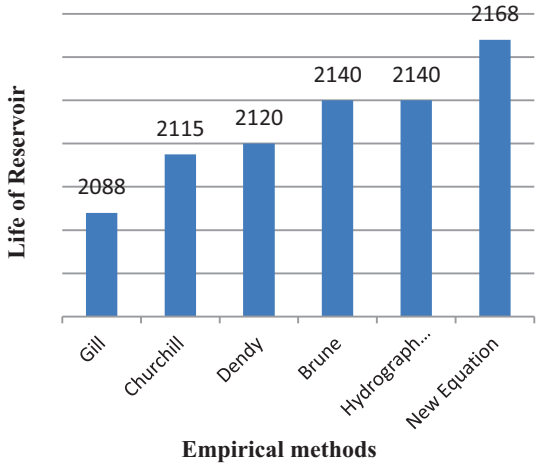

Fig. 15. Comparison of Life of Mangla reservoir.

D. Development of Equations for Trap Efficiency

In present study, considering C/I and S.I. factors, Trap efficiency equations have been developed. A comparison of influence of C/I and S.I. on trap efficiency for both Mangla and Tarbela reservoir is shown in Fig. 16 & 17 respectively, whereas, combined for both reservoirs is shown in Fig. 18.

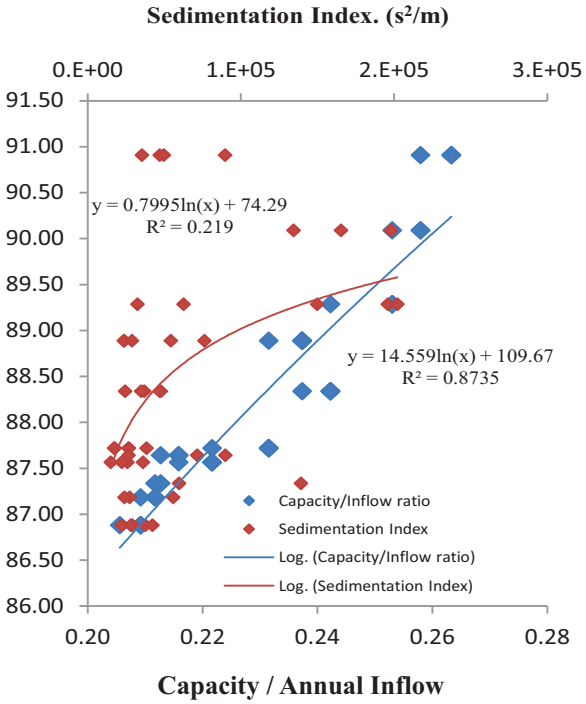

Fig. 16. Comparison of influence of C/I and S.I. on Trap Efficiency for Mangla reservoir.

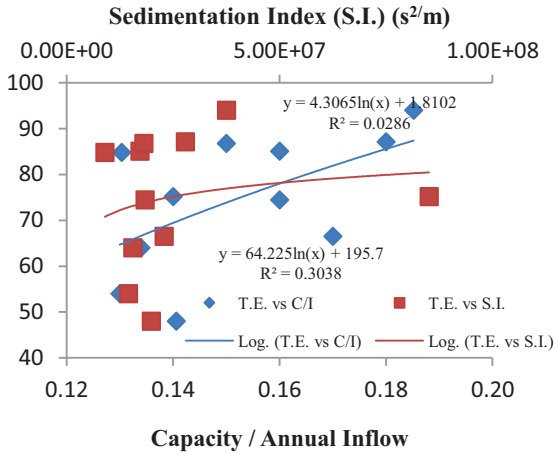

Fig. 17. Comparison of influence of C/I and S.I. on Trap Efficiency for Tarbela reservoir.

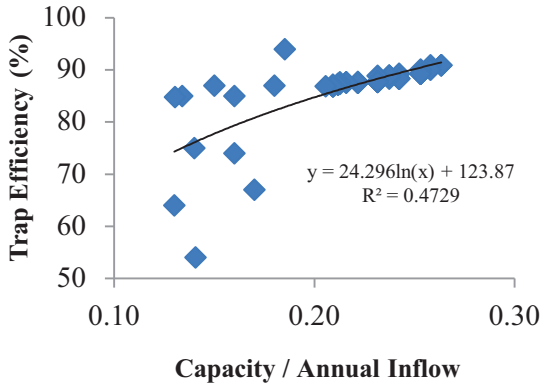

Fig. 18. Development of one combined equation for Tarbela and Mangla reservoir.

The developed correlations in this regard between C/I and T.E. given in Equations (11-13) respectively:

Mangla reservoir trap efficiency equation:

$$T.E. = 14.5 \ln\left(\frac{C}{I}\right) + 110 \quad (11)$$

Tarbela reservoir trap efficiency equation:

$$T.E. = 64.2 \ln\left(\frac{C}{I}\right) + 196 \quad (12)$$

Generalized trap efficiency equation:

$$T.E. = 24.3 \ln\left(\frac{C}{I}\right) + 124 \quad (13)$$

IX. Check the Performance of Newly Developed Equations

To check the performance of newly developed equations, these equations were used on Simly reservoir, which is located near Rawalpindi (330 43' 8" N and 730 20' 25"E) on Soan River. It was constructed in 1982; its storage capacity was 28.370 Mm3when developed, which was increased up to 40.70 Mm3 in 2005. Its watershed size is 153.5 km2. The elevation of Simly catchmentranges from 643-2274 meter. The comparison of performance of newly developed Trap Efficiency equations is shown in Table-IV and Fig.19.

Equation 12 gives higher results of Trap Efficiencies, so it is not recommended; moreover these equations are recommended for large reservoirs.

TABLE IV
TRAP EFFICIENCY OF SIMLY RESERVOIR USING NEWLY DEVELOPED EQUATIONS

Capacity (C), (Acre-feet)	Average Annual Inflow(I), (Acre-feet)	Capacity/Avg. Annual Inflow (C/I)	Equation-11 T.E.=14.5ln(C/I) +110	Equation-12 T.E.=64.2ln(C/I) +196	Equation-13 T.E.=24.3ln(C/I)+ 124
22919	77706	0.295	92.30	117.61	94.33
22838	77706	0.294	92.24	117.39	94.24
22757	77706	0.293	92.19	117.16	94.16
22676	77706	0.292	92.14	116.93	94.07
22595	77706	0.291	92.09	116.70	93.98
22514	77706	0.290	92.04	116.47	93.90
22351	77706	0.288	91.93	116.00	93.72
22189	77706	0.286	91.83	115.54	93.54
22027	77706	0.283	91.72	115.07	93.37
21865	77706	0.281	91.61	114.59	93.19
21703	77706	0.279	91.51	114.11	93.01
21541	77706	0.277	91.40	113.63	92.82
21338	77706	0.275	91.26	113.03	92.59
21135	77706	0.272	91.12	112.41	92.36
20933	77706	0.269	90.98	111.79	92.13
20730	77706	0.267	90.84	111.17	91.89
20487	77706	0.264	90.67	110.41	91.60
20244	77706	0.261	90.50	109.64	91.31
20000	77706	0.257	90.32	108.87	91.02
19757	77706	0.254	90.14	108.08	90.72
19514	77706	0.251	89.96	107.29	90.42
19271	77706	0.248	89.78	106.48	90.12

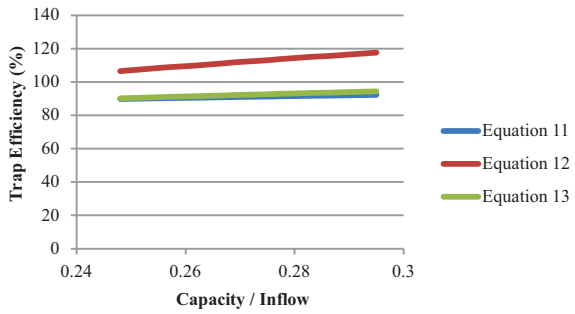

Fig. 19. Trap Efficiency of Simly reservoir using New developed equations.

X. CONCLUSIONS

In this study Trap Efficiency (T.E.) and useful life of Tarbela and Mangla reservoirs were investigated along with development and test of empirical equations. Firstly, the T.E. was estimated using Brown (1943), Churchill (1948), Brune (1953), Dendy (1974), Gill(1979), USDA-SDC (1983) and Siyam (2000) Methods and results were compared with the Trap Efficiency calculated through Hydrographic surveys. This comparison showed that Brune, Churchill, Gill and Dendy methods gave closer values to the Trap Efficiencies based on observed data. Secondly, the life of Tarbela and Mangla reservoirs was determined using the Brune, Gill, Dendy and Hydrographic survey methods and found to be 51 years (i.e. up to 2065) and 154 years (i.e. up to year 2168) respectively.

Finally, three empirical equations were developed between capacity/inflow and trap efficiency for Tarbela, Mangla reservoir along with a combine equation. During the tests of equations, it was found that empirical equationsgave fairly reasonable results when tested with Simly reservoir data.

REFRENCES

[i] B. G. Agarwal & K. Singh, "Sedimentation Studies for Tehri Dam Reservoir", Proceedings of Workshop on Reservoir Sedimentation, Mysore, Karnataka, India, May 17- May 19, pp. 171-179, 1994.

[ii] C. B. Brown, "Discussion of Sedimentation in Reservoirs", Proceedings of the American Society of Civil Engineers, edited by J. Witzig, 69, pp. 1493-1500, 1943.

[iii] G. M. Brune, "Sediment record in Midwestern United States", International Union of Geodesy and Geophysics, General Assembly, Brussels, Belgium, Aug., v. 2, pp, 29-39, 1953.

[iv] M. A. Churchill, "Discussion of Analysis and Use of Reservoir Sedimentation Data", Proceedings of Federal Interagency sedimentation Conference, edited by L.C. Gottschalk, Denver, pp. 139-140, USA, 1948.

[v] F. E. Dendy, "Sediment Trap Efficiency of Small Reservoirs", Trans. of ASAE, 17(5), 898-988, 1974.

[vi] H. A. Einstein, "Formulae for transportation of bed-load", Trans. ASCE, 107, 561-577, 1942.

[vii] V. Garg, & V. Jothiprakash, "Estimation of useful life of a reservoir using sediment trap efficiency", Journal of Spatial Hydrology, Vol. 8, No. 2 Fall 2008.

[viii] M. A. Gill, "Sedimentation and Useful Life of Reservoirs", Journal of Hydrology, 44, 89-95, 1979.

[ix] I. Haq & S. T. Abbas, "Sedimentation of Tarbela and Mangla Reservoirs",Pakistan Engineering Congress Publication, no, 659, 2007.

[x] D. N. Kulkarni, S. Y. Shukla, & V. S. Oka, "Sedimentation of Reservoirs in Maharashtra", Proceedings of Workshop on Reservoir Sedimentation, Mysore, Karnataka, India, May 17- May 19, pp. 158-165, 1994.

[xi] Mangla Dam Organization WAPDA,"River inflow and sediment measurement Records", April 2004.

[xii] Mangla Joint Venture, "Mangla Raising Project," Feasibility study Report, Volume II, Appendices – Appendix A: River inflows, February 2001.

[xiii] E. Meyer-Peter & R. Muller, "Formulas for bed-load transport",Rept 2nd Meeting Int. Assoc. Hydraul. Struct. Res., Stockholm, 39-64, 1948.

[xiv] G. L. Morris, & J. Fan, "Reservoir Sedimentation Handbook, Design and Management of Dams, Reservoirs and Watershed for Sustainable Use", Electronic Version 1.01, McGraw Hill, New York, 2009.

[xv] H. M. Morris, & J. M. Wiggert, "Applied Hydraulics in Engineering", New York: Ronald Press Co., 1972.

[xvi] B. N. Murthy, "Life of Reservoir", Technical Report No. 19, Central Board of Irrigation and Power (CBIP), New Delhi, India, 1980.

[xvii] H. M. Raghunath, "Hydrology Principles, Analysis, Design", Revised Second Edition, 2006.

[xviii] A. Rehman, "Sediment Management for Reservoirs", Pakistan Engineering Congress, Pakistan Engineering Congress, 69th Annual Session Proceedings, Lahore, pp.133-162, 2001.

[xix] A. M. Siyam, "Assessment of the current state of the Nile Basin reservoir sedimentation problems", Nile Basin Capacity Building Network (NBCBN), River morphology Research Cluster, Group1, 2000.

[xx] Surface Water Hydrology Project, Water and Power Development Authority, "Annual Reports 2004-2010".

[xxi] TAMS, "Tarbela Dam Sedimentation

Management Study", Final Report of the Study Prepared by TAMS Consultants Inc in association with HR Wallingford, March 1998.

[xxii] U. S. Bureau of Reclamation, "Design of Small Dams", Water Resources Technical Publication, Third Edition, 1987.

[xxiii] U. S. Bureau of Reclamation, "Technical Guideline of Reservoir Sedimentation", Denver, Colorado, October 1982.

[xxiv] USDA-SCS,"National engineering hand-book (2nd edn) (Section3: 'Sedimentation Chapter &'Sediment storage design criteria) Washington, D.C.US Department of Agriculture, 1983.

Harnessing the Potential of Tidal Currents in Indus Delta Creeks for Making Sustainable and Green Pakistan

M. H. Arsalan[1], H. Fatima[1], A. Khalid[1], I. Zia[2] , I. Ahmad[3]

[1] *Geo-informatics and Sustainable Development Research Lab, Institute of Space and Planetary Astrophysics, University of Karachi, Karachi, Pakistan*
[2] *National Institute of Oceanography, Karachi, Pakistan*
[3] *City and Regional Planning Department, University of Engineering and Technology, Lahore, Pakistan*
[3]haamsafar@hotmail.com

Abstract- Pakistan is facing serious energy crises. Presently the energy supplies are primarily fulfilled by natural gas and imported oil. The energy deficit is a major constraint to economic growth. However, Pakistan is blessed with natural resources, which can be utilized to tackle the energy deficit. Compared to other renewable energy technologies, tidal energy is still not capitalized in Pakistan.

It was estimated that around 900 MW power can be generated from tidal currents in the Indus Delta Creek areas. Among all creeks Chan Waddo, Korangi, Paitiani, Kajhar and Khai creeks have the highest power potentials.

In this study, a GIS based approach was used to analysee the sustainable use of the estimated tidal current power potential. The proximity of power potential sites to power grid, urban area, built up land and road network for easy access demonstrate the sustainable use of this energy.

Results showed that energy generated at these potential sites can be utilized in many ways as Korangi creek, Chann Waddo creek and Phitti are close to Karachi, while there are several towns in the vicinity of Pitiani creek and Khai creek. Other potential sites are close to the planned city Zulfikarabad.

As the tidal current potential of the Indus delta creek system is encouraging, it can be considered in future energy policies and sustainable development strategies for a green and sustainable Pakistan. Therefore, it is highly recommended that further research and pilot projects should be commenced on priority basis.

Keywords- Tidal Energy, Tidal Currents, Indus Delta Creeks, Sustainability, Renewable Energy, Resource Mapping, GIS

I. BACKGROUND

Renewable energy has become a hot area of research these days. Its utilization is now considered as an important step in sustainable development. Sustainable development can be defined in many ways. However, the Landmark definition of the Brundtland (1987) is "the development that meets the needs of the present without compromising the ability of future generations to meet their own needs" [i]. This goal can be achieved efficiently by utilizing renewable energy resources which give us unique opportunity not only to sustain natural capital, reduce greenhouse gas emission from conventional energy systems but also uplift economic conditions.

Technology associated life increased manifold global energy demands as well as increased knowledge of environmental issues that has made green energy a more favourable option for fulfilling global energy demands. Recent research [ii] showed a strong relation between the consumption of fossil fuels and the majority of global greenhouse gas emissions. Several countries around the world have integrated renewable energy policy in their sustainable development strategies. Green energy can be generated in form of Bioenergy, Direct Solar energy, Geothermal energy, Hydropower, Ocean energy and Wind energy.

Oceans cover about 70.8 % of the planet's surface. They not only provide heat and water to our atmosphere, but also they are potential resource of renewable energy [iii]. It has been estimated that if less than 0.1% of the renewable energy available within the oceans could be converted into electricity it would satisfy the present world demand for energy more than five times over [iv]. So far well-known ocean energy sources are waves, tidal range, tidal currents, ocean currents, ocean thermal energy conversion, and salinity gradients. All these sources have different origins and their distinct conversion technology. In comparison to other renewable energy technologies, Ocean energy systems are at an early stage of development, however, rapid advancement of ocean technologies still needs a number of pilot projects and intensive research [v].

Tidal power has more advantages than other renewable energy sources. It is highly predictable as compared to other resources like wind, solar, and wave power. The wind energy mills and tidal current turbines

work on the same mechanism, although the high density of seawater, which is about 830 times denser than wind [vi], makes tidal power more efficient than wind power.

Tidal energy can be extracted in two ways: Tidal barrages; and Tidal current turbines. Tidal barrages systems utilize the potential energy of tides and convert it into a usable form that is electricity. The tidal barrages work on the same principle of hydroelectric generation. The tidal barrages consist of dam, turbine, sluice gates, embankments, and ship lock. The coming tides are trapped in reservoirs behind the dam and when the tides go back, the trapped water let out turning the turbine and generating energy [vii]. However, the tidal current turbines utilize the kinetic energy of the tides. Tidal currents are the horizontal movement of water accompanied by the rising and falling tides. The strength of these tidal currents also varies with the tidal range [viii]. Except tidal barrages, many ocean energy technologies are in the pre-commercial prototype stage [v].

Pakistan like other developing countries of the region is facing a serious energy crisis. The total primary energy demand in Pakistan estimated about 60 million tons of oil equivalent (TOE) in 2006-07. During the last ten years, annual growth of primary energy supplies and their per capita availability has increased by nearly 50%. The per capita availability now stands at 0.372 TOE, which is, however, very low as compared to 8 TOE for USA [ix]. According to World Energy Outlook 2011 about 38% population of Pakistan didn't have access to electricity in 2009 [x].

According to a report by the Energy Expert Group entitled "Integrated Energy Plan 2009-2022", during 2007-08 the share of natural gas in primary energy supplies was 47.5%, followed by oil 30.5%, hydroelectricity 10.9%coal 9.2.2%, nuclear electricity 1.2%, LPG 0.7% and imported electricity 0.1% as shown in Fig. 1.

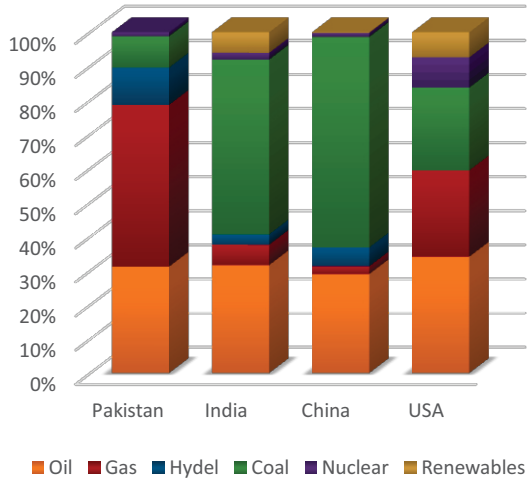

Fig. 1. Percentage of Energy Mix 2007-08 [xi]

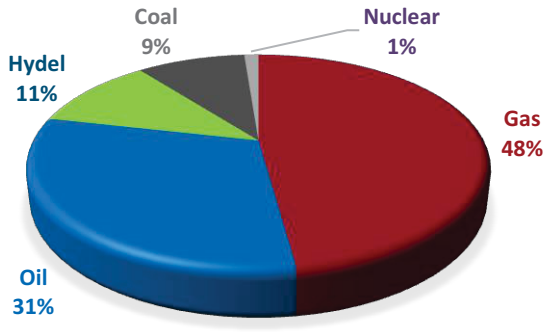

Fig. 2. Energy Mix 2008 [xi]

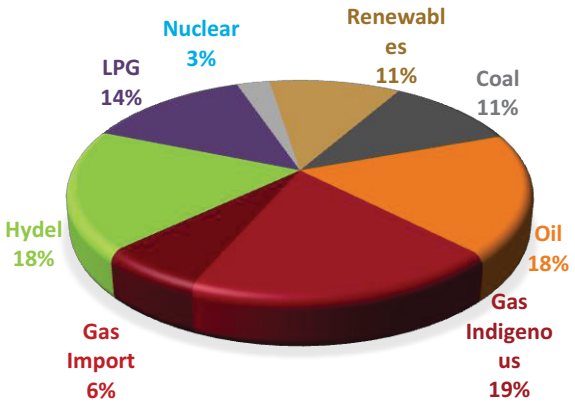

Fig. 3. Energy Mix 2022 [xi]

Pakistan's total primary energy demand is expected to increase from 62.9 MMTOEs (Million Tonnes of oil equivalent) in 2008 to 122.46 million TOEs in 2022[xi]. Figures 2 and 3 indicate the direction in which the Energy Expert Group expects to see the market grow in order to create greater self-reliance[xi]. The energy extraction from the renewable energy resources can help to achieve this expected renewable energy share in 2022 energy mix.

Pakistan's energy policies must be climate change concerned and energy secured. According to 2014 Key World Energy Statistics the net imports were 1.60 MTOE and CO_2 emissions were 0.20 Mt in year 2012 [xii] Table I. The renewable energy will reduce the proportional share of CO_2 emissions, if developed on a priority basis.

TABLE I
ENERGY INDICATORS FOR PAKISTAN YEAR 2012, (A) GROSS PRODUCTION + IMPORTS - EXPORTS -LOSSES, (B) CO2 EMISSIONS FROM FUEL BURNING [xii]

Energy Prod. (Mtoe)	Net Imports (Mtoe)	TPES (Mtoe)	Elec. Cons. [a] (TWh)	CO_2 emissions [b] (Mt of CO_2)
447	1.60	0.77	0.99	0.20

Pakistan is blessed with natural resources that can be utilized to generate electricity, such as Wind, Solar, Hydel, Biomass and tidal energy. The Government of Pakistan established the Alternative Energy Development Board (AEDB) in 2003 to promote investment from the private sector in renewable energy. "Government of Pakistan is putting greater emphasis on Renewable Energy and has set a target of 10% renewable energy or 2700 MW in the Country's energy mix by 2015" [xiii]. The Asian Development Bank (ADB) in its recent report titled '2011 Clean Energy Investments', pointed energy deficit as a major constraint on efficient economic growth in Pakistan [xiv], however this energy deficit can be overcome by utilizing renewable energy sources of Pakistan.

Pakistan has a coastline of about 990 Km [xv] with unique features of creeks in Indus delta. A network of creeks system formed over a period of time due to the flow of the Indus River into Arabian Sea. This creek system is spread over a distance of about 170 Km in the southeast of Karachi along the coast of Pakistan. These creeks meander about 50-69 Km inland where sea water flows into them with high velocity during flood and ebb tides, which is very favourable condition for the extraction of energy from tidal currents[xvi].

As compared to other renewable energy technologies, Tidal energy is still not working in Pakistan, however, the potential of tidal current energy of Indus delta creeks was estimated by Quraishee et al. [xvi] about 30 years ago. Since then the estimated potential has been cited several times, but no further research or pilot project has been initiated [xvii]. Throughout the world, several tidal power stations are working [xviii] say La Rance tidal power station in France, Annapolis Royal Generation Station in Canada, Kislaya Guba Tidal Power station in Russia, and Jangxia power station, China. The Indian state of Gujarat is also planning to host Asia's first commercial-scale tidal power station. British marine energy developer Atlantis Resources Corp. and Gujarat Power Corp. Ltd. signed a memorandum of understanding with the Gujarat government for the 50 megawatt tidal farm on India's west coast[xviii].

Now, it is the time for Pakistan to set its sustainable development goals higher than before and start capitalizing tidal power. If the estimated tidal current power is utilized it will uplift socioeconomic conditions of the coastal population of Pakistan as well as minimize environmental pollution. In this paper, we have highlighted the estimated tidal current power potential of the Indus delta creek system and have analysed its possible sustainable use.

Fig. 4. Indus Delta Creek System, Google Earth, 2014 [xiv]

II. Materials and Methods

A. Spatial Data Generation

Google Earth is a unique platform for base map creation. Its high resolution imagery is open access and free of cost for educational purposes, scholarly publications, and other non-profit uses. Its imagery can be easily captured and manipulated through the permission guidelines of Google Earth and Google Maps [xix] . We utilized images from Google earth to create base map and GIS data layers.

To assess the sustainable harnessing of energy from tidal currents, besides power generating potential many other physical, socioeconomic and environmental data were collected and analysed. To integrate the diversified nature of data layers, Geographical Information System (ArcGIS 10.2) was used. All the datasets were projected to Projected Coordinate System, UTM 1984 Zone 42N. The acquired data, their sources, and the processes involved are summarized in Table II.

TABLE II
COLLECTED DATA AND PROCESSING

Data Description	Type	Source	Processing
Shoreline	Physical	Landsat 7 (11 Apr, 2014), USGS, 2014, [xx]	Extracted in ArcGIS 10.2 using tasseled cap transformation [xxi, xxii]
Bathymetry		GEBCO, 2014, [xxiii]	GEBCO_08 Grid (a global bathymetric grid with 30 arc-second spacing) was extracted from GEBCO grid viewing and data access BODC software

Urban Area and built up land	Socioeconomic	Google Earth, 2014, [xix]	Digitized on Google Earth and processed in ArcGIS
Transportation lines		Google Earth, 2014, [xix]	
Fish Harbors		Google Earth, 2014, [xxiv]	
Ports		Google Earth, 2014, [xxv]	
Fairway and shipping lines		Google Earth, 2014 [xxvi-xxix]	
KESC Grid Station		Google Earth, 2014 [xix, xxx]	
HESCO Transmission lines		Google Earth, 2014, [xix, xxxi]	
Power Plants		Global Energy Observatory (GEO), 2014,[xxxii]	KML was downloaded and processed in ArcGIS

III. VISUALIZATION

Geographic Information system (GIS) provides a unique opportunity to visualize, query, analyse and interpret spatial data, conclude relationships, patterns, and trends. We utilized Visualization capability of GIS to map all input datasets and analysed outcomes in both raster and vector formats with their distinct attributes Fig. 5-14.

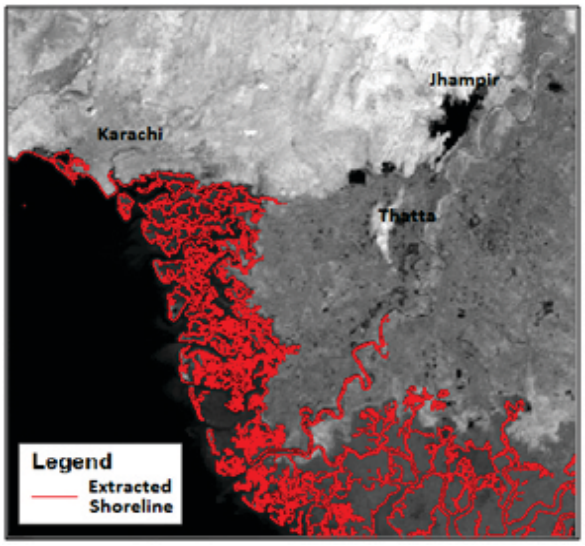

Fig. 5. Extracted Shoreline of Indus Delta

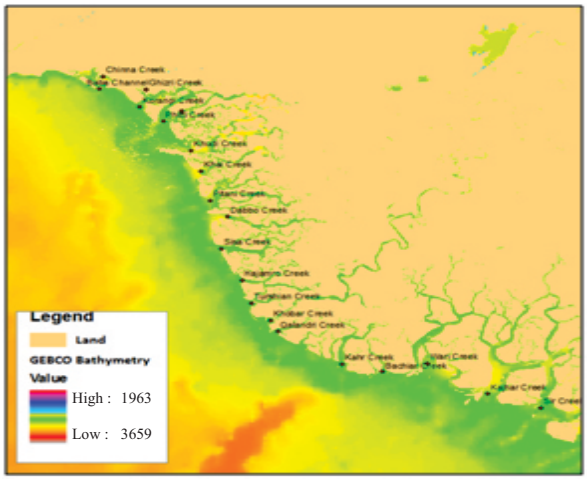

Fig. 6. GEBCO Bathymetry of Study area

Fig. 7. Fairway and Shipping Lines

Fig. 8. KESC Grid stations, Power Plants, and HESCO Transmission Lines

Fig. 9. Road Network

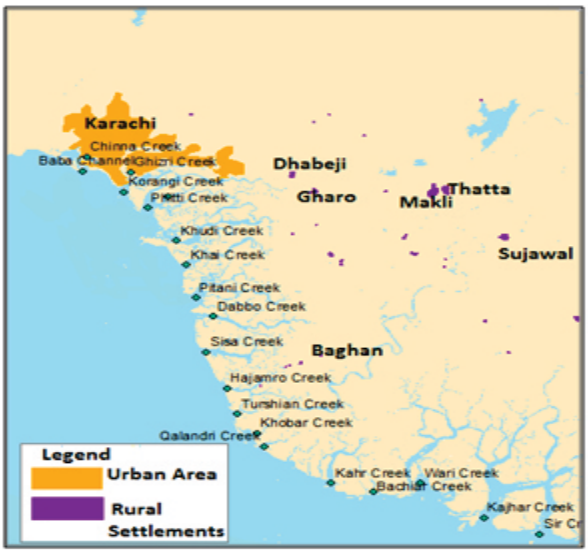

Fig. 10. Urban and Rural Settlements

Fig. 11. Ports and Fish Harbours

IV. Power Potential Analysis

The initial and critical step in tidal power generation is the reliable and comprehensive survey of temporal and spatial distribution of Tidal Energy along the coastlines. There is no regular tidal current monitoring program for creek areas of Pakistan. However a detailed project, named "Feasibility Studies for the extraction of Energy from current and Haliohydrogravity along Pakistan", was executed by [xvi]. It provides a sufficient Tidal power potential assessment for Indus Delta, Pakistan. As this project was the first of its kind and still there is not such a survey, the results of that survey is considered as Tidal power potential of Pakistan in this paper.

Reference [xvi] conducted an intensive survey of selected creeks through small boats. Galvanized Iron pipes and echo sounder were used for hydrographic and sounding purposes. Current velocities were measured in each creek at 0.5m below the surface, mid-depth and 0.5 m above the bottom with the help of Toho Deton and Ekman current meter. Tidal levels were computed by recorded tidal heights in the Khobar creek at Sajjan wari and Gharo creek at Pipri with the aid of tide poles [xvi].

As energy, extraction from current involves the installation of array of long bladed slow moving rotors. These rotors are appropriately designed depending upon various hydrodynamic and hydrographic parameters. Energy can be obtained from the rotation of rotors by the force of the flow of water. The maximum power that can be extracted from single rotor was calculated from this formula:

$$P_{max} = (16/27) * (1/2) \pi \rho V^3 R^2$$

Where,

P_{max} is the maximum power in megawatts

ρ is the average density of sea water in kg/m^3 (1027 kg/m^3)

R is Radius of the rotors in meters

V is the current velocity in Km/hour

16/27 is the Betz limits (max power coefficient for an open unrestricted environment). However, there are studies describing that the tidal turbines in a channel can theoretically have a power coefficient several times greater than 16/27 under certain circumstances[xxxiii].

The Research [xvi] proposed the diameter of the rotors of 1-3 m less than the depth of the creek (hence different radius of rotor for every creek) with a constant width of 0.5m. The number of rotors in one set was estimated for every creek, according to the average bottom width of that creek [xvi]. In this paper these proposed number of rotors Fig. 12 are considered and not calculated as it is out of scope of this paper.

D. Sustainable Use Analysis

Generally, the renewable power potential sites are far away from the users, hence for its utilization long-distance transmission infrastructure is needed. As Marine Current Turbine energy is highly dependent on the intensity of the current, it is difficult to regulate and conserve energy. Therefore, it will be economically efficient if the location is near to the electricity grid and the excess of generated energy will be distributed directly to the electricity grid[xxxiii].

For near shore locations (less than 10 km from the coastline), it is preferable to link individual Marine Current Turbine (MCT) transformer to an onshore transformer station using low voltage cable, although for offshore locations (more than 10 km from the coastline), it is preferable to link individual Marine Current Turbine (MCT) to an offshore transformer station[xxxiv].

After the preliminary engineering design of energy production and transmission, cost – benefit analysis can be determined. Nevertheless, Research [xvi] assessed the cost of production around USD 2.0/W at that time. Although it is the higher estimate of production in comparison with other ways of energy production, however, many studies suggest that the development timeframe and scale of projects have to be analysed in order to come up with the optimal entry point of cost and benefits [xxxv, xxxvi]. At large, small to medium-scale tidal projects are assessed more economically feasible due to experimental technologies. But new generations of technologies are gradually reducing the production cost as well as overall sustainability[xxxv, xxxvi].

To explore the sustainable use of the power potential of these sites, some spatial socioeconomic data of the study area was generated which is summarized in Table 2. The proximity of these power potential sites to national power grid, urban and built up land and road network for easy access is favourable. Along with tidal power potential these distances are important factors that are taken into account in site pilot project selection [xxxvii-xxxix].

V. Results and Discussions

Tidal energy is predictable as it is driven by gravity and not by the weather and it has less environmental impacts, hence it is gaining more and more attention these days. It is estimated that about 900 MW power can be generated from the Indus Delta Creek areas. It can be seen from Fig. 13 that Chan Waddo creek, Korangi creek, Paitiani creek, Kajhar creek and Khai creek have higher power potentials (i.e. 280 MW, 174 MW, 157MW, 127 MW and 58 MW respectively) while other creeks have power potentials below 20 MW.

Although Korangi creek, Chann Waddo creek and Phitti creek have great tidal potentials as well as they are close to Karachi- A populated city with enormous energy demand- they are navigational channels. Preferably a navigational channel should be avoided, but keeping these high potentials and energy crisis into account some engineering solutions are possible. If rotors are deployed in such a manner that rout of boat is not disturbed, then certainly they are the best which can be used for harnessing energy. Economically Chann waddo creek is the most feasible option, as energy generated here can be easily linked with national grid through Bin Qasim Power Plant. A pilot project in Chann Waddo creek is strongly suggested.

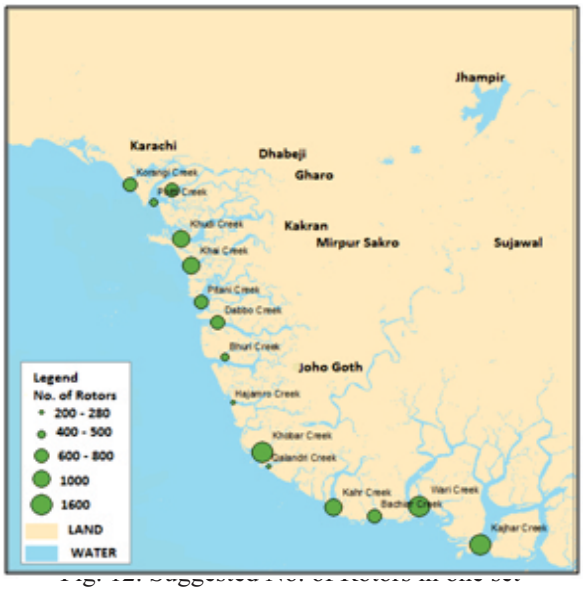

Figure 14 gives the sustainable use of analysis of energy with respect to the distances. It shows that within 20 – 30 km from the coastline favourable conditions exist in the form of HESCO transmission lines, KESC grid stations, power plants, road network, urban area, rural settlements and ports. The energy generated can be directly supplied to the national grid, neighbouring localities, to the warehouses at ports, to coast guards offices etc.

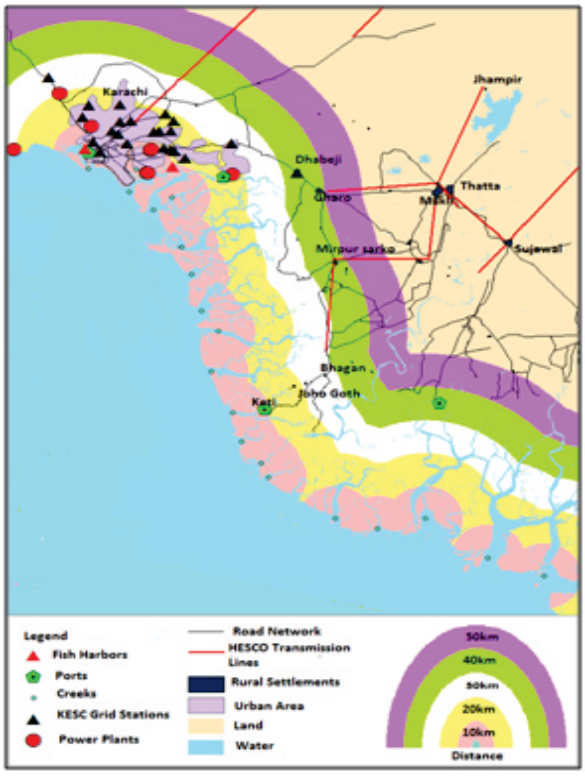

Fig. 14. Sustainable Use Analysis Map

Figure 15 show that some of the power potential sites (i.e. Pitiani creek, Dabbo creek, Bhuri creek, Hajamro creek, Khobar creek, Qalandri creek, Khar creek, Bachiar creek and Wari creek) are close to the planned city Zulfikarabad. Government of Sindh established Zulfikarabad Development Authority (ZDA) in 2010. ZDA is anticipated to facilitate the development of Keti Bandar, Kharo Chann, Shah Bandar and Jati (coastal sub-districts of District Thatta). These power potential sites should be taken into account for sustainable development of the city.

Fig. 15. Planned city Zulfikarabad

In future energy policies and sustainable development strategies tidal energy should be considered for a green and sustainable Pakistan. As the tidal current potential of the Indus delta creek system is encouraging and it can be utilized sustainability further research and pilot projects should be done.

VI. Conclusion

About 900 MW power can be generated from the Indus River Delta. Chan Waddo creek, Korangi creek, Paitiani creek, Kajhar creek and Khai creek have considerable tidal current energy potentials. Korangi creek, Chann Waddo creek and Phitti creek are close to Karachi and this proximity makes them more suitable for power production sites, but these are navigational channels, hence rotors may be deployed in such a manner that fairways are not disturbed. Further research is needed for this engineering challenge.

A pilot project in Chann Waddo creek is strongly suggested as it is economically most feasible. Energy generated here can be easily linked with national grid through Bin Qasim Power Plant.

Pitiani creek and Khai creek have good power potentials of 157 MW and 58 MW respectively, as well as they are close to Mirpur Sakro, Fatah M Kalmati, Kakran, and Lait. Bhuri creek has power potential of 12 MW and it is close to Joho Goth, Baghan, Dandari and Udasi. Kajhar creek has good power potential of 157 MW, but there is no settlement in its vicinity yet. However, Kajhar creek, Dabbo creek, Bhuri creek, Hajamro creek, Khobar creek, Qalandri creek, Khar creek, Bachiar creek and Wari creek are in vicinity of planned city Zulfikarabad. At least some of these sites should be considered in sustainable policies of this city. Besides the fair power potentials of these sites and their proximity to users, further research is needed to come up with optimized sites. So the optimized sites are utilized on priority basis.

While exploitation of tidal current energy in Indus

delta is anticipated to contribute to sustainable development, the protection of a delicate mangrove ecosystem was equally vital, especially in the case of the largest mangrove forest in the country. An independent environmental impact assessment (EIA) should be done.

REFERENCES

[I] I. Burton, " Our common future: The world commission on environment and development," Environment: Science and Policy for Sustainable Development, vol. 29, pp. 25-29, 1987.

[ii] W. Moomaw, F. Yamba, M. Kamimoto, L. Maurice, J. Nyboer, K. Urama, et al., "Renewable Energy Sources and Climate Change Mitigation: Special Report of the Intergovernmental Panel on Climate Change," Cambridge, United Kingdom and New York, NY, USA: Cambridge University Press2011.

[iii] M. G. Gross, Principles of Oceanography, 7th ed.: Prentice Hall College Div, 1995.

[iv] Green Energy News. (1999, Dec). Oceans of Power. Available: http://www.green-energy-news.com/arch/nrgs1999/19990040.html

[v] A. Lewis, S. Estefen, J. Huckerby, W. Musial, T. Pontes, and J. Torres-Martinez, "Ocean energy," IPCC Special Report on Renewable Energy Sources and Climate Change Mitigation, O. Edenhofer, R. Pichs-Madruga, Y. Sokona, K. Seyboth, P. Matschoss, S. Kadner, T. Zwickel, P. Eickemeier, G. Hansen, S. Schlömer, C. von Stechow (eds.), Cambridge University Press, Cambridge, United Kingdom, 2011.

[vi] N. Sveinsson, "Profitability Assessment for a Tidal Power Plant at the Mouth of Hvammsfjörður, Iceland," 2011.

[vii] F. O Rourke, F. Boyle, and A. Reynolds, "Tidal energy update 2009," Applied Energy, vol. 87, pp. 398-409, 2010.

[viii] Nicky Satyadharma Aziz, "Tidal energy resources assessment in Indonesia a case study in Alas Strait," Masters, University of Southampton, 2009.

[ix] Pakistan Water and Power Development Authority, "Hydro Potential in Pakistan," 2008.

[x] International Energy Agency, "World Energy Outlook 2011," 2011.

[xi] Energy Expert Group, "Integrated Energy Plan 2009-2022," 2009.

[xii] The International Energy Agency, "2014 Key World Energy Statistics," 2014.

[xiii] CDM- Excutive Board, "UEP 99 MW Wind Power Project," 2014.

[xiv] Asian Development Bank, "2011 Clean Energy Investments," 2012.

[xv] Hira Fatima, Mudassar H. Arsalan, Anam Khalid, Kashif Marjan, and M. Kumar, "Spatio -Temporal Analysis of Shoreline Changes along Makran Coast Using Remote Sensing and Geographical Information System," in Fourth International Conference on Space Science and Technology (ICASE) 2015, Institute of Space Technology-Islamabad, Pakistan, 2016.

[xvi] Quraishee G. S, "Feasibility Studies for the Extraction of Energy from Current and Haliohydrography along Pakistan Coast," ed: NIO,, 1986.

[xvii] Nayyer Alam Zaigham and Zeeshan Alam Nayyer, "Prospects of Renewable Energy Sources in Pakistan," in Renewable Energy Technologies & Sustainable Develoment, Karachi, 2005, pp. 65-81.

[xviii] Energy Daily. (2011, Dec). India plans tidal power station. Available: http://www.energy-daily.com/reports/India_plans_tidal_power_station_999.html

[xix] Google. (2015, Dec). Permission Guidelines For Google Maps and Google Earth. Available: http://www.google.com/permissions/geoguidelines.html]

[xx] USGS. (2014, December). Data sets. Available: http://earthexplorer.usgs.gov/

[xxi] C. Huang, B. Wylie, L. Yang, C. Homer, and G. Zylstra, "Derivation of a tasselled cap transformation based on Landsat 7 at-satellite reflectance," International Journal of Remote Sensing, vol. 23, pp. 1741-1748, 2002.

[xxii] L. R. M. Joseph W. Scott, William M. Harris, and Matthew D. Reed, "Using the Landsat 7 Enhanced Thematic Mapper Tasseled Cap Transformation to Extract Shoreline," 2003.

[xxiii] General Bathymetric Charts of the Oceans (GEBCO). (2014, 2014). Available: http://www.gebco.net/

[xxiv] P. Fishing. (2014, October). Fishing Industry in Pakistan. Available: http://www.pakistanfishing.com/fishing-info/fishing-industry-in-pakistan

[xxv] Sea Rates. (2014, May). Sea Ports of Pakistan. Available: http://www.searates.com/maritime/pakistan.

html
[xxvi] K. Y. Club. (2014, October). Karachi Harbor. Available: http://www.karachiyachtclub.com/map.htm
[xxvii] Alan Jhons. (2008, September). Keti Bandar What? Who? Where? Available: http://www.pgfa.org/Articles/Keti_Bandar_Karachi_Sindh_Pakistan
[xxviii] Port Qaim Authority. (2012, December). Navigation Channel and Channel Aids. Available: http://www.pqa.gov.pk/navigation_channel.php
[xxix] Wikipedia. (2014, June). Shahbandar. Available: http://en.wikipedia.org/wiki/Shahbandar
[xxx] General Electro-mecanique (GEL). (2014, September). Installation, Testing & Commissioning Of 22 Nos 132/11kv, Conventional Grid Stations In Kesc Network Under Contract No.Pak-031 For Kesc 5th Power Project Available: http://www.gelpak.net/ProjectCompleted.aspx?categoryid=8
[xxxi] HESCO. (2014, June). HESCO transmission lines. Available: http://www.hesco.gov.pk/htmls/images/hesco1.gif
[xxxii] G. E. O. (GEO). (2014, 2014). Power Plants. Available: http://globalenergyobservatory.org/constructNetworkIndex.php
[xxxiii] R. Vennell, "Exceeding the Betz limit with tidal turbines," Renewable Energy, vol. 55, pp. 277-285, 2013.
[xxxiv] L. Myers and A. Bahaj, "Simulated electrical power potential harnessed by marine current turbine arrays in the Alderney Race," Renewable Energy, vol. 30, pp. 1713-1731, 2005.
[xxxv] J. Houde, "Cost-benefit analysis of tidal energy generation in Nova Scotia: a scenario for a tidal farm with 300MW of installed capacity in the Minas Passage in 2020," 2012.
[xxxvi] Y. Li and H. K. Florig, "Modeling the operation and maintenance costs of a large scale tidal current turbine farm," in OCEANS 2006, 2006, pp. 1-6.
[xxxvii] H. S. Tang, S. Kraatz, K. Qu, G. Q. Chen, N. Aboobaker, and C. B. Jiang, "High-resolution survey of tidal energy towards power generation and influence of sea-level-rise: A case study at coast of New Jersey, USA," Renewable and Sustainable Energy Reviews, vol. 32, pp. 960-982 %@ 1364-0321, 2014.
[xxxviii] Z. Defne, K. A. Haas, and H. M. Fritz, "GIS based multi-criteria assessment of tidal stream power potential: A case study for Georgia, USA," Renewable and Sustainable Energy Reviews, vol. 15, pp. 2310-2321 %@ 1364-0321, 2011.
[xxxix] N. S. Aziz, "Tidal energy resources assessment in Indonesia: A case study in Alas Strait," TU Delft, Delft University of Technology, 2009.

An Experimental Study to Develop Bituminous Based Crack Sealant Using Rheological Data

I. Hafeez[1]

[1]Civil Engineering Department, University of Engineering & Technology, Taxila, Pakistan
[1]imran.hafeez@uettaxila.edu.pk

Abstract-Pavement maintenance in hot climatic areas requires a significant annual budget to keep it at a desired serviceability level. Filling of cracks during the pavement maintenance with an appropriate hot-poured crack sealant can save money. However, this cost can further be reduced by utilizing the local modifiers in a relatively higher penetration grade bitumen. This study presents optimizing the percentage rice husk as modifier in 80/100 penetration grade bitumen. A comparison of rheological properties among different crack sealants and bitumen modified with different percentages of modifier has been reported. Intermediate and high temperature performance characteristics of different crack sealants have been compared using stiffness parameters. Temperature and frequency sweep tests were run at different temperatures and frequency levels using a dynamic shear rheometer. The results showed a significant relationship of shear modulus (G*) with percentage addition of modifier and test temperatures. The developed sealant showed elastic behavior at lower temperatures and at higher percentage of modifier. The study recommends utilizing an effective and economical material, which is based on a soft bitumen and 9% rice husk.

Keywords-Flexible Pavements, Bituminous Crack Sealants, Complex Shear Modulus, Time and Temperature Superposition Principle, Yield Test

I. INTRODUCTION

Pavement performance under a specified traffic condition depends on many factors. Cracking associated with the pavement surface commonly reflects climatic variations. Cracks appear at the top surface is one of the signs of flexible pavement failure, associated with a significant temperature variation of that area. In order to achieve a cost-effective crack sealing and filling operation and proper field performance, two factors must be closely controlled: quality of sealant installation and sealant mechanical and rheological properties (such as viscosity, bulk stiffness, and adhesive bonding). Joint and crack sealants prevent the retention of incompressible materials in joints that protects pavement structure from moisture damage. Fend investigated the difference in performance of hot poured crack sealants and cold seal bands through laboratory and field studies. Different laboratory experimentation methods were also developed to characterize the seal bands. Also field investigation methodology was proposed to ascertain field performance and causes behind failures. The study recommended an improved strategies for application of seal bands [i].

A sealant losses its cohesion or adhesion with the passage of time mainly due to weather effects. A sealant fails to take external applied forces, when it losses inter particle cohesion. Such failure types are usually called as cohesion failure. An adhesion failure occur when sealant does not withstand the stress developed at interface between the asphalt surface and the sealant. Such stresses mainly develop due to shrinkage phenomenon during the winter season. The performance of crack sealant in terms of stiffness ability to dissipate tensile stresses also depends on its installation temperature and method of installation [ii].

Rice husk is produced from the rice crop that covers almost 1% of earth surface and is considered as the main food source [iii]. Husk is the rice kernel outer cover having two interlocking halves. Approximately 20% of rice paddy is husk that has been extracted from the two interlocking halves of kernel outer covers. In Pakistan about 1.15 million tons of husk out of about 6.0 million tons of rice has been produced every year [iv]. Rice husk is one of the main source of pozzolanic material that improves the stiffness [v].

Performance evaluation of crack sealants through laboratory experimentation have been proposed in different research studies in the past. The main purpose of such studies were to ascertain the parameters that could affect sealant's field performance at different temperatures [vi]. These parameters could be the mechanical properties of sealant, adhesion to different pavement materials, or chemical composition of sealant. Viscoelastic properties of silicone sealants by using dynamic shear rheometer (DSR) were investigated for six silicone sealants at different frequency levels and a temperature range of -30°C to +50°C with an increment of 10°C. Complex shear modulus (G*) and phase angle (δ), obtained from the DSR tests were used to construct master curves at a reference temperature.

Reference [vii] studied the critical requirement of sealing the cracks using crack sealants and reported that cost or sealing the crack be reduced by adopting the

methodology as proposed by this study. The study concluded that some specific cracks, which could not be identified with the help of laser guided tools had no sealing requirement. Different cracks were chosen to complete this study. The selection criteria was based on the type of crack and the dimensions of the crack. Reference [viii] used a cyclic shear and constant horizontal deformations to evaluate the performance of rigid pavement joint sealants. The horizontal deformation was used for simulating temperature loading, while the cyclic shear was used for simulating traffic loading. The scheme [ix] investigated the effect of rout geometry on crack sealants performance using an index and reported that sealants with clean and seal has relatively poor performance. At the same time over band improved the sealant adhesive and plow off strength. Reference [x] studied the linear viscoelastic behavior of hot-poured crack sealant at relatively low serviceability temperatures using bending beam rheometer. The test data was analyzed using a three-dimensional finite-element model and concluded that mechanical behavior of crack sealant can predicted by a linear viscoelastic model.

Several studies in the past have been conducted by using fine aggregate (filler) with bitumen. The main purpose was to stiffen the asphalt mixture and mastic. Such mixtures have been recommended for either seal coats or to improve the rut resistance of asphalt mixtures. Also, to improve the fatigue properties of asphalt mixtures in the cold areas.

The addition of mineral filler to bitumen stiffen the mastic and interrupt the crack growth in the mastic [xi]. Further, the acidic and basic nature of fillers may age the bitumen mastic by oxidative catalysis and chemical adsorption reactions [xii]. The size of mineral filler effect the adhesion properties of mastic as we go on increasing the diameter of filler, adhesion decreases [xiii]. No study as such recommends using a mastic as sealant. Therefore, based on the literature the function of both (rice husk and filler) are different.

Specific research areas depends on the intended functions and utility. As such rice husk modified bitumen as crack sealants have not been used in the cold climatic areas, but it is a common practice in Pakistan. In Pakistan, rice husk or saw dust is a common composition of sealants. It is important to characterize such mixtures.

II. Objectives and Research Methodology

Two phase study was planned to achieve the study objectives. The objectives of present study were to characterize intermediate and high temperature performance of crack sealants and to compare results with laboratory prepared sealant. This sealant was prepared using 80/100 penetration grade bitumen and rice husk. Also, to propose the optimum solution towards the utilization of local modifier such as rice husk. The scope of present study includes selecting three commonly available crack sealants (A, B, and C) and mixing of rice husk (at different percentages by mass) to 80/100 penetration grade bitumen. The program consists of adding four different percentages of rice husk (3%, 6%, 9% and 12%) by mass of bitumen in 80/100 penetration grade bitumen. The base bitumen was procured from Attock refinery, Rawalpindi, Pakistan. Conventional and rheological properties of base bitumen and the modified bitumen (sealant) were determined in the laboratory. Fig. 1 illustrate the testing program adopted for this research study.

The testing program involved two phases; mixing of rice husk was completed in the initial phase followed by comprehensive testing using conventional and rheological testing. Four different percentages of rice husk were selected and conventional testing was performed to confirm that the modified bituminous sealant should not be stiff enough that it losses viscosity and ductility level while applying in the field. A minimum ductility value of 30 cm was chosen to meet this criteria. Air dried rice husk material, grinded and passed through sieve no. 30 was utilized for modification of base bitumen.

Mixing of different percentages of rice husk for at least 30 minutes through a mechanical device at 160 ºC were made. The obtained samples after a uniform mixing were stored in a refrigerator till further testing. Both conventional and superpave testing were run on the samples. Mixture of base bitumen with 12% rice husk failed to achieve 30 cm ductility value. The other reason was the difficulty of handling this sample as the amount of rice husk was significant and the material crumbled while molding

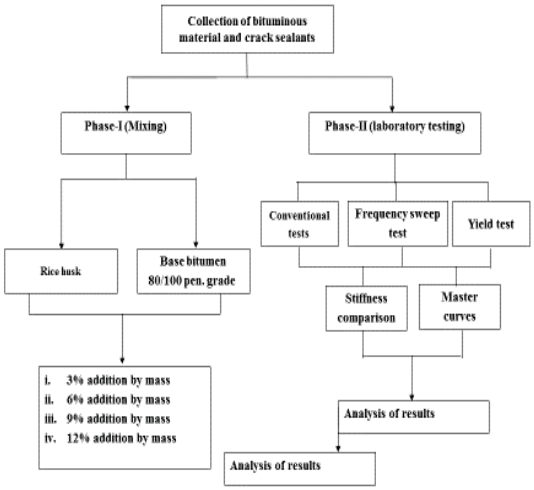

Fig. 1. Scope and methodology of the work

A. Conventional Testing

Several tests were conducted on bituminous crack sealants samples to ascertain the physical behavior. The results of ductility, penetration, softening point and

flash and fire point test have been reported in Table I.

TABLE I
STANDARD SPECIFICATIONS OF ASPHALT

Test Description	Test Method (AASHTO)	Test results of base bitumen and modification with rice husk				
		80-100	3%	6%	9%	12%
Ductility @ 25°C (cm)	T 51	105	65	47	35	12
Softening point, (°C)	T 53	46	51	57	64	76
Penetration @ 25°C (1/10mm)	T 49	86	67	58	49	38
Flash Point, Cleveland Open Cup Apparatus (°C)	T 48	232	229	220	221	196

It may be noted from Table I that the ductility value of specimens decreases with an increase in percentage rice husk. Similar trends have been noted in penetration values. The softening point increases with an increase in the percentage. It may also be noted that at 12%, the ductility value of specimen were about 12cm and the flash point reduced to 196°C. It would be difficult to handle the mastic as well. Therefore based on the conventional testing, a percentage of 12% was dropped from the present scope of the study and three percentages were selected for further rheological testing. Similarly, tests were run on all the three sealants as reported in Table II.

TABLE II
CONVENTIONAL TEST PROPERTIES OF CRACK SEALANTS

Crack Sealant (ASTM Type)	Pen. at 25°C. 150g, 5sec, cone	Soft. Point	Flow at 60°C, 5Hr.s	Bond test at -20°F (50% extendibility) as per manufacturer			Resilience percent
	(dmm)	(°C)	(mm)	1st Cycle	2nd Cycle	3rd Cycle	
Sealant A	69	61	0.45	P	P	P	70
Sealant B	27	81	0.4	P	P	F	68
Sealant C	63	65	7.6	F	P	F	62

The available sealants were bituminous based and qualify for application in hot climatic area. Crack sealants were homogenized before preparation of test samples. Aging of sealants was conducted using rolling thin film oven at a constant temperature for at least 16 hours. Specimens in replicates were tested under temperature and frequency sweep and the results were reported in the proceeding sections. Fig. 2 shows prepared crack sealant using rice husk.

B. Dynamic Shear Rheometer

Various tests using a 25 mm diameter test specimen of bitumen were carried out on a DSR in accordance with AASHTO T-315 test protocol [xiv]. A strain level of 10% was chosen to run the frequency sweep and temperature sweep testing on rolling thin film oven aged specimens. Anton Paar DSR as shown in Fig. II works within a shear modulus range of 100Pa to 10MPa with its parallel plate geometry and capable of maintaining a test temperature from -30 °C to 120 °C.

Temperature sweep and frequency sweep tests were run at a temperature range of 28°C to 82°C (with an increment of 6 °C) and at a frequency range from 0.1 to 100 rad/sec using a dynamic shear rheometer. Data obtained from the test like storage modulus, loss modulus and deflection was utilized to calculate the complex shear modulus (G*), and phase angle (δ), respectively. Phase angle and complex viscosity (η) rutting (G*sin/δ) and fatigue factor (G*sin δ) were also computed to assess intermediate and high temperature behavior. Results were elaborated with the help of plot against different parameters. Comparisons of results were shown at intermediate (28ºC, 46ºC) and high temperatures (64ºC and 80ºC). The viscoelastic characteristics of the sealants and modifiers based on time-temperature superposition principle (TTSP) were interpreted in the form of shifted master curves at a reference temperature of 46ºC.

Fig. 2. Crack Sealant Prepared for Dynamic Shear Rheometer Testing

III. Results and Discussion

Data obtained from the frequency sweep and temperature sweep test were analyzed using a statistical tool to investigate the effect of addition of rice husk, temperature and frequency of loading on the complex shear modulus (stiffness) values of base bitumen and in general on the selected crack sealants.

A. Development of Master Curves

Bituminous crack sealants are the viscoelastic material that follow time and temperature superposition principle. This means that the effect of temperature can be ascertain by changing the loading frequency and vice versa. Sigmoidal fit parameters were utilized in the following relationship to ascertain the horizontal shift function, while shifting the different temperature stiffness data on a reference. Fitting of sigmoidal functions (δ, α, β, & γ) were obtained using the following relationship in a nonlinear least square regression iteration process [xv].

$$Log|E^*| = \delta + \frac{\alpha}{1 + e^{\beta+\gamma(\log Tr)}} \quad (1)$$

The sigmoidal functions depend on aggregate gradation, binder content and air voids. These parameters also represents the minimum value of E*, the maximum value of E* and the shape of the sigmoidal functions. A reference temperature of 46 °C has been used for the development of master curves. Fig. 3 shows a comparison of developed master curves of different crack sealants and rice husk modified bitumen. It may be noted from Fig. 3 that all specimens are almost at the same stiffness range (complex shear modulus) except crack sealant B, which was relatively stiffer and showed higher softening point in Table II. The results of Table II are in line with the developed master curves in Fig. 3.

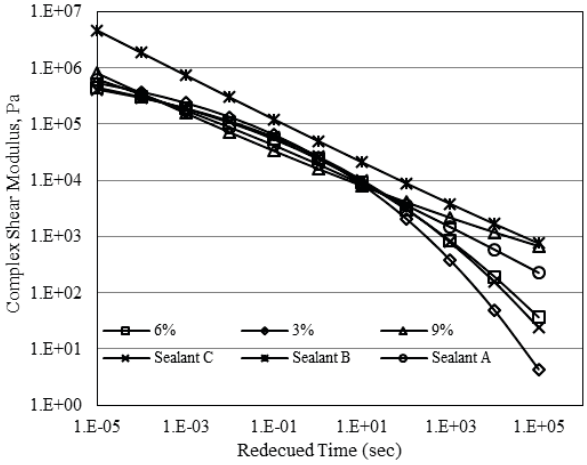

Fig. 3. Developed Master Curves of Different Crack Sealants and Bituminous Sealants

Master curves illustrates the time and temperature interdependency of material and temperature sensitivity in the form of a shift, which may be explained with the help of horizontal shift factors. It may be noted from Fig. 3 that all the sealants and modifiers showed almost similar range of stiffness at the highest frequency level, but the trends and lowest stiffness values changed with a decrease in frequency level. Moreover, the trend lines have shown different patterns. Fig. 4 and 5 showed a family of master curves with similar trends.

It may be noted from Fig. 4 that an addition of 9% rice husk yielded almost linear trend in the bituminous sealant, which is similar as sealant A and B. The stiffness value of bituminous sealant at lower frequency level was almost same as of sealant B. An addition of 9% rice husk in the bitumen therefore meet the desired criteria of producing a local modified sealant that can fulfill the stiffness requirement of available crack sealants. Similarly, Fig. 5 presents a comparison of master curves and their trends in case of 3% and 6% addition of rice husk and a soft sealant C. Almost similar range of stiffness may be noted at different frequency levels except at lower frequency range. Bitumen sealant with 6% rice husk showed better stiffness values.

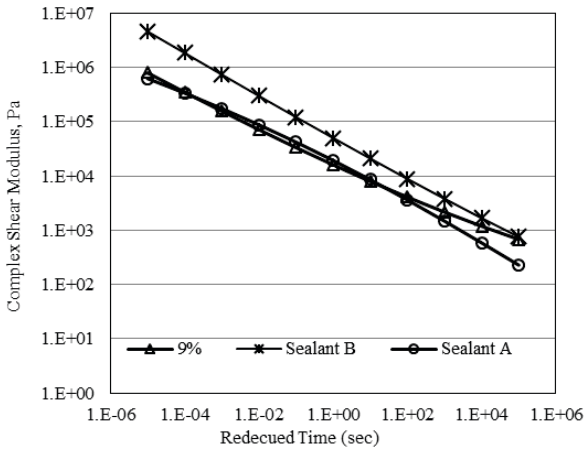

Fig. 4. Comparison of master curves of crack sealants with 9% modified bitumen

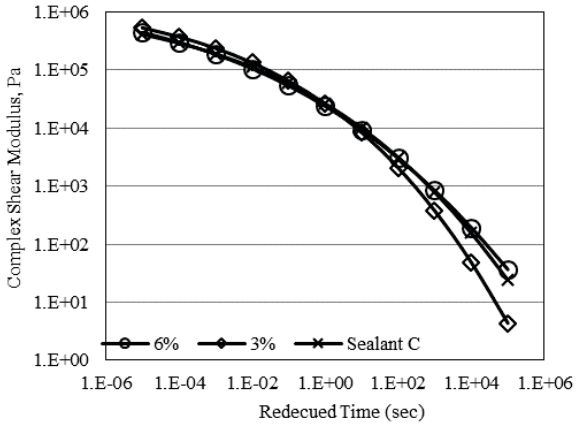

Fig. 5. Comparison of master curves of 3% and 6% modified bitumen with sealant

It may also be noted from Fig. 5 that master curves in case of softer crack sealants were in a curve like pattern. A comparison of shift factors were also made to see the effect of addition of rice husk to the temperature sensitivity of bituminous sealants. Shift factor (log a [T]) helps in moving the curves plotted at different

temperatures to a reference temperature. Fig. 6 shows trends of shift factor corresponding to each addition of rice husk.

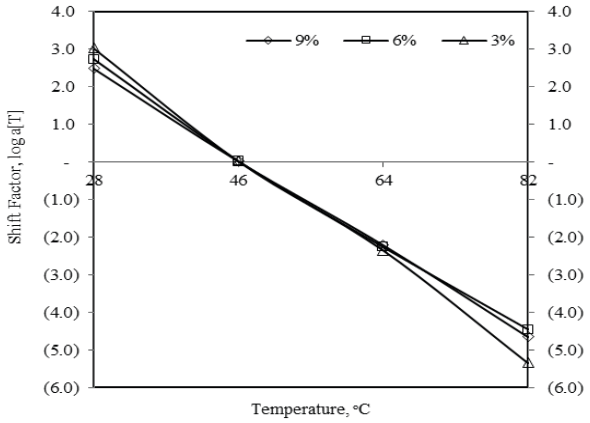

Fig. 6. A comparison of horizontal shift factors for bituminous

The basic purpose of comparing the horizontal shift factors was to ascertain the temperature sensitivity of bitumen with an increase in percentage rice husk. It may be noted from Fig. 6 that the addition of modifier (rice husk) decreases the sensitivity of sealants. As percentage rice husk increases, the complex shear modulus value also increases.

B. Yield Test

Yield test is relatively a simple and easy test to measure the grade of sealant. Yield test was performed at different temperatures using a DSR on 25mm diameter homogenized crack sealant specimens at a gap setting of 2mm. This test applies a monotonic constant shear-rate loading and measures resistance to yield-type failure. The test was performed in replicates at three different temperatures, which were at grade, above grade and below performance grade. The general pass/fail criteria of sealants was used as a minimum of 100% shear strain against a 150 Pa applied shear stress value. Same could be computed using the typical plot showing shear stress versus shear strain in Fig. 7.

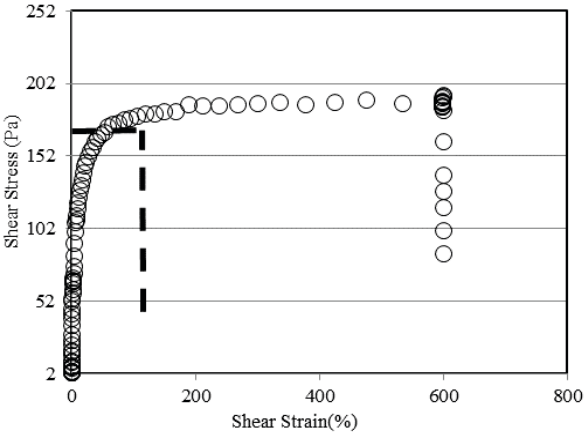

Fig. 7. Shear stress versus shear strain in a yield test

It may be noted from Fig. 7 that shear stress increases with an increase in shear strain to a maximum value and then stabilized at a certain shear strain value, which is a function of type of material. A drop of shear stress at which material failure to yield occurs, can be seen on the last limb of the curve. The results of yield tests at different percentages of strain for all crack sealants have been reported in Table III.

Table III
GRADING AT 150 PA SHEAR STRESS AND 100 % SHEAR STRAIN

Sealant type	Crack Sealants			Percentage rice husk in 80/100 Penetration grade		
	Sealant A	Sealant B	Sealant C	3%	6%	9%
Grade	76	82	70	64	70	76

It may be noted from Table III that with an increase in modifier (rice husk) percentage, the perfromance grade value increases. Yield test depicts an addition of percentage rice husk in the base 80/100 penetration grade bitumen.

C. Ranking of Crack Sealants

Based on the master curve date as developed through frequency sweep test the ranking of sealants was carried out to find the behavior of each material at different temperatures. The frequency and temperature sweep test and the yield test ranked different types of materials in similar order. A typical comparison of different sealants at 82ºC has been shown in Fig. 8.

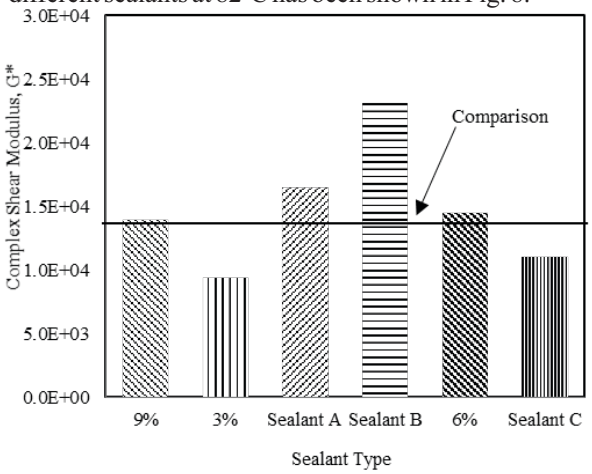

Fig. 8. Ranking of sealants based on complex shear modulus at 82ºC

It may be noted from Fig. 7 that the Sealant B showed the maximum value of G* at a stated temperature than sealant A and sealant C. The bitumen with 9% modifier produced higher value of G* and it decreased with a decrease in the percentage of

modifier. At 3% modifier, the value of G* was minimum compared with different sealants. None of the sealants showed lower than 1 kPa of complex shear modulus at the stated temperature.

Present study highlights the effective utilization of local modifiers for sealing the pavement cracks. An addition of rice husk developed similar stiffness properties in bitumen as that of a crack sealants. The rheological results obtained from different tests showed similar grading of different materials being used in this study. It may be concluded from the present study that adding local modifiers such as rice husk provides a viable solution for pavement crack sealing, similar as using crack sealant products of different manufacturers.

IV. Acknowledgment

Author gratefully acknowledged the support of Taxila Institute of Transportation Engineering, University of Engineering and Technology, Taxila in the provision of financial assistance and laboratory testing facilities. Author also acknowledged the technical assistantship of Engineer Zaid Ahmad.

V. Conclusion

This study presents characterizing the bituminous based sealants and a locally prepared bituminous based sealant by using rice husk. The criteria adopted to optimize percentage modifier was based on the linear visco-elastic range under a frequency and temperature sweep test. Yield test was also performed to confirm the results obtained from the other tests. The rheological testing phase was accomplished at intermediate and high temperatures, keeping in view the ambient temperature history. Following conclusions have been drawn from this study:

Developed master curves represent that the shear modulus has indirect relationship with the temperature as a decrease has been observed with an increase in temperature. Also, percentage increase in modifier increases the stiffness of sealants, which is in line with the results of previous studies. Sealant developed using rice husk showed a visco-elastic behavior. However, two different trends of master curves were obtained; curve and linear fits. Relatively stiffer sealants and bituminous sealant with 9% modifier showed linear fits, while the softer sealant showed a curve like trend. The percentage addition of modifier in the bitumen decreases the temperature sensitivity and increases the stiffness of the material. The conventional test results showed that both the penetration and ductility value of material had decreased with an increase in the percentage modifier. At the same time the softening point of sealant material had increased with an increase in percentage rice husk as modifier.

Based on the test data and plotted master curves at 46 ^{o}C, it was found that the stiffness in the form of complex shear modulus of bituminous sealant with 80/100+9% modifier yielded optimum value. With further increase in rice husk resulted in the brittleness of the material and causes a significant reduction in the flash point. The ranks obtained from the frequency and temperature sweep test and yield test were similar. Present study therefore recommends an optimum value of 9% rice husk to be used in the base 80/100 penetration grade bitumen for sealing the cracks in the pavements. With this percentage the modified bitumen was within the domain of sealants test results. The study thus recommends utilizing an effective and economical material instead of high cost crack sealants for hot climatic areas. This study reveals that both the ranking criteria of aggregate source yield similar results.

References

[i] H. F. Li, H. Li, and T. Li. (2015). Evaluation of Premature failure of asphalt pavement crack sealing bands. Journal of Materials in Civil Engineering. Doi:10.1061/(ASCE)MT.1943-5533.0001434, 04015149.

[ii] J. F. Masson, P. Collins, J. C. Margeson, G. Polomark. (2002). Analysis of Bituminous Crack Sealants by Physico-Chemical Methods ant its Relationship to Field Performance. Journal of Transportation Research Board, TRB, No. 1795, Washington D. C., pp. 33-39.

[iii] S. A. Memon, M. A. Shaikh, and H. Akbar. (2011). Utilization of rice husk ash as viscosity modifying agent in self-compacting concrete. Construction and Building Materials, 25: 1044-1048.

[iv] Agricultural Indicators-Federal Bureau of Statistics.
<http://www.statpak.gov.pk/depts/fbs/statistics/agrindicators/agri_indicators.html>.

[v] M. Jamil, A. B. Kaish, S. N. Raman, and M. F. M. Zain. (2013). Pozzolanic contribution of rice husk ash in cementitious system. Construction and Building Materials, 47: 588-593.

[vi] L. N. Lynch, and D. J. Janssen. (1999). Material Characterization of Silicon Sealants. Journal of Transportation Research Board, TRB, No. 1680, Washington D. C., pp. 44-46.

[vii] A. Mullion, J. Liu, and R. McHattie. (2014). Filed evaluation of crack sealing of AC Pavement in Alaska. Proceeding of the 2013 International Symposium on Climatic Effect on Pavement and Geotechnical Infrastructure. August 4-7, 2013. pp 39-51. doi: 10.1061/9780784413326.005.

[viii] I. L. Al-Qadi, S. Aboqudais, and R. E. Khuri. (1999). A Method To Evaluate Rigid

Pavement Joint Sealant Under Cyclic Shear and Constant Horizontal Deflections. Journal of Transportation Research Board, TRB, No. 1680, National Research Council, Washington D. C., pp. 30-35.

[ix] P. Solanki, H. Ozer, S. Yousefi, and I. L. Al-Qadi. (2014) Effect of Installation Parameters on Performance of Hot-Poured Crack Sealants. T&DI Congress 2014: pp. 142-152. doi: 10.1061/9780784413586.014.

[x] I. L. Al-Qadi, S. Dessouky, S. H. Yang. (2010). Linear viscoelastic modeling for hot-poured crack sealants at low temperature. Journal of materials in civil engineering, 22 (10): 996–1004. Doi.org/10.1061 (ASCE) MT.1943.5533.0000101.

[xi] Liao, M., Chen, J., and Tsou, K. (2012). "Fatigue characteristics of bitumen-filler mastic and asphalt mixtures". Journal of materials in civil engineering. 10.1061/(ASCE)MT.1943-5533.0000450, 916-923.

[xii] Wu, J., and Airey, G. (2011). "The influence of mineral fillers on mastic aging properties. ICCTP 2011:pp.3450-3461. Doi: 10.1061/41186(421)342.

[xiii] Lingyun, K., Shixiu, M., and Na, W. (2015). "High-temperature performance of asphalt mortar using surface and interface theory." Journal of material in civil engineering, 27 (8). Doi: 10.1061/ (ASCE) MT.1943-5533.0001185.

[xiv] AASHTO T 315 (2010). Standard method for determining the rheological properties of asphalt binders using a dynamic shear rheometer. American Association of State Highway and Transportation Officials, Washington, D.C.

[xv] I. Hafeez, F. Junaid, M. A. Kamal, J. Hussain, (2015). Influence of single and two-stage aggregate manufacturing mechanism on asphalt mixture's performance. Journal of Materials in Civil Engineering. doi:ASCE.10.1061/(ASCE)MT.1943-5533.0001480,04015180.

Section B
ELECTRICAL/ELECTRONICS

Low-Power Integrated Circuit Design Optimization Approach

Y. A. Durrani[1]

Electronics Engineering Department, UET, Taxila, Pakistan

[1]yaseer.durrani@uettaxila.edu.pk

***Abstract*—** In this tutorial survey, the paper presented a general review of the state-of-the-art techniques in optimizing the power dissipation on digital electronic systems. The source of power dissipation is focused on complementary metal-oxide-semiconductor (CMOS) circuits. This basic information cannot be implemented directly to optimize power dissipation due to the low abstraction level, but will be helpful to solve the power related problem. The major power factors are considered for the hardware and the software with the most trustful approaches of all levels of the design flow. The paper review is organized in three different types of digital system design: interpret conceptually, design flow, and management.

***Keywords*—** Low-power, Power Optimization, Power Estimation, CAD/EDA Tools

I. Introduction

Nowadays, the new trends of technology scaling brought serious challenges in nano-scale technologies. The size of the transistors became smaller and faster, other important issues like power consumption, cost, error tolerance, verification, testing and integrity are the new challenges in digital system design. Among these issues, low-power very-large-scale-integrated (VLSI) design has become the most focused research area in fabrication processes and design techniques. In response to the increasing demand of electronic industry, power efficient electronic design automation (EDA) tools are highly desirable to handle low-power problems at all steps of the design techniques. These tools are the beginning to market products that helps with the minimum power dissipation of ICs. At the cost of performance, the reduction of the voltage offers the power minimization in the digital circuits. Typically supply-voltage is kept high to permit high speed of the clock and limits the deep sub-micron (DSM) effects. As compared to other type of transistors, CMOS transistors dissipate less energy during non-conducting state. Therefore, low-power design is nowadays focused to reduce the transition activity at the lowest level that requires to perform different tasks. The low-power integrated circuit (IC) design techniques can be used at every step of the design.

This paper is the guideline for IC designers for all levels of abstraction and the low-power design flow. The section II of this paper demonstrates about the brief overview of the sources of power dissipation. This basic information cannot be implemented directly to optimize power dissipation due to the low abstraction level, but will be helpful to solve the power related problem. In section III gives the general review of the low-power design methodologies. Section IV explains about the power-reduction techniques at different levels of abstraction, which is the main part of this work. Finally, the section V is the conclusion. It is not possible to cover all related research in this specific area and we only discuss carefully selected topic in this paper.

II. Sources of Power Dissipation

The sources of power dissipation in CMOS circuit is comprised of dynamic and static power. Further, the dynamic power consists of capacitive switching power, short-circuit power and glitch power. The static power is divided into the leakage current and the dc standby power expressed in (1), (2), (3) and shown in Fig. 1.

$$P_{Total} = P_{Dynamic} + P_{Static} \tag{1}$$

where

$$P_{Dynamic} = Capacitive\ Switching + Short\ Circuit\ Power + Glitch\ Power \tag{2}$$

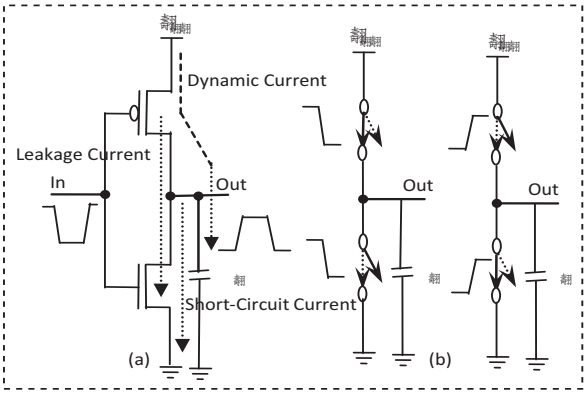

Fig. 1. (a) Sources of power dissipation in CMOS inverter (b) Charging/discharging the load capacitance C_L in equivalent circuit.

$$P_{Static} = Leakage\,Current + DC\,standby\,Power \quad (3)$$

In Fig. 2, the average power per clock period T_{clk} with current flow $I_{supply}(t)$ and supply voltage V_{DD} can be calculated as:

$$P_{avg} = \frac{1}{T_{clk}} \int_0^{T_{clk}} V_{DD} \bullet I_{supply}(t)\, dt \quad (4)$$

or power estimating by adding the total charge flow over each switching event through the circuit simulation.

A. Switching *Power:*

Switching power includes both short-circuit and dynamic power, resulting to charging and discharging of the output load capacitance C_L. It is observed that 50% of the energy is drawn as heat and other 50% of the energy dissipated from the power-supply that is stored in C_L. This output capacitance energy is released during the transition from the logical 0 to 1 or 1 to 0 as shown in Fig. 3. There are two activity factors involve in dynamic power:

- Factor 1: The fraction of clock periods when the output of the circuit has binary transition

$$P_{avg} = 0.5a\, C_L V_{DD}^2 f_{clk} \quad (5)$$

- Factor 2: The fraction of clock periods during the output is switching from high to low or low to high

$$P_{avg} = a_{0\to 1} C_L V_{DD}^2 f_{clk} \quad (6)$$

where V_{DD} is the supply voltage, C_L is the total load capacitance, f is the frequency and α is the factor of the switching activity. The C_L of the CMOS circuit consists of the input node capacitance, the output node capacitance of the driven gate and the effective capacitance of the interconnects/wires.

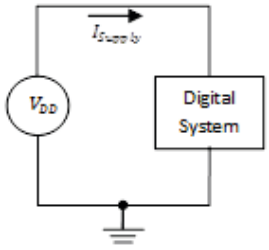

Fig. 2. Average power dissipation in digital system.

A. Short-Circuit Power:

Short-circuit power $P_{Short-Circuit}$ is dissipated due to the current path from V_{DD} to V_{SS} during NMOS and PMOS transistors are active at same time for short instant of time, when the signal switching at the input to the logic circuits. It is stated in (7), (8):

$$P_{Short-Circuit} = a_{0\to 1} f_{clk} I_{peak} \left(\frac{t_r + t_f}{2}\right) V_{DD} \quad (7)$$

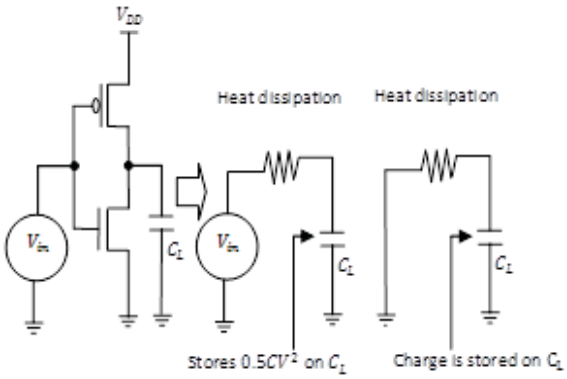

Fig 3. The switching activity factors involved in dynamic power.

$$P_{Short-Circuit} = K \frac{b}{12} (V_{DD} - 2V_T)^3 f t \quad (8)$$

where β is the CMOS transistor gain factor, V_T is the threshold voltage and τ is the rise and fall time of the logic gate input and K is the gain factor of the transistor. When K is zero then no power lost during $P_{Short-Circuit}$ can be minimize to a small amount of the overall power dissipation by using proper transistors sizing and reduction of the input rise-fall times in the circuit. Short-circuit power can also be reduced if the output rise-fall time of a gate is longer than the input rise-fall time. It consumes 10-20% of the overall power consumption. Normally, $P_{Short-Circuit}$ exists in the static CMOS logic families.

A. Dynamic glitch power:

Glitch or electronic pulse is an undesired switching activity for the short duration that occurs before the signal settles to its expected value. Glitches can cause sufficient amount of dynamic power dissipation due to the undesired transitions of the gate.

B. Leakage power:

Leakage power $P_{Leakage}$ is caused by the reverse-biased build between the diffusion regions of the source-drain and substrate-well in the transistors. Due to several internal factors, the transistor continuous to dissipate $P_{Leakage}$ at all junctions, even-though if it is an active mode and not switching. In other words, $P_{Leakage}$ is due to sub-threshold and substrate injection factors at pn-junctions, which can be determined during fabrication process. It can be ignored, because it only contributes not more than 1% of the total power.

However, it is considerable in deep-submicron level. $P_{Leakage}$ is expressed in (9):

$$P_{Leakage} = (I_{Diode} + I_{Sub\text{-}Threshold})V_{DD} \quad (9)$$

where I_{Diode} is the current flows in the reverse-biased diodes that are build between substrate and diffusion regions as shown in Fig. 4. V_{DD} is the supply-voltage and $I_{Sub\text{-}Theshold}$ refers the current flows through the transistor. $P_{Leakage}$ is due to the following five components:

- Reverse-biased diode leakage current at the transistor domains
- Sub-threshold current through a turned-off transistor channel
- Gate induced drain leakage
- Punch through
- Gate oxide tunneling

However, these current components can be controlled technologically. Diode leakage current occurs, when one transistor is not conducting while other transistors are conducting and charges up/down the drain to its substrate potential. Fig. 4 demonstrates a PMOS transistor with a negative gate bias V_{DD} to its substrate. Hence, the diode formed by the drain diffusion and the substrate is reverse-biased. The reverse bias current in (10):

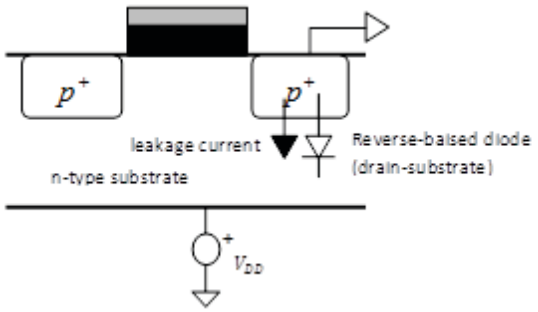

Fig. 4. The leakage current in a reverse-biased PMOS transistor.

$$I_{Leakage} = I_S\left(e^{\frac{V_{DD}}{V_T}}\right) - 1 \quad (10)$$

where $V_T = kT/q$ is the thermal voltage, V_{DD} is the biased voltage, and I_S refers to the reverse-saturation current.

Leakage power in DSM technologies is the most dominant factor in digital electronic circuits. The contribution of dynamic power dissipation also increases due to increased functionality requirements and clock frequencies. Consequently, the majority of existing low-power estimation techniques focus on this dynamic component of dissipation. Low-power design deals with the ability to minimize all sources of power dissipation in CMOS logic gates. To control power delivery cost, operational voltage V_{DD} is reduced 30% of each technology generation. To sufficiently overdrive large gates, threshold voltage V_t can be reduced with the same rate. However, due to the reduction of V_t, transistor sub-threshold current exponentially increases. In case of V_{DD} and V_t, both reduced, the leakage power can be comparable to the dynamic power. Dynamic and leakage power increases the temperature. If heat is not dissipated effectively, temperature and $P_{Leakage}$ may cause physical damage in the CMOS circuits. Therefore, power optimization can be achieved by focusing several complex problems from different dimensions. Technology improvements can enhance the design capabilities and contributes to the reductions of all components, mostly impact on dynamic switching and short-circuit power.

III. Low Power Design Methodologies

The major decisions for the low-power design starts with an understanding of the power consumption goals. The early strategy can severe effects the IC throughputs. These decisions can play important results in achieving the power specifications. With the changing environment, today's designers need a complete literate understanding to monitor and address the power at each level of the abstraction and obtain the maximum energy efficiency. As low-power has become major design parameter, the designers target on the sensible power designs where the power reduction approaches are applied. Nowadays System-on-Chip (SoC) requires a holistic and concurrent approach that includes the relationship among: system level design, architectural design, software/hardware co-design, intellectual property (IP) design, physical design, and Power verification.

The low-power design flow has several steps to perform designers and implement the digital electronic system. However, designers have to consider certain flow in the trajectory of the top-down technique, i.e. system to layout level, within each level there is no pre-defined design method. Every step includes several low-power design approaches. The low-power term includes all attempts that are possible to improve the logic circuits for power reduction. Power analysis follows power optimization. The accurate approaches must be adopted so that designers use proper power estimation function in the power reduction tools. The Low-power term can be sub-categories as:

- Power optimization and low-power synthesis
- Power estimation

A. Power optimization and low-power synthesis

In most cases electronic circuits are designed for small area and high speed, which are not the optimum circuit optimization. At all abstraction levels, the

dedicated low-power techniques and EDA tools must be developed to fully optimize the optimum implementation. The opportunities for power savings are the largest at system and architectural levels, whereas the accuracy is highest at the layout and gate levels as shown in Fig. 5. Modern low-power SoC requires concurrent and holistic techniques.

A. Power estimation

The computation and prediction of power dissipation is a challenging task, especially when the instantaneous

System Level	50…90%
Behaviour/Algorithm Level	40…70%
Architecture Level	30…50%
Logic Level	20…30%
Circuit Level	10…20%
Layout Level	5…10%

Fig. 5. Power reduction in low-power at top to bottom abstraction levels.

power is to be determined during the timing considerations.

Power estimation technique estimates the power consumption of electronic circuits. It is observed that power measurement approaches are more effective at high abstraction levels. The low-power estimation is interested in the optimization, analysis and trade-off of the circuit operation. Power does not only depends on typical power consumption factors (i.e. voltage, capacitance etc.), but it is also input patterns dependent. Furthermore, it is very difficult to determine an absolute estimate of the average power dissipation. More abstract variables such as correlation factors, transition density and signal probabilities are implemented in the power calculations. The main purpose of power measurements and analysis are to ensure the power consumption targets are achieved and not violated the power goals in the design of efficient low-power electronic system.

I. Power Optimization Techniques

A. System level

At system level the decisions making, the organizational and technological choices, the data representation, and the selection of algorithms for data processing have strong influence on the power dissipation. The power consumption in electronic system is scalable with the process technology scaling. System level optimization can be performed prior to the design of architecture that allows designers in short time to save all possible components of power. Several technological techniques have been adopted for the low-power based system design. Some of them are the multiple input voltages on a single chip; low supply-voltage operations, clock speed, variable supply-voltage, adoptive voltage scaling, dynamic clock frequency, voltage scaling, and the static voltage scaling. In portable systems, frequency reduction can save sufficient amount of power in the processors. Some techniques reduce power for specific applications, where noise is not an important issue and can be tolerated sufficiently.

The choice of exact algorithm may provide the required functionality of the system under the design limitations. Algorithms used for the estimation of power dissipation are influenced by overall complexity, basic operations, and communication requirements etc. Algorithm selection is an important factor for the low-power design that can be made through an object-oriented approach. Data-type selection has major factor on the overall power dissipation. The choice of algorithm may neglect the effect of interaction between executing the remained computations and the hardware implementation function. Hence, power estimation of the pre-characterizing function in isolation mode can be inaccurate. This issue must be considered by approach for low-power designs. During each operation of execution, many algorithms have branches, procedure calls and loops that create the distribution which is not uniform. Such non-uniformity is important for the energy-efficient system design. Execution of algorithm flow under the input patterns/signals can easily be detected in the kernels of the computations. To optimize sufficient amount of power, each kernel must be reduced in the implementation on hardware design. Approximate consumption algorithm technique [i] can be adopted to improve the quality to power constraints and the requirements of the users.

Electronic system modeling is very useful to abstract system characteristics and design goals. Several data processing engines can communicate between each other through these characteristics. For example in multimedia application with different processing engines such as digital signal processor core, microcontroller core and the general-purpose core can execute directly in hardware, some with different instruction set architecture (ISA) and some executing parallel threads of processing. Therefore, macro-modelling architecture is suitable at high abstraction level for implementation of the models. Power efficient system design modelling must be appropriate by low-power design flow in all stages. Power dissipation in later stages of the design may be not very effective due to the important decisions on system-level have already been considered.

Software and hardware partitioning is a well-known design methodology with the goal to minimize the power consumption. A large amount of off-chip operations can be reduced by partitioning. During switching activities of the transistors, these off-chip

operations sufficiently contribute to the overall power consumption at the system level. When two concurrent processes are implemented with different hardware, we can turn-off the clock of inactive hardware and power saving power can be made by preventing the transition activity in the circuit. Through the efficient power management system, processor can keep an idle state during doze, nap, and sleep modes.

Normally, data influences the power dissipation of communication resources and data access in memory affects the energy usage, while software compilation affects the instruction sets in the computational blocks. On the other side, software does not have physical hardware realization and efficient hardware-based system design addresses the power optimization in storage, computational and the communication units.

Several approaches use aggressive methods to reduce power in applications for dealing with noise can be tolerated. Approximate computation algorithms [ii] can optimize a large amount of power but in the expense of inaccuracies in the computation. Such technique can handle quality of power parameters and the user requirements. For example in digital filters, input bit-width can be altered. The power consumption can be reduced by disabling fan-in and fan-out of inactive bit lines. In computation, minimization of bit widths can cause inaccuracy and quality of output is affected by noise. In some applications noise can be tolerated under different operating conditions.

Power-modelling approach has been developed to focus the entire system's power consumption such as operating system, processors, re-configurable circuits, and memories. These models are used in the library in the context of multi level design exploration: to deal with the energy/power optimization and estimations at system level.

Re-configurable processors are high enough efficient than general purpose processors. For example, the power efficiency of XPP processor is higher than ARM-9. However, such processor still lower than

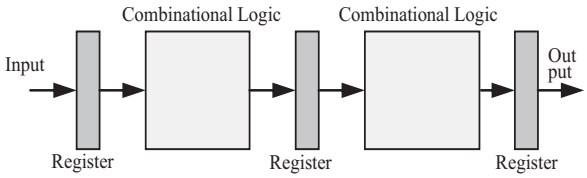

Fig. 6. A Synchronous Pipelined Model

application specific integrated circuit (ASIC) processing the same function due to run-time redundant logic circuit that is designed for the flexibility. Then the dual V_{DD} is applied to improve the power efficiency of reconfigurable processors. This approach is used to increase the slack time among several operations to minimize the power dissipation by executing the more fast operations with minimum voltage.

B. Architecture or Behavioral Level

For many electronic systems, the design entry point is architecture level. An accurate and clear power profile can be designed when the architecture is selected and register-transfer level (RTL) description is used for the specification of selected architecture. A huge variety of transformations from behavioural synthesis can be used such as unrolling, loop pipelining, control flow optimization and the design decisions have the dramatic effect on the requirements of power budget.

For improving performance parallelism is a well-known technique that optimizes power by reducing the supply voltage. A voltage reduction of up to 30-40% can be achieved depending on the data-path architecture. Architectural-based voltage scaling is the efficient technique at this level. It lowers the supply voltage V_{DD} and handles with the low circuit performance but compensate with a higher-throughput architecture. Parallelism technique compensates for the loss in throughput due to the voltage reduction.

Pipelining is another well-known technique for the power reduction. Adding the pipeline registers in the certain points of a data-path that decreases the critical path for allowing the data-path blocks to operate at the high rate as shown in Fig. 6. Increasing the level of pipelining may affect reducing the logic depth and power contribution because critical races are minimized. Simultaneously exploiting parallelism and pipelining approaches can obtain huge power optimization.

Today the designers have different alternatives to choose data representation such as: encoded vs. unencoded data, fixed-point vs. floating-point, sign-magnitude vs. two's complement methods. Each of these decisions involves a trade-off in accuracy between the power, the performance, and the simplicity of the design etc. The fixed-point representation has the minimum complexity that exhibits the low-power consumption but suffers the dynamic range difficulties. Software data scaling approach handles this problem; however, it must be incorporated into the processor micro-code. In contrast, floating-point alleviates the dynamic range difficulties at the expense of additional hardware. Two's complement method is widely used in arithmetic computations. In this type of representation, the most significant bit contains redundant information that causes additional switching activities and the high power dissipation. In contrast, signed data uses a single bit which also causes switching in one-bit of the data. Such problem can be solved through the data encoding, floating-point, and logarithmic companding techniques. In logarithmic scale many computations such as addition, the sign-magnitude do not have simple implementations; however, some arithmetic operations dissipate less power and become easier in the logarithmic scale: e.g. multiplication translates to additions. Applications such as large multiplications

can be helpful by using logarithmically encoded data.

Due to finite propagation delays several logic blocks can exhibit invalid transitions. Hence it is important that all signal paths have same propagation delays and reduce the logic-depth (through more cascading). Glitches are another reason of the additional switching activity in the logic circuits. Balanced circuits may have less glitches as the chain topology has been explained in [iii]. To increase the logic-depth may increase the capacitance due to glitches in the circuits and reduce the logic-depth may increase register power. So the selection of logic depth is the trade-off between the glitch capacitance and the register capacitance.

The selection of the hardware module for execution of a given instruction is an important aspect of the power optimization. For each different architecture of the same operation may have different area, performance and the power characterizations for example addition operation can be performed using ripple carry adder, carry save adder or carry look ahead adder [iv-v].

The global architectural technique for large memories and the driving signals across the chip for possible power dissipation tasks is the Global data transfer. Partitioning is another efficient technique for maximizing locality among different blocks. Exploiting locality through the distributed processors, controllers and the memories can improve sufficient power savings [vi].

C. Gate Level

Logic level has a huge impact on the power consumption, performance and area of its final gate level implementation. Several power optimizing techniques can be applied to the gate level design. Traditionally gate logic optimization can be divided into two steps: *technology-dependent* and *technology-independent* optimizations. Technology-dependent optimization can be made through the mapping of the library of a particular technology using technology-dependent algorithms for the power, performance, or area. Technology-independent optimization is the important factor for the logical functions. The commonly used algorithm for multi-level logic optimization is kernel extraction [vii]. From a given function kernels are extracted and the kernel with minimum literal counts is selected. For power dissipation, the main function is switching activity in the logic not the literal counts. The transition activity power can be optimized by Modified kernel extraction methods which are discussed in [vii]. The literal number of the factors represent in the logic gate function is effective technology-independent optimization. It may require an accurate power estimation of every network node to the mapped network power consumption.

In technology dependent approach, low-power technology mapping produces more accurate estimates by accurately estimating the gate input capacitances and their impact on the power. These technology mapping techniques have been used in design tools used commercially. Several prototype mappers have been proposed and reported 10-15% average power savings [viii]. The adaptation of the mapping graph data structure to implicitly explore alternative logic decompositions during library bindings. This technique helps in finding better matching, at the price of increased computational effort for power estimation. A pre-computation technique [ix] decreases the power and increases the multiplication process speed of the logic gates. In this technique all multiplication steps related with the accumulation and the generation of the partial products are eliminated at the end of the multiplication method. Such method reduces the clock and transition activity of the gates.

Retiming is the well-known optimization technique in the synchronous sequential logic circuits. In this technique, the necessary clock period is minimizes by repositions of the flip-flops [x]. The proposed algorithm for register retiming and minimum delay is Polynomial time-based algorithms [xi]. In synchronous logic circuits the transitions activity at the outputs of flip flops is less than the transitions activity at the flip-flop inputs. A large number of transitions activities are filtered out by the clock at the flip-flops inputs. The power consumption of sequential circuits is effectively reduced by retiming technique.

Boolean optimizations are more general, powerful, computationally intensive, and the propagation of don't cares are compared to the algebraic transformations. When especially targeting power, don't cares conditions are more complex, challenging issue and its simplification is a local problem. To restrict don't cares for optimization to a subset named power relevant don't cares [xii] that ensures the transitions activity in the fan-out of the optimized node does not increases. Power dissipation can be minimized through the logic restructuring techniques to prevent high switching frequencies from propagating the logic gates during their unwanted values.

Finite state machine (FSM) in logic level assigned codes that reduce the number of bits in the logic for similar state transitions [xiii]. State encoding technique namely weighted transition activity targets a power cost function [xiv]. If there are a large number of transitions between two states then the two states must be provided uni-distant codes to reduce the switching activity at the output of the flip-flops. Hence, the complexity of the logic circuit may increases the number of states that should not be avoided. Encode state transition graph technique [xv-xvi] produces the two-level and the multi-level implementations with the minimum power requirements. A method to re-encode sequential circuits at the logic level optimizes the power dissipation in [xvii]. Other techniques to encode to reduce the switching activities in the data-path logic

and minimize the switching on buses have been proposed in [xvii-xviii].

There are several power saving techniques that can be used both in dynamic and static logic circuits. Dynamic logic circuits can be more than 50% faster than static logic circuits. Static circuits are slower due to it's twice loading capacitance, high threshold voltages, and the slow P-type transistors. Dynamic logic can be harder to design and may be the only choice to increase the processing speed. Most processors run at giga-hertz that requires dynamic circuits and some manufacturers for power reduction such as Intel processors completely switched to the static circuits. Power reduction not only extends the running time with the batteries, but it also reduces the thermal design requirements to minimize the size of the heat-sink, fans, etc. In dynamic logic, clock gating and asynchronous methods are more effective power optimization techniques. Circuit level design techniques that vary widely with delay and power dissipation, such as static CMOS, NP Domino or NORA logic, Cascode Voltage Switch Logic (CVSL), Push-Pull Pass Transistor Logic (PPL), Differential Cascode Voltage Switch Logic (DCVSL), Pseudo-NMOS, Complementary Pass Transistor Logic (CPL), Pseudo-NMOS etc. CMOS transistors are suitable for building low-power circuits however, CMOS gate suffer other three power components discussed in section II.

Low-power dynamic logic is useful for the reduction of switching activities, reduction of the short-circuit power consumption and minimization of the internal capacitances. In the preceding cycle, each time power is consumed during the pre-charge phase and output of the discharged capacitors [xix]. Some approaches developed two and four-phase clock strategies to handle the problem of CVSL [xx]. Some further modified techniques used basic domino logic methods e.g. NP-CMOS Domino and NORA logic [xxi-xxiii]. Power consumption in Single Rail Pass-Transistor Logic (SPL) circuit is sensitive to the low-voltage operations. The NMOS pass transistor logic has better low voltage performance than standard CMOS circuits. For low threshold voltages the sub-threshold leakage may become serious problem for both SPL and CMOS low power design circuits [xxiv]. In [xxiv], using the same conditions, the delay is worse and significantly greater for low supply voltages. Pass-transistor logic can achieve significant power reduction if the problem of threshold voltage drop and static power of the inverter output is properly addressed. CPL-based full adder implemented with transmission gates saves half of power compared to the standard CMOS adder [xxv]. Booth algorithm based multiplier saves 18% power and speed increases more than 30%.

PPL is another good choice for low-power design. For example 40-stage full adder is a power-delay product of 60%, CMOS multiplier of 42%, CPL of 63% and SPL of 78%. Generally Pseudo-NMOS is not considered for low-power operation. This logic style can reduce power consumption only for complex logic function switching at high frequencies where savings to the dynamic power component due to reduced capacitances are dominant. DCVSL over conventional CMOS is faster switching due to reduced output capacitances. Compared to Pseudo-NMOS the DCVSL exceeds in that there is no static power consumption; however, the current during switching increases due to the large pull-up transistor. DCVSL logic style is suitable for implementing high fan-in gates and aims at reducing power consumption by limiting voltage swings in the internal nodes in the evaluation NMOS tree without any performance degradation. However, this style has some problems in different cases.

Domino circuit is normally used in high-speed applications. Domino circuit has faster speed but also have higher power dissipation. The low power dynamic logic gates works effectively at low supply voltages. The NMOS transistors are used instead of PMOS pull up transistors which reduce the voltage swing at the input of circuit.

Dynamic Latches are the simplest and most efficient timing circuits. There are different types of dynamic latch styles. According to simulation results in [xxvi], the non pre-charged true single phase clocked latch and 9T flip-flops dissipates lowest amount of power. The low-power dynamic latch can improve considerably their speed if they are designed without complementary outputs. A valuable comparison of the performance and power characteristics of flip-flops can be found in [xxvii].

D. Transistor Level

Transistor-level optimization and analysis in digital design is becoming critical for achieving possible unique solution of power, performance and area. Among several methods, transistor sizing is most common approach for various circuit optimization purposes. Most of the research work on transistor scaling has been on channel widths improvements of the transistor on the given circuit critical path delay. In [xxviii], the authors propose a novel method to incorporate into the transistor-level power optimization tools. The functional units are modeled by the graphical representation of the series parallel transistors. Then power budget are accurately allocate by using power budget distribution algorithm. The functional units' power consumption is optimized using these power budgets by transistor sizing technique.

In constant field scaling technique [xxix] a constant gate oxide field of the transistor is used to optimizes the transistor geometric features and maintains the silicon doping level. This technique remains the power density constant and power dissipation scales as k^2, while speed increases as k, Transistor size optimization can be performed with two types of algorithms:

- Algorithm that reduce the power dissipation by reducing the size of the gates and satisfies the timing constraint.
- Algorithm that performs sizing on each transistor for power optimization. The process may be completed, if power optimized layout satisfies the design constraints otherwise, power minimal size is applied to transistor sizes until the timing and delay constraints are required [xxx].

Advanced encryption standard (AES) technique [xxxi] is introduced in each stage of AES to optimize the low-power dissipation using multi threshold CMOS technique. The dynamic and sub-threshold power is reduced with different delays of the signals. The leakage current is minimized by implementing the most of the design part with low-power transistors with low speed. While the portion of design required high performance is implemented with faster transistors but high leakage current. This technique not only optimizes the leakage power but also allow propagation delay for the critical and non-critical paths closer. 10% power reduction can be made with AES technique of the system having throughput of higher than 18 GB/s.

Circuit parallelization is a well-known technique in which throughput of logic blocks on the critical path is maintain at a reduced voltage V_{DD} It can be obtained with N number of blocks in parallel clocked at $\frac{f}{N}$. Each block can calculate its result in a given time slot N time longer and provided at a reduced V_{DD} shown in (11).

$$P = C.\frac{f}{N}.V_{DD}^2 \tag{11}$$

Power dissipation is minimizes without reducing the V_{DD}. But, some factors have to consider such as results of the logic blocks and logic block repetition.

The most commonly used circuit-level dynamic power optimization technique is clock gating. Switching activity in a block which is not used can be eliminated by stopping the clock signals at that block. Transistor-level multiple voltage usage in CMOS circuits produces significant amount of leakage power when the low voltage gates drive high voltage gates. In this case, High voltage gate's PMOS transistor is not turned off at low voltage produced by low voltage gates. To handle this problem, clustered voltage scaling (CVS) [xxxii-xxxiii] and Module level voltage scaling (MLVS) are proposed in [xxxiv-xxxv]. In CVS technique, low voltages are assigned to the gates to produce clusters. In MLVS approach, dual supply voltage assign to large blocks of the circuit. Both techniques limit the power optimization by introducing low voltage assignment process. For the placement of high and low voltage transistors in dual voltage circuits it is necessary to understand its effect on the leakage current. To solve this issue, voltage level circuits are constructed to handle the leakage problem [xxxvi]. Voltage level converters convert a low to high voltage without increase of the leakage current. Further, CVS and MLVS techniques handle when no low voltage gate drives a high voltage gate. Both techniques consist of additional constraints to the dual voltage assignment process that reduces upto 8% of the total power dissipation in the circuit [xxxvi].

Reverse body bias (RBB) technique [xxxvii] increases the threshold voltages of transistors during an idle state. However, the performance of the RBB decreases as the V_{th} values are lowered or the channel lengths becomes smaller. 80% of the static power in CMOS circuits can be optimized by using multiple threshold voltages without decreasing the performance of the circuit [xxxviii]. A change of static logic provides a layout optimization for low-power by reducing the parasitic capacitances. Transistors are designed in series between output and the power supply. Nanotechnologies have been used with the limited number of standard cells for standard libraries. Such techniques achieve improved speed and low-power consumption compared to the conventional libraries [xxxix].

Several low-swing voltage technique have be introduced such as: conventional level converter (CLC), capacitive-coupled lever converter (CCLC), differential interconnect (DIFF), pseudo-differential interconnect (PDIFF), and pulse-controlled driver (PCD) etc. The most commonly used technique for power optimization on a long interconnect wire is low-swing voltage technique in which swing of the voltage is reduces on the wire. Power savings can be achieved with the minimum driver size due to the current delivered to the load capacitance by the driver in a certain time is smaller than the full-swing case. Second the charge required for charging and discharging of load capacitance is smaller. The dynamic energy E_{Dyn} of interconnect wire in one cycle can explained in (12).

$$E_{Dyn} = a.C_L.V_{Swing}.V_{DD} \tag{12}$$

where V_{swing} is the voltage across the wire and α is the switching activity of the signal.

E. Layout/Physical Level

Layout or physical level is an intermediate between the gate level and the geometric design of the electronic system. There are numerous layout design styles are used to place, route, partition and resize transistors. In zero-delay or glitch free models, the transition activity of the transistors remains unchanged during layout optimization and hence power reduction can be made through netlist partitioning, transistor sizing, and transistor reordering, routing and gate placement. In with glitch models, designing layout are more complicated and glitch activity may effected by layout optimization in various ways so glitch activity cannot be modelled accurately.

A large number of low power layout optimization

methods have been developed such as wire and buffer resizing, re-mapping and local restructuring. The transistor re-sizing in layout minimizes the short-circuit power dissipation and the parasitic capacitances. The optimal size for the transistor that drives the output should be larger than the minimum size. In [xxxx], power-delay optimal sizes algorithm runs until the power-minimal layout satisfies the delay constraints. Several authors [xxxxi-xxxxii] demonstrated 15-20% power reduction can be obtained through the transistor re-sizing techniques. The relation between power dissipation, signal delay, interconnect load and driver size is described by optimal buffer size technique [xxxxiii]. A layout interconnection propagation delay is reduces significantly by wire sizing and driver sizing. Power dissipation increases when the size of wire increases because of increase in driver load. Interconnect delay can be improve by using wire and driver sizing but at the cost of small increase of power dissipation. Another technique [xxxxiv] which avoids the monotonicity of the propagation delay model by using an optimal gate and wire sizing on convex programming. Such approach can find the gate size and wire width.

In digital systems, clock distribution network dissipates significant amount of power. Several clock routing algorithm techniques have been proposed. Among those, wire sizing and wire elongation [xxxxv] proposed the chain of drivers at the zero-skew. The non-zero skew clock routing approach was introduced for sized to find a prescribed skew bound [xxxxvi]. In another technique [xxxxvii], buffers were introduced at internal points in the clock tree for satisfying the source-sink path delay constraints and minimizing the area of the clock network. Due to the buffer insertion method for the partition of large clock tree into small number of sub-trees with the minimum wire widths that results 60-70% power savings in the clock tree compared to the single driver approach. The low power clock routing minimizes the load on the clock drivers to meet a tolerable clock skew.

With small supply voltage the noise margins are diminished and the power distribution can have large effect on speed of the digital circuits. The wire sizing topology in power distribution networks (PDN) was proposed in [xxxxviii]. The main goal was to reduce the layout area while limiting the average current density to avoid the voltage drops and the electron-migration induction problems. This approach observes that when the two sinks do not draw currents at same time, narrow wires can be used for power distribution. Thus reduction can be made through layout area up to 30% compared to the star routing scheme.

V. Conclusion

Power has to be addressed in all levels of abstraction through the use of different EDA/CAD tools. Based on the previous research, we discussed efficient techniques for the power optimization in digital electronic system. While system to layout level commercial tools is available but still many of the optimization techniques require manual interaction by the designer. For detailed discussions on different aspects of power consumption, the reader is referred to given below references.

References

[i] C. Yang, J. Chen, and T. Kuo, “An approximation algorithm for energy-efficient scheduling on a chip multiprocessor,” In proc. of the Design, Automation and Test in Europe conference, vol. 1, pp. 468-473, March 2005.

[ii] Y. A. Durrani, and T. Riesgo, “High-level power analysis for intellectual property-based digital systems,” Springer Circuits, Systems & Signal Processing, vol. 33, no. 6, pp. 10531-1051, Dec. 2013.

[iii] C. Nagendra, R. Owens, and M. Irwin, “Power-delay characteristics of CMOS adders,” IEEE Trans. VLSI systems, vol.2, pp. 377-381, Sept. 1994.

[v] A. Bellaouar, and M. Elmasry, “Low-Power Digital VLSI Design Circuits and Systems”, Kluwer Academic Publishers, 1995.

[iv] Y. A. Durrani, and T. Riesgo, "High-level power Analysis for IP-based digital systems," Journal of Low Power Electronics, American Scientific Publisher, vol. 9, no. 4, pp. 435-444, Dec. 2013.

[vi] Y. A. Durrani, and T. Riesgo, “Power estimation for intellectual property-based digital systems at architectural level” Elsevier Journal of King Saud University-Computer and Information Sciences, vol. 26, no. 3, pp. 1319-1578, 2014.

[vii] K. Roy and S. Prasad, “SYCLOP: Synthesis of CMOS Logic for Low Power Applications” In proc. of the Int’l Conference on Computer Design: VLSI in Computer and Processors, pp. 464-467, Oct. 1992.

[viii] S. Iman, and M. Pedram, “Logic Synthesis for Low Power VLSI Designs,” Kluwer Academic Publishers, 1998.

[ix] Y. Liu, and S. Furber, “The design of a low power asynchronous multiplier,” in Proc. ISLPED, pp. 301-306, 2004.

[x] L.-F. Chao and E. H.-M. Sha, “Scheduling data-flow graphs via retiming and unfolding,” IEEE Transactions on Parallel and Distributed Systems, vol.8, pp.1259–1267, 1997.

[xi] T. Soyata, E. Friedman, and J. Mulligan, “Incorporating interconnect, register, and clock distribution delays into the retiming process,” IEEE Transaction on CAD of

integrated circuits and systems, vol.16, no.1, pp. 105-120, Jan. 1997.

[xii] M. Pedram, "Power Estimation and Optimization at the Logic Level," Intl. Journal of High-Speed Electronics and Systems, vol.5, no.2, pp. 179-202, 1994.

[xiii] C-Y. Tsui, M. Pedram, and C-h. Chen, A. Despain, "Low power state assignment targeting two- and multi-level logic implementations," In proc. of the IEEE International Conference on Computer Aided Design, pp. 82-87, Nov. 1994.

[xiv] P. Ashar, S. Devdas, and A. R. Newton, "Sequential Logic Synthesis," Kluwer Academic Publishers, Boston, 1991.

[xv] K. Roy, and S. Prasad, "SYCLOP: Synthesis of CMOS Logic for Low Power Applications," In proc. of the Int'l Conference on Computer Design: VLSI in Computer and Processors, pp. 464-467, Oct. 1992.

[xvi] H-S. Jung, and M. Pedram "Uncertainty-aware dynamic power management in partially observable domains," IEEE Trans. on VLSI Systems, vol. 17, no. 7, pp. 929-942, Jul. 2009.

[xvii] G. D Hachtel, M. Hermida, A. Pardo, M. Poncino, and F. Somenzi, "Re-Encoding Sequential Circuits to Reduce Power Dissipation," In proc. of the Int'l Conference on Computer Aided Design, pp. 70-73, Nov. 1994.

[xviii] M. Stan and W. Burleson. "Limited-weight codes for low power I/O," In proc. of Int'l Workshop on Low Power Design, pp. 209-214, April 1994.

[xix] J. M. Rabaey, "Digital Integrated Circuits: A Design Perspective", Prentice Hall Publisher, 1996.

[xx] N. H: E. Weste, and K. Eshraghain, "Principles of CMOS VLSI Design," Addison Wesley Publisher, 1994.

[xxi] C. M. Lee, and E. W. Szeto, "Zipper CMOS," IEEE Circuits and Systems Magazine, pp. 10-16, May 1986.

[xxii] R. Krambeck et al., "High-Speed Compact Circuits with CMOS," IEEE Journal of Solid State Circuits, vol. SC-17, no.3, pp. 614-619, June 1982.

[xxiii] N. Gonclaves, and H. J. DeMan, "NORA: a race free dynamic CMOS technique for pipelined logic structures," IEEE Journal of Solid State Circuits, vol. SC-118, no. 3, pp. 261-266, June 1983.

[xxiv] K. Yano, Y. Sasaki, K. Rikino, and K., Seki, "Top-Down Pass-Transistor Logic Design," IEEE Journal of Solid State Circuits, vol. 31, no. 10, pp. 792-803, Oct. 1996.

[xxv] I. S. Abu-Khater, A. Bellaouar, and M.I. Elmasry, "Circuit Techniques for CMOS Low-Power High-Performance Multipliers," IEEE Journal of Solid-State Circuits, vol. 31, no. 10, pp. 1535-1546, October 1996.

[xxvi] C. Svensson, and J. Yuan, "Latches and Flip-Flops for Low Power Systems," Low Power CMOS Design", IEEE Press, 1998.

[xxvii] V. Stojanovic, and V. G. Oklobdzija, "Comparative Analysis of Master-Slave Latches and Flip Flops," IEEE Journal of Solid-State Circuits, vol. 34, no. 4, pp. 536-548, April 1999.

[xxviii] V. Sundararajan, S. S. Sapatnekar, and K. K. Parhi, "MINFLOTRANSIT: Min-Cost Flow Based Transistor Sizing Tool," Design Automation Conference, pp. 453-460, 2000.

[xxix] S. Borkar, "Design Challenges of Technology Scaling," IEEE Micro, vol. 19, no.4, pp. 23-29, July 1999.

[xxx] M. Borah, R. M. Owens, and M. J. Irwin, "Transistor sizing for low power CMOS circuits," IEEE Transactions on Computer Aided Computer-Aided Design of Integrated Circuits and Systems, vol. 15, no. 6, pp. 665-671, June 1996.

[xxxi] A. Alma'aitah, and Z. Abid, "Area efficienthigh throughput sub-pipelined design of the AES in CMOS 180nm," 5th International Design and Test Workshop, pp.31-36, 2010.

[xxxii] K. Usami, and M. Horowitz, "Clustered voltage scaling technique for low-power design," Low Power Design Symposium, pp. 3-8, 1995.

[xxxiii] M. Donno, L. Macchiarulo, A. Macii, E. Macii, and M. Poncino, "Enhanced clustered voltage scaling for low power," GLSVLSI '02. In proc. of the 12th ACM Great Lakes Symposium on VLSI, 18-20, pp. 18-23, April 2002.

[xxxiv] J.-M. Chang, and M. Pedram, "Energy minimization using multiple supply voltages," IEEE Transactions on Very Large Scale Integration Systems, vol. 5, pp. 436-443, 1997.

[xxxv] C. Chen, A. Srivastava, and M. Sarrafzadeh, "On gate level power optimization using dual-supply voltages," IEEE Transactions on Very Large Scale Integration Systems, vol. 9, pp. 616-29, 2001.

[xxxvi] S. H. Kulkarni, and D. Sylvester, "Fast and Energy-Efficient Asynchronous Level Converters for Multi-VDD Design," IEEE International SoC Conference, pp. 169-172, 2003.

[xxxvii] G. Sery, S. Borkar, and V. De, "Life is CMOS: why chase the life after," In proc. of Design Automation Conference, pp. 78-83, 2002.

[xxxviii] L. Wei, Z. Chen, K. Roy, M. C. Johnson, Y. Ye, and V. K. De, "Design and optimization of dual-threshold circuits for low-voltage low-power applications," IEEE Transactions on Very Large Scale Integration Systems, vol. 7, pp. 16-24, 1999.

[xxxix] J. M. Masgonty, S. Cserveny, C. Arm, P.-D. P. fister, and C. Piguet. "Low-Power Low-Voltage Standard Cell Libraries with a Limited Number of Cells," In proc. of 11th Int. Workshop on Power and Timing Modeling, Optimization and Simulation, Sept. 2001.

[xxxx] M. Borah, R. M. Owens, and M. J. Irwin. "Transistor sizing for minimizing power consumption of CMOS circuits under delay constraint," In proc. of the 1995 International Symposium on Low Power Design, pp. 167-172, April 1995.

[xxxxi] H-R. Lin, and T-T. Hwang, "Power reduction by gate sizing with path-oriented slack calculation," In proc. of the 1st Asia-Pacific Design Automation Conference, pp. 7-12, Aug. 1995.

[xxxxii] S. Sapatnekar and W. Chuang "Power versus delay in gate sizing: conflicting objectives," In proc. of the IEEE International Conference on Computer Aided Design, pp. 323-330, Nov. 1995.

[xxxxiii] A. Vittal, and M. Marek-Sadowska, "Power optimal buffered clock tree design," In proc. of the 32nd Design Automation Conference, pp. 497-502, June 1995.

[xxxxiv] N. Menezes, R. Baldick, and L. T. Pileggi, "A sequential quadratic programming approach to concurrent gate and wire sizing," In proc. of the IEEE International Conference on Computer Aided Design, pp. 144-151, Nov. 1995.

[xxxxv] J. Lillis, C-K Cheng, and T-T. Y. Lin, "Optimal wire sizing and buffer insertion for low power and a generalized delay model" In proc. of the International Conference on Computer Design, pp. 138-143, Nov. 1995.

[xxxxvi] S. Pullela, N. Menezes, and L. T. Pillage, "Reliable non-zero skew clock tree using wire width minimization," In proc. of the 30th Design Automation Conference, pp. 165-170, June 1993.

[xxxxvii] J. G. Xi, and W-M. Dai, "Buffer insertion and sizing under process variations for low power," In proc. of the 32nd Design Automation Conference, pp. 491-496, June 1995.

[xxxxviii] A. Vittal, and M. Marek-Sadowska, "Power distribution topology design," In proc. of the 32nd Design Automation Conference, pp. 503-507, June 1995.

Reactive Power Control of A 220kv Transmission Line Using PWM Based Statcom with Real Time Data Implementation

A. Mahmood[1], M. Amjad[2], . M. I. Malik[3], A. Ali[4], A. Muhammad[5]

[1,4]*Faculty of Electrical Engineering, Institute of Southern Punjab,Multan*
[2,5] *Department of Electrical Engineering, Islamia University Bahawalpur, Pakistan*
[3]*Faculty of Electrical Engineering BZU, Mulatn Pakistan*
[1]aatif_51@yahoo.com

Abstract-Static Synchronous Compensator (STATCOM) is the best device for reactive power compensation and power system stability. In this paper a novel STATCOM model is proposed. The STATCOM model used in this paper used a control algorithm. Pulse Width Modulation technique (PWM) is implemented with control algorithm for the generation of the gating pulses for IGBTs Installed in the Voltage Source Inverter (VSI). The STATCOM model is implemented in a 220KV existing transmission line located in Multan for reactive power compensation. The model is simulated in MATLAB/Simulink software and results are compared with the existing system. The results of STATCOM are compared with the capacitor which is already installed in the transmission system**.**

Keywords- STATCOM, Control Algorithm, PWM, VSI, MATLAB

I.INTRODUCTION

In recent past the demand of electrical energy has increased drastically which causes lots of problems for the power system stability. This will suggest that the electrical power system should be more flexible, reliable, accurate and should have faster response time. The transmission line is the major part of electrical system having high voltage and supply bulk amount of electricity from power generating ends to the substations that are located near to the population areas. Transmission and distribution system normally have the losses in between 6% to 8% [i].During past years the increased demand of electrical energy have created problems like reactive power deficiency, power transfer capability and power system stability. Severe blackouts happened in the recent past due to transient stability problems[ii-iii]. So for the improvement of transient stability many solutions have been provided which includes superconducting faults current limiters [iv-v], superconducting magnetics energy storage units[vi-viii] and thyrsitor controlled braking resistors [ix]. These solutions have the disadvantage of rigidity and slower reponse time.

Flexible AC transmission system (FACTS) devices are the most viable option for the power system performance, transient stability and reactive power compensation [x]. FACTS devices include TSC (Thyristor Switched Capacitor),SSSC (Static Synchronous Series Compensator) ,TCR (Thyristor Controlled Reactor), TCSC (Thyristor Controlled Series Compensator),SVC (Static VAR Compensator) and STATCOM (Static Synchronous Compensator). FACTS devices are implemented using power electronics converters and thyristors for reactive power compensation and to improve power system stability[xi-xiii].The FACTS devices are categorized by series and shunt connected compensators. Series compensators include Thyristor Switched Capacitor, Static Synchronous Series Compensator, Thyristor Controlled Reactor and Thyristor Controlled Series Compensator. And shunt compensators include Static VAR compensator and static synchronous compensator [xiv].

STATCOM is considered to be one of the best devices for reactive power compensation, transient stability improvement, better voltage support capability, better power transfer capability and have faster response time. Moreover, a STATCOM does not need thyristor-switched capacitors (TCS) or thyristor-controlled reactors (TCR) and it does not generate harmonic order distortions [xv-xvi]. A STATCOM model is connected to the 230KV transmission line for the improvement of transient stability and reactive power compensation of the system. This model is implemented with the help of PID controller along with feedback signals to control the firing angle of the converter [xvii]. STATCOM model is used for the power system improvement in [xviii-xix].A comparison is made between SVC and STATCOM of the same ratings for the shunt compensation and proves STATCOM gives better results [xx, xxi].

II.PROBLEM STATEMENT

Now a days demand of electricity is increased a lot due to this reason an existing electrical system is require transferring more power than its standard

ratings. This problem can be overcome by simply installing new transmission lines. But this solution is not a best solution. This solution obviously will increase the cost of the system and also will take much time for the installation. And another important factor which comes into existence is the environmental impacts of the transmission system which has to be installed. We have to provide other solutions for this problem.

Due to high demand of electricity voltage of the system decreases which will increase the demand of high current. High current will in return damage the transmission line conductors. And also the reactive power of the system will increase exponentially. Severe blackout happens due to these reasons in the past.

To maintain the reactive power balance in transmission line FACTS devices are installed. And amongst the FACTS devices STATCOM controllers provide better performance for system stability and reactive power compensation. STATCOM controllers provide leading and lagging reactive power, faster response time and improve transient stability of the system.

In this paper a 220KV transmission line known as Multan Samundri-1 transmission line is modeled in MATLAB/Simulink. The line already provided with capacitor banks for reactive power compensation which is an older technique. A STATCOM controller is implemented for this transmission line in MATLAB/Simulink. A comparison will be made between STATCOM response and capacitor bank response for reactive power compensation.

III. STATCOM

A STATCOM is one of the most promising devices for improvement of power system stability. STATCOM may have many topologies, for most practical applications it uses DC to AC converter also known as Voltage Source Inverter (VSI). A STATCOM mainly consists of Voltage Source Inverter, DC capacitor, link reactor and filter components.Voltage source inverter thyristors, MOSFETs or IGBTs. The essential hypothesis of VSI is to create an arrangement of contorllable 3-phase yield voltages/currents at the fundamental frequency of the AC line voltage from DC source voltage, for example, a charged capacitor or any DC energy supplying device. By adjusting the phase angle and magnitude of the output current and voltage, the system can provide active as well as reactive power between AC and DC buses, and stabilize AC bus voltage.

The performance of a STATCOM for reactive power compensation is directly related to the performance of VSI, and VSI is directly linked with the control techniques. Amongst many ways of controlling techniques of VSI pulse width modulation (PWM) and hysteresis current control are the famous ones.

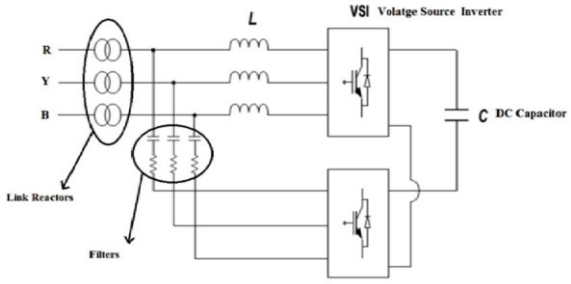

Fig. 1 Basic STATCOM Block

A. PWM STATCOM

PWM voltage control of STATCOM presents the control of three phase output voltage and phase angle with respect to the voltage of transmission line, thus controlling output current indirectly. In STATCOM PWM is done by comparing a high frequency triangular carrier wave with the sinusoidal waveform which in turn creates the desired gating pulses for the IGBTs. The gating signal just controls the switching of the VSI and exchange the active/ reactive power to the power system. There are many ways of generating the gate pulses. In this paper a control technique is developed for PWM for gating signals.

B. Control Block Methodology

The control signals of gate pulses are generated with the help of current computations. Figure 3 shows a single line diagram of current computations for the generation of gating pulses. The reference voltage V_s is multiplied with power factor angle and pass through a bandpass filter. V_{dc} is the DC bus voltage which subtracted from a reference voltage V_{dc*} and pass through a PID controller and generates the current I_{sm*}.

The unit vectors are used for wave shaping. Subtraction of PID controller current with source currents gives source reference currents(I_{sR*},I_{sY*},I_{sB*}). Subtraction of source reference currents with load currents(I_{LR},I_{LY},I_{LB}) gives the command currents (I_{cR*},I_{cY*},I_{cB*}). The difference resulting from I_{cR*},I_{cY*},$I_{cB*}$and I_{cR},I_{cY},I_{cB} pass through a low pass filter set at 10kHz.The output is the compare with the triangular carrier wave and produce sinusoidal PWM. SPWM is very effective for reducing switching losses of IGBTs.

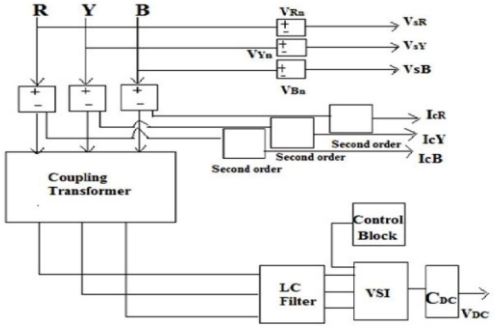

Fig. 2. STATCOM MATLAB Model

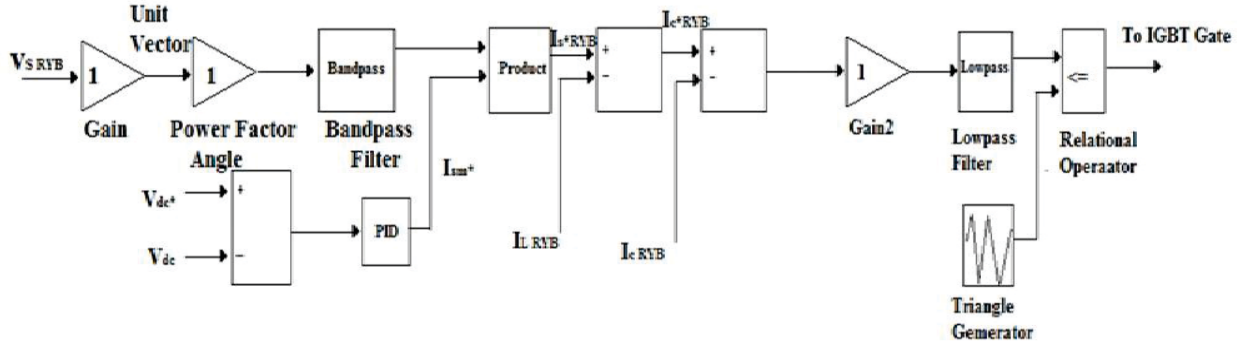

Fig. 3. Single Line Diagram of Control Methodology

C. Mathematical Modeling

The mathematical expressions for the control algorithm are given below.The equations for the three-phase Source Reference Currents (SRC) are given as:

$$I_{SR}^* = I_{sm}^* \times U_{SR} \tag{1}$$

$$I_{SY}^* = I_{sm}^* \times U_{SY} \tag{2}$$

$$I_{SB}^* = I_{sm}^* \times U_{SB} \tag{3}$$

Where,

$$U_{SR} = \frac{v_{RS}}{V_S} \tag{4}$$

$$U_{SY} = \frac{v_{SY}}{V_S} \tag{5}$$

$$U_{SB} = \frac{v_{SB}}{V_S} \tag{6}$$

Here v_{SR}, v_{SB} and v_{SB} are peak phase voltages. V_S is the peak source voltage it can be calculated as:

$$V_S = \frac{2}{3}\sqrt{v_{SR}^{\,2} + v_{SY}^{\,2} + v_{SB}^{\,2}} \tag{7}$$

The value of *SRC* (I^*_{sm}) is calculated through the PID controller. At nth instant the output of PID controller is given below:

$$Z_{0(n)} = Z_{0(n\text{-}1)} + K_{pdc}\{v_{dce(n)} - v_{dce(n\text{-}1)}\}K_{idc}\, v_{dce(n)} \tag{8}$$

$$Z_{0(n)} = I_{sm}^* \tag{9}$$

In equation (8) $K_{idc}K_{pdc}$ are considered to be the integral and proportional gains of PID controller. $v_{dce(n-1)}$ is the error signal and $Z_{0(n-1)}$ is the output of PID controller at instant (n - 1). vdce(n) is the DC error signal at the instant n .$Z_{0(n)}$ is the required output for calculating the SRC.

The DC error signal can be calculated by taking the difference between the reference DC voltage $v^*_{dc(n)}$ and the sensed DC voltage v_{dc} of DC bus capacitor.

$$v_{dce(n)} = v_{dc(n)}^* - v_{dc(n)} \tag{10}$$

After the calculation of *SRC* the difference between SRC and measured load currents yields the active filter currents as:

$$i_{CR}^* = i_{SR}^* - i_{lR} \tag{11}$$

$$i_{CY}^* = i_{SY}^* - i_{lY} \tag{12}$$

$$i_{CB}^* = i_{SB}^* - i_{lB} \tag{13}$$

The error Active Filter current is obtained by taking the difference of reference currents and the measured Active Filter current i.e.

$$i_{CRe} = i_{CR}^* - i_{CR} \tag{14}$$

$$i_{CYe} = i_{CY}^* - i_{CY} \tag{15}$$

$$i_{CBe} = i_{CB}^* - i_{CB} \tag{16}$$

The error currents of active filter will pass through a low pass filter and after that it is compared with carrier triangular wave of frequency 10 kHz then following things happen:

If,

i_{cRe} < carrier wave magnitude

{The upper Switch of IGBT is turned on}

Else if,

i_{cRe} > Carrier wave magnitude

{The lower switch of IGBT is turned off}

End.

D. System Under Study

A 220KV transmission line is taken into account. The line is installed in Multan and is known as Multan Samudri-1 transmission line. This system is implemented in MATLAB/Simulink program to study the STATCOM and capacitor behavior on the specified line. A single line diagram of the system is shown in figure 4. Two loads are connected to transmission system. One load is of 300MW and given the step of 0.2seconds and the other load is of 350MW and will connect after a 0.5 seconds interval. The behavior of

capacitor and STATCOM is studied when these two loads are connected to the system.

E. Simulation Results

The simulation results are represented by the Fig. 5-12. Initially the sytem shows its response before 0.2 second. After 0.2 second capacitor or STATCOM is connected to the system and after 0.5 second the other load is connected to the system and shows the system response. Figure 5 and figure 6 shows the voltage waveforms of capacitor and STATCOM. As shown in figures initially before 0.2 second the the system is unstable and there is no
sinusoidal response as the system requires some compensation. After 0.2 second when capacitor is connected to the system the system voltage stabilizes and become sinusoidal. After 0.5 second the voltage remains the

same as when the second load is connected to the system. So, voltage waveform is constant which shows that the system implemented is stable. When STATCOM is connected to the system it also shows the same response as in the case of capacitor it is because of the fact that the voltage have no influence on the reactive power which satisfies the condition of system's performance. The Fig. 7-8 shows the current waveforms of the system when capacitor and STATCOM are connected to the system. Figure 7 shows the reponse of capacitor. Initially before 0.2 second the system response is very unstable when capacitor is connected at 0.2 second the system currents requirement decreses as capacitor starts supplying the current.

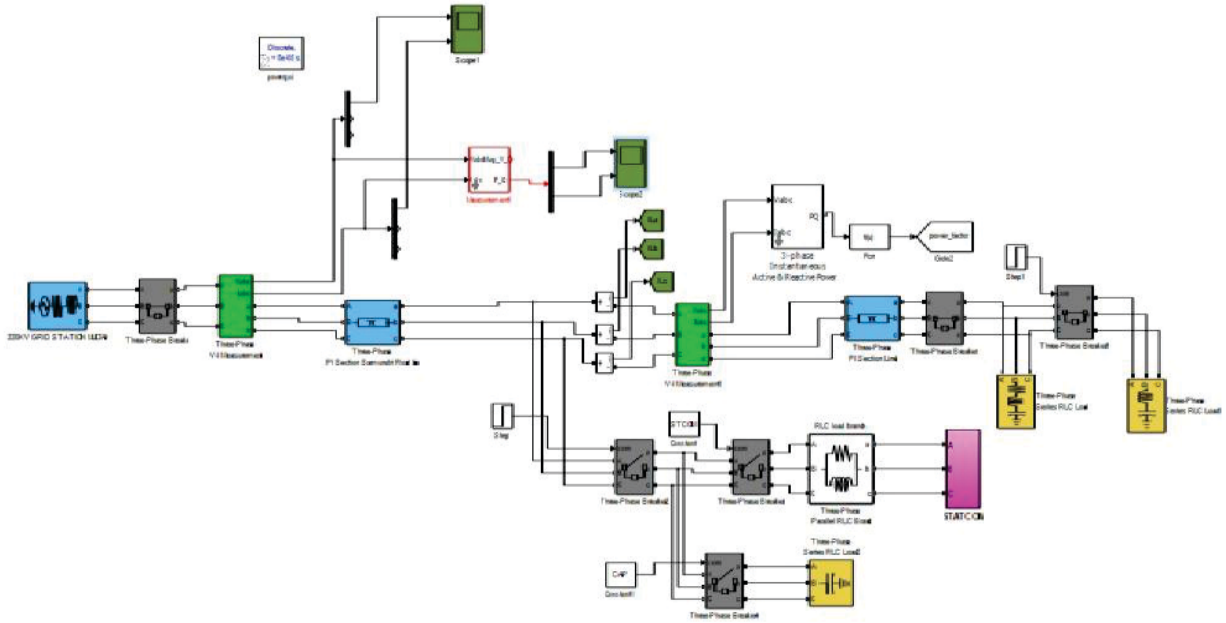

Fig. 4. MATLAB/Simulink Model of 220KV Transmission line with Capacitor and STATCOM Implementation

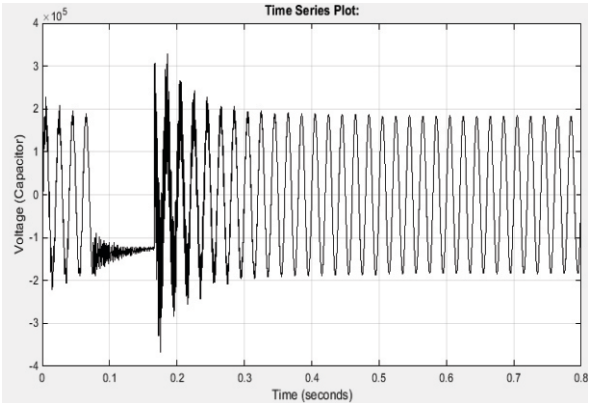

Fig. 5. Voltage of System when Capacitor is Connected

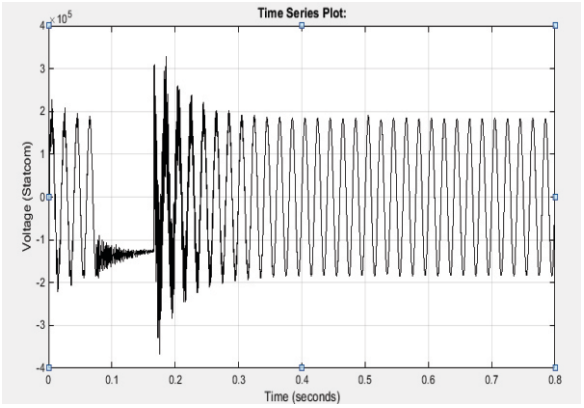

Fig. 6. Voltage of the System when STATCOM is connected

But when the second load is connected to the system at 0.5 second the system's current increses which in turn increase the reactive power of the system.

Fig. 8 shows the response of the STATCOM. At 0.2 second the STATCOM is connected to the system and STATCOM supplies the current. The wavform shows the response of the current waveform as the current requirement is decreased. At 0.5 second the other load is connected to the system which should increase the current demand of the system but it does not happen as the STATCOM supplies the current itself and the syetm's current requirement is decresed which shows that STATCOM stabilizes the system.

In Fig. 9-10 the active power of the system is shown when capacitor and STATCOM are connected the system under consideration.

As shown in Fig. 9-10 the active power remains the same for capacitor as well as for STATCOM. This shows that the system implemented is stable.

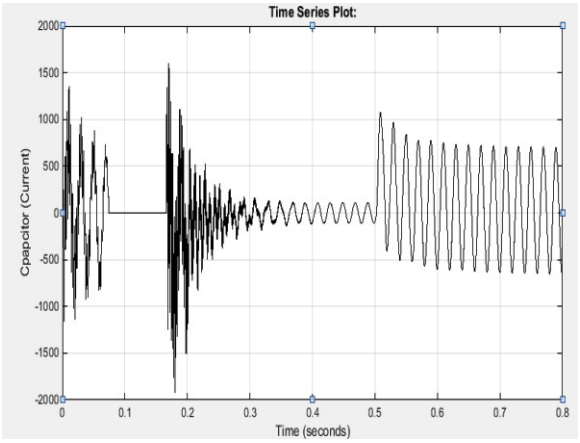

Fig. 7. Current of the System when Capacitor is Connected

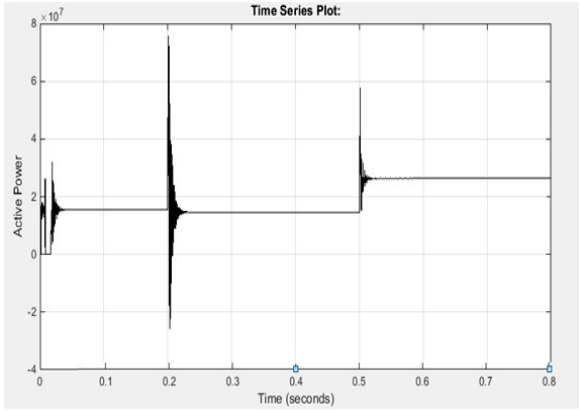

Fig. 8. Active Power of the System when Capacitor is Connected

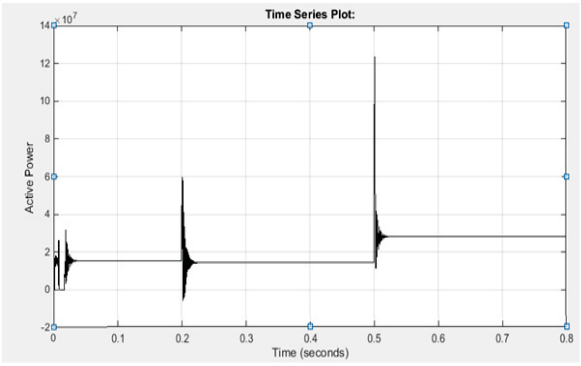

Fig. 9. Active Power of the System when STATCOM is Connected

Now the wavefoems of reactive power are shown in Fig. 11-12. As shown in Fig. 11 when capacitor is connected to the system at 0.2 second the capacitor compensates the system's reactive power. But when the second three phase load is connected to the system at 0.5 second the system's reactive power increases as the capacitor is not suitable for variable loads. Capacitor shows the disadvantage of fixed compensation in this case. So, capacitor will never be used for variable loads.

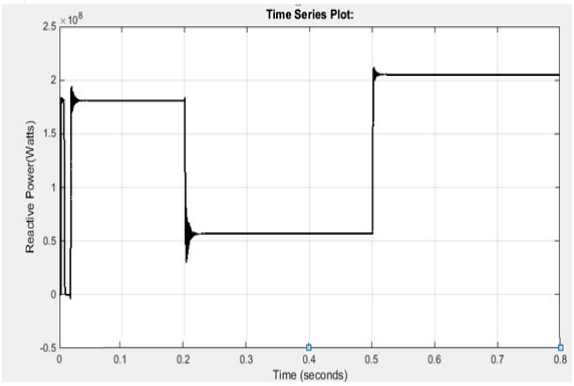

Fig. 10. Reactive Power of System when capacitor is connected

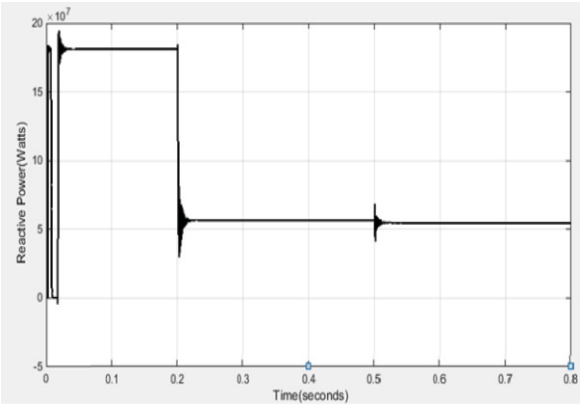

Fig. 11. Reactive Power of System when STATCOM is connected

Fig. 12 shows the response of reactive power when STATCOM is connected to the system at 0.2 second. After 0.2 second the STATCOM compensates the reactive power of the system and decreases the reactive power demand of the system. When the second load is connected to the system at 0.5 second the STATCOM try to reduce the reactive power demand of the system again. And the reactive power of the system remains nearly constant for both the loads as STATCOM is used for variable loads. So these results shows that the STATCOM is the best device for reactive power control and system stability.

IV. CONCLUSIONS

The results of simulation revealed that a STATCOM behaves better in reducing harmonics as compared to existing installed capacitor in the transmission system. The voltage and current waveforms also indicate that a STATCOM is better in maintaining the system's current and voltage sinusoidal waveforms. Moreover, the result of active power show that the system implemented is stable and provides better voltage regulations. From our results of all available waveforms, we can conclude that the STATCOM is the best choice for the reactive power compensation and power system stability for the transmission line under study. And furthermore, STATCOM can be implemented to the other transmission lines having the problem of reactive power compensation.

APPENDIX

Two Loads: Active Power: 300 MW and 350 Mw, Freq: 50 Hz, Phase to Phase Nominal voltage **Transmission Line:**220KV, Line Length 196Km, Conductor ACSR(Zebra), Positive Sequence Impedance (0.06774 + j0.40211) Ω/km, Zero Sequence Impedance (0.22623 + j1.1653) Ω/km, Positive Sequence Resistance (0.0677 Ω/km),Zero Sequence resistance (0.22623 Ω/km)Positive Sequence Inductance (1.28 mH/km), Zero sequence Inductance (3.709 mH/km), Positive Sequence Capacitance (12.74 nF/km),Zero Sequence Capacitance (7.751 nF/km)
STATCOM Parameter: 220KV, $\pm$150MVAR, R=0.3 , L= 0.33, C_{dc}=300 mF, V_{dc}= 2.5KV , V_{ref} =1.0

REFERENCES

[I] P. Suman, P. Kumar , N. Vijaysimha and C. B. Saravanan " Static Synchronous Series Compensator for series compensation of EHV transmission line," International Journal of Advanced Research in Electrical, Electronics and Instrumentation Engineering Vol. 2, Issue 7, Jul. 2013

[ii] G.Andersson, P. Donalek, R. Farmer, N. Hatziargyriou, I. Kamwa, P. Kundur, N. Martins, J. Paserba, P. Pourbeik, J. Sanchez-Gasca, R. Schulz, A. Stankovic, C. Taylor and V. Vittal"Causes of the 2003 major grid blackouts in North America and Europe and recommended means to improve system dynamic performance," Power systems, IEEE Trans. on Power Syst., Vol.20, pp.1922-1928, Nov. 2005

[iii] M.D.Ilic , E.H.Allen , J.W.Chapman , C. A. King , J. H. Lang and E. Litvinov, "Preventing future blackouts by means of Enhanced Electric Power Systems Control: From complexity of order," Proc. of the IEEE , Vol. 93, pp 1920-1941, Nov. 2005

[iv] M.Yagami, S.Shibata, T.Murata and J.Tamura, "Improvement of power system transient stability by superconducting fault current limiter," in Transmission and Distribution Conference and Exhibition 2002: Asia Pacific. IEEE/PES, vol.1 pp. 359-364, Oct. 6-10, 2002.

[v] M. Sjostrom, R. Cherkaoui and B. Dutoit, "Enhancement of power system transient stability using superconducting fault current limiters," Applied Superconductivity, IEEE Trans. on App. Supercond. , vol.9, pp.1328-1330, Jun. 1999.

[vi] M. Ebadian and M. Alizadeh, "Improvement of power system transient stability using Fault Current Limiter and Thyristor Controlled Braking Resistor," in Int. Conf. on Electric Power and Energy Conv. Syst., EPECS, Sharjah, pp. 1-6, Nov. 10-12, 2009

[vii] C. T. Hsu, "Enhancement of Transient Stability of an Industrial Cogeneration System with Superconducting Magnetic Energy Storage Unit," Power Engg. Review, IEEE, vol. 22, pp. 63, Aug.2002.

[viii] T. Y. Lin and W. Youyi, "Stability enhancement using SMES and robust nonlinear control," Energy Management and Power Delivery, Proc. of EMPD Int. Conf. , vol.1. , pp. 171-176 Mar. 1998

[ix] A. Abu-Siada and S. Islam, "Application of SMES Unit in Improving the Performance of an AC/DC Power System," IEEE Trans. Sustain. Energy, vol. 2, pp. 109-121, Mar. 2011

[x] M. Karthikeyan and P. Ajay-D-Vimalraj " Optimal location of shunt FACTS devices for power flow control," IEEE proc. Int. Conf. on Emerging Trends in Electrical and Computer Technology (ICETECT) , pp154-159, Tamil Nadu, Mar. 23-24, 2011

[xi] J. Dixon, L. Moran, J. Rodriguez and R. Domke, "Reactive Power Compensation Technologies, State-of-the-Art Review,"

Proc. of IEEE, Vol. 93, Issue 12, pp 2144-2164, Dec. 2005

[xii] M. Kowsalya, K. K. Ray and D. P. Kothari," Positioning of SVC and STATCOM in a long transmission line," International Journal of Recent Trend in Engg., Vol.2, No. 5, Nov. 2009.

[xiii] V. K. Chandrakar and A. G. Kothari, "Optimal Location for Line Compensation by Shunt Connected FACTS Controller," The fifth Int. Conf. on Power Electronics and Drive Systems, Vol.1, pp 151-156, Nov. 17-20, 2003

[xiv] SCADA growing in Power Transmission and Distribution, 2011. www.automation.com

[xv] A. F. Abdou, A. Abu-Siada and H. R. Pota, "Application of a STATCOM for Damping Subsynchronous Oscillations and Transient Stability Improvement," AUPEC conf. Brisbane, Australia, Sept. 25-28, 2011.

[xvi] A. M. S. Yunus, A. Abu-Siada and M. A. S. Masoum, "Application of STATCOM to Improve the Low-Voltage-Ride-Through Capability of Type-D Wind Turbine Generator," IEEE Innovation Smart Grid Technologies conf., Perth, Nov. 13-16, 2011

[xvii] A. Pahade and N. Saxena "Transient stability improvement by using shunt FACT device (STATCOM)with Reference Voltage Compensation (RVC) control scheme,"International Journal of Electrical, Electronics and Computer Engg. Vol.2 , Issue 1, pp 7-12, Jan. 2013,

[xviii] L. M. Castro, E. Ache and C. R. Fuertes-Esquivel "A Novel Statcom Model for Dynamic Power System Simulations,"IEEE power syst. , vol. 28, no. 3, Aug. 2013

[xix] K. Li, J. Liu, Z. Wang and B. Wei "Strategies And Operating Point Optimization Of Statcom Control For Voltage Unbalance Mitigation In Three-Phase Three-Wire Systems," IEEE Trans. on Power Delivery ,Vol 22, pp 413–422, Jan. 2007

[xx] M. Kowsalya, K. K. Ray and D. P. Kothari, "Positioning of SVC and STATCOM in a Long Transmission Line" International Journal of Recent Trends in Engineering, Vol. 2, No. 5, Nov. 2009.

[xxi] Y.L. Tan, "Analysis of line compensation by shunt connected FACTS controllers: a comparison between SVC and STATCOM", IEEE Trans. on Power Engg. Review, Vol.19 , pp 57-58, Aug. 1999

[xxii] N. Agashe, R. D. Kulkarni and A.R.Thorat "Simulation Study for Reactive Power Compensation Using STATCOM, " International Journal of Advanced Research in Electrical, Electronics and Instrumentation Engg., Vol. 4, Issue 6, Jun. 2015

[xxiii] P. K. Mani and K.S.Naidu "Simulation and hardware implementation of STATCOM dynamic voltagerestorer (s-d) device," ARPN Journal of Engg. and App. Sciences Vol. 11, No. 2, Jan. 2016

Section C

MECHANICAL/INDUSTRIAL/ MATERIAL/ENERGY ENGG. AND ENGINEERING MANAGEMENT

Design of Mini PLC based on PIC18F452 Microcontroller using Concepts of Graceful Degradation

M. Asif[1], A. Raza[2], A. Sultan[3], F. Malik[4]

[1,3,4]Mechatronics Engineering Department, University of Engineering and Technology Taxila, Pakistan
[2]Mechatronics & Control Engineering Department , University of Engineering and Technology Lahore, Pakistan
[1]asifscara@gmail.com

***Abstract*—** Programmable logic controllers (PLCs) which are able to interact with peripherals play a key role as a controlling unit in most of the industries now a day. Main objective of this research is to design a PIC18F452 microcontroller based low cost mini PLC which is gracefully degrading to support ladder logic programming language- one of the programming languages of standard IEC61131-3. A compiler with selected features has been designed in C# language. An operating system of the microcontroller of this mini PLC has also been designed in C language. To interface programming device and mini PLC, USB to RS232 communication protocol has been used. It is easy to envision the scheme of wiring, power supply, input & output channels, microcontroller, circuits of optical isolators etc. in the mini PLC thereby providing the students a platform to understand the internal architecture of most of the PLC systems.

***Keywords*—** Mini PLC, Graceful Degradation, Redundant, Robust, Ladder Logic Compiler, Operating System

I. INTRODUCTION

Programmable Logic Controller (PLC) is a controlling device having different number of inputs/outputs (I/Os). PLC is specially designed to control a typical process or a machine. Programmable logic controllers were initially introduced to replace the conventional relay based circuits. Now these are extensively used for the implementation of systems based on logic, arithmetic, sequencing, timing, and counting [i].

According to the number of inputs/outputs, PLC market can be classified into the five groups as Fig. 1 illustrates [ii].

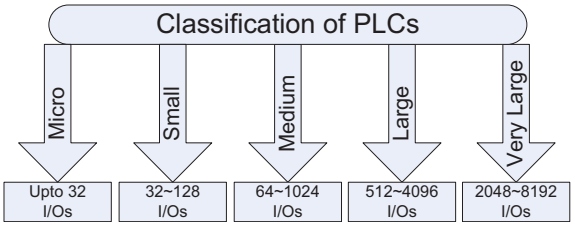

Fig. 1. PLC grouping according to I/Os.

PLCs are available in different configurations even from the same vendor. Some of the most essential & common components of a PLC are power supply, central processing unit, input/output channels, & indicator lights [iii].

Different environments of programming & debugging, addressing methods, structures of grammar etc. lead to the incompatibility and issues in use as a teaching tool at the university. International Electro-technical Commission (IEC) published the standard IEC61131-3 in 1999 which offers a uniform criterion for the manufacturers of PLCs [iv]. This standard offers the graphical and textual programming languages. Graphical programming includes ladder logic diagram, functional block diagram, & sequential function charts while text programming includes structured text & instruction list [v].

Ladder diagram is easy to understand and mostly used for programming the PLCs. It defines the instructions such as logic/Boolean and switching operations [vi]. Microsoft Visual Studio 2012 has been used to develop the ladder logic editor. On compilation of editor, it provides a text file of alphanumeric code which is sent to microcontroller of the mini PLC [vii]. The operating system of the mini PLC based on PIC18F452 microcontroller has been developed in C language [viii].

Graceful degradation/fault tolerance is the property of the system that enables it to continue functioning even in case of failure for one or more of its components. Graceful degradation occurs due to interaction of 3 aspects of system design i.e., hardware, software, and human interface between hardware & software. Graceful degradation improves the reliability of systems by increasing the robustness & redundancy [ix].

Capability of systems to resist the changes or disturbances is referred as robustness. Robust systems stablize their original configuration when subject to any change. Systems or parts of systems are designed efficiently to tackle the disturbance and noise [x].

Duplication of different functions or components of the system is termed as redundancy. It increases reliability of systems by providing backup or fail-safe capabilities. Redundant systems possess the ability to switch to other components/functions of system to exhibit the same feature in case of certain failure [xi].

Redundancy of 1st order has been incorporated in this mini PLC.

Some of the features of the microcontroller used for the mini PLC have been described here. Microcontroller is being operated at 5V DC and at a frequency of 4 MHz by using external ceramic capacitors of value 15pF each. It has the current sink/source capability 25mA/25mA. It has three external interrupt pins with a feature of assigning a high or low priority level. It contains the timers named as: Timer0 module: 8-bit/16-bit timer/counter with 8-bit programmable prescaler; Timer1 module: 16-bit timer/counter; Timer2 module: 8-bit timer/counter with 8-bit period register (time-base for PWM); Timer3 module: 16-bit timer/counter. Two of the timers have been used as timers and one as counter in the ladder logic programming. The microcontroller has compatible 10-bit Analog-to-Digital (A/D) Converter module [xii].

The PLCs work in different phases of input scanning, logical solving, and output scanning. In input scanning, it takes the data from sensors to send it to memory of the processor of the PLC. Then processor logically solves all the problems to issue the commands to the actuators. In output scanning, actuators perform accordingly [iii].

II. Methodology

A. Design of Hardware

Figure 2 shows the complete diagram of the mini PLC. Physical size of the mini PLC is (4.25″ x 4.25″ x 4.25″). Push buttons, toggle switches, indicators, and female connectors with internal diameter of 3mm & 1mm have been shown at the top of the mini PLC. To display the status of mini PLC working, LCD (liquid crystal display) has been installed at the top of the mini PLC. A relay control board is also shown at left side of the Fig. 2. A DC motor control experiment is being tested on the mini PLC.

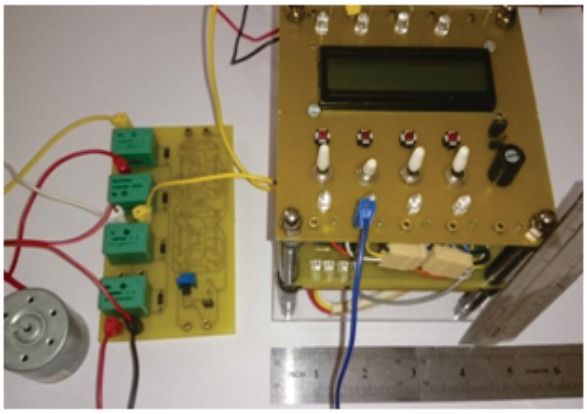

Fig. 2. Mini PLC.

System diagram of the mini PLC is shown in Fig. 3. Input module, output module, central processing unit, power supply, and programming device are shown here.

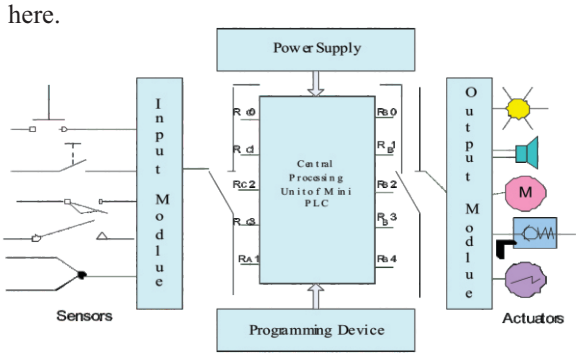

Fig. 3. Block diagram of the mini PLC.

First “4” pins of Port “C” of microcontroller are used as digital inputs, first pin of Port “A” of microcontroller is used to take analog input from the sensors and first “5” pins of Port “B” are used as digital output pins.

i) Controlling Unit

The controlling unit of the mini PLC comprises microcontroller inserted on ZIF (zero insertion force) socket, connecting pins & cables, power indicator, and crystal oscillator.

ii) I/O Section

Circuits of power section, optical isolation, input & output module, automatic power shut down system, and power feedback are shown in Fig. 4.

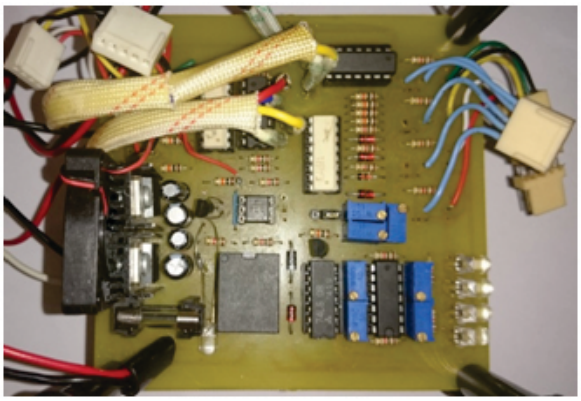

Fig. 4. I/O section of the mini PLC

This board has “5” I/O (out of 5, 4 are digital inputs, 1 is analog input, and 5 digital outputs) channels. I/O channels are optically isolated through optocoupler TLP523-4.

Initially, ladder logic code is developed in ladder logic editor and after compilation the result is sent to the microcontroller. The microcontroller will read the data and solve for the required output to send to the actuators at the output module of the mini PLC. Working of mini PLC is explained in Fig. 5.

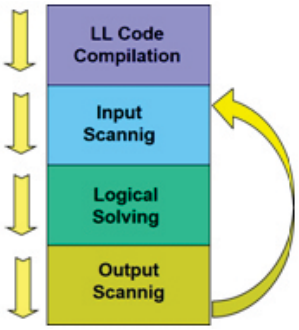

Fig. 5. Working of the mini PLC

iii) Power Source & its Feedback System

Power supply of 5V DC & 24V DC is used for microcontroller & I/O module respectively. Microcontroller is optically isolated from the transducers making both the power sources independent of each other.

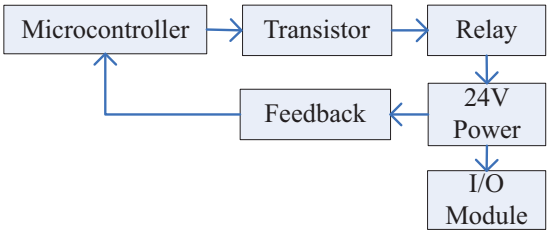

Fig. 6. Power source with feedback.

To avoid the manual troubleshooting in case of power failure of 24V DC power supply of transducers, a power feedback system has been developed. In this system, microcontroller is capable to automatically troubleshoot and take the corresponding action.

iv) Gracefully Degrading Design

Graceful degradation has been implemented in context of redundancy & robustness to improve the reliability of the system.

a. Redundancy of Zener diodes

Zener diodes work as zener in reverse bias and are used to regulate the voltage values [xiii]. Zener diodes have been duplicated at I/O module.

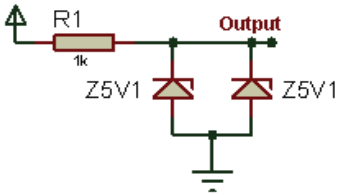

Fig. 7. Redundancy of zener diodes.

These zener diodes are used to provide constant values of 5V and 24V at different nodes of the circuits of mini PLC. In case of open circuit failure of one zener, the other zener will be conducting, providing constant voltage where required.

b. Redundancy of optical isolators

Like Zener diodes, optical isolators have also been duplicated in the mini PLC. It has been tested through switches and shows that signal will adopt the alternative path in case of open circuit failure of one IR LED of optical isolator. Fig. 8 shows redundancy of IR LEDs.

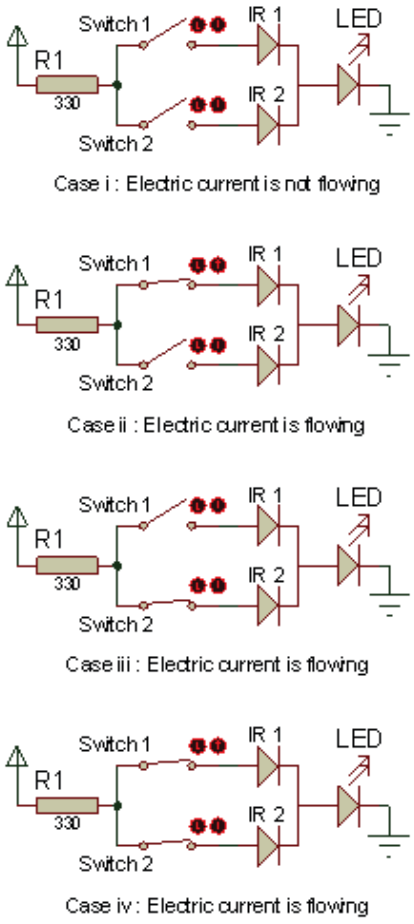

Fig. 8. Redundancy of IR LEDs.

Figure 9 shows overall working of optoisolator being redundant. IR LEDs will work fine when redundant but phototransistor will be fail-safe. Phototransistor/s of the corresponding IR LED/s will be in saturation or in cutoff mode.

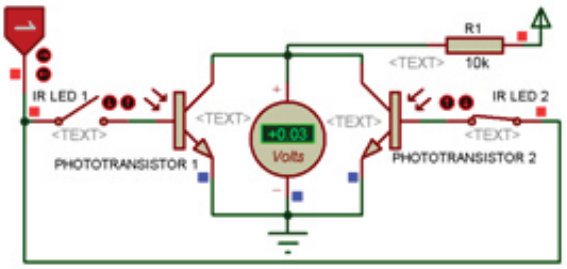

Fig. 9. Redundancy of optoisolator.

c. Robustness

The leads of the components like transistors, zener diodes etc. have been used as long as it possible to save the components from thermal effects. The long leads increase the metallic area of the components thereby increasing the heat sinking capability. A lot of electronic components exist e.g. BJTs in plastic package which are heat sensitive but there is no space/option to attach heat sinks on them. Components used in metal packages also provide robustness to the system.

In the circuit of mini PLC, relay has been used to switch ON/OFF the power of sensors and actuators. The coil of relay is made fail-safe using the circuit of back EMF (electro motive force) eliminator. Applying the fuse is common to most of the circuits. Referring to Fig. 10, a capacitor C_4 is used to avoid voltage fluctuations and zener diode D_3 is used to regulate the voltage at the coil terminal. If LEDs D_{24}, D_{25} will glow, it indicates the successful operation and switching ON the power of sensors and actuators.

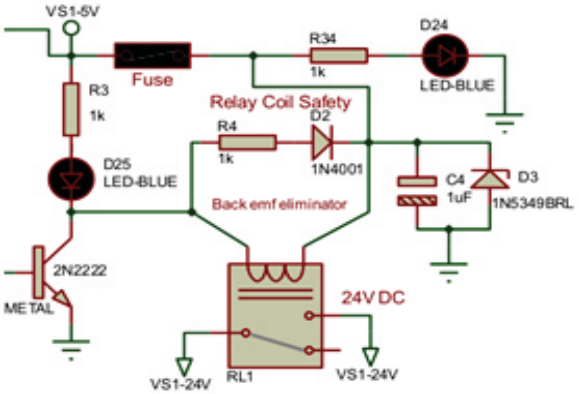

Fig. 10. Robust circuit for relay.

Fans and heat sinks are also used to avoid the components from thermal effects. A small fan of 5V DC has been incorporated to provide cooling to the electronic components of the mini PLC. It is located near the voltage regulator of power supply circuit. Voltage regulators are continuously performing the functions of input & output load regulations, therefore they may heat up due to increase of load current.

B. Design of software

To interface the mini PLC hardware, a software platform is required. This software allows editing and compiling ladder logic programming. Microsoft Visual Studio 2012 has been used to develop the graphical user interface for ladder logic editing.

i) Ladder logic editor

Using Microsoft Visual Studio 2012, the ladder logic editor has been developed in C# language. Fig. 11 shows the main window of the software. It contains the symbols of NO (normally open), NC (normally closed), branches, wire, timers, counters, analog input. All these symbols are given at the left side of the ladder logic editor.

Compiled output of alphanumeric code can be visualized at the right side of Fig. 11. User can also write comments/working of ladder logic code in the window of compiled output.

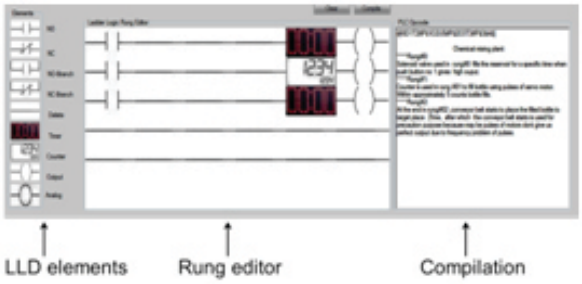

Fig. 11. Ladder logic editor.

ii) Ladder logic simulator

It is illustrated in Fig. 12, simulation of ladder logic compiler. The simulation has been prepared in Proteus v7.8 [xiv] with the hex file loaded into the microcontroller of the mini PLC.

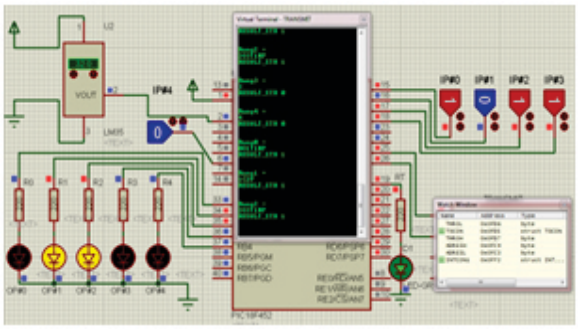

Fig. 12. Ladder logic simulator.

C. Operating the mini PLC

Check to ensure that all the wires and connections are in proper order. After receiving a signal of power feedback circuit, microcontroller of the mini PLC would power up the circuits of input/output module. Build code in the ladder logic editor using required number of rungs. Perform the compilation of ladder logic code. Now send the alphanumeric code produced to the microcontroller of mini PLC developed.

After receiving alphanumeric code, safety conditions would be checked by the mini PLC. Now mini PLC shall wait for the inputs from different sensors according to ladder logic code. All the functions would be performed through output modules after logical solving by the microcontroller.

III. Experimentations

Different experiments performed on the mini PLC designed are given here.

A. Handling the graceful degradation for the increased

voltage signal at inputs and outputs of the mini PLC

Purpose of this experiment is to gracefully degrade the exceeded voltage at inputs & outputs of mini PLC by using circuits of zener diode. Zener diode operates in the reverse bias mode & starts to conduct at nominal value of voltage as shown inFig. 13.

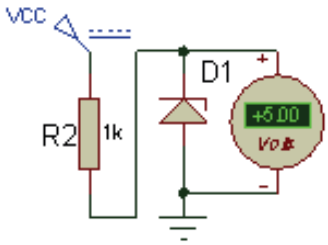

Fig. 13. Handling the graceful degradation.

B. Switching off input signal at infrared LED of optoisolators in case of exceeded voltage at the input of mini PLC

This circuit has been made by using voltage comparator along with AND gate logic IC. Voltage signal of the value 8V has been fixed as a reference voltage by using combination of resistors at inputs. The signal is then fed at negative terminal of gates of voltage comparator IC. All positive terminals of each gate of voltage comparator IC are fixed with values of "8.1V", "8.3V", "8.5V", & "8.7V".

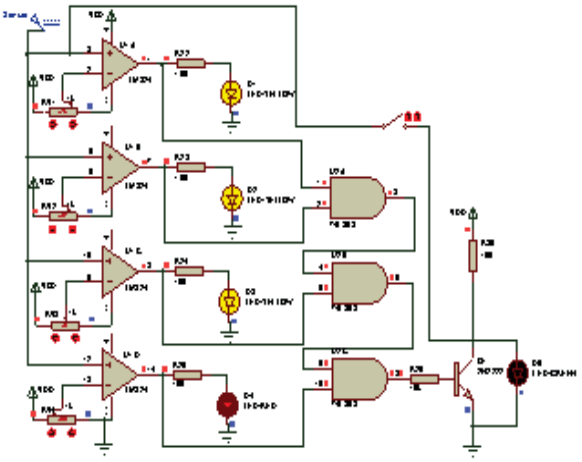

Fig. 14. Automatic power shut down circuit

When input voltage will exceed 24V, the 8V signal will start to increase and at the value of 8.1V, 1st yellow LED will start to glow. At 8.3V, the 2nd LED will start to glow and so on. All "4" outputs received due to increased voltage level will be given as inputs to AND gate. The output will become high when all inputs are high. High signal will switch the transistor into saturation mode giving zero volts at the input module.

C. Implementation of the ladder logic branching

In this experiment, the implementation of ladder logic branch using one branch has been shown in Fig. 15.

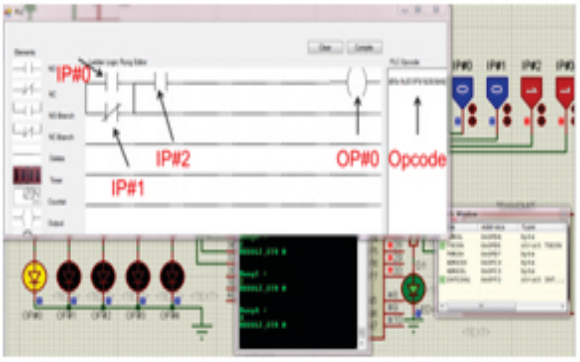

Fig. 15. Ladder logic branching.

D. Measurement of temperature using analog input channel

The experiment is designed to measure & control the temperature of room. The sensor LM-35 used here has a resolution of 10mV/ C°. Thermostat control has been implemented. Threshold value of thermostat is 25°C. Fan will be ON when temperature goes above 25°C & is shown in Fig. 16. Similarly fan will be OFF when the temperature goes below 25C°.

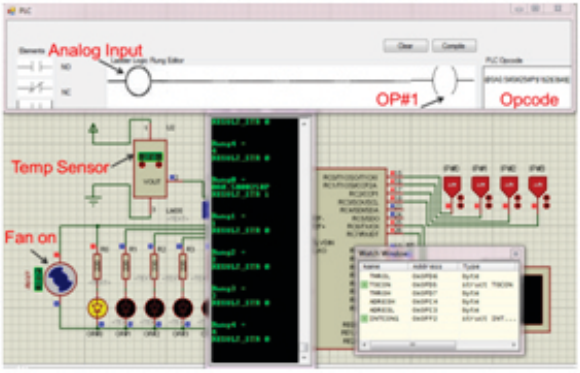

Fig. 16. Temperature control fan switched ON.

IV. Results

The property of graceful degradation offers the systems a capability to stablize on its own. PLC systems having ability of graceful degradation continue to perform rather than failing completely when faults occur in the system.

Redundancy of zener diodes and optical isolators enabled the mini PLC to remain in fail-safe mode due to open circuit failure mode. Statistical review of open circuit failure mode in Table I, shows, the probability is 0.75 for the electric signals of transducers at digital channels to flow even in case of failure.

TABLE I
STATISTICAL DATA ON REDUNDANCY

Binary Data	Cases	Best Cases	Worst Case	Redundancy order	Probability
$2^0 = 1$	2	1	1	0^{th}	0.50
$2^1 = 2$	4	3	1	1^{st}	0.75

Zener diodes are capable to bear the increased value of voltage signal and provide regulated voltage as an output. Redundancy of zener provides an alternative path to the signal in case of open circuit failure mode.

Using this mini PLC, students of the university have tested the sensors (PT-100 RTD, LM-35 temperature sensor, limit switch, proximity sensor, tilt sensor, LDR, and IR sensor etc.) and actuators (DC motor, DC servo motor, pumps, SOVs,) in different projects.

The power section with feedback circuit works successfully in circuit hardware thereby avoiding the operator effort for troubleshooting in case of power failure. When there is a failure of power, operator has to trace out where problem was occurred & will find the solution accordingly. After incorporating the circuit, the corresponding actions have been taken by microcontroller of mini PLC and if required, specific problems may be communicated to the user.

Automatic power shut down circuit successfully switched off the sensor input at the input module. When voltage signal increased to 24.5 V, 1^{st} yellow LED started to glow, 2^{nd} yellow LED started to glow at 25, 3^{rd} yellow started to glow at 25.5 V. Finally at 26 V, 4^{th} LED (red) started to glow and switch off the signal through microcontroller at input module.

The basic logic gates including NOT gate, OR gate, AND gate, & X-OR gate have been tested on this mini PLC. Operating system & hardware showed the successful results.

The slope equation i.e., $y=mx+c$ has been programmed into the microcontroller of mini PLC. A threshold value is required to get high or low output accordingly e.g. a threshold value of 25°C has been shown in Fig. 17.

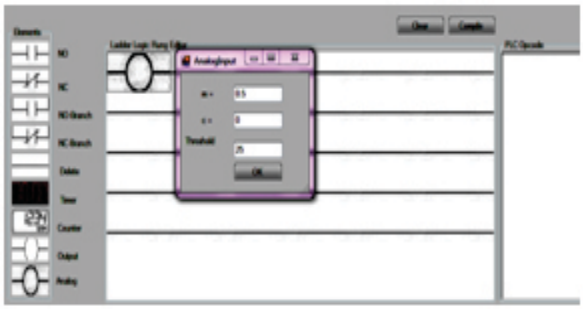

Fig. 17. Analog input editing.

Operator would enter the values of parameters into this equation to obtain the required output.

The results of temperature measurement using LM-35 temperature sensor have been shown in Fig. 18.

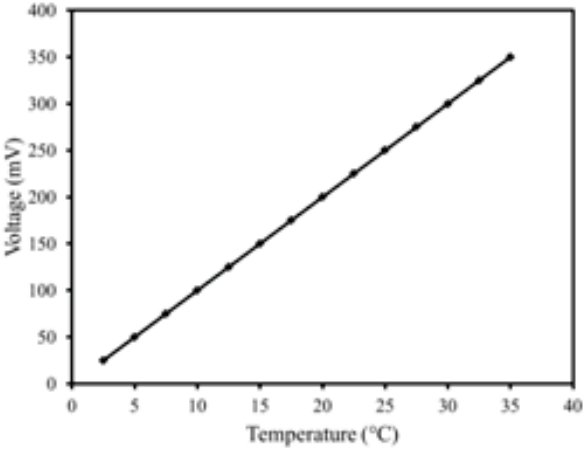

Fig. 18. Temperature Vs Voltage plot of thermostat.

V. CONCLUSIONS

It has been observed that the mini PLC gracefully degrades the electrical noise in such a way that it remained functional even when voltage signal was increased from 24V~26V DC at the input/output of the mini PLC.

Graceful degradation enhanced the reliability of the mini PLC by implementing redundant and robust circuits. Redundancy of optical isolators and zener diodes in the mini PLC provided the alternative path to the electrical signals in case of open circuit failure mode. Probability of biasing the digital electric signals is 0.75 by means of redundancy of 1^{st} order. Without redundancy, probability is 0.50 to bias the digital electric signals. Robust circuit of relay is able to oppose the voltage over flow & fluctuations due to zener & capacitor circuitry respectively.

Power feedback system provided a capability to the mini PLC to automatically troubleshoot the possible faults in case of power failure. Voltage signals of 5V, 12V, and 24V were successfully sent to corresponding electronic components and also checked through power feedback system.

Students are using this mini PLC at Department of Mechatronics Engineering UET Taxila, Sub-campus Chakwal in "Robotics and Automation Lab". During and after the practice they found it useful due to user friendly ladder logic editor, low cost hardware, and easy troubleshooting.

Short circuit failure mode for the said electronic components may be considered in future study. Using the same schematic & programming approach, input and output channels can be increased. If we have a team of engineers, a PLC can be developed to present to industry locally meeting the requirements. The

successful team effort having well defined goals may lead Pakistan to become a gracefully degrading PLC manufacturer.

Availability of persons for installation/ maintenance/ troubleshooting/ repairing within Pakistan may provide ease to the industries. This mini PLC being low cost provides the greater productivity and avoids the shipping charges.

REFERENCES

[i] W. Bolten, "Programmable Logic Controllers", ISBN-10: 0-7506-8112-8, 4th Edition, Elsevier, 2006, pp. 2-3.

[ii] L. A Bryan, E. A. Bryan "*Programmable Controllers, Theory and Implementation*", ISBN 0-944107-32-X, 2nd Edition, Industrial Text and Video Company, 1997, pp. 10–23.

[iii] H. Jack. (2010, April 15). *Automating Manufacturing Systems with PLCs.* [Online]. Available: http://engineeronadisk.com/book_plc.

[iv] J. Huang, Y. LI, W. LUO, X. LIU, K. NAN "The design of new-type PLC based on IEC61131-3," in *Proc. ICMLC* in IEEE, 2003, pp.809-813.

[v] J. Huang, Y. LI, W. LUO, X. LIU, K. NAN"An Open Source IEC 61131-3 Integrated Development", in IEEE, Vienna, 2007, pp.183-187.

[vi] M. A. Murti, A. N. Jati, L. Mawardi, and Siti A. N. F. Agustina "Software Architecture of Ladder Compiler to Opcode for Micro PLC Based on ARM Cortex Processor", in JOACE, 2014, pp.363-366.

[vii] F. Y. S. Siang "Ladder Logic Editor for Programmable Logic Controller (PLC)", Electrical-Electronics, Universiti Teknologi Malaysia, Malaysia 2012.

[viii] M. E. Rida, F. Liu, and Y. Jadi, "Design Mini-PLC based on ATxmega256A3U-AU Microcontroller," in ISEEE, Sapporo, 2014, pp.1034-1037.

[ix] Dr. J. E. Czarnecki, COL. K. T. Chamberlain "Graceful Degradation: A C2 Design Virtue for Our Times", in ICCRTS, Alexandria, 2013.

[x] Richard C. Dorf, Robert H. Bishop "*Modern Control Systems",* ISBN 978-93-325-1862-9, 12th Edition, Pearson, 2014, pp. 936-937.

[xi] W. Nace, P. Koopman "A Product Family Approach to Graceful Degradation", in Springer, 2001, pp.131-140.

[xii] Microchip Technology Inc. (2006), Data sheet PIC 18FXX2 Microcontroller. [Online]. Available: "ww1.microchip.com/downloads/en/.../39564c.pdf".

[xiii] T. L. Floyd "*Electronic Devices, Conventional Current Version"*, ISBN: 81-7758-354-9, 6th Edition, Pearson, 2006, pp. 110–111.

[xiv] Labcenter electronics, Proteus v7.8. [Online]. Available: http://www.labcenter.com/index.cfm

Design and Analysis of Packed Bed Activated Carbon Reactor for the Enrichment of Biogas

M. Farooq[1], A. Qamar[2], M. Asim[3], F. A. Siddiqui[4], M. Amjad[5], A. Yousaf[6]

[1,2,5]Mechanical Engineering Department, University of Engineering & Technology Lahore, Pakistan KSK Campus
[4]Mechanical Engineering Department, Bahauddin Zakariya University Multan, Pakistan
[3,6]Mechanical Engineering Department, University of Engineering & Technology Lahore, Pakistan
[1]engr.farooq@uet.edu.pk

Abstract- Biogas produced by anaerobic digestion of organic matters has reasonable potential to replace natural gas need of the world energy consumption. According to the UK National Non-Food Crops Centre (NNFCC), the anaerobic digestion (AD) industry experienced rapid growth in recent years. Thus, there is an increasing demand for the enriched biogas, to be used as vehicle fuel or injected to the natural gas grid. Since a typical biogas contains 50-65% methane, 30-45% carbon dioxide, 1000 - 10,000 ppm hydrogen sulphide, the removal of carbon di-oxide and hydrogen sulphide is required for upgrading the biogas. A number of methods exist for enriching biogas including water scrubbing system, membrane separation, chemical absorption, cryogenic separation and physical adsorption. Among these methods, adsorption by activated carbons (AC) is considered as an efficient and economical approach. The uniqueness of the activated carbon as adsorbents is due to their high surface area, developed pore volume and surface properties. Accordingly, this research has been focused on adsorption of activated carbon. An activated carbon packed-bed reactor designed and commissioned at laboratory scale. Biogas mixture passed through the packed bed reactor and benchmarked against the Standard Industrial Activated Carbon (SIAC). Break through curves were used to assess the adsorption capacities. It is envisioned that this method can transform the enrichment of bio-gas for power generation systems. The results obtained from the current research could be utilized as a guide for the further design and operation of the industrial system.

Keywords- Biogas, Packed Bed Reactor, Physical Adsorption, Standard Industrial Activated Carbon.

I. INTRODUCTION

AD is the biological treatment of biodegradable organic waste in the absence of oxygen, utilizing microbial activity to break down the waste in a controlled environment [i]. The AD of organic material basically takes place in four steps, namely hydrolysis, acidogenesis, acetogenesis and methanogenesis as shown in Fig. 1 [ii].

There is an increasing local interest in the use of biogas as an alternative to fossil fuels, and hence, there has been a steady increase in the renewable power derived from anaerobic digestion system.

An exponential growth in the world's population and rapid economic development has led to a tremendous demand for energy [iii-vii]. Fossil fuels are currently the main energy source for this global energy demand [viii-ix]. However, the reserves of fossil fuels are limited and often placed in geo-political challenged locations [x-xi]. Also negative environmental effects of using fossil fuels include acid rain, ozone layer depletion and global climate change [xii-xvi]. The result has been a rapid growth in the level of greenhouse gas emissions and an increase in fuel prices, which are the main driving forces behind efforts to utilise renewable energy sources [xvii-xviii].

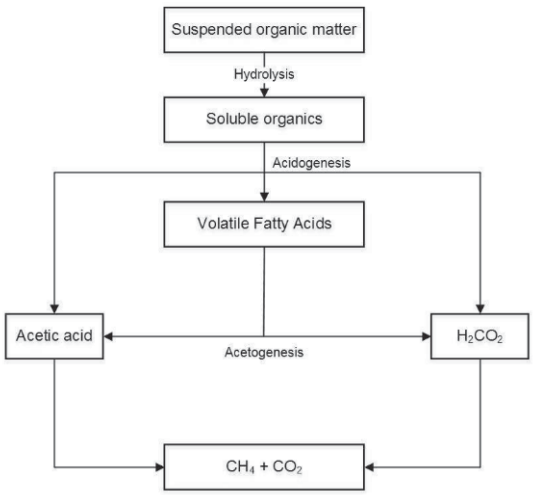

Fig. 1. Steps in the anaerobic digestion process [xix]

Biogas usually refers to a gas formed by the biological breakdown of organic matter in the absence of oxygen. Biogas derives from biogenic material, biofuels type. Biogas is produced through anaerobic digestion or fermentation of biodegradable materials which includes biomass, sewage, manure, municipal waste, green waste, and plant material and energy crops. This type of biogas comprises primarily methane and carbon dioxide. Also the gas produced by the use of biomass which is wood gas created by gasification of wood or other biomass. This type of gas consists

primarily of nitrogen, hydrogen, and carbon monoxide, with trace amounts of methane.A typical biogas composition is shown in Table I.

TABLE I
TYPICAL BIOGAS COMPOSITION [xx]

Content	Composition
Methane	50-60 %
Carbon Dioxide	30-45 %
Hydrogen Sulphide	1000-10,000 ppm
Hydrogen	0-1 %
Oxygen	0-2%

Agricultural organic streams include manure and slurries of different animals, energy and crops. Industrial organic waste streams includes by-products from food processing such as milk and cheese manufacture, slaughter houses and vegetable canning, from the beverage industry, such as fruit processing, distilleries, coffee, soft drinks, and from industries, including paper and board, sugar plants, rubber and pharmaceuticals. Municipal solid waste contain organic fraction of household waste. Methane content is 50-60% on average but its percentage is higher for the waste from agro food industry. The CO_2 is 30-45 % on average from all sources. The H_2S concentration varies with the different sources, but it is higher for sewerage, agriculture and animal waste from 600 ppm to 20,000 ppm average, as compared to municipal and landfill, where the concentration of H_2S varies from 3 ppm to 3000 ppm. Most intended uses of H_2S have considerable lower threshold for H_2S content and removal of H_2S is thus required to ensure the H_2S content is below the allowed amount.

Hence, there is a strong political drive towards the enrichment of biogas, since its properties are comparable to natural gas. Hence it could be used as a fuel for the same applications as fossil natural gas [xxi].

A range of techniques are available for the up gradation of biogas into bio-methane. Fig. 2 lists these techniques. Several processes are available in the literature for the upgrading the biogas into bio-methane, including high pressure water scrubbing, chemical absorption, cryogenic separation, membrane separation, and physical adsorption. High pressure water scrubbing is currently the most commonly used, since gases dissolves into the water while CH_4 does not because of their difference in solubility.

Physical absorption technique used the water with high pressure as absorber. The unrefined biogas supplied in a packed column from down side & the water with high pressure sprayed from the top side of the column reactor. Hence this process becomes with the counter current flow direction. The unwanted components of biogas i.e. carbon dioxide & hydrogen sulphide separated from the gas on the basis of the solubility in the water. These gases separated at the bottom of the column [xxii]. Chemical absorption involves formation of reversible chemical bonds between the solute and the solvent. Regeneration of the solvent, therefore, involves breaking of these bonds and correspondingly, a relatively high energy input. Chemical solvents generally employ either aqueous solutions of amines, i.e. mono-, di- or tri-ethanolamine or aqueous solution of alkaline salts, i.e. sodium, potassium and calcium hydroxides. [xxiii]. Membrane separation technique is another possible method for the biogas up gradation. With the help of a thin membrane some gas elements from the unrefined biogas could be transported. Normally the elements with less than 1 mm thickness separated by the membrane, while the other keep hold as it is. Due to the difference in the partial pressure the respective components are transported through the membrane, which is depending upon the component's permeability in the membrane. Permeability should be higher to get the high methane transparency [xxiv]. This process undergoes with a pressure of 25-35 bar and normally the solid membranes are used for this purpose. These membranes are of acetate cellulose materials which has the permeability with higher values. . This method is not suitable for high purity needs Consumes relative more electricity per unit of gas produced [xxv].The cryogenic method of purification involves the separation of the gas mixtures by fractional condensations and distillations at low temperatures. The process has the advantage that it allows recovery of pure component in the form of a liquid, which can be transported conveniently.

However, attempts to apply the cryogenic process for the removal of CO_2 from digester gas by Los Angeles County sanitation have not proven successful. Rather complicated flow streams are involved and thermal efficiency is low. Capital cost high Requirement of large sites. Longer start-up and shut down process Limited scalability in production. Capital cost and utility requirements are also high [xxvi].

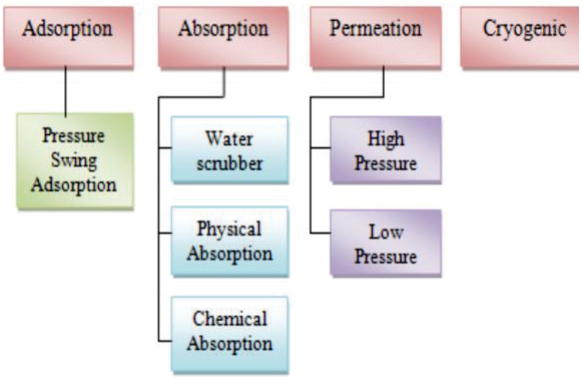

Fig. 2. Biogas upgrading technologies options [xxii]

However activated carbon adsorption is the most efficient method for enriching biogas system. Hence, the aim of this research is to establish an effective method for up-grading by physical adsorption of activated carbon.

II. Experimental

A. Materials and Methods

A packed bed activated carbon reactor installed and commissioned for the adsorption analysis of activated carbonfor biogas enchainment process. Adsorption unit made of stainless-steel tube (25mm OD, 290mm length). Different samples of standard industrial activated carbon were used as adsorption material of the packed bed reactor. Samples were given names as C-1, C-2 and C-3 respectively. All the samples of activated carbon were selected with different physical structure. The sample C-1 is granular and it is produced by steam activation at high temperature using a propriety process, which does not involve the use of any impregnant. C-2 has a structure of pallets. It is developed for the purification process from air streams and eliminating odours. It is the cost effective solution for the removal of "nuisance" type odours. As a result the risk of bed fires due to exothermic reactions is greatly reduced. C-3 is the powdered activated carbon. A powdered activated carbon with high adsorptive capacity, good filterability, and above average purity that is particularly suited for many purification applications.Glass wool was used at the bottom end of the rig to prevent the activated carbon to fall into the tube below. Similarly, a filter paper was used on the top side for smooth flow of the gas. Methane and carbon dioxide gases were used from the gas lines in the laboratory where as a special gas cylinder (BOC Ltd) was used with 1%H_2S/ 99%N_2. Physical adsorption method was used for the adsorption analysis at different flow rates.

TABLE II
SPECIAL GAS CYLINDER SPECIFICATIONS

Gas Mixture:	1% Hydrogen Sulphide/Nitrogen
Material number:	151885-AV -C
Cylinder size:	AV* (680mm x 181mm - 10 liquid litre capacity)
Pressure (bar):	200
Contents:	1.9m^3
Valve outlet:	BS15
Shelf-life:	36 months

B. Experimental Set-up of Packed-bed Reactor

A packed bed reactor of activated carbon was used for the present research. Different gas mixture were used for the biogas as shown in Fig. 3. Methane and carbon di-oxide gases from the gas lines while a cylinder of special gas mixture of $H_2S/N_2$was used. This cylinder consist of 1% hydrogen sulphide with 99% mixture of nitrogen gas. The properties of the special gas mixture has been shown in Table II. Pressure regulators andflow meters were used for controlling the pressure and volume flow of the gas in the reactor. Pressure regulators were fixed with the gas lines whereas flowmeters (Omega Ltd. UK) were installed with the rig at the time of assembling the unit. A safety valve was mounted with adsorption unit and the rig was placed inside the fume-hood for the safety reasons. A mass-spectrometer (Hiden Analytical Ltd. UK) is attached at the exit side of the rig, which is used to analyse the gases. Mass-spectrometer was further attached with the mass-soft to quantify the adsorption amount.

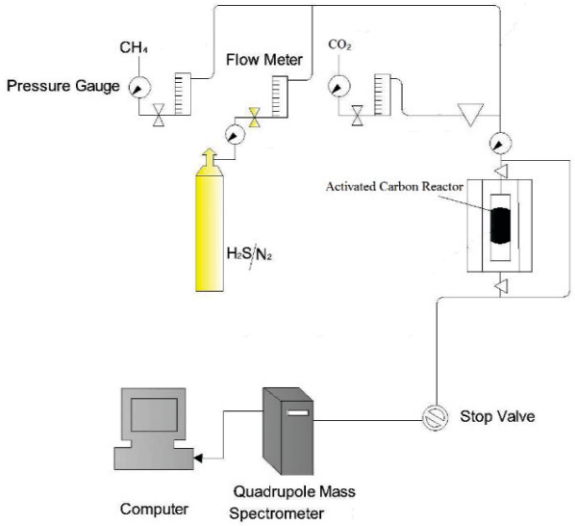

Fig. 3. Experimental set-up of the adsorption unit

C. Activated Carbon Characterization

CHN (Carbon, Hydrogen & Nitrogen) analyses were conducted on 440 Elemental Analyser (Control Equipment Cooperation). Isotherms of nitrogen were taken using Micrometrics Gemini VII. The catalyst degassed at temperature of 200°C for half a day with nitrogen gas by using Micrometrics Flow prep 060. Specific surface area is one of the imperative properties which affect the adsorption capacity of activated carbon significantly. Different surface areas for all the samples were measured and shown in Table IV below.

III. Overview of the Process Analyses

In the present study, biogas enrichment was carried

with the physical adsorption system. Activated carbon material was selected for this purpose and different analyses were conducted for finding the adsorption capacities of activated carbon samples. These analyses includes surface area, elemental and adsorption analyses. Risk assessment was prepared before the analyses to determine the process viability of the adsorption system. This includes COSHH (Control of Substances Hazardous to Health) and MSDS (Material safety Data Sheets) provided by the manufacturer for all the materials used. Leak test was conducted every time before filling the new sample in the reactor. Breakthrough curves were used for the adsorption capacities of the process.

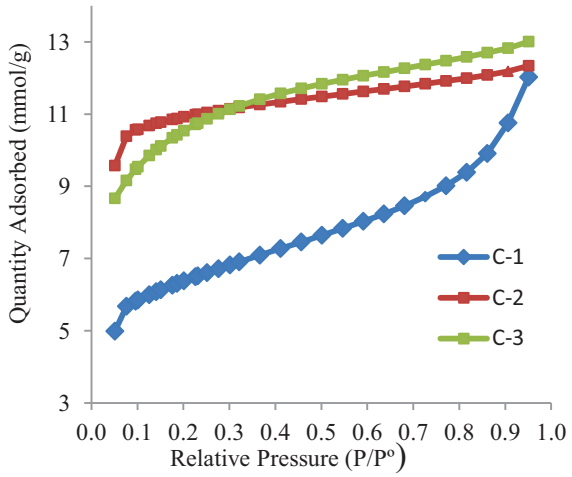

Fig. 4. Overview of the process analysis

IV. Results and Discussions

A. Elemental Analysis

CHN analyses were conducted on 440 Elemental Analyser (Control Equipment Cooperation). In the analyser carbon, hydrogen and nitrogen content in organic and inorganic compounds can be determined. Combustion of the samples occurs in pure oxygen under static conditions. Helium was used to carry the combustion products through the analytical system to atmosphere because it is chemically inert relative to tube packing chemicals, and it has high co-efficient of thermal conductivity. The percentage of carbon, nitrogen and hydrogen obtained from elemental analysis for all samples of activated carbon is given in Table III.

TABLE III
ELEMENTAL ANALYSIS OF AC SAMPLES

Sample	% C	% H	% N
C-1	76.21	0.59	0.3
C-2	82.25	0.13	0.37
C-3	81.38	0.2	0.11

B. Surface Area Analysis

Nitrogen isotherms were used to calculate the specific surface area, micro-pore volume, and total pore volume. All parameters and pore size distributions were calculated using the Density Functional Theory (DFT) [xxv]. The surface area was calculated using the BET method. The internal surface area of the activated carbon is usually determined by BET method (Brunaurer, Emmett and Teller). This method utilizes the low pressure range of the adsorption isotherms of a substance of known dimension which is usually nitrogen. This region of isotherms is generally distributed to monolayer adsorption. Hence, by considering the material is only adsorb one molecule deep on the surface of the carbon, the surface area can then be measured by using the following equation

$S = X_m NA$

S = Specific surface in m2/g

X_m = sorption value (ratio of the weight of the nitrogen adsorbed and carbon sample)

N = Avagardo's number, 6.025 E+23

M = Molecular weight of the nitrogen

A graph of adsorbed quantity for different activated carbon samples is shown in Fig. 4. Figure shows the quantity of the different activated carbons absorb with respect to the relative pressure. C-1 found with the linear increase of pressure. C-2 and C-3 absorption gives the smooth curves for the adsorption for the relative pressure values.

Table IV shows surface areas of activated carbon samples used for the analysis. There are normally four different type of surface area are used. These includes Single point, BET, Langmuir and t-Plot External Surface Area. However, BET surface adsorption theory is based on multilayer adsorption which addressed some flaws in Langmuir theory which is monolayer adsorption.

TABLE IV
BET ANALYSIS OF ACTIVATED CARBON SAMPLES

Samples	Single Point Surface Area	BET Surface Area	Langmuir Surface Area	t-Plot External Surface Area
	m^2/g	m^2/g	m^2/g	m^2/g
C-1	0.301107	202.8039	839.1614	258.1577
C-2	0.301109	265.6395	1,200.3939	153.8693
C-3	0.301257	277.6921	1,239.4617	443.3491

C. Adsorption Capacity of Activated Carbons

Adsorption capacities of all the activated carbon samples were calculated at different temperatures ranges from 25°C to 75°C as shown in Fig. 5. Each sample of activated carbon was chosen with different

physical structure. C-1 is small grains physical appearance, C-2 in pallet form whereas C-3 is in powder form. These capacities of samples were calculated on the basis of the material quantitative analysis. It can be seen that at 25°C, C-1 &C-2 has good adsorption capacity of about 50-60% compared to C-3, 38%.However, C-2 seems to have good adsorption capacity than the other samples at 50°C.

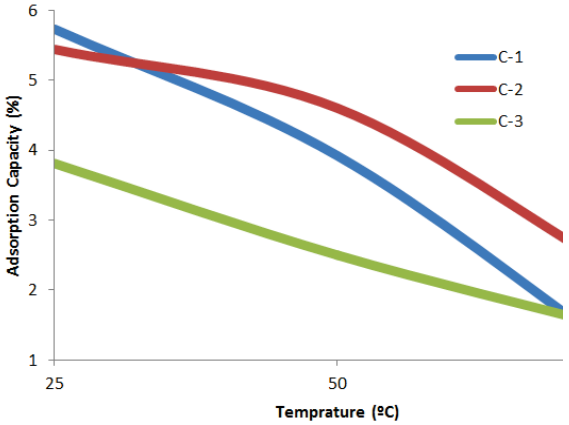

Fig. 5. Adsorption capacities of activated carbons at different temperatures

Anaerobic digestion takes place in the thermophilic region where digestion occurs at higher temperatures between 50 and 57 °C which is suitable for thermophilic bacteria. However, C-2 has comparatively high adsorption rate than the other two samples used for the analysis.

Thus, temperature range 50 to 60 °C are the best described for adsorption capacities of the activated carbon for the anaerobic digestion process. On the contrary, capacities of all activated carbon samples at 75°C are very small.

V. Conclusions

In the present energy crisis, biogas utilization after enrichment can be one of the most affordable methods for renewable power generation applications and home heating. Different technologies for the biogas clean-up technologies were studied. A number of methods are available for the upgradation of the biogas. However, there is need to find a potential solution for upgrading the gas which are environmental friendly. The present research was focused to find out the efficient way for the biogas purification system by activated carbon adsorption. The uniqueness of activated carbons as sorbents is related to their high surface area, high pore volume, and hydrophobicity of the surface.

In the present research, different gas mixtures passed through the packed bed activated carbon reactor. Measurements of the gases before and after treatment with the adsorption reactor were taken. Reduction of the carbon dioxide was observed from the mass spectrometer, which is coupled with the computer system through software. Results were analysed withadsorption curve with different activated carbon samples as explained in the results section. Hence, the results obtained from the current research could be utilized as a guide for the further design and operation of the industrial system.

References

[i] D. H. Maassen, J. V. Meel, S. Shazad, and J. M. P. Vaessen, ‘’Comparing different biogas upgrading techniques’’. Eindhoven University of Technology, The Netherlands, 2008.

[ii] A. L. Appels, C. J. Baeyens, A. J. Degreve and R. Dewil, “Principles and potential of the anaerobic digestion of waste-activated sludge,” in Progress in Energy and Combustion Science 755–781.

[iii] P. Chen, A. Overholt, B. Rutledge and J. Tomic, “Economic Assessment of Biogas and Bio methane Production from Manure,” in CALSTART March 20, 2010.

[iv] Q. H. Escobedo, F. M. Agugliaro and A. Z. Sierra, “The wind power of Mexico,” Renewable & Sustainable Energy Reviews 2010; 14(9):2830–40.

[v] A. T. Becerra, X. L. Bravo and F. B. Barcena, “Proposal for territorial distribution of the EU2020 political renewable energy goal,” Renewable Energy 2011; 36(8):2067–77.

[vi] F. M. Agugliaro and J. C. Valle, “Location of air in leakage in power plants condensers by helium test,” DYNA 2011; 86(2):173–81.

[vii] A. Demirbas, “Energy issues and energy priorities,” Energy Sources, Part B: “Economics, Planning and Policy” 2008; 3(1):41–9.

[viii] A. Demirbas, “Recent advances in biomass conversion technologies,” Energy Education Science and Technology 2000; 6:19–40.

[ix] M. Vinichuk, K. Rosen, K. J. Johanson and A. Dahlberg, “Correlations between potassium, rubidium and caesium (133Csand137Cs) in sporocarps of Suillus,” variegatus in a Swedish boreal forest. Journal of Environmental Radioactivity 2011; 102(4):386–92.

[x] I. Galvan, T. A. Mousseau and A.P. Møller, “Bird population declines due to radiation exposure at Chernobyl are strong erin species with pheomelanin-based coloration,” Oecologia2011; 165(4):827–35.

[xi] O. Kuchma and R. Finkeldey, “Evidence for selection in response to radiation exposure: pinussylvestris in the Chernobyl exclusion zone,” Environmental Pollution 2011;

159(6):1606–12.

[xii] E. Cardis and M. Hatch, "The Chernobyl accident—an epidemiological perspective," Clinical Oncology 2011; 23(4):251–60.

[xiii] S. F. Gluzman. "The Chernobyl accident—a personal perspective". Clinical Oncology 2011; 23(4):306–7.

[xiv] F. C. Peragon, J. M. Palomar, P. J. Casanova, M. P. Dorado and F. M. Agugliaro, "Characterization of solar flat plate collectors," Renewable and Sustainable Energy Reviews 2012; 16(3):1709–20.

[xv] F. M. Agugliaro, Q. H. Escobedo and A. Z. Sierra, "Use of bovine manure for exsitu bio remediation of diesel contaminated soils in Mexico," Itea- informacion Tecnica Economica Agraria 2010; 106(3):197–207.

[xvi] F. M. Agugliaro, M. J. S. Muros, F. G. Barroso, A. M. Sanchez, S. Rojo and C. Ban˜o´n, "Insects for bio diesel production" Renewable and Sustainable Energy Reviews 2012; 16(6):3744–53.

[xvii] Q. H. Escobedo, F. M. Agugliaro, J. A. G. Parra and A. Z. Sierra, "Is the wind a periodical phenomenon,". The case of Mexico Renewable & Sustainable Energy Reviews 2010;15(1):721–8.

[xviii] R. Banos, F. M. Agugliaro, F. G. Montoya, GilC, A. Alcayde and J. Go´mez, "Optimization methods applied to renewable and sustainable energy: a review," Renewable and Sustainable Energy Reviews 2011; 15(4):1753–66.

[xix] J.B. Holm-Nielsen, T. Al Seadi and P. O. Popiel, "The future of anaerobic digestion and biogas utilization," Bio- resource Technology (2009); 5478 -5484.

[xx] M. Farooq, I.A. Chaudhry, S. Hussain, N. Ramzan and M. Ahmed, Biogas up gradation for power generation applications in Pakistan," JQTM, Vol. VIII (II) (2012), pp. 107–118

[xxi] W. W. S. Charters, "Developing markets for renewable energy technologies," Renewable Energy 2001; 22:217–22.

[xxii] Q. Zhao, E. Leonhardt, C. MacConnell, C. Frear and S. Chen, "Purification Technologies for Biogas Generated by Anaerobic Digestion," CSANR Research Report 2010; 2010 – 001.

[xxiii] W. C. Savery and D.C. Cruzon, "Methane recovery from chicken manure," in Water Pollut Control Fed, PP. 2349–54.

[xxiv] R. Ciccoli, V. Cigolotti, R. Lo Presti, E. Massi, S.J. McPhail, G. Monteleone, A. Moreno, V. Naticchioni, C. Paoletti, E. Simonetti and F. Zaza, "Molten carbonate fuel cells fed with biogas," Combating H2S; Waste Management 2010; Vol. 30 PP. 1018–1024.

[xxv] A. Wellinger and A. Lindeberg, "Biogas upgrading and utilization," in Energy from biological conversion of organic wastes 1999, PP. 1–19.

[xxvi] A. Alonso-Vicario and A. Domínguez, "Purification and upgrading of biogas by pressure swing adsorption on synthetic and natural zeolites; Micro porous and Mesoporous Materials," Vol. 134 PP. 100–107.

Modeling and Simulation of MEMS-Based Comb Drive Actuator for Development of Single Axis Gyroscope, Using Bond Graph

[1]A. Raza, [2]S. Khushnood, [3]A. M. Malik,

[1,2]*Mechanical Engineering Department, UET Taxila*
[3]*DME, Air University, Islamabad.*
abbasraza812@yahoo.com

Abstract-A comb drive is an important component of MEMS-based actuators used in many applications such as a dispenser and a fluidic pump, and as a sensor in an accelerometer and in MEMS gyroscope. These energy systems, generally called mechatronic systems, are coupled multi-domain. Modeling and simulation of mechatronic systems is a challenging task. For coupled multidomain energy systems recently Bond Graph Method (BGM) has emerged as a method of choice. The system is seen as an interplay of power and energy variables, thus introducing the immortal concept of cause and effect. The two primary forces, electromechanical and electrostatic, are cast into the cause and effect paradigm whilst expressing power into effort and flow variables.

In this research work the main focus is on the investigation of the control parameters of laterally vibrating electrostatic comb-drive actuators. 20-SIM, a commercial bond graph package, is used to investigate the influence of control parameters on performance of the comb drive. The design process of system-on-chip (SoC) MEMS can be improved by this type of analysis. The comb-drive is represented here as a main source of actuation which is vibration in lateral direction. The work can be used as any design application as a cooling system for microprocessors used in space vehicles or a drug delivery system based on fluidic pump in on-a-chip systems. The multi-physics system of a robust comb-drive is modeled and solved using the 20-SIM, a commercial bond graph software. In this model, the driving voltage is taken into account. The comb drive displacement and electrostatic force are in direct relation to the square of the driving voltage. In this method, a model based on BGM is developed and then directly simulated using 20-SIM (a commercial software of Bond Graph modeling). Since bond graph is a precise mathematical model, the **state**-space equations of physical dynamic system can be solved. The bond graph simulations lead to the desired state space equations, which unfold the dynamic response of the physical system.

Keywords-Comb Drive, Gyroscope, MEMS, Modeling and Simulation, Bond Graph Method

I. INTRODUCTION

The drive for miniaturization propelled technology towards smaller devices. Micro Electro Mechanical Systems (MEMS) or the more European term Micro Systems Technology (MST), are devices whose applications are being discovered.

The comb-drive actuator is a basic building block of MEMS. Comb drive basically works on the generation of the electrostatic between the integrated conducting fingers moves relatively. As it is capable of generating the force, it has numerous applications in micro-mechanical systems. As an actuator MEMS Micro-gripper [I], probe based scanning devices [ii], on chip MEMS seismic accelerometers [iii], bi-directional rotation in MEMS actuators [iv], laterally oscillating gyroscopes [v] and RF filters [vi]. Therefore, improvements in comb drive actuators will have lasting effects in MEMS.

Particularly, in electrostatic actuator our interest is always in comb finger designs. These designs would generate more deflection profiles with the change of electrostatic force with linear shapes. These linear relationships, due to the action of a linear suspension spring, Reference [vii] will partially compensate for the mechanical restoring force. The drive voltage of these electrostatic actuators can be lowered by the electrostatic force of the spring. Moreover, this force may cause a change in resonant frequency.

In some researches people have investigated different comb shapes. Scheme [vii] reported fabrication methods for fingers, which are sensitive to small amount of displacements and drastically reduces the separation gap. These fingers were design supports maximum possible force output which is needed to minimize the voltage requirements at a nearly constant rate. The search of high-force actuators continued in the work of Scheme [viii].

The synthesis process demands efficient tools to enable designing of complex MEMS. This involves physical interchangeability with robustness between different domain of energy like electrostatic, mechanical, thermal optical, fluidic and magnetic energies. Several groups are working on this and reported the deficiency in different MEMS design

tools, including CAEMEMS [ix] (Univ. of Michigan). (Microcosm/ M.I.T.), IntelliCAD [x] (IntelliSense Corp.), MEMCAD [xi]. These design tools focus on two perspectives:

i) numerical simulation processes of self-consistent electromechanical integrated comb drive,
ii) 3D modeling of layout.

Now the product life cycle of MEMS is made cumbersome by the modeling and simulation using these software, and FEM packages, such as ANSYS. This research work is aimed provide an ease to MEMS design and to cut down the length of the whole effort by employing the power of Bond Graph Method. The multiphysics approach and cross-domain reach of bond graph method enables us to use the coupled domains and work under the supposition that the domains have decoupled under some assumed approximations. Such approxima-tions have usually made the model to deviate from real system specifications as it is not considering the unexpected behavior of physical conditions and fabrication limitations. It is expected that theoretically the Bond Graph approach shall bring the model closer to empirical results as all physical conditions can be incorporated in it. Though the methodology has been in use since the last three decades, its power has been fully realized recently, while its object oriented modeling capabilities and merging of genetic programming has been exploited to the greatest benefit.

Bond graph method has been applied to RF MEMS comb drive switches by Rosenberg et al [xii]. The same was tried on vertical comb drive actuator in this paper. The initial effort has been focused on formulating the bond graph while tuning it to have a system approach of the model available for further results to be extracted by specifying the various parameters in the state space of the bond graph method.

II. Physical and Mathematical Model

Developing a bond graph model and thus state space of a comb drive actuator with capability of continuous motion and large static displacement has always been the main focus of research in micro domain.

The actuators consist of two inter-digitized fingers, with one connected to a suspension and the other is fixed. The actuator is designed to be stiff in the orthogonal direction and only respond in the displacement direction [xiii]. The electrostatic forces, generated by applied voltage, cause deflection of the movable comb and vary directly with the square of the applied voltage.

Different comb designs, investigated for variations in displacement due to electrostatic driving forces generated by the applied voltage, have already been modeled by a robust finite element method and commercial multi-physics FEM package ANSYS [xvi].

The authors in this paper introduce the implementation of BGM by constructing a Bond graph model to get the variation of electrostatic force and displacement of comb drive with voltage. The model acquired is directly solved and simulated on 20-SIM, commercially available BGM software. BGM provides an easy way to investigate the system behavior with the variation of different parameters directly, without changing the basic design of system. It is a special ability of BGM which enhances the robustness of parametric study of multi physics system with reliability and repeatability.

The electrostatic Comb-drive actuator performance relies on its electrostatic characteristics [xiii]. In Fig. 1 voltage difference is applied between the two fingers, keeping the moving finger at ground potential; thus, a potential difference causes the fingers (electrodes) to be electrically charged. This results in an induced capacitance in the two electrodes. The electrostatic force displaces the movable finger in x direction. The driving force F can be expressed as:

$$F = \partial U / \partial g = nt\varepsilon_o\varepsilon_r V^2 / 2g \quad (1)$$

here
U = Energy related to applied potential V,
ε_o = Permittivity in the free space, equal to 8.85 pF/m,
ε_r = Relative permittivity of the dielectric material between the two electrodes
n = Number of the electrode pairs,
t = Electrode thickness and
g = Gap between two fingers.
Considering an elastic displacement in the movable finger, according to Hooke's Law:

$$Fs = K_x x \quad (2)$$

x is the displacement of the movable finger and K_x is the stiffness in x direction. Scheme [xv] and Scheme [xvi] has showed in their work to derive the stiffness of the spring. In equilibrium, the two forces Fs and F are equal, in this case x is a function of the driving potential (V), thickness of comb (t), the gap (g), the stiffness (K_x) and the number of electrodes (n) as:

$$x = nt\varepsilon_o\varepsilon_r V^2 / 2K_x g \quad (3)$$

Equation 3 shows that the actuator displacement deviates from the linear behavior (increase in applied voltage causes an increase in displacement) and follows the voltage-stroke relation for the Combo-drive.

II. Modelling the System Through Bond Graph Method

The Modeling of a MEMS device carries with it certain inherent problems, which have lead to a method

of formulation that does not always yield the most practical results. The designer has to bank upon numerous assumptions. The numbers of assumption widen the chasm between ideal and real system. The factors distancing the ideal or assumed system from the real system are:

1) Multi-domain system where the power flows from electrical to mechanical domains due to the capacitance variation (piezoelectric effect) which results in the Carioles Forces in the comb drive.
2) The relationship of various parameters is non-linear.

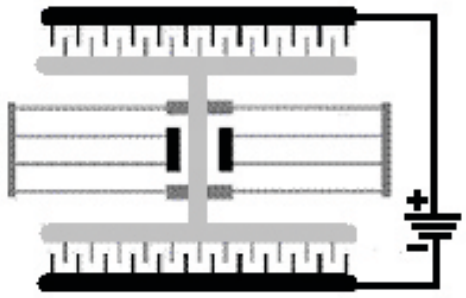

Fig. 1. The original actuator with folded-flexure suspension. This is a traditional actuator design with symmetry about x- and y-axis. [xvii]

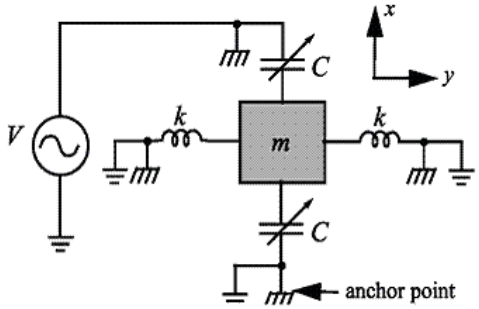

Fig. 2. A Mixed domain structure view of comb drive with a voltage source. [xiii]

3) A single model of a comb finger with the flexure alley has to be extended to the whole comb drive (with an average of 20 fingers). This requires an ability to generate algebraic loops, thus enabling the use of advanced techniques such as Genetic Algorithm [xii].

The authors linearized the system and used some approximations to unfold domain information; these approximations enable the system to give empirical results through BGM.

BGM is based on ancient "cause-effect" theory and provides the domain independences in multi-domain system modeling. Four system variables are to be defined for any domain. To implement BGM on multidomain system firstly the identification of two power variables for that domain are needed. Some examples of power variables of system are shown in Table I. These variables are selected in such a manner that the product of these variables is always equal to the "power" in that domain. These variables are the effort and flow of that specific domain. After identifying these variables, the causality assignment come i.e., the classification of these elements into cause and effect in the system. The other two variables are called co-energy variables. As energy is the integral of power so these two variables are the integrals of effort and flow variables. The co-energy variables help to understand the energy flow of the system.

These elements consist of two energy sources, the source of flow (Sf) and source of effort (Se). Three energy elements, first for kinetic energy storage, i.e. inductor (I), second for potential energy storage, i.e. capacitor (C) and the third for system energy dissipation i.e. resistor (R).

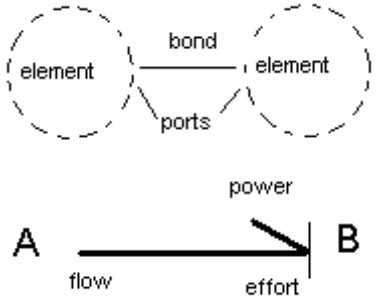

Fig. 3. Ports and bonds of Bond Graph

To interplay between different domains and incorporate the causality change between variables, two convertors are used i.e. Transformer (TF) and Gyrator (GY). These two convertors use to incorporate the change of domain, like Electrical to mechanical in our system, and to step up and down the power variables, like transformer in electrical system. Last two are the junctions, i.e. 0 and 1 junctions, use to define the parallel and series combination of the elements. With the help of these nine elements one can model the universe as it is a complete unified modeling technique. The system of every domain like electrical, mechanical, mechanical rotation, hydraulic and thermal or combination of any of these can be built by taking appropriate domain variable as detailed in Table (I) and the system elements.

These nine elements are connected with each other through the ports Fig. 3. These ports contain the information of causal and the energy flow directions of the system.

The connections of elements through ports having causal and energy information in accordance with the precise physics of the system, give a complete augmented Bond Graph of the system. Unlike the traditional modeling techniques BGM defines the system flow and unfold the mathematics of the system through the physical information incorporated in

model.

TABLE I
VARIABLES OF DIFFERENT DOMAIN IN BOND GRAPH METHOD.

Domain	Variables of Effort	Variables of Flow
Mechanical	Force (F)	Velocity (v)
	Torque (τ)	Angular Velocity (ω)
Electrical	Potential Diff. (V)	Electric Current (I)
Hydraulic	Hydraulic Pressure (P)	Volume flow rate (dQ/dt)
Thermal	Thermodynamic Temperature(T)	Rate of Entropy change (ds/dt)
	Pressure (P)	Volume change rate (dV/dt)
Chemical	Chemical potential (μ)	Mole flow rate (dN/dt)
	Enthalpy (h)	Mass flow rate (dm/dt)
Magnetic	Magnetomotive force (e_m)	Magnetic flux (φ)

Our comb drive is based on electrical and mechanical domains. The interconnectivity of mechanical and electrical domain variables Fig. 4 for the comb drive system has been developed according to the physics of the system and rules of BGM.

The Bond Graph of a physical system is developed by identification of domain specific system elements and connecting them according to the power flow pattern and causality assignments. This Bond Graph will have the sufficient information of the system energy flows and it precisely unfolds the mathematical model i.e. direct facilitation in the dynamic response of the physical system. Now by assigning the value to elements of bond graph model, according to physical system, the simulations are being done on the commercial Bond Graph software, 20-SIM.

Our developed bond graph model Fig. 4 for a comb drive actuator is derived from a physical design

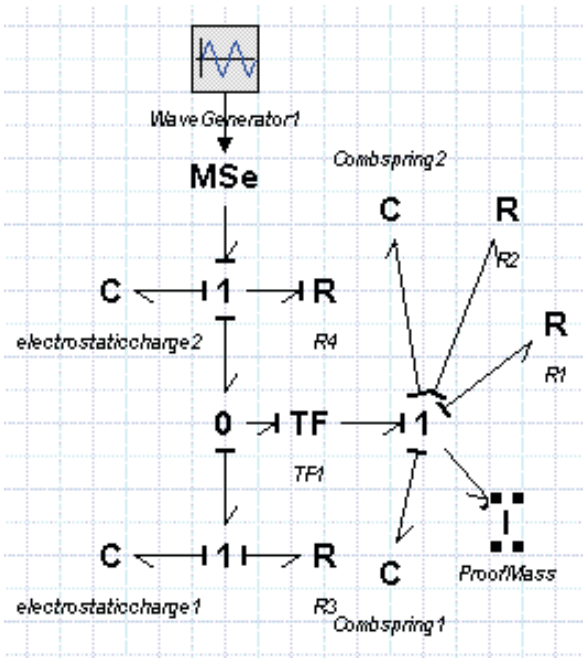

Fig. 4. Bond Graph Model of electrostatic comb-drive.

of a traditional x and y-axis symmetric comb drive Fig.1 [xvii]. A mixed domain structure of that system with voltage source, V, is shown in Fig. 2 [xiii]. It consists of a mass suspended by two folded beams flexures, thus constituting a mass spring damper system. This derived model is then simulated and trend of results, for different values of parameters, have been compared with the results of FEM [xiv].

III. Results and Discussion

The variation in comb displacement and electro-static force in the comb spring against the applied voltage is studied. Eq. (1) and (3) show that the displacement of combs and the force generated is directly proportional to the square of applied voltage. The authors have developed bond graph model of the system Fig. 4 with the help of physical model only, and simulated the Bond Graph Model on 20-SIM. Fig. 5 shows the relationship of applied voltage, against displacement and electrostatic force. This relationship of physical model exactly follows the trend represented in mathematical Eq. (1) and (3).

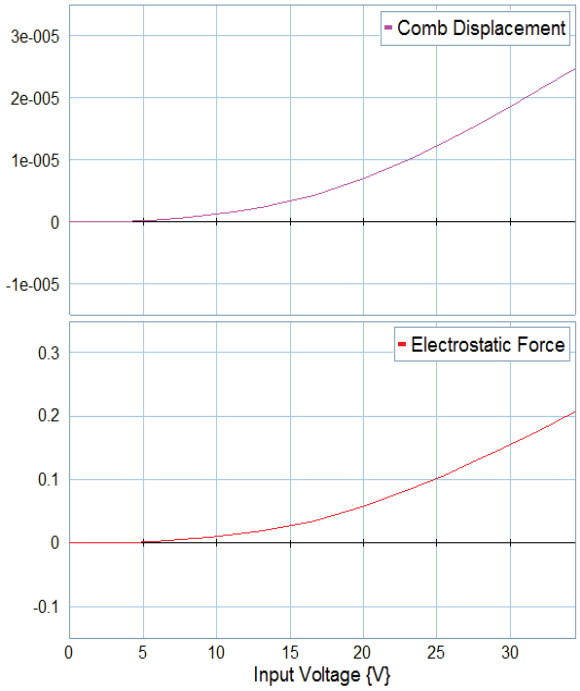

Fig. 5. Simulation of Comb Drive displacement and electrostatic force against driving voltage at initial parameters.

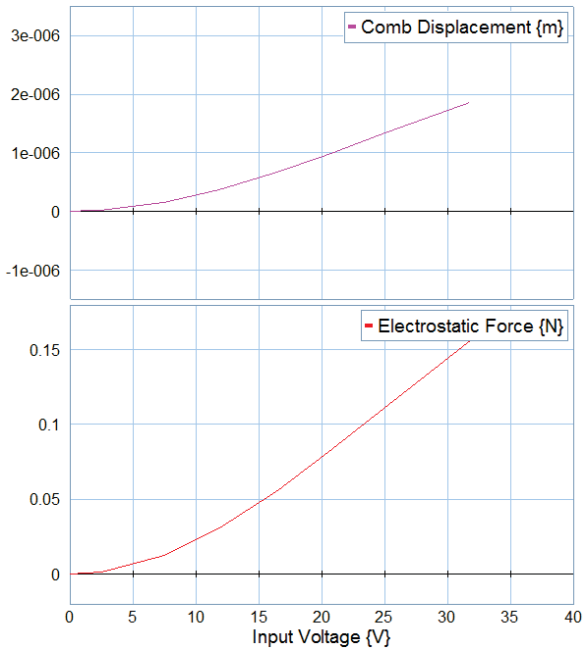

Fig. 6. Current Frequency doubled from initial value.

In the current study, the Bond Graph Method is applied to check the effects of Comb's design parameters on the actuation performance Figs. 1-9. Fig. 5 shows the variation of the Comb displacement and generated electrostatic force with the driving voltage of 40 volts. Figure shows that electrostatic force and displacement is linearly related to voltage squared with constant spring stiffness and other parameters.
The initial parameters of the system are taken as :

MSe	= Input Voltage	= 40V
f	= Current frequency	= 50rps
R3	= Elec. Resistance	= 0.05ohm
R4	= Elec. Resistance	= 0.05ohm
C	= Charge on fingered cap. 1	= 1.456exp-8C
C	= Charge on fingered cap. 2	= 1.456exp-8C
R1	= Mech Damping	= 0.00323Ns/m
R2	= Mech Damping	= 0.00323Ns/m
C	= Comb Spring Stiffness1	= 83333N/m
C	= Comb Spring Stiffness2	= 83333N/m
I	= proof mass	= 0.5g

The natural frequency for the free undamped vibration of a uniform cantilever affects the displacement and is a function of its length, cross-section, and boundary conditions. Fig. 6 shows the effect of doubling thr frequency of current on the electrostatic force and comb displacement observed in comb-drive. This dependence of displacement and force on natural frequency has been simulated at 40V and the results are displayed which shows that the displacement of the system decreases with the increase in current frequency, as expected.

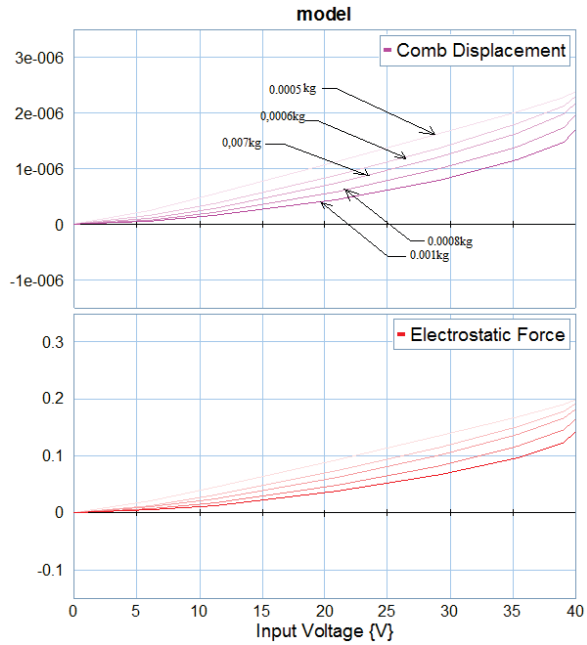

Fig. 7. Increasing Proof Mass giving decrease in Comb displacement and force

The results shown in Fig. 7 indicate that for a driving voltage of 40 volts, as the value of proof mass is increased from 0.0005 to 0.001kg, the inertia of the drive increased and so is the Comb displacement decreased. This effect of the Comb is also expected.
The displacement variation rate is shown to decrease with the decrease of the proof mass (m) as well. This effect verifies the above result.

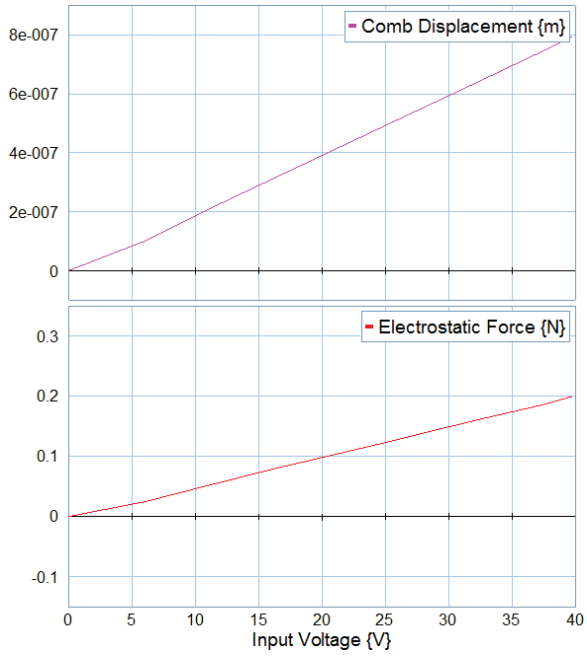

Fig. 8. Stiffness increased by three times

If the value of stiffness is increased from 83333 to 250000, the comb displacement decreases. Fig. 8 concurs with the relation between stiffness and Comb displacement for 40V driving voltage; other parameters are same as in Fig. 5.

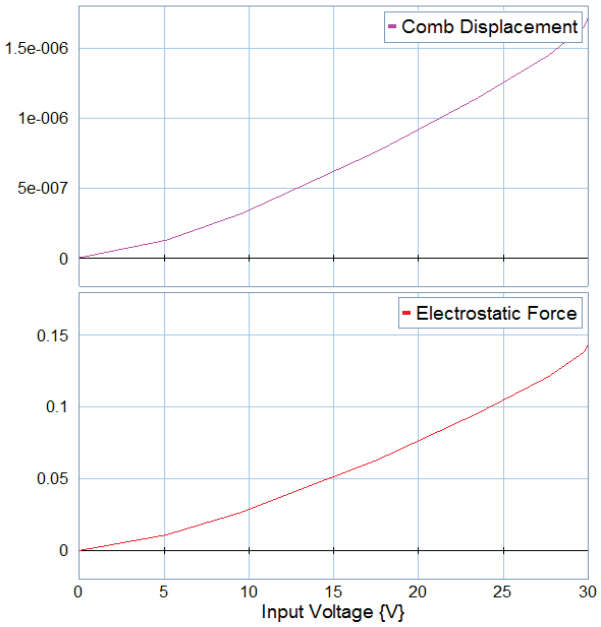

Fig. 9. 30V

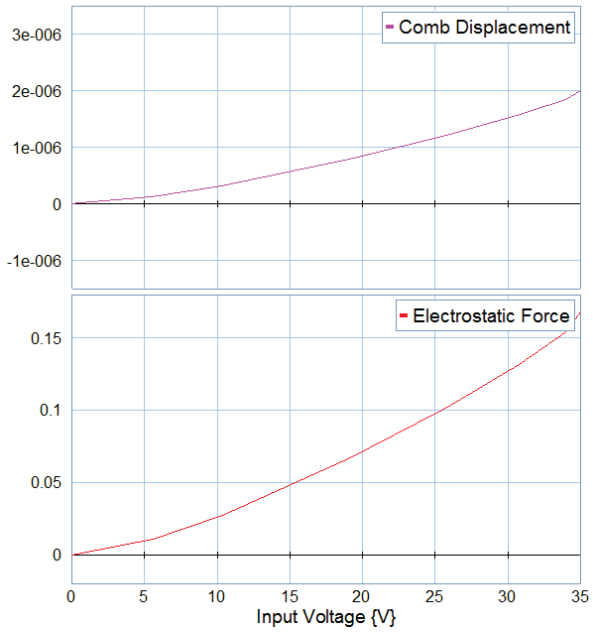

Fig. 10. 35V

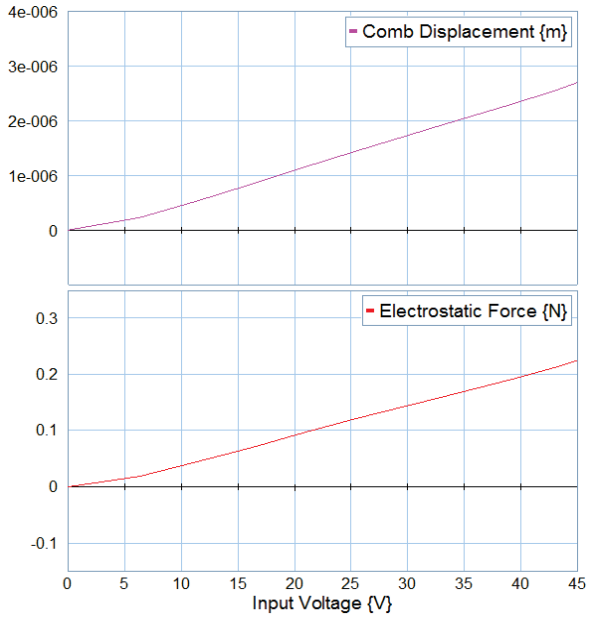

Fig. 11. 45V

When supplied voltage is decreased as in Fig. 9-12, the displacement of the comb drive will also decrease. In case if we increase the supplied voltage, an increase in the comb resistance is observed for the taken comb design, as shown in Fig. 11 and 12. In these figures, variation rate in the displacement of comb drive is changed with supplied voltage.

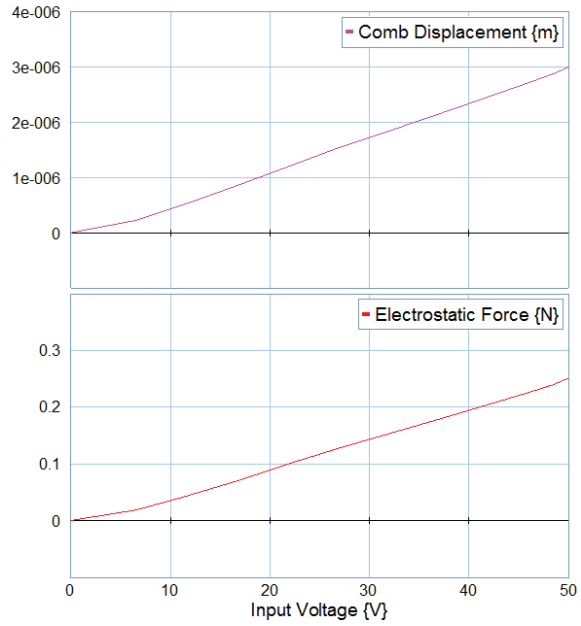

Fig. 12. 50V

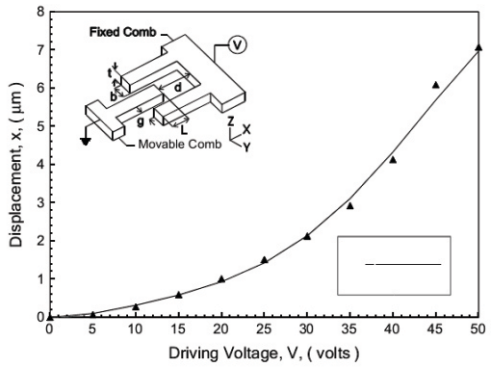

Fig. 13. Graph indicating variation of displacement versus the applied voltage, (V) of Comb-drive. [xiv]

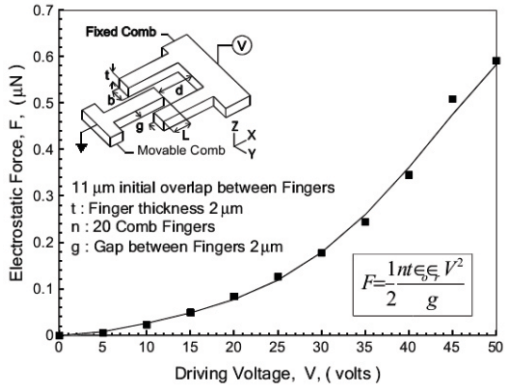

Fig. 14. Graph indicating variation of electrostatic force and applied voltage [xiv].

In order to utilize the current study results in the design optimization of comb drives with linear nature, we have made an effort to condense these results into non-dimensional compact form that correlates the studied geometric parameters of the modeled comb-drive with its displacement. Utilizing Newton Raphson Method, built-in with 20-SIM, it is observed that the displacement values in Fig. 6-10 are effectively represented by Eq. (1) and (3) and results of FE and Mixed domain method presented in [xiv] also confirms the trends of these simulations.

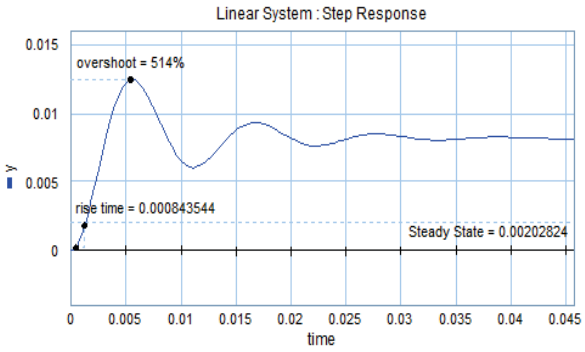

Fig. 15. Step Response Plot

The step response of the system is extracted, Fig. 15 and its shown that the settling time of the system is found 0.05 sec.

With sinusoidal input it is observed the system oscillated sinusoidally in response time of 0.05sec.

The simulation through the bond graph model is studied with the variation of different parameters and it is evident that the system design parameter are successfully studied and altered through this method and system followed all the expected trends.

IV. Conclusion

In this work, Bond Graph Analysis is used to explore the effect of the design parameter of laterally actuated electrostatic comb drive on the actuation performance. The comb displacement induced and the generated electrostatic force in comb are directly proportional to the square of driving voltage. The bond graph method is successfully applied to the MEMS system to study the variations of considered variables with the change of parameters. The variation follows the expected trends of comb drive actuation. Now from these results, by considering the actual parameters of comb drive, an optimized design of this kind of a system can be developed without indulging in an extensive mathematical modeling. Bond graph method basically depends on correct physical model of the system and supports to develop the mathematical equations of the physical system itself. Assumptions discussed earlier can be tackled by taking suitable values of system variables and improving the system performance by inserting the values of parameters ignored in this model.

The effect of comb-drive design parameters on actuation performance is explored. Eq. (1) and (3) shows that the displacement of combs and the force generated is directly proportional to the square of applied voltage. The same results are indicated by the results of FEM and PolyPUMP. The relationship of our developed physical model follows the trend represented in these results.

In this research, the coupled electrostatic and mechanical analysis of MEMS Comb-Drive has been performed. Mechanical Analysis done through Finite Element Method (FEM) and Electrostatic Analysis is done by the Boundary Element Method. Several design parameters of comb drive like overlap of the fingers, folded flexure spring length which effect the stiffness and the voltage applied to the comb fingers were addressed and their effects were studied on different variables like mass, system's natural frequency and comb displacement, using ANSYS by [xiv]. Simulations on 20-SIM through bond graph method are following the same trends and generating the same effects as ANSYS results.

V. RECOMMENDATIONS

An optimized comb drive based gyroscope is to be designed with Bond Graph Method, in which the gyroscope's design issues and problems can be simulated, studied, optimized and verified.

REFERENCES

[i] Y. Jia , Q. Xu, "MEMS Microgripper Actuators and Sensors: The State-of-the-Art Survey", Recent Patents on Mechanical Engineering 04/2013; Vol. 6(2).

[ii] T. Y. Harness and R. A. Syms "Characteristic modes of Electrostatic Comb-Drive X-Y Microactuators", J. Micromech. Microeng. 10 (2000), pp. 7-14

[iii] A. Neeshpapa, A. Antonov and V. Agafonov, Article "A Low-Noise DC Seismic Accelerometer Based on a Combination of MET/MEMS Sensors" J. Sensors 2015, 15, 365-381

[iv] MEMS actuators with combined force and bidirectional rotation, Patent: US 8729770 B1

[v] W. C. Tang, T. Cuong, H. Nguyen and R. T. Howe "Laterally Driven Polysilicon Resonant Microstructures", Proc. 1989 IEEE Micro Electro Mechanical Systems, pp. 53-59, February 1989

[vi] R. Legtenberg, A. W. Groeneveld and M. Elwenspoek "Comb-Drive actuators for large displacements", J. Micromech. Microeng. 6 (1996), pp. 320-329.

[vii] M. A. Rosa, D. D. Bruyker, A. R. Völkel, E. Peeters, and J. Dunec, "A novel external electrode configuration for the electrostatic actuation of MEMS based devices," Journal of Micromechanics and Microengineering, vol. 14, no. 4, pp. 446–451, Apr. 2004.

[viii] Hirano, T., L. S. Fan, T. Semba, W. Lee, J. Hong, S. Pattanaik, P. Webb, W. H. Juan and S. Chan "High bandwidth hdd tracking servo by a moving-slider micro-actuator". IEEE Transactions on Magnetics 35, 3670–72.(1999).

[ix] S. B. Crary, O. Juma, and Y. Zhang, "Software Tools for Designers of Sensor and Actuator CAE Systems," Technical Digest of the IEEE Int. Conference on Solid-State Sensors and Actuators Transducers '91), San Francisco, CA, pp. 498-501, June 1991.

[x] IntelliCAD, IntelliSense Corporation, 16 Upton Dr., Wilmington, MA 01887.

[xi] S. D. Senturia, R. Harris, B. Johnson, S. Kim, K. Nabors, M. Shulman, and J. White, "A Computer-Aided Design System for Micro-electro-mechanical Systems, "J. of Microelectromechanical Systems, v .1, no.1, pp. 3-13, Mar. 1992.

[xii] Z. Fan, K. Seo, J. Hu, R. C. Rosenberg, E. D. Goodman "System-Level Synthesis of MEMS via Genetic Programming and Bond Graphs"

[xiii] G. K. Fedder and T. Mukherjee "Physical design for surface-micromachined MEMS", 5th ACM/SIGDA Physical Design Workshop, Reston, VA USA, April 15-17, 1996, pp. 53-60

[xiv] W. A. Moussa, H. Ahmed, W. Badawy, M. Moussa, "Investigating the Reliability of Electrostatic Comb-Drive Actuators Utilized in Microfluidic and Space systems Using Finite Element Analysis"

[xv] Jaecklin V. P., Linder C, de Rooij N F , Moret J M "Micromechanical comb actuators with low driving voltage" Journal of Micromechanics and Microengineering. Vol. 2, (1992) p250-255

[xvi] R. Legtenberg, A. W. Groeneveld and M. Elwenspoek "Comb-Drive actuators for large displacements", J. Micromech. Microeng. 6(1996), pp. 320-329.

[xviii] J. D. Grade, H. Jerman and T. W. Kenny, "Design of Large Deflection Electrostatic Actuators" Journal Of Microelectromechanical Systems, Vol. 12, No. 3, June 2003

Identification of Factors Affecting Cost Performance of Construction Projects

M. Abas[1], S. B. Khattak[2], R. Akhtar[3], I. Ahmad[4], M. Ullah[5], I. U. Haq[6]

[1] Mechanical Engineering Department, GIK, Topi, Pakistan
[2,3,5] Industrial Engineering Department, UET Peshawar, Pakistan
[4] Management Sciences Department, Iqra National University, Peshawar, Pakistan
[6] Institute of Mechatronics Engineering, UET, Peshawar, Pakistan
[3]rehman_akhtar@uetpeshawar.edu.pk

Abstract-Construction projects are measured in terms of cost, quality and time. Project success is related to completion of projects within a specified budget. Khyber Pakhtunkhwa (province of Pakistan) is facing project management related issues such as cost overrun. Cost is among the most important contemplations throughout the project management life cycle. It can be looked upon as one of the most significant parameters of a project and the driving force for its success. In order to point out the significant factors that cause cost overrun of construction projects. In this paper, a total of 31 factors are selected. Data is in the form of feedback from construction practitioners and subject matter experts. The statistical tools such as mean and relative importance index are used to identify significant factors related to cost.

Keywords-Construction projects, Cost Overrun, Khyber Pukhtunkhwa, Factors, Mean, Relative Importance Index.

I. INTRODUCTION

Cost overrun occurs when the final project cost surpasses the original estimations [i]. Cost overrun is a very common phenomenon and is practically associated with nearly all projects in any industry. This tendency is more severe in developing countries like Pakistan, where these overruns sometimes exceed 99% of the estimated cost [ii]. The major causes of cost overrun arise due to client actions, such as financial instability, making slow decision and lack of involvement in the planning phase of the project [iii]. The other causes include delays in funding, poor site management, revision of project scope and lack of resources[iv].

To date, agriculture sector construction is the second largest contributor to Pakistan economy. It contributions considerably lead to socioeconomic development. Construction industry contributes more than 2.4 percent of the total GDP [ii]. However, it suffers due to lack of investment in infrastructure development. The construction projects suffer cost overrun due to change in scope of project, fluctuation in prices of key materials, inappropriate government policies and lack of proper planning [v]. More than 90 percent of projects get over budgeted or completely abandoned due to either lack of funds or mismanagement at different levels. Poor site management, corruption, political interest and extra work contributes to cost overrun [vi]. Hence, special consideration is required to overcome the issues of cost overrun, although numerous researchers identify significant factors that cause cost overrun, but their significance level varies from region to region [ii, vi,ix]. This paper highlights the factors that adversely affect the cost of construction projects in the Khyber Pakhtunkhwa, a province of Pakistan.

II. LITERATURE REVIEW

Cost is among the key considerations throughout the project management lifecycle. Regardless of its recognized importance, it is not infrequent to see a construction project dwindling to accomplish its objectives within the identified cost.

Cost overruns are critical for both developing and developed countries. The authors in [x] concluded that the major causes of cost overrun in Pakistan are incompetent consultants, price escalation, exchange rate fluctuation, approval issues, weather related issues, and permit approval process. A case in point, the authors in [xi] identified cost related risks in their study. The identified risks are stern schedule of project, inappropriate planning, design variation, and error in cost estimation.

The authors in [xii] have done study related cost risk to the West Rail project of Hong Kong. The study suggested fifteen (15) risks concerned with project cost. The factors are divided into three groups: resource factors, management factors and parent factors. Escalation material prices are related to resource factors, imprecise budget cost and supplier or subcontractor's failure is related to management factors, where as excessive interface for project management is related to parent factors.

The study of the authors in [ii] about Pakistan construction industry concludes that instability of raw material prices, high cost of machineries, low bid, poor site management, and changes in government policies related to construction sectors and associated fields are responsible for cost overrun. The authors in "[xiii]

holds ineffective communication between project team responsible for negative impacts such as low productivity, cost and time overruns, and inadequate design specifications. The authors in [xiv] showed that in longer term lowest bid is not necessarily the most economical solution. It affects the project in terms of cost overrun and time delay.

The authors in [xv] discussed top three factors affecting construction cost. These factors have significant effect on the project cost, which includes cash flow problem, financial instability, ineffective site management, lack of supervision, and lack of communication among parties. According to the authors in [xvi] the causes of poor cost estimation are related to documentation, design, project management, financial resource management and contract administration.

The above literature concludes that the level of importance of factors affecting cost of construction projects varies. It is difficult to identify the factors that have significant effect on project cost. This research is conducted to highlight the factors that have substantial effect on cost performance of construction projects in Khyber Pakhtunkhwa, a province of Pakistan. The analysis method deployed in this research includes cronbach alpha test, Analysis of Variance (ANOVA), Arithmetic Mean and Regression Analysis. The analysis methods are explained in methodology and data analysis section in detail.

III. METHODOLOGY

Keeping supply chain perspective in view, a total of 31 factors are identified and selected for this research. Table I shows the 31 identified factors. Factors identification is done through literature review. The selected factors are finalized in consultation with academic and construction experts. For effective cash flow risks and benefits sharing among the major participants are very important [xvii]. Implementing continuous improvement in construction projects increases the profitability. Reducing waste is basically evaluated by assessing input and final project outcomes [xvii]. No blame culture is extremely important when the project is complex and unachievable. It aids in decision-making, team building and improve cost performance. Incorrect implementation of joint working or partnering will have disastrous effects on the cost performance of the project [xix]. With trust, the company can share sensitive information freely with no fear to their suppliers and clients. This helps them to solve many problems related to their clients and supplier, which results in better quality and cost control of material [xx].

As first hand and reliable information was not available with any government and private organization. A questionnaire based on 31 selected factors is designed. The questionnaire is designed into four main sections. As shown in Table II, each section has independent and different types of questions. Additionally, the respondent is asked to share their experience relating to these factors (e.g., how weather affected the cost of their project, any incident they faces related to terrorists activities, situation in which the government policies affected project cost).

TABLE I
CONSTRUCTION SUPPLY CHAIN FACTORS

S. No	Factors	S. No	Factor
1	Planning Commission Proforma 1 (PC-1)	17	Trust with supplier
2	Funding	18	Communication
3	Procurement Unit of Contractors	19	Problem Solving
4	Financial capability of Contractor	20	Risk Allocation
5	Management team of Contractor	21	Continuous Improvement
6	Communication Infrastructure	22	Incentive Mechanism
7	Escalation of Material Prices	23	Pain and Gain Sharing
8	Technical Person Availability	24	Performance Measurement
9	Cash Flow	25	Joint Working
10	Shortage of Material/ Equipment	26	No Blame Culture
11	Law and Order Situation	27	ISO Certification
12	Low Bid	28	Benefit Shared
13	Weather Condition	29	Mutual Objective
14	Bureaucracy and Political Influence	30	Government Policies
15	Terrorism	31	Inflation
16	Regulatory Authorities		

As first hand and reliable information was not available with any government and private organization. A questionnaire based on 31 selected factors is designed. The questionnaire is designed into four main sections. As shown in Table II, each section has independent and different types of questions. Additionally, the respondent is asked to share their experience relating to these factors (e.g., how weather affected the cost of their project, any incident they faces related to terrorists activities, situation in which the government policies affected project cost).

TABLE I
QUESTIONNAIRE SECTIONS

Sections	Description
1	Questions related to Respondent Qualification and Demography
2	Questions related to Company Information
3	Questions related to external and internal factors with weightage 1-9
4	Questions relating internal and external factors to cost, quality and time

The questionnaire was sent to respondents through

mails, emails, by hands. In some instances interviews and discussion session were held with groups of senior construction practioners. A total of One hundred and fifty (150) questionnaires were distributed. Hundred and ten (110) were received out of which Nine (9) were discarded due to insufficient information. The profile of the respondents of the received questionnaire is shown in Table III. The youngest respondent as shown in Table III holds 9-year practical experience.

TABLE III
RESPONDENTS PROFILE

S.No	Organization	Designation	Experience
1	Contractors of Class A and B	Quantity Surveyors	12-15 years
2	UET Peshawar	Professors (Academic Experts)	9-13 years
3	Peshawar Development Authority (PDA)	Executive and General Director	18-23 years
4	Contractor of Class A and B	General Director	17-21 years
5	Irrigation Department Peshawar	Civil Engineers	16-18 years

The maximum number of receiving responses belongs to medium and large firms as shown in Table IV. CA and CB category contractors are placed in large firms, whereas C1 and C2 category contractors are termed as medium firms. This CA, Pakistan Engineering Council (PEC) does CB, C1 and C2 categorization. The categorization criteria are based on the number of completed projects and project budget.

Table IV
RESPONSES CATEGORIZATION

S.No	Organization	Number of Responses
1	Large Construction Firms	35
2	Medium Construction Firm	25
3	Small Construction Firm	15
4	Government Organization	15
5	Private Organization	11
	Total	**101**

Upon receiving the responses, the data was streamlined via Microsoft Excel. The filtered data is subjected to cronbach alpha and ANOVA tests.

Cronbach alpha (α) test is deployed to check the reliability of the collected data. Reliability is at low level and not acceptable when Cronbach α is less than 0.3. Reliability is at a highly acceptable level when Cronbach α is more than 0.7. To check the reliability of the data it is transferred to SPSS software. The reliability based on Cronbach alpha (α) test is 0.801, which shows that the data is highly reliable and valid for analysis.

Additionally, the respondents involved in the study are from different organization having different designation and experience. Hence, it is important to check whether their opinions are same or different about the factors affecting the cost of construction projects. For this aim, One Way ANOVA test is conducted with the help of SPSS software. The test is conducted on randomly four questionnaires from each category of respondents. The summary of ANOVA results and the respondent categorization is shown in Table V.

TABLE V
ONE WAY ANOVA TEST RESULTS

S.No	Category	F	P Value
1	Contractors – Government official	1.558	0.216
2	Contractors – Academic experts	2.287	0.082
3	Contractors – Private organization	2.448	0.067
4	Private organization-Academic Experts	2.737	0.070
5	Government officials – Private organization	1.978	0.121

All the values of ***"P"*** are greater than 0.05, so it is concluded that the test is insignificant and opinions of all the respondents are same about factors affecting the cost of a construction project.

I. Data Analysis

First the dependency of factors on the criteria (cost) is evaluated with the help of regression analysis. The Table VI shows the model summary (ANOVA) of regression analysis. The value of ***"P"*** is less than 0.05; the test is significant, highlight the factors affecting cost. The Table VII shows the t-test and P-values results for each factor depends on cost. Values less than 0.05 shows significant effect on the cost, while greater than 0.05 implies less significance. The data is analyzed by two different methods. One is method of measure of central tendency i.e., Arithmetic Mean (AM) while the other is Relative Importance Index (RII).

TABLE VI
ANOVA RESULTS

S.No	Model	Sum of Squares	Mean Square	F	Sigma
1	Regression	48.163	2.833	3.566	0.023[a]
2	Residual	07.945	0.794		
	Total	56.107			

Where "a" is independent variable and "b" is dependent variable (time)

Arithmetic Mean (AM) is one of the best ways to calculate the average value of data, because it gives

equal importance to all of the data under analysis. Equation 1 shows the generalized form for AM.

$$AM = \sum W/N \quad (1)$$

Where

$\sum W$ = Summation of weights assigned
N = Numbers of responses to that factor

The relative importance index is the statistical methods used to quantify the data. The weight of each factor from different responses are summed and divided by the product of highest weight and the number of respondents –[xxi]. The general formula is shown in below equation:

$$RII = \text{Sum of weights } (Y1 + Y2 + Y3 + \ldots + Yn) / Wx N \quad (2)$$

Where, Y = Weights given to each factor by the respondents and will range from 1 to 9.

If '1' is less significant and '9' is extremely significant.

W = highest weight (i.e., 9 in this case), and N = total number of respondents.

As shown in Table VII, the results of these two methods were same. Escalation of material prices, inflation and terrorism are highly significant by RII and the arithmetic mean. No blame culture and ISO certification is on the lower side.

Table VII
Factors Ranking

Statistical Measures				Regression Analysis	
Ranking	**Factors**	**RII**	**Mean**	**t- Test**	**P-value**
1	Escalation of Material prices	0.9074	8.17	3.631	0.005
2	Inflation	0.8889	8.00	2.888	0.016
3	Terrorism	0.8667	7.80	-2.792	0.019
4	Financial Capability of Contractor	0.8556	7.70	-3.388	0.007
5	Cash Flow	0.8519	7.67	2.793	0.019
6	Low Bid,	0.8111	7.30	-1.076	0.028
7	Shortage of Material/Equipment	0.800	7.20	2.2614	0.047
8	Technical Person Availability	0.7852	7.07	0.255	0.197
9	Management Team of Contractor	0.7778	7.00	0.092	0.121
10	Funding	0.7704	6.93	0.179	0.033
11	Continuous improvement	0.763	6.87	0.363	0.023
12	Bad Weather	0.7556	6.80	-1.156	0.012
13	Procurement Unit of Contractor	0.7481	6.73	0.235	0.043
14	PC-1 Preparation	0.7444	6.70	0.455	0.037
15	Problem Solving	0.7333	6.60	-0.578	0.043
16	Risk Allocation	0.7296	6.57	0.247	0.010
17	Law and Order Situation	0.7222	6.50	0.028	0.021
18	Bureaucracy and Political Influence	0.7185	6.47	-0.777	0.043
19	Performance Measurement	0.7037	6.33	0.910	0.044
20	Government Policies	0.7037	6.33	-0.832	0.041
21	Communication	0.6926	6.23	0.851	0.040
22	Communication Infrastructure	0.6889	6.20	0.137	0.038
23	Mutual Objective	0.6741	6.07	-0.423	0.037
24	Trust with supplier	0.663	5.97	-0.115	0.037
25	Joint working	0.6148	5.53	-0.673	0.033

26	Regulatory Authority	0.6074	5.47	-1.029	0.031
27	Incentive Mechanism	0.600	5.40	0.694	0.030
28	Pain and Gain sharing	0.563	5.07	1.130	0.475
29	Benefit shared	0.5407	4.87	0.800	0.612
30	No blame Culture	0.5185	4.67	1.301	0.561
31	ISO certification	0.4111	3.70	-1.315	0.401

V. Results and Recommendations

The five most significant factors affecting the cost of a construction projects are graphically depicted in Fig. 1. The most significant factor based on both mean and RII is an escalation of material prices. The AM value for escalation of material prices is 8.17, while RII value is 0.9074. The regression analysis with ***"P"*** value of 0.0178 shows escalation of material prices has significant effect on the cost of construction projects. The risk of escalation of material prices can be mitigated through the early purchase of materials that are subject to escalation risk. However, commitment to early supply material with corresponding suppliers may resolve price escalation issue. In addition, the other possible solution is to treat the escalation as an allowance in subcontracts. Duel surcharges in pricing agreement and delaying construction project until prices become stable are another way to force client for proper funding. Buy material in bulk to take advantage of discount and to avoid escalation risk.

Inflation is a second significant factor with both AM and RII value of 8. In regression analysis, the "P" value of inflation is 0.016, which is less than 0.05. Inflation reduces the time value of money. Entire project exceeds allocated budget due to expensive material, costly labor and equipment. Contractor should include inflation clauses in the contract.

The third most significant factor is terrorism. The mean value of terrorism is 7.8 whereas RII value is 0.867. The "P" value in regression analysis for terrorism is 0.0191. It highlights the significance of terrorism on the cost performance. Due to terrorist activities, the number of check posts has increased on major routes. This not only causes traffic congestion, but also interrupts the daily supplies and routine work on the construction site. Trucks containing materials have to wait for hours at a single check posts for security clearance. The government needs to focus on these issues and relax the policy related to security reason for the contractors and suppliers.

With a AM value of 7.7 and RII 0.856, financial capability is the fourth most significant factor. In regression analysis, the "P" value is 0.0294, which is less than 0.05. If the financial capability of the contractor is strong, materials, and the equipment's can be purchased/hired on time. Skilled and sufficient number of labor may be hired, which may decrease lead-time of the project and saves money. Inversely, if the financial capability of the contractor is not that strong, the project won't be completed in pre-assumed span of time. Contractor has to bear penalties, which directly affect the cost of the project.

To mitigate such risk, one need to develop trust with supplier and communicate openly and share the pain and gain with the supplier.

Cash flow with a mean value of 7.67 and an RII value of 0.852 is a fifth significant factor. Its regression value is 0.0362, showing importance. Cash flow is the movement of money through the various parts of construction projects. Effective flow has a positive influence on the outcome of the project. The cash flow is highly affected by low bids, incorrect estimates, poor management, and inadequate budget. Corrective control is not exercised in time, and the scope of work increases drastically. For better cash flow, the contractor needs to constantly audit the project. Double-check the estimate for any mistakes. Keep in view the trend of inflation and escalation of material prices. Penalties might be the solution to compel project managers to achieve project goals on time.

Factors such as problem solving, risk allocation, government policies, and PC-1 preparations are the intermediate significant factors. These factors might be most important for time and quality but not for cost. "ISO Certification" turned out to be the least significant factors. In addition, neither contractors nor their suppliers are interested in getting ISO certification. The government is also not keen to have ISO certified contractors on board. Hence, the cost and tedious paper work with no genuine return is the main reason practioners do not opt for these certifications.

VI. Conclusions

The study is carried out to identify major factors causing cost overruns in construction projects of Khyber Pukhtunkhwa. Five significant factors affecting cost of a construction project were selected on the basis of mean, and RII. These factors are an escalation of material prices, inflation, and terrorism, financial capabilities of the contractor, and cash flow. Results of the study reveal that considerable attention is required to build a policy to ensure reduction in impacts of identified factors for infrastructure development in Khyber Pukhtunkhwa. The findings of this study and the methodology are useful for research in construction

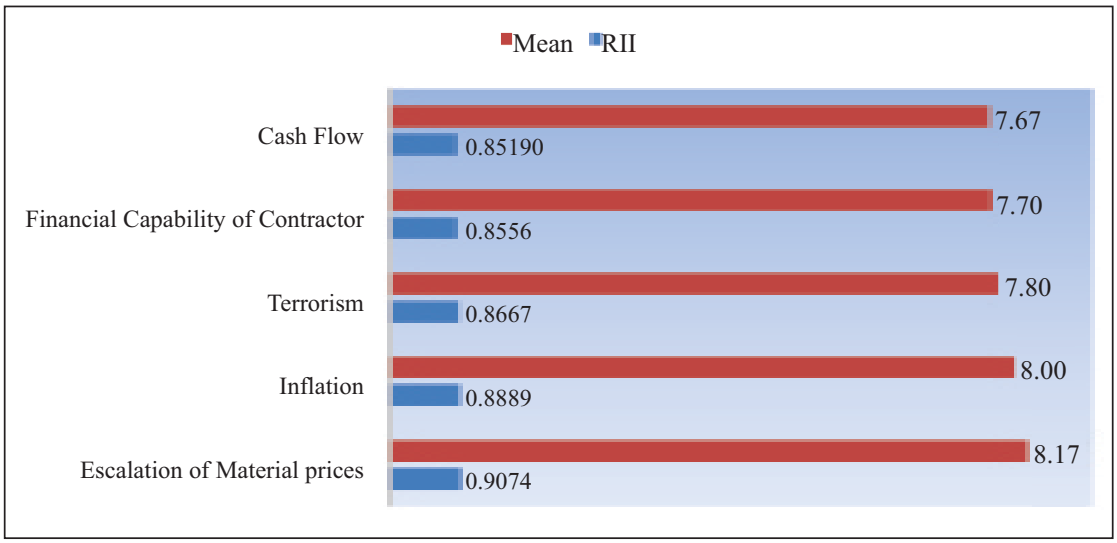

Fig. 1. Significant Factors

domain. Furthermore, the study can aid professionals in taking proactive measures for reducing cost overruns construction projects. Both contractor and government agencies can save exchequer money by improving and implementing laws related to construction environment. Since a key contribution of this study is development of a framework to address project overruns related issues, several other research areas for future work can spin-off from this study. Notably, opportunities exist to integrate our analysis with other project management methodologies such as risk assessment, supplier-supplier relationship, and inventory management etc; to contribute to the knowledge in the field of project management. Finally, although the developed methodology was applied specifically to Khyber Pukhtunkhwa, the same methodology can be implemented to other regions of Pakistan.

REFERENCES

[i] Avots, "Cost-Relevance Analysis for Overrun Control," International Journal of Project Management, vol. 1, no.3, 1983, pp. 142-148.

[ii] N. Azhar, Rizwan U. Farooqui, and S. M. Ahmed, "Cost Overrun Factors In Construction Industry of Pakistan," First International Conference on Construction In Developing Countries (ICCIDC–I), August 4-5, Karachi, Pakistan 2008.

[iii] S. H. Han, "Analyzing Schedule Delay of Mega Projects Lessons Learned From Korea Train Express," IEEE Transactions on Engineering Management, vol.56, no.2, 2009.

[iv] S. Murali, "Causes of and Effects of Delays in Malaysian Construction Industry," International Journal of Project Management, 2007.

[v] R. M. Choudhry, A. Rehman Nasir, H. F. Gabriel, "COST AND TIME OVERRUNS IN HIGHWAY PROJECTS IN PAKISTAN," Centenary Celebration (1912 – 2012), 2012.

[vi] T. Nawaz, N. A. Shareef, and A. A. Ikram, "Cost Performance in Construction Industry of Pakistan," Industrial Engineering Letters vol.3, no.2, 2013.

[vii] X. Meng, "Assessment framework for construction supply chain relationships: Development and evaluation," International Journal of Project Management, vol. 28, 2010, pp. 695-707.

[viii] X. Meng, "The effect of relationship management on project performance in construction," International journal of project management, vol. 30, 2012, pp. 188-198.

[ix] R. U. Farooqui, & J. Aziz, "Assessing the Viability of Total Quality Management Implementation in Contracting firms of Pakistani Construction industry," presented at the First International Conference on Construction In Developing Countries (ICCIDC–I), "Advancing and Integrating Construction Education, Research & Practice", Karachi, Pakistan, 2008.

[x] N. Azhar, R. U. Farooqui, and S. M. Ahmed, "Cost overrun factors in construction industry of Pakistan," Advancing and Integrating Construction Education, Reseach & Practice, 2008, pp. 499-508.

[xi] P. X. Zou, G. Zhang, and J. Y. Wang, "Identifying key risks in construction projects: life cycle and stakeholder perspectives," in Pacific Rim Real Estate Society Conference, 2006.

[xii] H. Chen, Hao, G., Poon, S.W. and Ng, F. F, "Cost Risk Management in West Rail Project

of Hong Kong," 2004.

[xiii] P. Trkman, Groznik, "Current Issues and Challenges of Supply Chain Management," European and Mediterranean Conference on Information Systems Abu Dhabi, UAE 2010.

[xiv] M. M. Kumaraswamy, "Contractor evaluation and selection: a Hong Kong perspective," Building and Environment, vol. 31, 1996, pp. 273-282.

[xv] Memon, I. A. Rahman, M. R. Abdullah, and A. A. A. Azis, "Factors Affecting Construction Cost in Mara Large Construction Project: Perspective of Project Management Consultant," International Journal of Sustainable Construction Engineering & Technology vol. 1, December 2010.

[xvi] Memon, I. A. Rahman, and A. A. A. Azis, "Time and Cost Perfomance in Costruction Projects in Southern and Cenrtal Regions of Penisular Malaysia," International Journal of Advances in Applied Sciences (IJAAS) vol. 1, pp. 45~52 March 2012.

[xvii] Barlow, "Innovation and learning in complex offshore construction projects,". Research Policy, 2000, pp. 973-989.

[xviii] R. Takim, A. Akintoye, And J. Kelly, "Performance measurement systems in construction," 19th Annual ARCOM conference, University of Brighton,, vol.1, 2003, pp. 423-431.

[xix] G. Packham, B. Thomas, and C. Miller, "Partnering in the Welsh construction industry: A subcontracting perspective," University of Glamorgan Business School, 2001.

[xx] J. T. I. Stephen K. Hacker, Laurent Couturier, "Building Trust In Key Customer - Supplier Relationships," 1999.

[xxi] Kometa, Olomolaiye, and Harris, "Attributes of UK construction clients influencing project consultants performance," Construction Manage Econ, vol. 12, 1994, pp. 433–43.

Fabrication of Polycaprolactone-Cellulose Acetate Hybrid Electrospun Fiber Blends

S. Ali[1], F. Ahmed[2], A. Khatri[3], M. Khatri[4]

[1,2,3,4]Textile Engineering Department, Mehran University of Engineering and Technology, Jamshoro 76060, Pakistan
[3]awais.khatri@faculty.muet.edu.pk

Abstract- Series of Poly(ε-caprolactone) (PCL)/Cellulose Acetate(CA) hybrid electrospun fibers mats (EFMs) were prepared via electrospinning process. The EFMs were characterized by X-ray photoelectron spectroscopy (XPS), thermogravimetric analysis (TGA), field emission-Scanning electron microscopy (FE-SEM) and water contact angle (WCA) measurements. XPS analysis revealed that the carbon content (%) was gradually decreased and the oxygen content (%) was enhanced steadily with the increasing composition of the CA present in the PCL/CA hybrid EFMs. Better thermal stability of the PCL/CA hybrid EFMs was found in comparison to the neat PCL EFM and the neat CA EFM, as revealed by TGA analysis. The fiber morphology under FE-SEM showed that the surface of EFMs were smooth and beadless. The WCA results revealed that EFMs were hydrophobic. The PCL/CA hybrid EFMs may be used as scaffold in tissue engineering and in other biomaterials where low wetting properties are required.

Keywords- Poly(ε-caprolactone), Cellulose Acetate, Electrospinning, Thermal Stability, Smooth Surface

I. Introduction

The rapid evolution of nanotechnology has paved the way for researchers worldwide to explore the unique properties of nanoscale materials [i]. Electrospinning is a well-known method for producing polymer fibers in the submicron to nanometer diameter ranges [ii]. Electrospun fibers and mats offer several advantages including high surface to volume ratio, tunable porosity and good physico-mechanical properties making them a suitable substrate for various applications [iii]. Significantly, desired properties in electrospun fibers and mats can be achieved by manipulating the polymer solution and process parameters [iv].

Poly(ε-caprolactone) (PCL) is a non-toxic polyester having good biocompatibility and environmental degradability, as well as good mechanical properties [v-vii]. It has poor thermal properties due to its low melting temperature preventing wide scale use [viii-ix]. However, PCL can be blended with other polymers to achieve improved properties [vi]. Significantly, PCL is suitable for blending with other polymers due to its good processability and blend compatibility [v].

Cellulose acetate (CA) is an important organic ester of cellulose and is extensively used to make fibers, plastics and coatings [vi], [x]. It is a cost-effective organic polymer with limited water absorption property due to the presence of acetyl groups in its chemical structure [xi]. Furthermore, CA offers higher melting temperature making its processability difficult [viii].

There are various reports available in which PCL was successfully blended with different polymers to enhance the desired properties of either one or both constituent polymers. We are providing three such examples here. Firstly, the blend of long-chain cellulose ester (LCCE) and PCL showed that the addition of PCL into LCCE raised the tensile stress at break slightly as well as enhanced the thermal stability of LCCE in the blends [xii]. Secondly, the PCL-PLLA blend was prepared to make nanofibers tubes. In the blend, PCL provides a better physical and mechanical stability, and the PLLA enhances the biodegradability [xiii]. Thirdly, cellulose/PCL blends were prepared successfully. The blends showed considerable enhancement of thermal stability in comparison to the regenerated cellulose when the proportion of PCL content is more than 40 wt% [xiv].

In this study, we prepared PCL-CA hybrid EFMs by blending different proportions of the PCL and CA polymer solutions followed by electrospinning. Furthermore, the surface and thermal properties of the EFMs were characterized by X-ray photoelectron spectroscopy (XPS), Field emission-Scanning electron microscopy (FE-SEM) and thermal gravimetric analysis (TGA) respectively. The wetting property of EFMs was also evaluated by water contact angle (WCA) measurements.

II. Experimental

A. Materials

Poly(ε-caprolactone) (PCL, weight average molecular weight = 80,000) and Cellulose acetate, CA (39.8% acetyl content having weight average molecular weight = 30 kDa) were obtained from Sigma-Aldrich (USA), and used as-received.

B. Preparation of the polymer solutions

A 9 % (w/w) PCL solution in dimethylformamide/

chloroform and a 17% (w/w) CA solution in acetone/ dimethyl formamide were prepared to fabricate the neat PCL electrospun fibers mat (EFM) and the neat CA EFM respectively. For PCL/CA hybrid EFMs, four different blend ratios were prepared as 4:1, 3:1, 2:1 and1:1 (w/w). Each PCL/CA polymer solution was stirred at 50°C for 24 h before electrospinning. All the PCL/CA polymer solutions were clear and homogeneous.

C. *Electrospinning*

The electrospinning set up (NanoNC, Korea) was used as reported previously [xv]. The polymer solutions were pumped with a 10 mL plastic syringe at a controlled feeding rate of 0.1 mL/h (KD Scientific, Korea) through a 23 gauge needle. The voltage of 12 kV was applied and the tip-to-collector distance was fixed at 15 cm. Electrospun fibers were collected over the metallic drum covered with aluminum foil. The average thicknesses of EFMs were in the range of 40-50 µm; measured by Digital Micrometer MCD130-25 with a measuring sensitivity of 1 µm.

D. Measurements

The chemical compositions of the EFMs were examined by XPS (Theta Probe Base System, Thermo Fisher Scientific Co.) with Al Kα radiation. Survey spectrum was recorded over the 0-1350 eV binding energy range at detector pass energy of 200 eV. TGA (PerkinElmer TGA-7,Korea) was performed to investigate the thermal properties of EFMs from 30°C to 500°C at a heating rate of 10°C per minute under a nitrogen gas atmosphere. The morphology of EFMs were examined under FE-SEM (JSM 6701F, JEOL Japan). All samples were sputtered with platinum under vacuum before assessment. WCA of the EFMs was measured by sessile drop measurements using a Drop Shape Analysis System, DSA 100 (Krüss, Hamburg, Germany). Five contact angle measurements were averaged to get a reliable value.

III. Results and Discussion

A. XPS analysis of EFMs

Fig. 1 depicts the average chemical composition of the surfaces of the EFMs at a 10 nm depth. The C 1s peaks and O 1s peaks are present at 285 eV and 532 eV respectively. The elementary compositions of the EFMs obtained from the survey spectrum are also compiled and given in Table I. The PCL EFM showed greater carbon content (77.49%) in comparison to the carbon content (62.54%) of CA EFM. In contrast, PCL EFM showed lower oxygen content (22.51%) in comparison to the oxygen content (37.46%) of CA EFM. The results showed that carbon content (%) was gradually decreased and the oxygen content (%) was enhanced with the increasing composition of the CA

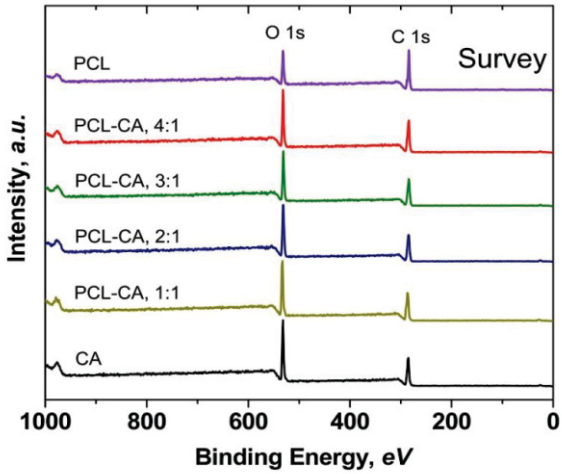

Fig. 1. XPS results of PCL, CA and PCL-CA hybrid EFMs.

present in the PCL-CA EFMs as given in Table I. comparison to the oxygen content (37.46%) of CA EFM. The results showed that carbon content (%) was gradually decreased and the oxygen content (%) was enhanced with the increasing composition of the CA present in the PCL-CA EFMs as given in Table I.

B. TGA analysis of EFMs

Sample	Carbon (%)	Oxygen (%)
PCL	77.49	22.51
PCL-CA, 4:1	68.61	31.39
PCL-CA,3:1	67.91	32.09
PCL-CA,2:1	65.61	34.39
PCL-CA,1:1	65.7	34.3
CA	62.54	37.46

Fig. 2. TGA results of PCL, CA and PCL-CA hybrid EFMs.

The TGA thermal curves of PCL, CA and PCL-CA hybrid EFMs are shown in Fig.2. All the EFMs exhibited a single step in the loss of their weight. Significant weight loss occurred at around 350-400°C, and continued to decrease until the temperature reached up to 500°C. The thermal stability of the PCL-CA hybrid EFMs was found better than the PCL EFM and the CA EFM. Hence, blending PCL with CA resulted into a higher thermal stability than the neat PCL and the neat CA EFMs.

Fig. 4 shows the results of WCA of EFMs. It can be seen from Fig.4 that all the EFMs remained hydrophobic producing WCA results in the range of 110-115°. Therefore, blending of CA and PCL did not produce significant effect on the surface wetting of the EFMs.

C. *FE-SEM analysis of EFMs*

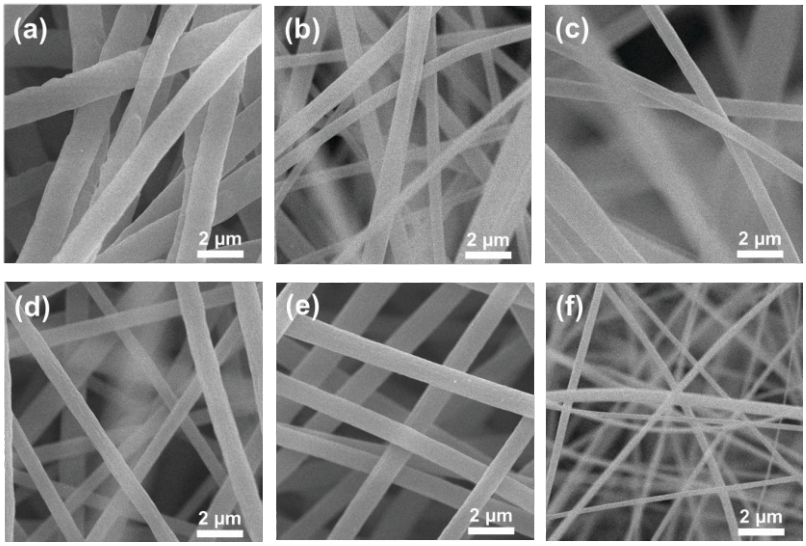

Fig. 3. FE-SEM images of as-spun EFMs. *(a)* PCL, (1:0), *(b)* PCL-CA, (4:1), *(c)* PCL-CA, (3:1), *(d)* PCL-CA, (2:1), *(e)* PCL-CA, (1:1) and *(f)* CA, (0:1).

Figure 3 demonstrates the morphologies of the PCL, CA and PCL-CA hybrid EFMs. All the samples showed a beadless and smooth morphology, which suggests that the polymer concentrations used, the selection of solvent system as well as the electrospinning parameters used were optimal. Moreover, FE-SEM images showed that the CA electrospun fibers are finer than PCL electrospun fibers Fig. 3.

D. WCA analysis of EFMs

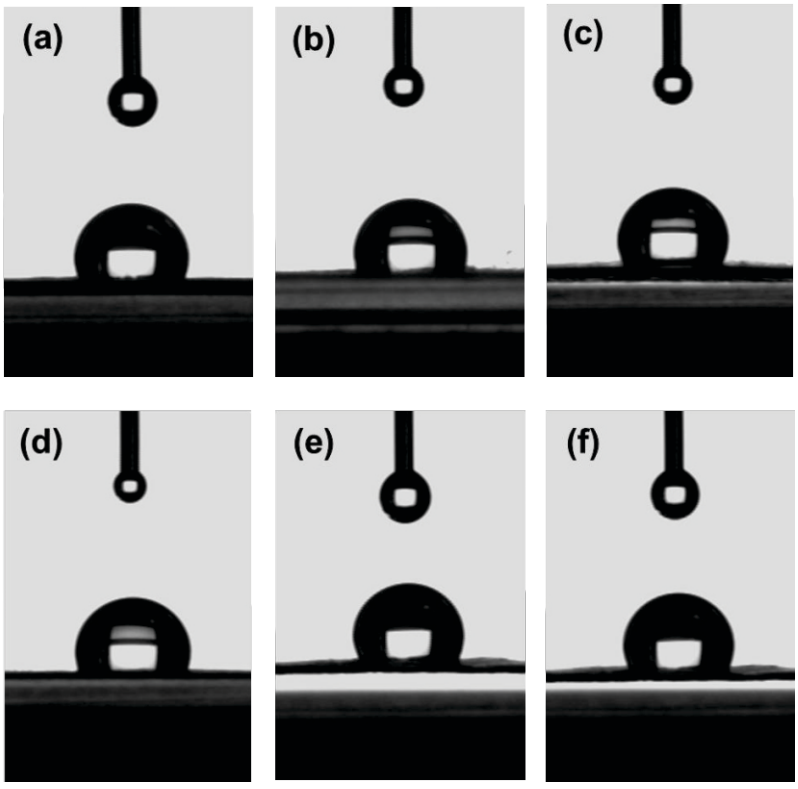

Fig. 4. WCA (°) of EFMs *(a)* PCL, (1:0), *(b)* PCL-CA, (4:1), *(c)* PCL-CA, (3:1), *(d)* PCL-CA, (2:1), *(e)* PCL-CA, (1:1) and *(f)* CA, (0:1).

IV. Conclusions

PCL/CA hybrid EFMs were successfully fabricated via electrospinning process. XPS analysis showed that the carbon content (%) was gradually decreased and the oxygen content (%) was enhanced steadily with the increasing composition of the CA present in the PCL/CA hybrid EFMs. TGA analysis revealed better thermal stability for PCL/CA hybrid EFMs in comparison to the neat PCL EFM and the neat CA EFM. FE-SEM results demonstrated the bead-free surface morphology of EFMs. The WCA results revealed that EFMs were hydrophobic. The potential application of PCL/CA hybrid EFMs include scaffold in tissue engineering and in other biomaterials.

V. Acknowledgements

Mr. Shamshad Ali is thankful for the financial support received from HEC Pakistan under the HRDI-UESTPs/UETs scholarship and MUET Jamshoro Pakistan.

References

[i] N. Bhardwaj & S. C. Kundu, "Electrospinning: a fascinating fiber fabrication technique," Biotechnology advances, vol. 28, pp. 325-347, 2010.

[ii] A. Greiner & J. H. Wendorff, "Electrospinning: a fascinating method for the preparation of ultrathin fibers," Angewandte Chemie International Edition, vol. 46, pp. 5670-5703, 2007.

[iii] S. Tan, X. Huang, & B. Wu, "Some fascinating phenomena in electrospinning processes and applications of electrospun nanofibers," Polymer International, vol. 56, pp. 1330-1339, 2007.

[iv] S. Agarwal, A. Greiner, & J. H. Wendorff, "Electrospinning of manmade and biopolymer nanofibers—progress in techniques, materials, and applications," Advanced Functional Materials, vol. 19, pp. 2863-2879, 2009.

[v] I. Steyaert, L. Van der Schueren, H. Rahier, & K. De Clerck, "An Alternative Solvent System for Blend Electrospinning of Polycaprolactone/Chitosan Nanofibres," in Macromolecular Symposia, 2012, pp. 71-75.

[vi] F. Bragança & D. Rosa, "Thermal, mechanical and morphological analysis of poly (ε‐caprolactone), cellulose acetate and their blends," Polymers for Advanced Technologies, vol. 14, pp. 669-675, 2003.

[vii] D. Rosa, C. Guedes, F. Casarin, & F. Bragança, "The effect of the M w of PEG in PCL/CA blends," Polymer testing, vol. 24, pp. 542-548, 2005.

[viii] R. Kusumi, Y. Inoue, M. Shirakawa, Y. Miyashita, & Y. Nishio, "Cellulose alkyl ester/poly (ε-caprolactone) blends: characterization of miscibility and crystallization behaviour," Cellulose, vol. 15, pp. 1-16, 2008.

[ix] Y. Nishio, K. Matsuda, Y. Miyashita, N. Kimura, & H. Suzuki, "Blends of poly (∈-caprolactone) with cellulose alkyl esters: effect of the alkyl side-chain length and degree of substitu tion on miscibility," Cellulose, vol. 4, pp. 131-145, 1997.

[x] R. Konwarh, N. Karak, & M. Misra, "Electrospun cellulose acetate nanofibers: the present status and gamut of biotechnological applications," Biotechnology advances, vol. 31, pp. 421-437, 2013.

[xi] Z. Khatri, K. Wei, B.-S. Kim, & I.-S. Kim, "Effect of deacetylation on wicking behavior of co-electrospun cellulose acetate/polyvinyl alcohol nanofibers blend," Carbohydrate Polymers, vol. 87, pp. 2183-2188, 2012.

[xii] Y. Xu, C. Wang, N. M. Stark, Z. Cai, & F. Chu, "Miscibility and thermal behavior of poly (ε-caprolactone)/long-chain ester of cellulose blends," Carbohydrate Polymers, vol. 88, pp. 422-427, 2012.

[xiii] Z. Khatri, R. Nakashima, G. Mayakrishnan, K.-H. Lee, Y.-H. Park, K. Wei, & I.S. Kim, "Preparation and characterization of electrospun poly (ε-caprolactone)-poly (l-lactic acid) nanofiber tubes," Journal of Materials Science, vol. 48, pp. 3659-3664, 2013.

[xiv] R. Xiong, N. Hameed, & Q. Guo, "Cellulose/polycaprolactone blends regenerated from ionic liquid 1-butyl-3-methylimidazolium chloride," Carbohydrate polymers, vol. 90, pp. 575-582, 2012.

[xv] S. Ali, Z. Khatri, K. W. Oh, I.-S. Kim, & S. H. Kim, "Zein/cellulose acetate hybrid nanofibers: Electrospinning and characterization," Macromolecular Research, vol. 22, pp. 971-977, 2014.

Salt Gradient Solar Pond Heat Transfer Model for Lahore

S. Kanan[1], M. Asim[2], M. Amjad[3,*], R. Kumar[1], M. Farooq[3]

[1] School of Mechanical, Aerospace and Civil Engineering, University of Manchester, M13 9PL, Manchester, UK
[2] Mechanical Engineering Department, University of Engineering & Technology Lahore, Pakistan
[3] Mechanical Department, Mechatronics and Manufacturing Engineering (City Campus), University of Engineering & Technology Lahore, Pakistan
[3]amjad9002@uet.edu.pk

***Abstract*—**A solar pond with salt gradient is a system used to collect, convert and store heat energy absorbed from solar energy. Basic salt gradient operation in a solar pond is presented in this study. A numerical model is developed and simulated for mass and heat transfer behavior of a solar pond. Pond's water temperatures and salt concentration distributions are observed. The results are obtained for the climatic conditions of Lahore and established that system is viable to operate in this climatic condition.

***Keywords*—**Solar Pond, Solar Thermal Energy Lahore, Solar Pond Heat and Mass Transfer.

I. Introduction

Solar energy is widely available renewable and clean energy resource with its direct use as solar radiation and indirect use as wind, biomass, hydro, and ocean and wave energy [i]. The global annual energy consumption in 2013 was approximately 0.154 Million TWh, which is very less than the solar energy availability on earth. [ii] Pakistan lies in a region with sufficient potential for solar thermal application. The annual average solar insolation is 5-6 kWh/m^2.day with 8-10 sunshine hours a day [iii].

Solar pond is a water reservoir which is used for solar energy collection and storage. For a normal water body, hot water rises to the surface when sunlight heats up the water, and exchanges its heat with surface air. The salt gradient solar pond technology controls this process of hot water heat loss with depth by the salt concentration, makes a density gradient at the middle layer. The difference of salt concentration acts as membrane to avoid mixing. The pond is 1 to 3 meter deep with the black color lined bottom surface to increase solar energy absorption. The solar pound has three salt gradient layers as shown in Fig. 1. Upper Convective Zone (UCZ) is the top layer, which is cold and in contact with ambient conditions, having lowest salt concentration. The thickness of UCZ layer is normally from 10cm to 40cm. The Non Convective Zone (NCZ) is the second layer, it works as insulator. The thickness of this layer is from 60 - 100m. The bottom layer is Lower Convection Zone (LCZ) with highest salt density and works as heat storage layer. The salt density in NCZ is more than UCZ and less than LCZ, this creates a non-convection layers system which inhabits heat transfer between layers by thermal convection. The conductivity of water is lower and solar radiation passes NCZ to LCZ and get absorbed. The temperature of bottom layer is almost constant and in can be up to 100°C [iv]. Solar pond area varies with the heat energy requirement and application. Solar pond is used for multiple applications such as water desalination, refrigeration, cooling and heating in buildings and low temperature heat application in industry.

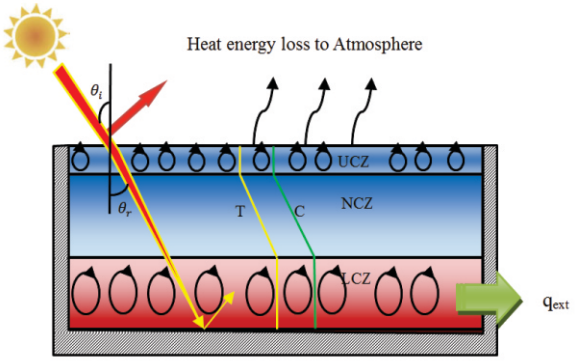

Fig. 1. Construction of simple salt gradient solar pond

Many studied have been carried out about salt diffusion and heat transfer with in solar pond to predict its performance. Researchers of [v] was the first who presented the mathematical model to study behavior of salt gradient solar pond. He analyzed processes like absorption of solar radiation, heat energy loss to atmosphere and ground surface. He used partial differential equation and obtained the analytical solution for the transient temperature distribution of the solar pond. Reference [vi] designed a salt gradient solar pond for experimental plant. The pond was used to investigate the behavior and use of solar pond for collection and seasonal storage of solar energy. Authors of [vii] has predicted the time-dependent behavior of the interface between the convecting and the non-convecting zones of the solar pond by developing a numerical model. Reference [viii] modified the

Weinberger model for two-zone simple pond with Lower and Non Convective Zones only.

For solar pond models with complex boundary conditions, numerical methods are suitable. The authors of [ix-xii] used finite difference method for solar pond. Reference [xiii] used a finite element method to develop and simulate a one-dimensional model and studied the dynamic performance of a salt-gradient solar pond. Researcher [xiv] also used finite element method.

In this paper, simple mathematical equation (one dimension) model for mass and heat transfer is used to simulate solar pond located in Lahore (31.5497° N, 74.3436° E) Pakistan. The temperature profile for the pond layers is analyzed for the month of May and salt concentration behavior is observed for 2 year period. The 22 years monthly average solar insolation and weather data for Lahore is shown in Table I.

TABLE I
MONTHLY AVERAGE WEATHER DATA FOR LAHORE [XV]

Month	Insolation kWh/m^2 day	Ta °C	V m/s	RH %
January	3.31	10.6	3.77	53.9
February	4.3	13.5	3.89	49.2
March	5.41	19.6	3.94	40
April	6.53	26.2	4.08	30.2
May	7.34	30.6	4.42	30
June	7.26	32.5	4.53	39.4
July	6.14	30.1	3.68	63.5
August	5.69	28.4	3.34	71
September	5.58	26.8	3.59	61.8
October	5.04	22.9	3.67	42.3
November	4.01	17.7	3.82	38.2
December	3.24	12.5	3.85	45.9

II. Mathematical Formulation

The mathematical heat equation of salt gradient solar pond is solved in Matlab.

A. Solar Radiation and Heat Transfer in Pond

The solar radiation penetration in the water body is not linear. Reference [xvi] proposed an exponential formula for solar energy penetration in the pond.

$$\frac{H_x}{H_o} = \left\{0.36 - 0.08 \ln\left(\frac{x}{\cos\theta_r}\right)\right\} \quad (1)$$

where
H_O =Mean monthly solar insolation on horizontal (W/m^2)
Hx =Incident solar radiation flux at depth $^1x^1$ (W/m^2)
θ_r =Angle of refraction for Pond's surface

The angle of refraction can be calculated from Snell's law and zenith angle, declination angle and hour angles from basic solar energy equations. [xvii]

The heat transfer system model for solar pond is shown in Fig. 2 The value of depth $^1x^1$ is zero at surface and increases towards bottom of the solar pond. For this work mathematical model is developed for energy balance in each layer of the pond.

Each layer energy input is equal to energy absorbed/stored and energy loss by that layer.

For UCZ energy balance is described the following equations;

$$[H_o + q_{cond1}] = [H_1 + q_{loss}] + \rho C_p \frac{\partial T}{\partial t} X_{UCZ} \quad (2)$$

where
q_{loss} = pond surface total heat loss including evaporation (q_e), convection (q_c) and radiation (q_r).[xviii, xix]
ρ = Density of sodium chloride brine (kg/m^3)
Cp=NaCl brine specific heat (kJ/Kg.°C)

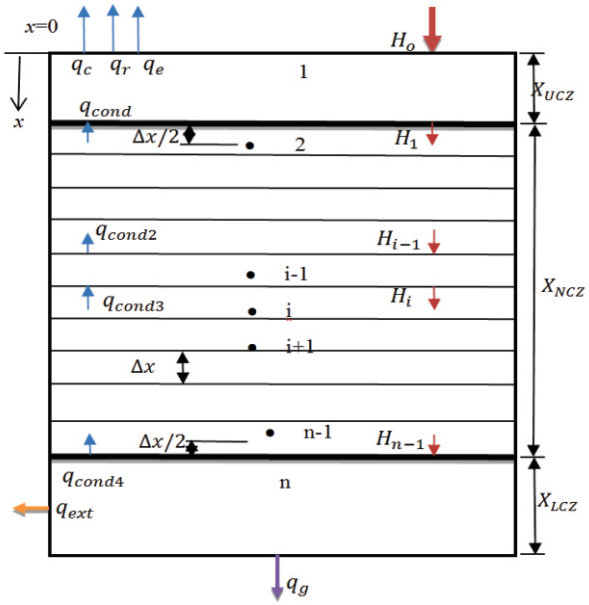

Fig. 2. Representation of solar pond's mathematical model.

The convection heat transfer between atmosphere and upper layer depends on wind speed and temperature difference between atmosphere and pond's surface.

The finite difference equation for UCZ heat balance for temperatures can be written as;

$$T_1^{i+1} = T_1^i + \frac{\Delta t}{\rho C_p X_{UCZ}}\left[(H_o - H_1) + k\left(\frac{T_2^i - T_1^i}{\frac{\Delta x}{2}}\right) - q_{loss}{}^i\right] \quad (3)$$

where;

k = NaCl brine thermal conductivity (W/m °C)

X_{UCZ} =Thickness of UCZ

The boundary for NCZ ranges from 2 to n-1 and energy balance for this layer is written as;

$$[H_{i-1} + q_{cond3}] = [H_i + q_{cond2}] + \rho C_p \frac{\partial T}{\partial t} \Delta x \quad (4)$$

The finite difference equation for NCZ heat balance for temperatures can be written as;

$$T_i^{j+1} = T_i^j + \frac{\Delta t}{\rho C_p \Delta x}\left[(H_{i-1} - H_i) + k\left(\frac{T_{i+1}^j - T_i^j}{\Delta x}\right) - k\left(\frac{T_i^j - T_{i-1}^j}{\Delta x}\right)\right] \quad (5)$$

The thickness of LCZ is X_{LCZ}, the heat balance equation can be written as;

$$[H_{n-1}] = [q_{cond4} + q_{ext} + q_g] + \rho C_p \frac{\partial T}{\partial t} X_{LCZ} \quad (6)$$

The finite difference equation for LCZ heat balance for temperatures can be written as;

$$T_n^{j+1} = T_n^j + \frac{\Delta t}{\rho C_p X_{LCZ}}\left[(H_{n-1}) - k\left(\frac{T_n^j - T_{n-1}^j}{\frac{\Delta x}{2}}\right) - q_{ext}{}^j - U_g(T_n^j - T_g^j)\right] \quad (7)$$

where, U_g= Ground over all heat transfer coefficient [xx]

B. Mass Transfer Model for Solar Pond

During operation of solar pond different mass transfers processes occur due to temperature, heat and density gradient. In the NCZ diffusive mass-transfer occurs, whereas in UCZ and LCZ convective mass-transfer occurs. For this model, total mass of pond is constant with in fix volume, and only molecular diffusion creates mass transfer. Thermal gradient based mass transfer is neglected. The one dimensional mass transfer in x direction with thickness of Δx in NCZ is written as:

$$\frac{\partial}{\partial x}\left(D \frac{\partial C(x,t)}{\partial x}\right) = \frac{\partial C(x,t)}{\partial t} \quad (8)$$

This equation can be transformed for salt concentration as;

$$C_{(i)}^{j+1} = \frac{D\Delta t}{\Delta x^2}\left[C_{(i-1)}^j - 2 * C_{(i)}^j + C_{(i+1)}^j\right] + C_{(i)}^j \quad (9)$$

where;

C = Salt concentration (kg/m^3)

D = Diffusion co-efficient of saline water (3×10^{-9} m^2/s) [xxi]

The mass transfer equation for UCZ is as:

$$D \frac{\partial C}{\partial x} = \frac{\partial C}{\partial t} X_{Ucz} \quad (10)$$

The mass transfer equation for LCZ is as:

$$-D \frac{\partial C}{\partial x} = \frac{\partial C}{\partial t} X_{Lcz} \quad (11)$$

The above equation the initial conditions of salt concentrations are assumed for UCZ and LCZ as 10kg/m^3 and 178 Kg/m^3 respectively with linear distribution in NCZ.

III. Methodology

The heat and mass transfer equations (3), (5), (7), (9), (10) and (11) have been solved by MATLAB codes to obtain the temperature profile and salt concentration of the solar pond. The boundary conditions are shown in the Fig.2. The NCZ is divided into equally sized layers (n-1). Where it is assumed that n=100, Δx = 0.01m and Δt =300 sec.

The upper and lower convective zones are supposed as one grid point. The explicit formulation of numerical stability criterion is

$\tau = \alpha \Delta t / \Delta x^2 \leq 0.5$, where α is thermal diffusivity.

The results are obtained from simulation with monthly average solar insolation on a horizontal surface and monthly average ambient temperature and. From Lahore weather data, 22 years monthly average insolation is 7.34 kWh/m^2.day and ambient temperature is 30.6ºC for the month of MAY is used. In the simulation the input data used as; pond depth of 2m, thermal diffusivity and thermal conductivity of saline water are 3×10^{-9} m^2/s, and 0.566 W/m ºC respectively. The specific heat, density and thermal diffusivity of saline water at constant pressure and temperature of 40ºC with salinity of 10% NaCl by mass are 3758.3 J/kg. ºC, 1063.8 kg/m^3 and 1.4156×10^{-7} m^2/s respectively. The thicknesses of upper, non-convective and lower zones are 0.30m, 1.0 m and 0.70m respectively. The other parameters used are ground heat loss kg = 2.15 W/m ºC [xxii] and Tg = 23.2 ºC at Lg = 6m depth [xxiii].

This simulation outputs are pond three zones temperatures and salt concentration profile inside zones. The start time of simulation is 1st January and ends on 31 December for one year and the output of one month used input to next month. The initial temperature of pond is considered at 25°C.

VI. Results and Discussion

A. Solar Pond Temperature Distribution Profile

The temperature of solar pond depends on pond's depth and is shown in Fig.3. The selected month is May as the maximum average solar energy available in this month. The result shows that pond's temperature increases with increase in depth. The maximum temperature is at LCZ in the end of month is about 67°C including heat loss to surface and ground. After two weeks of time; temperature in LCZ rose with respect to

depth and is about 50°C. The next month simulation starts with this temperature and heat availability thus produce high temperature and more heat energy. The available heat energy can be extracted and used for any application for heating, cooling or thermal process.

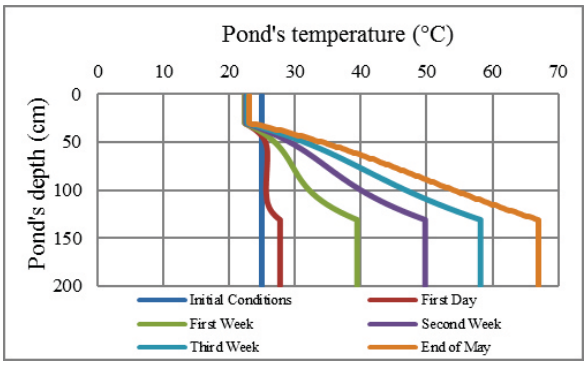

Fig. 3. Temperature profiles in solar pond in the month of May

B. Solar Pond Salt Concentration Profile

For the selected duration of simulation (1st to 31 MAY), the salt concentration for solar pond is shown in Fig. 4. The UCZ has lowest (10kg/m^3) and LCZ has highest (178kg/m^3) salt concentration, the concentration of NCZ is supposed as linear. During simulation time the concentration in zones changes but its effect is negligible as system is stable.

The simulation was also run for one and two year time period to observe the effect on salt concentration inside pond with long time operation. The results showed that for UCZ the salt concentration is increasingly continuously both for 1st year and second year as shown in Fig. 4.

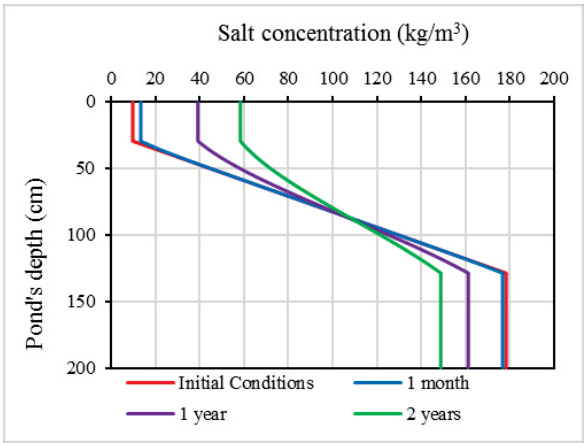

Fig. 4. Solar pond salt concentration profile

For LCZ the salt concentration has decreased continuously in both of the years. This is due to mass transfer and salt concentration diffusion over the long time period. It is assumed that fluid inside the pond is static. The change of concentration will disturb the NCZ layer and can be avoided by replacing the brine in the LCZ after few months.

C. Heat Extraction from Solar Pond

The simulation runs from 1st of January to 31st December for a complete year. The heat is extracted in summer season from April to October. Different loads are applied to extract heat from pond and the respective pond temperature with NCZ thickness is shown in Fig. 5.

The heat extracted from the pond for 24 hours each day. It is clear that more the load less will the pond LCZ average temperature. The maximum temperature is in month of July and the LCZ temperature depends upon heat extracted, ambient and initial temperature, solar radiation and relative humidity. Comparing the weather conditions of June, July and August, the pound temperature and heat energy is availability is more than other months of the year.

The more the heat is extracted the lower the LCZ temperature and vice versa with the given heat extraction the temperature more than 60°C which can be used for heating, cooling and other thermal energy application. The pond temperature in winter season is lower but it's enough to use as domestic hot water for washing and bath.

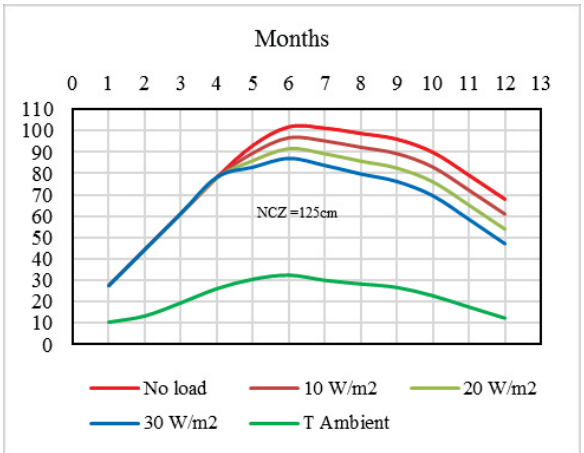

Fig. 5. LCZ monthly maximum temperature with heat extraction

D. Simulation Validation

Researcher [xii], carried out similar simulation for salt gradient solar pond for Iraq. The simulation results were in good agreement with the experimental work.

V. Conclusions

This paper work was to simulate both mass and heat transfer model of salinity gradient based solar pond and investigate the potential of using solar pond in Lahore climatic conditions. The temperature distribution and salt concentration of the different

layers were studied. The following conclusions are established;

- Solar ponds work as collector and storage systems and can provide handsome amount of thermal energy during summer. The hot water can be used for multiple thermal energy applications.
- The efficiency of solar ponds is in range of 15-20 % similar to Photovoltaic system and can be easily used in rural or remote areas for multiple application i.e. fruit drying and water desalination.
- With1.25m NCZ thickness, the maximum temperature of LCZ is 101°C without load extraction and 87°C with 30W/m^2 load extraction in month of July. The total power output for a typical (100 ×100) m^2 pond is 300kW. This model can also have same output during summer with temperature 70-80 °C.

NOMENCLATURE

Symbol	Quantity	Units
C	Salt concentration	kg/m^3
C_p	Specific heat capacity of salt water	J/kg °C
D	Salt diffusion coefficient	m^2/s
h_c	Convective heat transfer coefficient	W/m^2°C
H_O	Monthly average insolation incident on horizontal surface	W/m^2
H_x	Incoming radiation flux at depth x	W/m^2
k	Thermal conductivity of NaCl brine	W/m °C
q_c	Convection heat transfer	W/m^2
q_{cond}	Conduction heat transfer	W/m^2
q_e	Evaporation heat transfer	W/m^2
q_{ext}	Heat extracted from the pond	W/m^2
q_g	Heat loss to the ground	W/m^2
q_{loss}	Pond's surface heat loss	W/m^2
q_r	Radiation heat transfer	W/m^2
RH	Relative humidity	%
T	Temperature	°C
T_a	Ambient temperature	°C
T_g	Ground water temperature	°C
t	Time	s

REFERENCES

[i] B. Sorenson "Renewable Energy Focus Handbook"; Elsevier Ltd, ISBN:9780123747051, Ch.6.1, Pg,321,2009

[ii] Global Energy Statistical, Yearbook2014, http://yearbook.enerdata.net/

[iii] U. K. Mirza, M. M. Maroto-Valer and N. Ahmad, "Status and Outlook of Solar Energy use in Pakistan". Renewable and sustainable energy review 7(2003) 501-504

[iv] C. Angeli, & E. Leonardi "A one-dimensional numerical study of the salt diffusion in a salinity-gradient solar pond". International journal of heat and mass transfer, 47(1), pp.1-10, (2004).

[v] H. Weinberger "The physics of the solar pond". Solar Energy, 8(2), pp.45–56, (1964).

[vi] D. Tinaut and A. Calera (1987), "Design of the C. S. I. C. Research Salt Gradient Solar Pond", Solar Energy Utilization, Springer Netherlands. 129: 519-524.

[vii] K. A. Meyer, "A Numerical Model to Describe the Layer Behavior in Salt-Gradient Solar Ponds." ASME. J. Sol. Energy Eng. 1983;105(4):341-347.

[viii] A. Rabl, & C. E. Nielsen, "Solar ponds for space heating" Solar Energy, 17(1), pp.1-12, (1975).

[ix] H. Rubin, B. A. Benedict, S. Bachu, "Modeling the performance of a solar pond as a source of thermal energy" Solar Energy, 32, pp.771-778, (1984).

[x] J. R. Hull, "Computer simulation of solar pond thermal behaviour" Solar Energy, 25, pp.33-40, (1980).

[xi] K. Hüseyin, M. Ozkaymak, and A. K. Binark. "Experimental and numerical analysis of sodium-carbonate salt gradient solar-pond performance under simulated solar-radiation."Applied energy 83(4), pp. 324-342, (2006).

[xii] S. Kanan, J. Dewsbury and G. Lane-serff. "A Simple Heat and Mass Transfer Model for Salt Gradient Solar Ponds" International Journal of Mechanical, Aerospace, Industrial, Mechatronic and Manufacturing Engineering, Vol 8, pp27-33 (2014)

[xiii] Z. Panahi, J. C. Batty, and J. P. Riley. "Numerical simulation of the performance of a salt-gradient solar pond."J. Sol. Energy Eng. ;(United States) 105(4), (1983).

[xiv] T. S. Jayadev, and J. Henderson. "Salt concentration gradient solar ponds-modeling and optimization." Proceedings of International Solar Energy Society. Atlanta, vol. 1, pp. 1015-1019, (1979).

[xv] NASA (2014). "Surface meteorology and solar energy." renewable energy source website 6. Retrieved 30-11-2014, 2014.

[xvi] H. C. Bryant, and I. Colbeck. "A solar pond for London?"Solar Energy 19(3), pp.321-322, (1977).

[xvii] Jaefarzadeh, M. Reza. "Thermal behaviour of a small salinity-gradient solar pond with wall shading effect."Solar Energy 77(3), pp.281-290, (2004).

[xviii] V. V. N. Kishore, and V. Joshi. "A practical collector efficiency equation for nonconvecting solar ponds."Solar Energy 33(5), pp. 391-395, (1984).

[xix] K. Hüseyin, F. Halici, and A. K. Binark.

"Solar pond conception—experimental and theoretical studies."Energy conversion and management 41(9), pp. 939-951, (2000).

[xx] J. R. Hull, J. Nielsen and P. Golding. "Salinity gradient solar ponds." (1988).

[xxi] J. Srinivasan "Solar pond technology. "Sadhana (Academy Proceedings in Engineering Sciences). Vol. 18. Indian Academy of Sciences, 1993.

[xxii] S. J. Bash AlMaliky, "Investigation of the Readiness of Ground Soils for the Installation of Ground Heat Exchange Systems in Baghdad City." Journal of Geography and Geology 3(1), pp.200, (2011).

[xxiii] A. A. Karamallah, H. M. Hussen, H. A Hoshi, "Experimental model of ground-source heat pump." The 7th Jordanian International Mechanical Engineering Conference (JIMEC'7), Sept. (2010).

Institution-wise Feasibility for Establishment of Inter-Disciplinary Postgraduate Engineering Program in Southern Punjab

S. U. Abdi[1], K. Iqbal[2]

[1] *Engineering Management Department, University of Ottawa, Canada*
[2] *Systems Engineering Department, University of Arkansas at Little Rock, USA*
[1]umerabdi@hotmail.com

Abstract **-** Southern Punjab region has remained largely deprived after 68 years of independence when it comes to higher education in engineering & technology or development of industrial research culture. Due to political, socio-economic, cultural, and geographical reasons more than 60 million people living in this region have faced lack of opportunities to higher education in engineering and professional development. In this paper a feasibility study is conducted for possible establishment of a postgraduate level inter-disciplinary engineering program in Southern Punjab region to fill this gap. A successful inter-disciplinary engineering management program at *University of Ottawa* is adopted as a model. The institutions of higher learning in Southern Punjab are evaluated for their preparedness to institute such a program on a matrix of indicators. The study determines that establishment of such program will allow engineers, architects and town planners from multiple disciplines to acquire higher education and develop managerial and entrepreneurial skills in close proximity to their homes. The study concludes that such a program is feasible, highly desired and can be launched with minimum additional financial and human resources.

Keywords: Engineering Management, Feasibility, Evaluation Matrix

I. Southern Punjab: Background & Statistics

Southern Punjab is the home ofover one-third of the population of Pakistan. Southern Punjab region does not have well-defined geographical boundaries, but may be defined in terms of the Seraiki belt, i.e., the region where Seraiki is spoken as the mother tongue. Unofficially, the lower 3 divisions of Punjab, i.e., Multan, Bahawalpur, and Dera Ghazi Khan are considered Southern Punjab. These divisions comprise of 11 districts with a total area of 99,572 sq. km (48.5% of the total area of Punjab Province). This shows that area wise the southern Punjab region is almost half of the Punjab province [i]. In addition, southern parts of Sahiwal and Sargodha divisions are included in the Seraiki Belt.

Punjab province inhabits more than 56% ofcountry's population. Almost, 36% of its rural inhabitants are poor, 2nd highest among the provinces of Pakistan. The Seraiki belt can be easily categorized as the underprivileged part of Punjab based on several development or welfare indicators. As compared to rural parts of Sindh province where the incidence of poverty is 31-35%; rural Southern Punjab has a higher level of poverty documented up to 50% [ii]. Other studies [iii] place poverty in Southern Punjab at40%, which is at par with rural Khyber Pakhtunkhwa and Balochistanprovinces. Three districts of Punjab (Lodhran, Muzaffargarh and Rajanpur from Southern region of province) show least recorded literacy rate (30.23% and below) in the survey. Whereas remaining eight districts of South Punjab have lower level (30.23-45%) of literacy rate [iv] compared to districts located in Northern regions of Punjab.

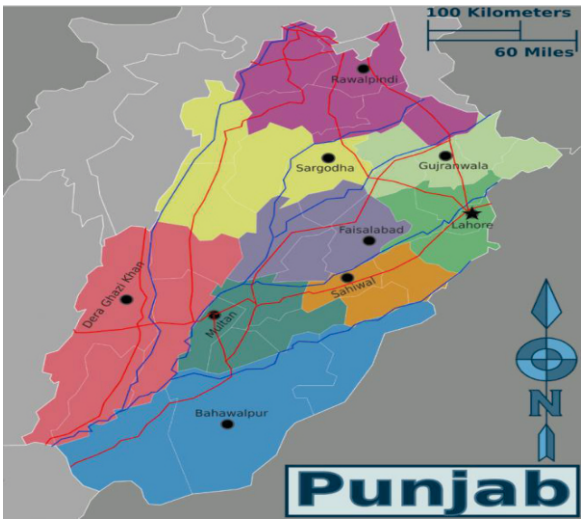

Fig. 1. Map of Punjab province (Division-wise)

Southern Punjab hostsseveral high-tech and process industries including power generation, fertilizer manufacturing plants, crude and edible oil refineries, textile spinning and weaving units, uranium, minerals, oil & gas reserves, nuclear power plants,

sugar and ghee mills, tobacco manufacturing facilities and cement industries. Despite recent initiatives from Federal and Provincial governments for improving higher education in the region, only two post graduate engineering programs in Electrical and Civil Engineering are available [v, vi] with very limited intake for engineers to improve their technological skills in this industrially rich but educationally deprived region that was a hub of knowledge, tradition and civilization for several centuries. This has resulted in lack of sustainable development, absence of industry-academia linkage, and non-availability of multi-disciplinary programs to incubate entrepreneurial activities and solve technical and managerial problems of the local industry.

In the year 2014-15, Punjab government distributed Rs. 48.31 billion, more than twice as compared toprevious year's funding, for 532 development projects for education (325 under process& 207 new schemes), which included Rs.14.05 billion for higher education**.** Although, Northern Punjab performed well on education indicators, Southern Punjab continued to lag behind due to poor planning and lack of execution. Home to one third of country's population, South Punjab has only two public sector universities (general category) and one recently established federally chartered degree awarding institute dedicated for engineering and technology education. A couple of Federal Institutes have established campuses in Southern Punjab; however, they only provide limited opportunities for higher education and research in the engineering field.

II. Higher Education as Precursor to Development

"Education is better safeguard of liberty than a standing army" is a legendary quote of Sir Edward Everett (1794-1865), Governor of Massachusetts state in USA and President of Harvard University [vii]. It has become a universal human right anda vital component to grab opportunities and gain empowerment [viii]. Higher Education is the key to sustainable development in a society asthis hasan impact on productivity effects and reduced income inequality [ix]. There is a substantial positive correlation between economic productivity and education. Life Satisfaction Index and Material Wealth Index also identify Higher Education as Indicator of Prosperity in Life [xxvii].

Education is the most significant instrument for human resource development.When individuals are educated, their living standards improve as they gain access to productive ventures, which eventually improves in their livelihoods [x]. Education melts away ignorance and fundamentalism in society, leading to a critical mind combined with knowledge, wisdom and tolerance, thus preventing corruption, crime and environmental damage in society [xxvii].

Higher incomes are associated with higher level of education. US Census Bureau reports higher earnings ratio of people with higher qualification Fig. 2. The purpose of education is not only to impart knowledge and skills which enables the recipients to perform as agents for economic and social change in the community, but also to increase the substantial impacts on ideologies, ambitions and rationales, which are essential prerequisites for the progression of sustainable development [xi]. The up-front linkage between studies is through development of skill-set, which as a result increases opportunities for well-paid productive employment, consequently, facilitating people to fully exploit their potential confidently [xii].

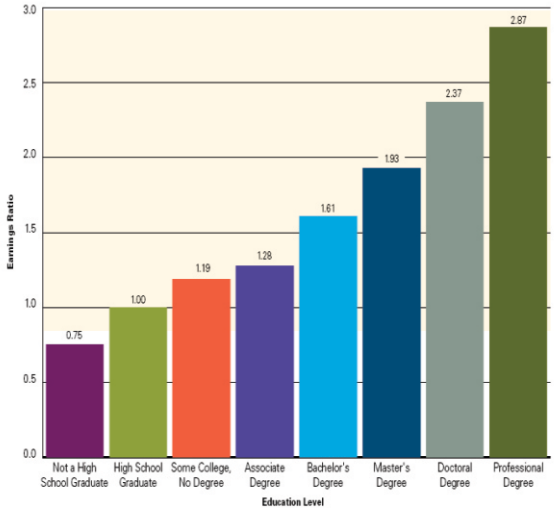

Fig. 2. Life Time Earnings of people with different education levels [xxvii]

Higher education ensures sustainable economic development and prosperity in the society. It also generates improved economic conditions; regrettably, disadvantaged countries like Pakistan face considerable economic deficiency as far as higher education is concerned [xiii]. Poor quality education system may be one of the most vital rationales why deprived countries like Pakistan remain underdeveloped [xv]. Quite interestingly, deficient areas in Pakistani society like lack of Liberty, Freedom of Choice, Exploitation of Innovation, Capital Investment and Good Governance belong to subsets of Education [xxvii].

Human capital development studies correspond that it is infact the human resources of a country (and not its capital or natural resources) that finally determine the speed of its economic growth, and social development. Education hasa significant inverse relationship with poverty as it provides employment opportunities and rejects poverty [viii]. The real wealth of any nation is its people who strive to develop new ideas and then create processes and mechanism to bring wealth to the society [xxvii]. Development studies related to Southern Punjab have consistently advanced

the possibilities for development and progress in higher education in this region. The development process aims to eradicate poverty and ongoing displacement based on region's resources, institutes and cultures. One factor that proves to lessen inequality and poverty has been the investment in human capital, which is replicated in the investment to development of knowledge and professional skills [xv].

As of 2007, only 6% Pakistanis (9% male and 3.5% female) were university graduates. This figure is expected to increase to 10% until 2015 and 15% by 2020 [xiv]. Government of Pakistan spends only 2% of GDP on Education (primary to tertiary level) for the last one decade of which major portion is spent on recurrent expenses like staff salaries leaving behind a very small budget for quality enhancement, faculty development, and establishment of new programs.

III. Significance of Master's Program in Engineering Management

Engineers equipped with technical management skills can better contribute in developing economies of countries like Pakistan. The developingcountries are facing challenges like sustainability, technology innovation and environmental protection, necessitating a need for integration of technical and management skills to counter these problems. There is an emerging need for organizations to integrate technical and business skills to solve these difficulties [xvi]. This is especially true in Pakistan where mega construction projects and industrial development particularly in the fields of energy, transportation, manufacturing and mining are expected to occur in the coming years. Thus, there is a dire need to establish an educational setup where engineers can acquire advanced management skills to outperform in their fields.

Universal trend demonstrates that engineers who are well-versed with the principles of business and management are bestowed with leadership responsibilities in an organization. Understanding ability ofadvanced technology and conforming management strategy is basic essence behind securing a competitive position in any high-tech firm or public sector organization. Due to emerging interdependence between technology, industry, economy and society, more opportunities would be available for engineers to use their potential as leaders, not only in business but also in the multinational and government organizations [xvii]. In today's competitive environment, employers seek technical people that not only understand technology they use, but also know the business needs of the company. According to Engineers of 2020, a report published by the National Academy of Engineering, business savvy attitude and leadership potential are among the desirable skills for future engineers [xxvii].

Research on approachesto improve engineering education has identified management and innovation skills as essential to success in an engineering career. Researchers [xviii] also believe that engineering curricula that do not address innovation and higher-level technical management are depriving students of essential competencies for engineering success in the global marketplace. Such deficiency precludes career enrichment and advancement in public and private sector, and perhaps more significantly, makes it harder for them to reach their full potential. Progressive organizations increasingly desire interdisciplinary knowledge of both engineering and management [xix] of their employees. These facts clearly demonstrate that there is ever increasing demand for engineering professionals to acquire management and entrepreneurial skills [xx].

A Master's program in Engineering Management is distinctive due to its highly integrated nature. Such program can fulfil the demand of professionals in the fields of business knowledge, technology entrepreneurship, technical management and engineering in the complex environment of technology driven industry. Engineering Management program enables engineers to think on a broader spectrum in a wider world; they are not just bound in a single paradigm. In addition to doing technical jobs, they can compete in money making and knowledge making business and consultancy. Engineering Management program enables the graduates to factor in business related issues in their decision making. This program also reduces resources required for training fresh engineers in management. The combination of management concepts and technical focus presented in Engineering Management program allows new graduates and working professionals to acquire the management skills necessary to excel in today's technical world. Engineering Management program also encourages development of 'Business Eco-system' design, a process to develop an environment to incubate entrepreneurial activities, especially technology start-ups, and to create jobs for the workforce.

Unlike a Master's degree holder in Science or conventional Engineering disciplines, Engineering Managementdegree offers business perspective needed by technical managers. Compared to traditional MBA programs, an Engineering Management program emphasizes skills suited for technology-based organizations. Fig. 3 [xvi] compares the expected acquisition of skill set for an engineer entering Masters in Business Administration or Master's in Engineering Management degree program.This is why World's top notch universities like Georgia Tech, Stanford University, MIT, University of Ottawa and number of others mentioned in Appendix I offer successful inter-disciplinary MS Engineering Management program. American Universities listed in Appendix II and

identified in [xxvi] also offer PhD program in Engineering Management.

It may be worthwhile to note that as per Agenda No. 7 of 59th EA&QEC meeting of Pakistan Engineering Council a body which regulates engineering programs in Pakistan, MS Engineering Management is considered as an 'engineering degree' in Pakistan.The Higher Education Commission (HEC) and the National Business Education Accreditation Council (NBEAC) in Pakistan recommended 3.5 years of study for engineers who wish to get an MBA degree [xxi-xxii]. Comparatively, only 1½-2 years are required to get a Master's in Engineering Management with an option of getting a degree with thesis or simply on course work basis.

MEM graduates have brighter job prospects of becoming CEOs, Chief Operating Officers, Chief Technology Officers, Entrepreneurs, General Managers, Production and Manufacturing Managers, Business Analysts, Technology Consultants, Business Strategists and academicians in Engineering Management faculties around the globe.

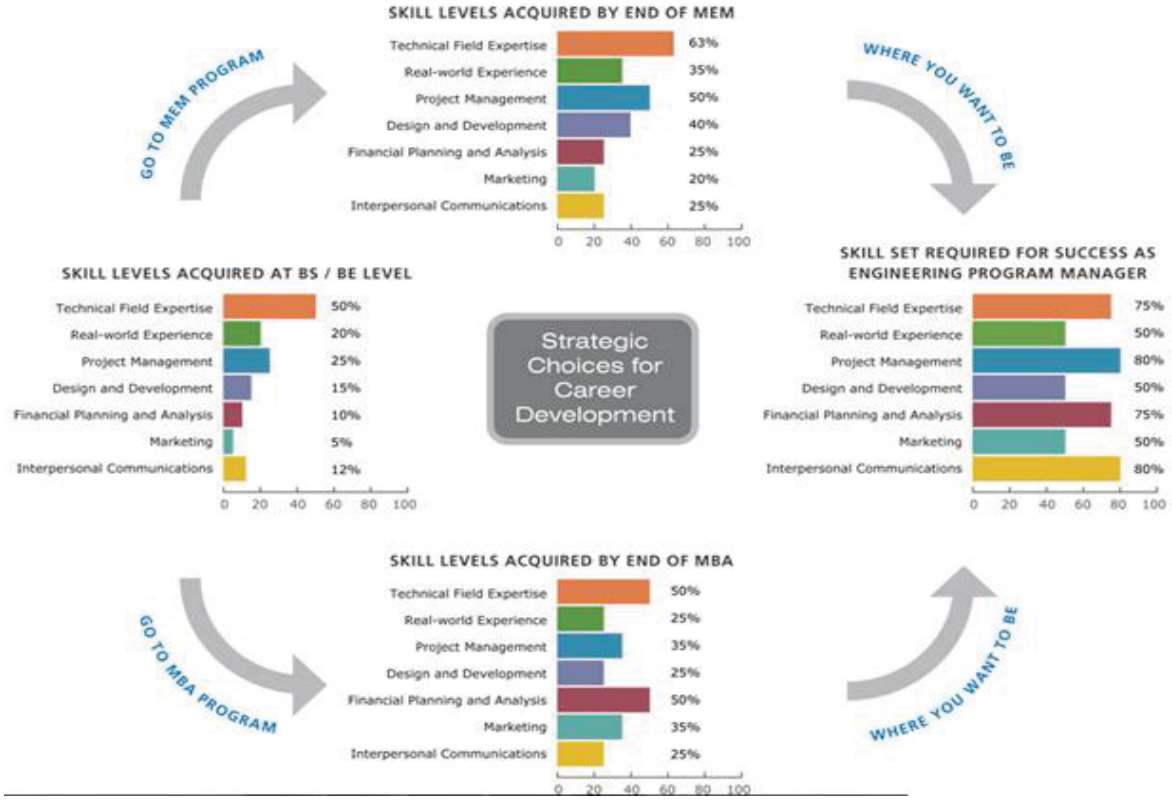

Fig. 3. MBA v/s MEM: An outcome based comparison [xvi]

IV. University of Ottawa Model of Masters of Engineering Management

The Masters of Engineering program in Engineering Management at University of Ottawa, Canada is run by sharing resources from Faculties of Engineering, School of Information Technology& Computer Science, and Telfer School of Management. Professors from different faculties teach Engineering Management courses, and Engineering Management students attend classes with Business Administration, Engineering or Computer Science students to study the courses of their choice to complete their credit hours. Class rooms, computer labs, library and admin staff are also shared by different departments. There is minimum expenditure to run this inter-disciplinary program as it hardly requires sophisticated research lab facilities, and courses taught in this program are of generalized nature. Despite the above stated facts, MEM is a highly popular program among students due to the availability of diversified courses and research areas. Due to its high demand, the MEM program offers admissions three times a year and has a higher merit as compared to conventional M. A. Sc. and M. Eng. admissions three times a year and has a higher merit as compared to conventional M. A. Sc. and M. Eng. programs. Most importantly, the MEM program generates handsome revenue for Canada's capital university and fulfils the higher education needs of engineers working in technology parks andhi-technology industries around theregion.

The essence behind the success of the inter-disciplinary MEM program is a peaceful environment and streamlined educational and administrative system of University of Ottawa, Canada. This is supported by excellent inter-departmental communication,

coordination and tolerance to share resources and faculty, and flexibility offered to the students to select any graduate level course offered in the entire university. This helps the students to tailor their degree according to their professional needs and make the MEM program high in demand for the North American employers. University of Ottawa is among top universities in the World [xxiii] with its Telfer School of Management among top most North American business schools [xxiv] located in Canada's National Capital Regionandnear World's largest Project Management Institute and World's 2nd largest IT industry in the Kanata region [xxv].

V. Resource Availability for Instituting a MEM Program in Southern Punjab

Feasibility Study to establish an inter-disciplinary Master's program in Engineering Management (based on University of Ottawa model) at Higher Education Institutes in Southern Punjabwas carried out through surveys. Institutions were evaluated on the basis of availability of PhD faculty, charter of institution, geographical location, operational engineering programs and financial resources. As per the University of Ottawa model, existing Engineering and Business programs will be required to contribute towards a proposed postgraduate Master's in Engineering Management program.

The resource availability and preparedness of these institutions towards initiating an MEM programs was studied through an evaluation matrix (Table I) that measured these institutions on the following factors: engineering programs, business programs, postgraduate programs, PhD faculty, accreditation, industry, industrial liaison, admission strategies, and infrastructure. The following study discusses the practicality of starting MEM program at institutions of higher learning in Southern Punjab. The results are tabulated at the end of the study (Table II).

TABLE I
THE EVALUATION MATRIX TO ASSESS RESOURCE AVAILABILITY AT SOUTHERN PUNJAB INSTITUTIONS OF HIGHER LEARNING.

Resource Availability					
	Engineering Programs	Bachelor's level multi-disciplinary engineering programs	Bachelor's level engineering programs in 3 or more disciplines	Bachelor's level engineering programs in 1 or 2 discipline	No bachelor's level engineering program
	Business Programs	Offers both BBA and MBA degrees	Offers BBA and plans to offer MBA and MS degrees	Offers BBA only	No business program but have program in computer science
	Postgraduate Programs	Postgraduate programs in both engineering and business administration	Postgraduate program in business administration	Postgraduate program in computer science	No postgraduate program
	PhD Faculty	Experienced PhD faculty in engineering and business admin.	PhD faculty in businessadministration / management	PhD faculty in engineering and computer sciences	Limited PhD faculty
	Accreditation	PEC, NBEAC, HEC	PEC and HEC	NBEAC and HEC	Only HEC
	Industrial Presence in Vicinity	Several industrial units with technical manpower / engineers	Corporate Offices and Service Industry only	Some Industrial Units	Limited presence of industry (3 or less)
	Industrial Liaison	Strong industry-academia linkage.Joint research & consultancy projects	Managed to get R&D funded projects, internships and trainings	Establishing Contacts with Local Industry	Limited industry–academia linkage
	Admission Campaigns & Marketing Strategy	Well-developed and managed admission campaigns. Availability of need based and talent scholarships	Institute is renowned and already have tough competition for admissions and scholarships	Developing marketing strategy for institute. Admission campaigns and scholarship hunts are in progress	Little or no attention towards admission campaigns and marketing of institute
	Academic & Civil Infrastructure	Fully furnished academic blocks, library, lecture theatres, research labs	Shared academic blocks, class rooms and labs	Academic Block, shared labs and class rooms	Rental building, no labs, limited class rooms
		Excellent = 4	Good = 3	Fair = 2	Poor = 1
		Maximum Score: 36			

A. COMSATS IIT, Sahiwal Campus

Available academic and administrative resources at COMSATS Institute of Information Technology, Sahiwal are nearly adequate to successfully launch and run a broad spectrum MS program in Engineering Management with minimalcapital and recurring costs. Such a program will be popular and is expectedto generate higher revenue than the current MS programs in Management, Computer Science and Bio-Sciences. Lecture theatres, class rooms, library and academic blocks are already available on campus during evenings / weekends, and can be improved with the passage of time, for potential EM students. It is noted that the Institute is already running an executive MBA program on weekends.

CIIT Sahiwal hasfour Engineering Management graduates from World's renowned universities and Project Management Professional certified among its faculty. It also has seven PhDs each in Mechanical Engineering and Management Sciences departments, six PhDs in Computer Sciences department, two in Civil Engineering, and three in Electrical & Computer Engineering department, as well as several faculty members enrolled in PhD programs in different local universities who can teach a diversified variety of core and elective courses and supervise research projects. Since this institute is running under the administrative control of Federal Ministry of Science & Technology, the availability of funds would not be an issue. It is recommended that Engineering Management program should run under the administrative control of well-established Mechanical Engineering department.

CIIT Sahiwal is located on almost central location on Lahore-Multan G.T Road. It has in close proximity engineering industries like Engro Foods, FaujiFresh n Freeze Pak Pattan, Yousafwala Grid Station, Michell'sOkara, Lakson Tobacco, Philip &Moris Tobacco Okara, Qadirabad Coal Fired Power Plant, Ittefaq Sugar Mill Pakpattan, as well as engineers working in service industry like PTCL, MEPCO, Sui Gas and Cellular Network Providing Companies. A majority of those engineers will be candidates for admission into the MEM program when it is launched.

CIIT Sahiwal has strong and well-established network of admission campaigns, career counselling and marketing. It can easily motivate engineers working in industries in this region to improve their qualification in evening/weekends.CIIT Sahiwal can expect a higher number of students in the proposed MEM program. It is so because of high demand and lack of competitors in the region, who offer a similar kind of unique program from which architects, town planners and engineers from any background can equally get benefit.

B. NFC Institute of Engineering & Technology, Multan

NFC IET Multan was established in 1994 after it was upgraded from Technical Training Centre of National Fertilizer Corporation. NFC IET is the oldest engineering institution in Southern Punjab, and was once the only engineering institution from Lahore to Hyderabad. The institute imparts engineering education in Chemical, Electrical, Petroleum & Gas, Civil and Mechanical Engineering in addition to Bachelor's program in Business Administration, Computer Science, Environmental Science and several BS Technology programs.

NFC IET have PhD faculty in Civil, Mechanical, Chemical, Environmental, Computer and Power Engineering;five MBAs, two MPhil Computer sciences, and several faculty enrolled in PhD in Engineering and Computer Science disciplines who can teach a variety of core and elective courses.After being declared an independent Federal Degree Awarding Institution in 2012, NFC IET has launched new programs in engineering, technology and other non-engineering disciplines. Teaching staff, who have years of industrial and teaching experience, but could not get Master's degree due to non-availability of such opportunity in the region, can take admission in the pioneer batch of MEM and after completing this degree, can start teaching the forth coming batches.

NFC IET has an advantage of well-established research laboratories and industrial liaison with process industries nationwide.In addition to fresh engineers, architects and town planners who are still looking for jobs, potential students could include professional engineers working in industries in 150 Km radius such as KAPCO, PARCO, Pak Arab fertilizers, AES Lalpir, Rousch power plant, Nestle Food, Fauji Kabirwala Power plant, SNGPL, WAPDA/NTDC, DG Cement, Fatima Sugar & Textile mills, PAEC's uranium fields etc. These corporate employees can pay a higher tuition fee and can easily come to attend classes on evening / weekends.

C. Bahauddin Zakariya University, Multan

Located in Multan, Bahauddin Zakariya University (BZU) is the largest university of south Punjab. It is a degree awarding institute in more than 60 disciplines, including Pharmacy, Medical, Engineering, Humanities, Business Administration, Law, Art, Music, Computer/IT/Telecom, Agriculture and Languages. Subsequent to a presentation delivered to the Vice Chancellor and Registrar of BZU on the potential for establishment of MEM program, the following observations were recorded: BZU hasthree PhD faculty members in College of Agricultural Engineering and 4 PhDs in Institute of Computing to teach MS Telecommunication program. Faculty of Engineering & Technology at BZU, comprised of College of Engineering & Technology, Institute of Advanced Materials and College of Textile Engineering, collectively have six dedicated PhD faculty members and several who are enrolled in PhD

programs in engineering disciplines in local universities. These faculty members can teach diversified elective courses and supervise projects in their own areas of interest. Three existing PhDs, and others with M.Phil. degrees in Management/Business Administration, who arefaculty members at the Institute of Management Sciences, can easily take care of core management courses to be taught in the MEM program. BZU Multan has recently started MS programs in Electrical and Civil engineering.

Cost-Benefit Analysis made on the request of Campus Director an initial setup of MEM program at BZU Sub-campus Sahiwal is given in Appendix III. If proper marketing strategy is adopted, BZU Multan can expect more students in the MEM program because of its high demand and absence of competitors in the region. However, deficiency of inter-departmental coordination and sharing of administrative and human resources, students' union strikes, and intervention of political elements has been observed and confirmed from a number of sources inside the University.

D. The Islamia University of Bahawalpur

The Islamia University of Bahawalpur is one of the two public sector universities in Southern Punjab. It has University College of Engineering & Technology imparting Electrical Engineering education at undergraduate and postgraduate level with different specializations. UCET IUB, which is already running MS Electrical Engineering program with couple of specializations, hasthree permanent PhD faculty members and several others with postgraduate qualification in Electrical or Computer Engineering. This college serves the need of higher education in Engineering for the people of Bahawalpur, R.Y Khan, Fort Abbas, Bahawalnagar districts. Launch of Master's level Engineering Management program in UCET IUB is feasible due to availability of PhD faculty in Faculty of Management Science. Potential students / target beneficiaries includeengineers from Fauji Fertilizer Company and Fatima Fertilizers Ltd. Sadiqabad, Liver Brothers R. Y. Khan, and several sugar and ghee mills in the area.

E. Namal College, Mianwali

Founded by Imran Khan in 2008, the college began as a technical training and diploma awarding institute, and now awards University of Bradford degrees for its undergraduate programs. Presently, the college offers two academic programs: four-year engineering degree program, namely a BEng (Hons) in Electrical and Electronic Engineering and a four-year computer sciences undergraduate program of BSc (Hons) in Computer Science.Namal College has attracted six PhDs each in their Computer Science and Electrical Engineering faculty. Prof. Dr. Muhammad Abbas Chaudhary, PhD Engineering Management from USA and former Vice Chancellor of UET Taxila is also serving on the faculty.

A proposal to establish an Engineering Management program at Namal College was forwarded to Director Administration of the college.If a post-graduate program in Engineering Management is launched at Namal College, professional engineers working in Pak-American Fertilizers and Maple Leaf Cement in Iskanderabad; Salt Mines of Kala Bagh, Nuclear power plant in Chashma and service industry of adjoining areas like Bhakkar, Khushab, Layyah, Nowshera and Mianwali can benefit from it.

F. MNS University of Engineering & Technology, Multan

Mohammad Nawaz Sharif UET Multan was running under administrative control of UET Lahore, has recently received charter from Govt. of the Punjab foran independent university status recognized by HEC. This is in-fact the very first initiative of Government of Punjab to establish a dedicated Engineering & Technology University in Southern Punjab. Classes for Engineering and Technology programs were temporarily started in buildings of Government College of Technology, Multan. This nascent institution is not yet ready to launch a Master's level program on its premises.

G. Air University Multan Campus

Air University, a Federally Chartered University, opened its campus in 2011 at Multan on the then Prime Minister Yousaf Raza Gillani's initiative to cater the need of students of Southern Punjab and adjoining areas of KPK, Balochistan and Sindh provinces. The Campus operates in a rented building in Multan cantonment area. Management and Computer Science departments are operational which offer undergraduate and graduate programs in Business Administration, CS, Maths and Economics. Launch of Electrical and Computer Engineering programs are being planned in Phase II, subject to land acquisition and construction of purpose-built campus in the suburbs of Multan, for which land at Bahawalpur Bypass has already been acquired. Although Air University has managed to attract PhD faculty in Management, Mathematics, Computer Science and Economics,its Multan Campus is pre-mature for launch of any postgraduate level engineering program pending the construction of a purpose-built campus and a well-established engineering department.

H. Institute of Southern Punjab

Institute of Southern Punjab, Multan is the very first and only degree awarding private institute in Southern Punjab and has established purpose-built campus on Bosan Road near BahauddinZakariya University's main campus. The Institute has Southern School of Engineering & Technology, which is offering

Bachelor's program in Electrical and Civil Engineering, for which Pakistan Engineering Council has also given green signal. However, scarcity of PhD faculty and permanent staff is currently a hindrance in the start of a postgraduate level engineering program at ISP.

I. Quantitative Comparison of Resource Availability

Table II offers a quantitative comparison in terms of resource availability at eight Southern Punjab institutions of higher learning for possible launch of a MEM program. As seen from the table, COMSATS, Sahiwal, and BahauddinZakariya University Multan exhibit highest preparedness for instituting a MEM program. The Islamia University, Bahawalpur also has similar readiness in terms of resource availability. The remaining five Southern Punjab institutions, however, need to strengthen their existing engineering and business programs to qualify for a launch of MEM program at their campus.

TABLE II
INSTITUTION-WISE COMPARISON OF RESOURCE AVAILABILITY TOWARDS LAUNCH OF INTER-DISCIPLINARY ENGINEERING

		COMSATS IIT Sahiwal	NFC IET Multan	BZU Multan	IU Bahawalpur	Namal College Mianwali	MNS-UET Multan	AU Multan	ISP Multan
Resource Availability	Engineering Programs	3	3	4	3	2	2	1	2
	Business Programs	4	2	4	4	3	1	4	4
	Postgraduate Programs	3	1	3	3	2	1	3	3
	PhD Faculty	4	2	4	4	2	2	3	1
	Accreditation	3	3	4	4	2	3	2	1
	Industrial Presence in Vicinity	4	4	4	3	4	3	4	3
	Industrial Liaison	4	4	3	3	2	2	4	2
	Admission Campaigns & Marketing Strategy	4	2	3	3	4	1	4	2
	Academic & Civil Infrastructure	4	4	4	4	4	1	4	3
		33	25	33	31	24	16	26	21

VI. Concluding Remarks

Quality higher education is vital in promoting economic progress and an affluent lifestyle of people in any geographical region. Higher education is positively correlated with better quality of life, better infrastructure and working conditions, prosperity, poverty alleviation, improved social fabric, law & order situation and decline in terrorism, some of the challenges faced by our country.

Residents of Southern Punjab have long been deprived of opportunities toward higher education in engineering and technology. Feasibility study and feedback received from Engineering Institutes in Southern Punjab state that a graduate level multi-disciplinary engineering program in Engineering Management can be launched with low capital cost, minimum recurring expenditures, nominal additional faculty and administrative resources.

Launch of a postgraduate engineering program at the geographically central region of Pakistan will link professional engineers with universities and institutions of higher education that will not only benefit people of Southern Punjab, but also serve adjoining areas of KPK, Sindh and Baluchistan. Such an initiative will spawn technology innovation and development of entrepreneurial skills, and promote industry-university liaison. It will initiate business &technology incubation and provide inter-disciplinary research culture to solve technical management problems of the industry as well as socio-economic problems of the people. In conclusion, establishment of post-graduate engineering management program in Southern Punjab will strengthen the industry-university liaison and provide quality higher education to the loving and soft spoken people of this educationally deprived region.

References

[i] *Special Report on Southern Punjab* (2012), Youth Parliament of Pakistan.

[ii] Gazdar, Haris (1999) *Poverty in Pakistan: A review*. In Shahrukh R. Khan (Ed.), *50 years of Pakistan's economy: Traditional topics and contemporary concerns*, pp. 241-326. Oxford, Karachi, etc.: Oxford University Press.

[iii] Federal Bureau of Statistics (2002). *Poverty in the 1990s' PIHS*, Government of Pakistan: Islamabad.

[iv] *Literacy Trends in Pakistan* UNESCO Report (2003). http://unesco.org.pk/education/life/nfer_library/Reports/4-39.pdf.

[v] University College of Engineering & Technology, Bahauddin Zakariya University, Multan http://www.bzu.edu.pk/v2_engineering.pdf.

[vi] The Islamia University of Bahawalpur College of Engineering http://www.iub.edu.pk/department.php?id=14.

[vii] William B. Fowle, *"The Common School Journal and Educational Reformer"* (1852), recorded in, p. 28.

[viii] I. S. Chaudhry, S. Rahman (2009) *"The Impact of Gender Inequality in Education on Rural Poverty in Pakistan: An Empirical Analysis"* European Journal of Economics, Finance and Administrative Sciences.

[ix] N. Birdsall, D. Ross, R. Sabot (1995). Inequality and growth reconsidered: lessons from East Asia. The World Bank Economic Review, 9(3), 477-508.

[x] Nconco. F. (2006). *"A comparative study of leadership and management approaches in further education and training colleges."* A PhD Education submitted dissertation, Nelson Mandela Metropolitan University.

[xi] R. E. Anderson, S. Dexter "School technology leadership: An empirical investigation of prevalence and effect." Educational Administration Quarterly 41, no. 1 (2005): 49-82.

[xii] Aikman, S. and Unterhalter, E. (2005). "*Beyond access: Transforming Policy and Practice for Gender Equality in Education*." London: Oxford.

[xiii] A.R. Chaudhary, A. Iqbal, S. Y. M. Gillani (2009). "The Nexus between Higher Education and Economic Growth: An Empirical Investigation for Pakistan. "Journal of Commerce and Social Science, Vol.3, pp. 137-145.

[xiv] UNESCO Institute for Statistics. (2009) http://www.uis.unesco.org/Library/Documents/ged09-en.pdf.

[xv] Aisha Khan (2009) *Education Order in Punjab: A District Level Study*. Centre for Research in Economics and Business, Lahore School of Economics.

[xvi] Engineering Management programs consortium, USA. http://www.mempc.org/whyMEM.Lee, J. J. Lee, S. Y. Kang, J. H. Heo Lee, Joosung

[xvii]J So Yeon Kang, and Jun-Haeng Heo. "Business and management competency of engineers: Curriculum and assessment." In Education Engineering (EDUCON), 2010 IEEE, pp. 295-302. IEEE, 2010.

[xviii] C. J. Steiner, (1998) "Educating for Innovation and Management: The Engineering Educators' Dilemma" IEEE Transactions on Education, Vol 41, No. 1.

[xix] Korea Industrial Technology Association, (2007) *"University Science and Technology Education that Companies Desire"*.

[xx] Kim, E. H., (2002) "*Threats and Opportunities for Science and Engineering Human Capital Resources Supply*" Samsung Economic Research Institute.

[xxi] National Business Education Accreditation Council http://www.nbeac.org.pk/index.php/roadmap

[xxii] Higher Education Commission of Pakistan http://www.hec.gov.pk/insidehec/divisions/aeca/curriculumrevision/documents/roadmapbusinesseducation.pdf.

]xxiii] TIMES Higher Education World Ranking of Universities https://www.timeshighereducation.com/world-university-rankings/university-of-ottawa?ranking-dataset=1083.

[xxiv] QS Top MBA 2014-15 Business School Report http://www.topmba.com/mba-rankings/region/us-canada/2015#sorting=rank+custom=478983+order=desc+search

[xxv] University of Ottawa, Engineering Management program. http://www.grad.uottawa.ca/Default.aspx?tabid=1727&page=SubjectDetails&Kind=M&SubjectId=233.

[xxvi] Ipek Bozkurt, (2014) "*Quantitative Analysis of Graduate Level Engineering Management Programs*" IEEE Technology Management Conference (ITMC) pp 1-8.

[xxvii] Asrar Sheikh, (2008) *"Prosperity through Education and Research"* Keynote speech in IEEE ICEE.

APPENDIX I

World renowned universities that offer successful Masters of Engineering Management programs include:

USA:

University of California at Berkley, University of Michigan, UCLA, Purdue University, University of

Wisconsin at Madison, University of Illinois at Urbana Champaign, Virginia Polytech University, Texas A&M University, Ohio State University, Iowa State University, Kansas State University, Wayne State University, University of Louisville, University of Colorado New Jersey Institute of Technology, University of Pennsylvania, Missouri University of Science and Technology, George Washington University, University of Southern California, University of Florida, Stevens Institute of Technology, California State University, Columbia University, Florida Institute of Technology, George Washington University, John Hopkins University, Penn State University, Rochester Institute of Technology, Stevens Institute of Technology, Syracuse University, University of Texas at Arlington, University of Wisconsin, University of New Orleans,

Canada:
University of Alberta, Memorial University of New Foundland, University of Waterloo, University of Calgary

Saudi Arabia:
King Fahd University of Petroleum and Minerals, King Saud and King Abdul Aziz University

Korea:
KAIST, Yonsei University, Seoul National University

China:
Peking University, Tsinghua University, Dalian University of Technology, Wuhan University, Shanghai - Jiaotong University, Harbin Institute of Technology, Beijing Institute of Technology, University of Science & Technology Beijing, Huazhong University of Science & Technology, University of Science & Technology China, UCAS

EU:
Oxford University, Swiss Federal Institute of Technology, London South Bank University, University of Warwick, University of York, Teesside University, University of Warwick, Technical University of Denmark, Istanbul Technical University

Pakistan:
NUST E&ME College Rawalpindi, GIK Institute Topi, UET Lahore and Taxila, University of Lahore, NED Karachi, QUEST Nawabshah, MUET Jamshoro, CASE and MAJU Islamabad.

APPENDIX II

American Universities offering PhD in Engineering Management.

Airforce Institute of Technology, George Washington University, Missouri University of Science & Technology, Oklohoma State University, New York Institute of Technology, Old Dominion University, Southern Methodist University, Stevens Institute of Technology, Texas Tech University, University of Alaska Fairbanks, University of Huntsville Alabama, University of Tennessee Space Institute, Western New England University, Michigan Technological University, Norwich University

APPENDIX III: COST BENEFIT ANALYSIS

Keeping in view resource requirements at BZU sub-campus Sahiwal and after having detailed discussion with Campus Director; a rough estimate for *kick starting* MEM program is as follows:

Expenditure:
01 Associate Professor / HoD = Rs.195,000/-month
PhD + experience + publications (fixed Salary /all inclusive) = Rs. 2,340,000/year
01 Asst. Prof/Conv. Admissions & Campaign
= Rs. 130,000/month
PhD Qualified / MS 4 years' exp. (Fixed Salary /all inclusive) = Rs. 1,560,000/year
01 Lecturer = Rs. 70,000/month
(MS Engg Mgt. qualified) = Rs. 840,000/year
01 Visiting Faculty Member = Rs.50,000/Sem
(MEM qualified hourly remuneration 2 courses)
= Rs.100,000/year
01 Naib Qasid = Rs. 15,000/month
Salary / year = Rs. 180,000/year
Cost of Marketing / Admission Campaigns in 150 Km Radius = Rs. 200,000/year
TOTAL COST = Rs. 5,220,000/year

Earnings:
Admission Fee = Rs. 25,000 (at time of admission only) X 45 = Rs. 1,125,000/-
Tuition Fee = Rs. 45,000/semester/student X 45 students X 2 semesters/year = Rs. 4,050,000/-
Exam Fee = Rs. 5,000/semester X 45 students X 2 semesters / year = Rs. 450,000/-
Security = Rs. 10,000/ semester X 45 students / year
= Rs. 450,000/-
Registration Fee = Rs. 2,000/ semester X 45 students X 2 semesters / year = Rs. 180,000/-
Library Fee = Rs. 1,500 / semester X 45 students X 2 semesters / year = Rs. 135,000/-
TOTAL EARNING =Rs. 6,390,000/-

TOTAL REVENUE / YEAR
= Earning *minus* Expenditure
= Rs. 6,390,000/- *minus* Rs. 5,220,000/-
= Rs 1,170,000/-

Estimated Profit of Rs. 1.17 Million per year

Flame Resistance of Chemical Protective Clothing Materials at Various Washing Intervals

M. Ijaz[1], S. Kalsoom[2], N. A. Akthar[3]

[1]Lahore College for Women University, Lahore, Pakistan
[2]Govt. College of Home Economics Lahore, Pakistan
[3]University of Engineering and Technology, Taxila, Pakistan
[1]mehreenijaz@hotmail.com

***Abstract*—**The study investigates the fire resistance of chemical protective clothing materials over repeated number of washing cycles. This research work was experimental in nature, performed and completed at a reputable textile mill. The sample of protective coveralls was collected from fertilizer-manufacturing units. These coveralls were evaluated for their fire-resistant ability through the determination of after-flame time and char length by following Vertical Flame Test ASTM D 6413. An experimental fabric was manufactured with various construction parameters to improve the results. Data was presented in the form of mean±S.D along with their minimum and maximum value. The results of experimental and existing clothing materials were compared. The conclusion drawn from this study was that the existing clothing materials failed to meet the international requirements and their condition became even worse with the repeated washing. Whereas, experimental clothing material performed well even with repeated laundering. These findings can be helpful for the manufacturers to review and alter the construction parameters to develop protective coveralls for the safety of workers.

Keywords—Protective Clothing, Fire Resistance, After-Flame Time, Char length, Washing Cycles.

I. Introduction

In a typical setup at a chemical industry, workers are threatened by toxic chemicals, fumes or gases. These threats may cause severe injuries and casualties [i]. Number of different chemicals is used in different industries. Behavior, nature and reaction of chemicals vary so much that safety becomes a cumbersome task. However, considering the serious nature of threats, safety measures become pertinent [ii]. Industries in both, public and private sector need protective clothing for safeguarding their employees against such hazards. Accurate protective ensembles can help the wearer to get a few extra seconds of escape [iii].

Chemicals when exposed to different atmospheric conditions or other chemicals, may respond in the form of a chemical reaction. Nature of chemical reaction depends on number of factors such as temperature and types of participating chemicals. In an industrial setup, such chemical reactions are routine; small sparks or temperature-change may result in big fire. Ignition, fuel and oxygen are necessary elements for a fire. Therefore presence of toxic chemicals with plenty of oxygen in a chemical industry poses fire-hazard-threats. Fire never burns at the same rate/speed. Some fuels burn quickly and others burn slowly. Chemical composition, amount and available oxygen affect the speed of burning [iv].

The chemical structure of fibers determines its behavior under given conditions. Chemical behavior determines the flammability of yarns and fabrics. For example, fibrous polymer, a thermally stable polymer, has high decomposition temperature and its decomposition reaction is endothermic in nature [v]. Flammability refers to the ease with which a substance may ignite and support a fire. In order to reduce flammability and/or reduce speed of fire, chemicals known as flame-retardants are applied on a flammable materials such as textiles and plastics [vi-vii]. These flame-retardants can be added in the spinning solution for making the yarns or applied on the surface of textile materials to make them resist fire and prevent the burning process [viii]. Compounds of sulfuric and phosphoric acid are usually used as flame retardant for cellulosic and synthetic polymers in textile manufacturing. Phosphoric acid forms a layer of char, which acts like boric acid, borax and hydrated aluminum oxide. It is mostly used in combination with nitrogen. These combinations are effectively used for natural and synthetic textile materials such as cellulose, polyurethane and polyester [iv].

Flammability of fabrics is evaluated based on the nature of burning hazard and fabric's ability to self-extinguish. Self-extinguishing fabric stops burning when flame is removed. The flammable fabric starts burning when exposed to an ignition source for a time period of up to 12 seconds and continues to burn even when flame is removed [v].

Flame-retardant fabrics are designed to resist ignition when exposed to a flame. Flame-retardant fabrics are of two types: inherently and treated flame-retardant fabrics. Inherently flame-retardant fabrics such as aramids have the property of resisting fire without use of additives. This makes them durable even after laundering processes [ix]. Treated flame-retardant fabrics are processed chemically to induce flame-resistant characteristics. They can also be manufactured by laminating or coating of additives on the surface of fabric. These coatings may lose their strength with laundering process [x]. Determining the

effect of laundering on the performance of protective-clothing ensembles involves deep understanding of fabric construction parameters, its geometry, stability as well as the forces that hold within the fabric [xi].

II. Materials and Methods

A total of fifteen chemical protective coveralls (locally-made) were randomly obtained from the fertilizer-manufacturing units and evaluated for their ability to resist fire. The coveralls were categorized into three groups (100% polyester, 100% cotton, and blend of cotton/polyester) based on their fiber content and irrespective of their brand names. The construction specifications of these coveralls are given in the Table I

TABLE I
CONSTRUCTION SPECIFICATIONS OF EXISTING PROTECTIVE COVERALLS

Group	Sample Code	Fiber Content	Fabric Weight (GSM)	Thread Count (per inch)	Linear Density (tex)	
					Warp Direction	Weft Direction
Polyester	P1	Polyester 100%	153	216	17.216	17.938
	P2	Polyester 100%	151	160	18.746	18.981
	P3	Polyester 100%	152	104	36.575	35.542
	P4	Polyester 100%	160	125	15.254	15.968
	P5	Polyester 100%	210	165	29.525	29.525
Cotton	C1	Cotton 100%	257	228	26.599	26.362
	C2	Cotton 100%	208	170	28.946	29.233
	C3	Cotton 100%	141	190	13.451	12.564
	C4	Cotton 100%	223	184	26.013	35.572
	C5	Cotton 100%	143	224	14.726	15.064
Blends	B1	Cotton 97% Polyester 3%	264	142	13.921	14.351
	B2	Cotton 98% Polyester 2%	215	133	15.743	16.236
	B3	Rayon 70% Polyester 30%	145	171	16.53	16.932
	B4	Cotton 95% Polyester 5%	221	136	13.301	15.321
	B5	Cotton 45% Polyester 55%	146	140	19.949	18.806

The samples were laundered by following AATCC Monograph M6 [xii] with front loading machine at a speed of 45±10 rpm. They were washed at 54±2.9°C for about 11±1 minutes while 0.1g/liter ECE reference detergent was added into the machine. The samples were rinsed for about 2 minutes during the first rinsing cycle and for 5 minutes during second rinsing cycle by adding liquid softer. The spinning was carried out at 1300±150 rpm for about 12 minutes. They were tumble dried at 68±6°C for 1.5 hours. All samples of protective coveralls were given 20 laundering cycles. After every 5 cycles, their ability to resist fire was evaluated by conducting Vertical Flame Test ASTM D 6413 [xiii].

Five specimens in lengthwise direction were taken with the measurement of 76mm x 300mm. They were brought to the moisture equilibrium according to the specifications of ASTM-D1776 test method [xiv]. After removing specimen from standard atmosphere, it was exposed to flame within 4 minutes. Test specimen was held by a holder; two clamps at top and two clamps at the bottom of the holder held specimen very tightly. Holder along with the test specimen was inserted into the cabinet; inside the cabinet, burner was placed 19mm below the specimen. The timer for flame was set and the specimen was exposed to it for 12 ±0.2 second. It was noted for its melting or dripping behaviour. In order to note the after-flame time, stop watch was immediately started as soon as the holder along with specimen was removed from the cabinet. Once holder was removed, specimen was allowed to cool down. The char length was measured by making a crease in the specimen through peak of charred area and parallel to the specimen sides.

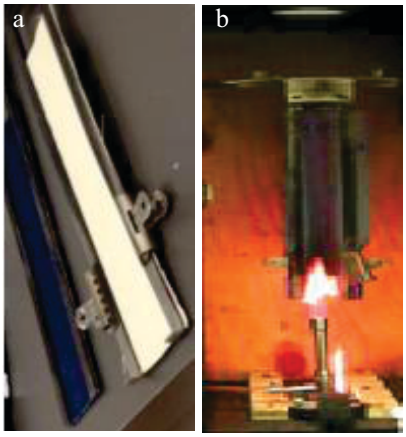

Fig. 1. (a). Samples clamped in the holder (b) Fire tester

In addition to testing existing fabrics, an experimental fabric was manufactured at a reputable textile mill with the aim of achieving better results. A woven fabric was manufactured using ring spun yarns. Inner layer of this fabric was made of a Polyester-Cotton (65 / 35) blended yarn which was treated with a fire retardant agent (FPK 8001). Linear density (warp and weft) was fixed at 19.68 tex. Aramid yarn with a linear density of 15.06 tex for both warp and weft directions was used for the outer layer. Finally plain weave was followed for the interlacing of yarns to make a fabric. The fabric density was 60 ends (per inch) and 5 picks (per inch).

Fabric weight was 135 GSM. According to the of the sample loom, length and width of the prepared fabric was 236 x 19 inches. The construction specifications of the experimental fabric are given in Table II.

TABLE II

CONSTRUCTION SPECIFICATIONS OF EXPERIMENTAL FABRIC

Linear density (Polyester / Cotton blend)	Linear density (Aramid)	Weight	Fabric density (ends/picks)	Thread Count	Length /Width
19.68 tex	15.06 tex	135 GSM	60/55 per inch	115	236 x 19

Lastly, following the same test methods used while testing existing fabrics, this new fabric was laundered and evaluated for its fire-resistance characteristics.

III. Results and Discussion

Table III describes descriptive statistics of all three groups for their after-flame time and char length. The mean value of after-flame time for polyester was recorded at 15.24±0.96 for zero wash and it increased to 48.81±1.13 for 20th wash. After-flame time for Cotton was noted at 6.87±0.36 for zero wash and it increased to 44.69±0.92 for 20th wash. Similarly, mean after-flame time for blend of cotton / polyester was recorded at 14.95±0.93 for zero wash and increased to

TABLE III
FLAME-RESISTANT ABILITY OF EXISTING PROTECTIVE CLOTHING

Washing Cycles	Specimen		After-Flame Time (Seconds)				Char length (Inches)			
		N	Mean	S.D	Min.	Max.	Mean	S.D	Min.	Max.
0	Polyester	5	15.24	0.96	14.20	2.93	2.45	0.50	3.46	2.93
0	Cotton	5	6.87	0.36	6.50	2.49	2.20	0.42	2.98	2.49
0	Blend	5	14.95	0.93	14.10	3.28	3.20	0.10	3.40	3.28
5	Polyester	5	21.82	1.14	20.70	7.39	7.28	0.13	7.54	7.39
5	Cotton	5	15.93	0.95	15.00	5.64	5.40	0.34	6.04	5.64
5	Blend	5	26.09	1.75	24.50	8.68	7.40	1.89	10.86	8.68
10	Polyester	5	34.81	0.91	33.90	9.37	8.10	2.17	11.86	9.35
10	Cotton	5	28.42	1.28	27.40	8.34	7.20	1.48	10.02	8.34
10	Blend	5	33.59	1.62	32.20	9.35	8.90	0.41	9.70	9.37
15	Polyester	5	43.14	2.74	40.10	10.06	9.10	0.94	10.98	10.06
15	Cotton	5	42.85	0.64	42.30	10.06	8.90	1.32	11.50	10.06
15	Blend	5	45.38	1.34	44.20	11.56	10.80	0.66	12.00	11.56
20	Polyester	5	48.81	1.13	47.64	11.13	10.00	1.02	12.00	11.13
20	Cotton	5	44.69	0.92	43.88	10.83	10.00	1.04	12.00	10.83
20	Blend	5	47.64	0.43	47.14	11.73	11.20	0.46	12.00	11.73

47.64±0.43 for 20th wash. Results clearly show that after-flame time rises with increase in number of washing cycles for existing clothing coveralls. The mean value of char length for polyester was recorded at 2.45±0.50 for zero wash and increased to 10.00±1.02 for 20th wash. Charlengthfor cotton was recorded at 2.20±0.42 for zero wash and increased to 10.00±1.04 for 20th wash. Char length for blended fabric was recorded at 3.20±0.10 for zero wash and 11.20±0.46 for 20th wash. There is an increase in char length of existing materials with repeated number of washing cycles.

Lastly, following the same test methods used while testing existing fabrics, this new fabric was laundered and evaluated for its fire-resistance characteristics.

Results and Discussion

Table III describes descriptive statistics of all three groups for their after-flame time and char length. The mean value of after-flame time for polyester was recorded at 15.24±0.96 for zero wash and it increased to 48.81±1.13 for 20th wash. After-flame time for Cotton was noted at 6.87±0.36 for zero wash and it increased to 44.69±0.92 for 20th wash. Similarly, mean after-flame time for blend of cotton / polyester was recorded at 14.95±0.93 for zero wash and increased to 47.64±0.43 for 20th wash. Results clearly show that after-flame time rises with increase in number of washing cycles for existing clothing coveralls. The mean value of char length for polyester was recorded at 2.45±0.50 for zero wash and increased to 10.00±1.02 for 20th wash. Charlengthfor cotton was recorded at 2.20±0.42 for zero wash and increased to 10.00±1.04 for 20th wash. Char length for blended fabric was recorded at 3.20±0.10 for zero wash and 11.20±0.46 for 20th wash. There is an increase in char length of existing materials with repeated number of washing cycles.

Table IV describes descriptive statistics of experimental fabric for its after-flame time and char length. The after-flame time was noted at 0.56±0.05 for zero-wash and increased to 0.86±0.05 for 20th wash. The char length was recorded at 0.50±0.10 for zero wash and increased to 0.63±0.25 for 20th wash.

TABLE IV
FLAME-RESISTANT ABILITY OF EXPERIMENTAL FABRIC

Washing Cycles	After-Flame Time (Seconds)				Char length (Inches)			
	Mean	S.D	Min.	Max.	Mean	S.D	Min.	Max.
0	0.56	0.05	0.50	0.60	0.50	0.10	0.40	0.60
5	0.56	0.05	0.50	0.60	0.50	0.10	0.40	0.60
10	0.60	0.10	0.50	0.70	0.53	0.15	0.40	0.70
15	0.80	0.10	0.70	0.90	0.56	0.15	0.40	0.70
20	0.86	0.05	0.80	0.90	0.63	0.25	0.40	0.90

Figure 2 shows after-flame time of existing and experimental clothing materials. This graph clearly depicts that after-flame time (in seconds) of existing materials increased with every washing cycle whereas, experimental fabric had not significant increase in its after-flame time even at 20th wash. According to the test procedure specifications, after-flame time should not exceed 2 seconds. It was observed that all the three groups of existing materials failed to meet safety standards in regards to protection against fire. Coveralls from the cotton group performed better at zero wash as compared to the other two groups. Experimental fabric recorded after-flame time of less than 2 seconds even at 20th wash. Thus experimental fabric meets the safety standards.

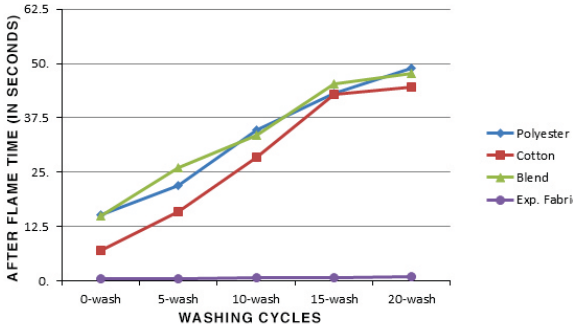

Fig. 2. After-flame time of experimental and existing clothing materials

Figure 3 illustrates char length of existing and experimental clothing materials. This graph clearly shows that char length (in inches) of existing materials increased at a significant rate as the number of washing cycles increased from zero to twenty. On the other hand, experimental fabric had no significant increase in its char length over repeated washings. According to the test method specifications, char length of test specimen should not exceed more than 4 inches. At zero wash, all existing materials passed this test specification. However, with increasing number of washing cycles, their performance dropped drastically. Coveralls from cotton group exhibited better performance than the other two groups but these coveralls also failed to meet 4 inches barrier with increasing number of washing cycles. Experimental fabric recorded a char length of less than 4 inches even at 20th wash. Thus, it passed this test.

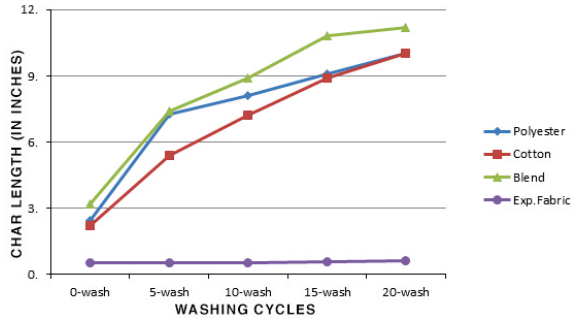

Fig. 3. Char length of experimental and existing clothing materials

One possible reason for poor performance of existing materials was the use of inferior quality finishing, which easily cracked and lost its strength after laundering. It was also highlighted by [xv] that when finish breaks out from the outer layer, it exposes the inner layer directly to the flame. The nature and kind of finish is very important in manufacturing fire-resistant fabrics. As explained by [xvi], cotton and a blend of cotton/ polyester fabrics burn within few seconds and continue ignition until the whole sample is consumed. Polyester fabrics melt and burn easily, if no finish is applied over their surface. Experimental fabric passed the test based on international safety standard because of inherent flame-resistant characteristics of Aramid fiber. On exposure to fire, these fibers swell up and make a barrier between source of ignition and human body. This barrier lasts till it cools thus provides few precious seconds to the wearer to escape [vi]. Moreover, a blend of polyester/cotton yarn was given a flame retardant treatment that did not break even at 20th wash. It was highlighted by [xvii] that an aramid layer in combination with flame-retardant fabric provides better protection to the wearer.

V. Conclusion

Chemical Protective clothing safeguards it wearer from fire hazards. It was concluded that none of the collected sample was able to perform well against fire hazards according to the international test standards. Furthermore, ability of the coveralls to withstand against ignition deteriorated with laundering. Considering the threats posed by chemicals in an industry, high quality protective clothing should be worn by the workers which maintain its performance even after repeated use and laundering. The experimental clothing material met these requirements, as mentioned in international safety-standards. Correct selection of fibers and finishing treatment played a vital role in manufacturing standard-compliant protective clothing.

References

[I] M. Raheel, "Chemical protective clothing", in Protective clothing systems and materials, vol. 25, New York, CRC Press, 1994, pp.39-78.

[ii] Z. N. Jaspal, and N. Haider, "Management of Chemicals in Pakistan: Concerns and challenges", Research Journal of South Asian Studies,vol. 29, no. 2, pp.497-517, Dec. 2014.

[iii] T. E. Neal, and S. L. Lovasic, "Industrial Flash Fire and Burn Injury Fundamentals with an Instrumented Manikin Demonstration of Protective Clothing Performance", in ASSE Professional Development Conference and Exposition., American Society of Safety Engineers, Nashville, Tennessee, 2002.

[iv] C. Stephanie, "Retarding the flame", http://www.selah.k12.wa.us/soar/sciproj2002/StephanieC.html, 2002.

[v] S. Nazare and A.R. Horrocks, "Flammability testing of fabrics", in Fabric testing, H. Jinlian,Ed.vol. 76, New York, CRC Press, 2008, pp.339-385.

[vi] A. Grad, (2013, April). "Specialist work clothing" [online]. Avaliable: http://specialistworkclothing.wordpress.com/2013/04/29/understanding-flame-retardant-fabrics-nomex-cantex-and-proban/].

[vii] A. Pettigrew, "Halogenated flame retardants", in Kirk Othmer's Encyclopaedia of Chemical Technology, New York:John Wiley and Sons, 1993.

[viii] T. U. Onuegbu, E.T. Umoh and I.E. Iwuchukwul, "Flame retardant effects ON flexible polyurethane foam treated WITH potassium aluminum sulphate",ARPN Journal of Science and Technology, vol. 2, no.11, pp.1097-1102, Dec. 2012.

[ix] "Fire retardant clothing requirements for welders and cutters. Workers Compensation", Sep. 2012. [online]. Available: www.wcb.pe.ca/.../Document/pub_fireretardantclothingrequirements.pdf

[x] W. Zhou, N. Reddy and Y. Yang, "Over view of protective clothing" in Textiles for protection, R. A. Scott, Ed. Cornwall, Woodhead publishing limited, 2005, pp.3-25.

[xi] B. Hepworth, "Investigating the dimensional Properties of 1x1 Rib Fabrics" Knitting International, 48-51, July. 1989.

[xii] Standardization of home laundry test conditions, AATCC Monograph M6, 2013.

[xiii] Standard test method for flame resistance of textiles (Vertical test), ASTM D6413, 2013.

[xiv] Standard practice for conditioning and testing textiles, ASTM D1776, 2015.

[xv] H. Makinen and S. S. Mustonen, "Comparing the flammability of fabrics in accordance with EN 531 and ENV 50354, International Journal of Occupational Safety and Ergonomics, vol. 10, no. 3, pp.207-213, July. 2004.

[xvi] Sellers, R. D., & Carr Jr, V. J. (2007). Performance of Nomex Military Uniforms in Attacks by Flame Field Expedient Weapons-A Literature Study. Applied Research Associates, Technical Report, Mar. 2007.

[xvii] M. W. King, X. Li, B. E. Doupe and J. A Mellish, "Thermal protective performance of single layer and multiple layer fabrics exposed to electrical flashovers", in Performance of protective clothing, S. Z Mansdorf, R. Sagar and A. P Nielsen, Eds. Baltimore, American Society for Testing and Materials, 1988.

Expert System for Lean Manufacturing at Tobacco Industry

S. B. Khattak[1], R. Akhtar[2], I. Hussain[3], M. Ullah[4], S. Maqsood[5], I. U. Haq[6]

[1,2,3,4,5] *Industrial Engineering Department , UET Peshawar, Pakistan*
[6] *Institute of Mechatronics Engineering, UET, Peshawar, Pakistan*
[2]rehman_akhtar@uetpeshawar.edu.pk

Abstract- Machine breakdown is inversely proportional to productivity. Breakdowns on critical machines disrupt the desired productivity significantly. To date, many procedures have been deployed to reduce the breakdown time. This paper deals with the application of expert system using the key principles of lean manufacturing. We developed systematic operating procedure to reduce the breakdown time of a specified machine in a cigarette manufacturing industry. In addition, this research explains to industries as how to get expert opinions irrespective of the expert's availability.

Keywords- Expert System, PW-2 Machine, Total Productivity Maintenance, Cigarette Manufacturing

I. INTRODUCTION

All manufacturing organizations are striving to eliminate different types of wastes. Waste minimization is mandatory to stay competitive in any market. Breakdown time that causes delay directly relates to the production capacity of a machine. However, eliminating the variation completely is a daunting task. Hence, to reduce the breakdown time a systematic approach is to be adopted to identify and remove the defects from machine. Availability of spare parts and tools, experts and maintenance procedures are mandatory. Principles of Total Productivity Maintenance (TPM) allow the operator of the machine to do routine maintenance. It is difficult for worker to remember each and every defect of the machine along with its root cause. Furthermore, experts are not always available. Artificial Intelligence (Expert System) helps them to generate a system of expert opinion dealing with machine malfunction and its root causes.

II. LITERATURE REVIEW

In global market intelligent production systems, maintenance techniques and trainings are essential to have a competitive system [i]. Systematic elimination or reduction of unneeded resources or waste is the key principle of lean philosophy [ii].

Knowledge Based Systems (KBS) make decision similar to those of human experts [iii]. It makes decision on the basis of observation and experience depending on how the expert opinions are entered into the expert database.

KBS or Expert System (ES) are the computer programs, which hold a set of rules for user to access the already fed data in specific domains. The main elements of a KBS are shown in Fig. 1. The user with the help of an interface asks queries from the inference engine. These queries could be in the form of push buttons, radio buttons, or even some alphanumeric entry. The knowledge database in a synchronize manner process a specific query. The knowledge base is developed through continuous expert inputs. The expert inputs are incorporated via knowledge acquisition module. The knowledge acquisition module includes different set of questions that are processed by different production rules in the inference engine. Once the production rules are applied to the specific query, the results could be displaced on the screen or in printed form.

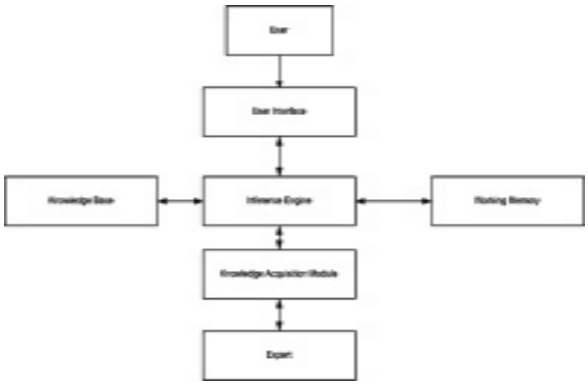

Fig. 1. Components of KBS/ES

Human experts are not always available. In addition, their consistency is doubtful and their reliability is less than hundred percent. They are subject to worldly matters. Expert System can be used everywhere at any time. Over a past couple of decades, expert system applications have been found in almost all the ways of life. The authors in [iv-xiv] have reviewed a number of KB systems applications. Table I summarizes the different applications of an expert system over a period of time.

TABLE I
EXPERT SYSTEM APPLICATIONS IN VARIOUS FIELDS [IX-XXVI]

Application	Contributor (Year)
Job Shop Scheduling	Authors in [ii, x, xx]
Material Handling and Supplies	Authors in [ii, xv, xxvi]
Robots	Authors in [viii, xxiii]
Design of Flexible Manufacturing Systems	Authors in [ii, xxi]
CAD/CAM	Authors in [xxiv, ii, xvi]
Quality Control	Authors in [xix, xi, xii]
Facilities Layout	Authors in [xxv, ix]
Network Problems	Authors in [xiii, xviii]
Health Care	Authors in [xix, xvii]
Military	Authors in [xxii]
Urban Planning	Authors in [vi]

Different commercially available softwares are available to develop ES applications. These softwares have edge over the conventional programming tools. They have a number of facilities, which are lacking in the conventional programs such as ready written sub-routines, strong user interface, ease of integration with various modules and a number of databases etc. Application Manager (AM) is one of the available softwares. It is selected for the application under consideration.

III. Methodology

PW-2 machines are the technologically advanced cigarettes packing and wrapping machines. Millions cigarettes could be processed through it in an 8 hour shift. However, an ordinary breakdown degrades daily production considerably. A PW-2 machine has a built-in display screen. It shows the breakdown title but cannot guide the operator through its root causes for resolving. The operation either has to use his skills or has to engage the maintenance department. Total Productivity Maintenance (TPM) will boast worker ability to do the routine maintenance. An ES consisting of the breakdown along with its root causes can help the worker in effective and efficient problem resolving.

Technological and managerial advancement are very rapid in tobacco industry. Nothing could be proposed or inferred if a system is not studied thoroughly. For on-hand knowledge and experience of the current system, different parameters were identified. These parameters were related to different faults and maintenance procedures. The identification was carried out via literature review and manually recording the breakdowns occurred in many 8 hours long shifts.

With the help of manual sheets data is collected for a number of complete shifts. The data collected is analyzed through Pareto and Five why analysis. Based on these findings, information base is developed. Information base as discussed in Fig. 1 is responsible for keeping the database related to the identified parameters. Information base leads to the development of production rules. Testing phase of the expert system is initiated to remove bugs and errors. Fig. 2 gives a step-wise view of how this research progresses. This figure gives a pictorial view regarding data collection and analysis methods to be deployed for information base development.

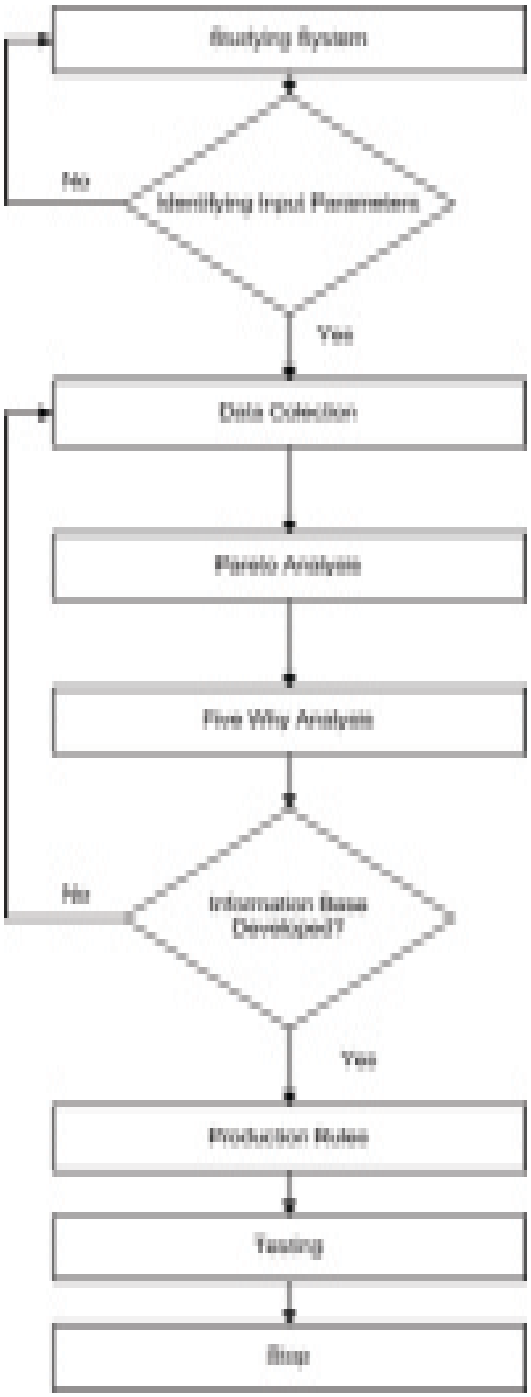

Fig. 2. Analysis Progress

Current system was studied for both operational and managerial perspective. It was unanimously decided to gather an eight hour-long shift data encompassing all types of breakdowns that occur. Manual sheets were initially used which were later transferred to an excel sheet. Table II depicts the type of data collected.

TABLE II
SAMPLE DATA FOR BREAKDOWN OF A SINGLE MACHINE

Sr. No	Run Time	Time (hours)		Detail Of Stoppages	Down time (hours)
		From	To		
1	0:05:00	6:00:00	6:05:00	No Cigarette from hopper detector	0:00:19
2	0:01:21	6:05:19	6:06:40	No Cigarette from hopper detector	0:00:25
3	0:04:04	6:07:05	6:11:09	Magomate problem	0:01:05
4	0:00:08	6:12:14	6:12:22	Blank jam in magazine	0:00:37
5	0:02:08	6:12:59	6:15:07	No Cigarette from hopper detector	0:00:45

For three weeks data is collected for the available three machines simultaneously. The collected data is analyzed with the help of Pareto analysis (i.e., 20% is responsible for 80%). The significant breakdowns both with respect to frequency and downtime are identified. The identified breakdowns are then shared with the maintenance experts to assess the breakdowns and generate data related to Fault Tree Analysis (FTA). Root cause identification is based on Five-Why technique. Fig. 3 illustrates how five why analysis is used for a specific fault. The same procedure was applied to all the identified faults.

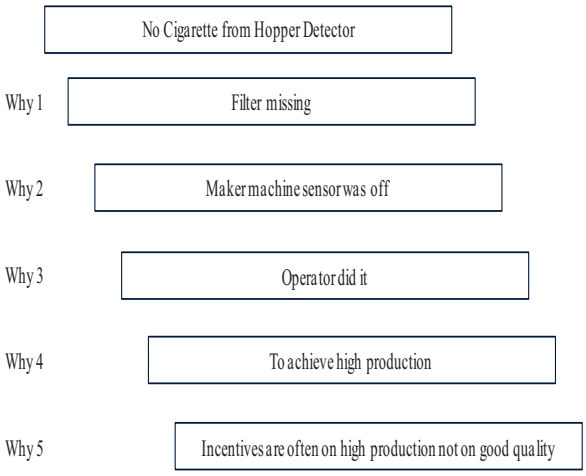

Fig. 3. Deploying Five Analysis

Fig. 3 depicts that "No cigarette from hopper detector" is the main problem. The Five Why analysis revealed that the root cause was related to organization policy and not with the maintenance procedures. The company was more interested in production than quality; hence, the operator would turn off the machine sensor for higher production.

A theme of information base is developed incorporating different production rules of the KBS. The developed ES is then tested on real production line and the improvement and suggestions are documented. Production rules for different breakdowns are developed using IF, AND, THEN, and OR rules. Forward chaining depth strategy is employed to execute rules. Rule for one of the breakdown "No cigarette from hopper detector" is shown below:

IF The breakdown occurred is "No Cigarette from hopper detector"

AND reason for it is cigarette jam

THEN check the incoming raw material
OR

IF The breakdown occurred is "No Cigarette from hopper detector"

AND its is due to loosen

THEN Check the machine

OR

IF The breakdown occurred is "No Cigarette from hopper detector"

AND the breakdown is due to filter missing

THEN the check the maker machine

OR

IF The breakdown occurred is "No Cigarette from hopper detector"

AND the breakdown is due to dust particles

THEN clean the machine

In this study, we developed a generic KBS, which can work for all available machines and equipment. The information base first input is related to the desired production and shift number. The desired production is usually on the higher side to motivate the operator. The first hour of the shift is categorized as cleaning and streamlining hour. The operator is asked to clean and

check the inputs for machine carefully.

At the end of first hour actual hourly production is entered which is less than the desired production. The FTA screen of parent breakdown appears after entering the actual production. The operator then selects the occurred breakdown. The operator can access the root cause of the breakdown as shown in Fig. 4. At the end of second hour the operator again enter the actual hourly production and is able to access the FTA.

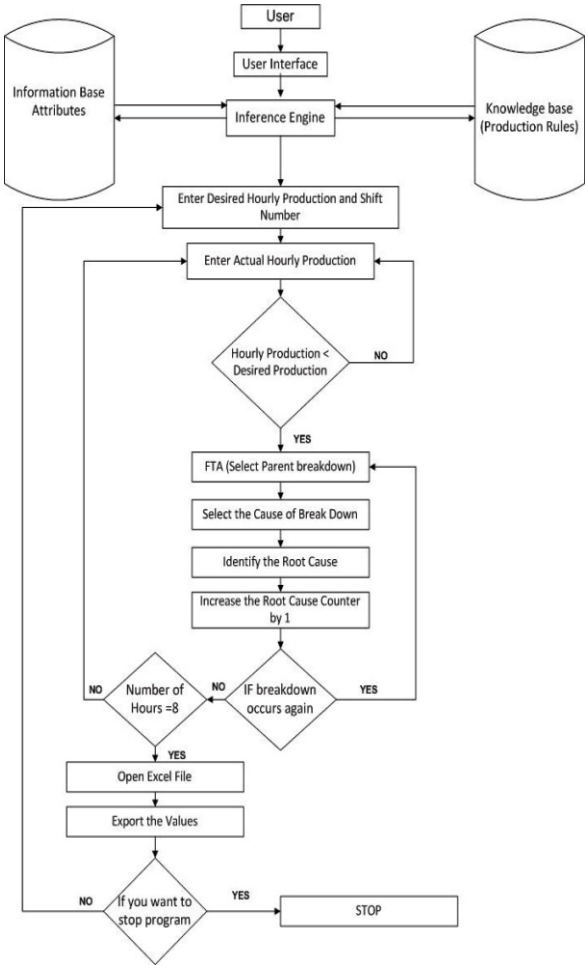

Fig. 4. Flow Chart of Expert System

A counter is attached to each of the parent breakdown and root cause. The counter increases every time the operator accesses a certain breakdown and its cause. At the end of shift all the production and counter values are exported to an excel sheet. The excel sheet is saved by a specific number with respect to date and shift. The saved excel sheet is used for upgrading the already developed information base and a printed version is kept in folder for management review. Fig. 4 gives an insight view of how the information base is utilized, improved and developed. Initially, such systems are run and tested for a warm up period. New problems and new issues may arise, which are then fed into the expert system in coordination with the respective expert.

The expert system developed was verified by the academic and industrial experts and was then validated on twenty one (seven on each machine) readings as shown in Table III.

TABLE III
SUMMARIZING MACHINE BREAKDOWNS

Sr. No	M/c No	Downtime/ Shift (Hrs: Min: Sec)	Remarks
1	1	02:10:03	Database updated and root causes verified
2	2	01:49:34	Database updated and root causes verified
3	3	01:53:43	Database updated and root causes verified
4	1	01:59:50	Database updated and root causes verified
5	2	01:56:32	Database updated and root causes verified
6	3	01:48:48	Database updated and root causes verified
7	1	01:56:12	Database updated and root causes verified
8	2	02:01:48	Database updated and root causes verified
9	3	01:45:09	Database updated and root causes verified
10	1	01:51:11	Maintenance Performed (Warm up run)
11	2	01:43:35	Maintenance Performed (Warm up run)
12	3	01:49:57	Maintenance Performed (Warm up run)
13	1	01:48:19	Maintenance Performed through ES
14	2	01:53:29	Maintenance Performed through ES
15	3	01:42:53	Maintenance Performed through ES
16	1	01:18:30	Maintenance Performed through ES
17	2	01:23:45	Maintenance Performed through ES
18	3	01:19:23	Maintenance Performed through ES
19	1	01:12:13	Maintenance Performed through ES
20	2	01:09:09	Maintenance Performed through ES
21	3	01:03:10	Maintenance Performed through ES

V. Results and Discussion

The downtime is significantly reduced after eliminating the root causes using the expert system. The Bar chart in Fig. 5 shows the reduction in downtime for the first, second and third collected data. The numbers shown in the bars are in the hours/minutes/seconds format. The reduction is approximately 30 minutes in each shift.

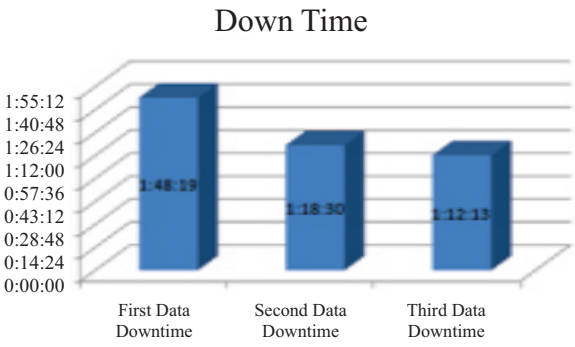

Fig. 1. Downtime of a single PW-2 Machines

After implementing the expert system, approximately 30 minutes of breakdown time was reduced. Hence, it is concluded that the downtime and production time are inversely proportional to each other. Any decrease in one of them will increase the other by the same amount of time. The bar chart in Fig. 6 shows the increase in the production (run) time of one machine up to thirty minutes.

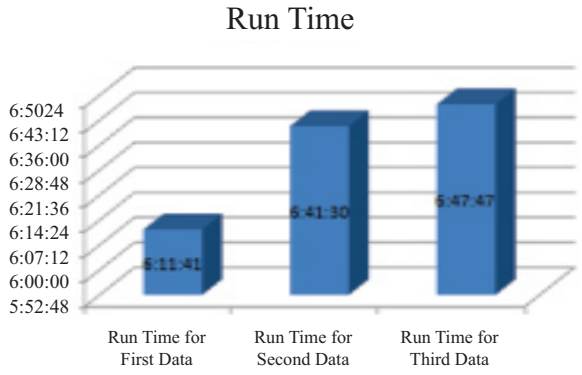

Fig. 2. Runtime for a single PW-2 Machine

The hourly production is also recorded. Fig. 7 depicts that that around 720 packets per shift for a single machine is rejected initially. After implementation of the ES and removal of the root cause, the rejections are reduced to 520 packets. The third bar in Fig. 3 shows the third reading depicting that the rejections are reduced to 480 packets. This leads to waste minimization and ultimately contribute towards the increase in production.

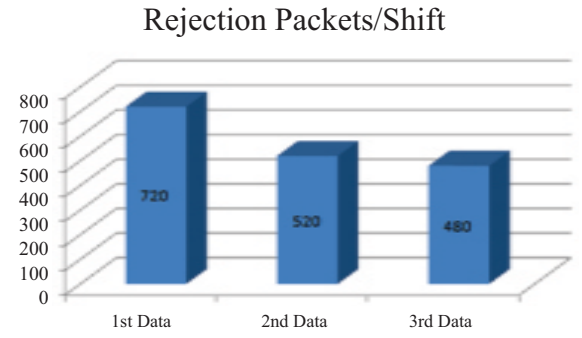

Fig. 3. Rejection of Packets per shift for single machine

The increase in uptime due to identification and subsequent removal of the root cause leads to reduction in the rejections of the packets. The production for single machine was increased over a series of readings as shown in Figure 8. A single machine production was increase from 2480 to 2720 (the increase is around 9.6 percent).

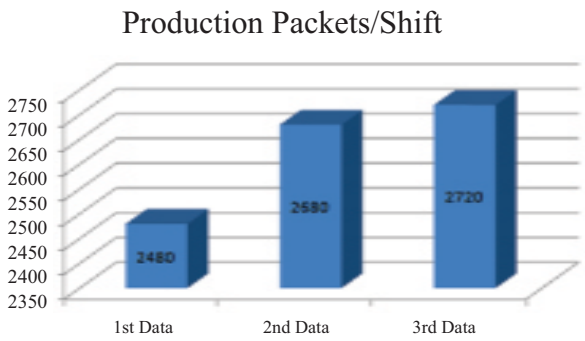

Fig. 4. Production per shift of single machine

VI. Conclusions

Maintenance is often ignored and overlooked whereas it is one of the important aspects of the overall manufacturing. It is directly related to production cost and productivity. It can rightly be termed as center theme line for a good manufacturing unit. Employing appropriate preventive and corrective maintenance measures increases the production time significantly. For a good maintenance system to be in place a continuous training program needs to be developed to properly train operators and technicians. By imparting a thorough knowledge of the breakdowns, scheduled maintenance and replacements of machine parts the breakdowns are reduced efficiently. Expert system not only helps to generate the database of all the breakdowns along with their root causes, but also guide the operator/technician to quickly search for the real root cause. It results in making informed steps to reduce the downtime on time. Managers and researchers may incorporate following recommendations for much better results. Expert system can be further extended to all the other machines available at the shop floor. Managers can deploy expert system for more accurate and precise decision-making. In addition, sensors may be integrated to automatically detect the breakdown and show the root cause. Furthermore, real time data form sensors could be used to expedite or defer (incase schedule maintenance already performed) routine maintenance. Different probabilities can be assigned to the causes of the breakdown depending on the real shop floor environment.

References

[I] K. Amasaka, “New JIT: A new management technology principle at Toyota," International Journal of Production Economics, vol. 80, 2002, pp.135-144.

[ii] A. B. Badiru, "Expert systems applications in engineering and manufacturing", Prentice Hall, 1992.

[iii] I. Hussain, AL-Ahmari, "Knowledge Based System for Planning and Design of Computer

Integrated Manufacturing", King Saud University (KSU), 2000.

[iv] R. Maus & J. Keyes, "Handbook of expert systems in manufacturing," McGraw-Hill, 1991.

[v] G. I. Doukidis & R. J. Paul, "Artificial Intelligence in Operational Research", Scholium Intl, 1992.

[vi] W. L. Stefanov, M. S. Ramsey, & P. R. Christensen, "Monitoring urban land cover change: An expert system approach to land cover classification of semiarid to arid urban centers," Remote Sensing of Environment, vol. 77, 2001, pp.173-185.

[vii] M. C. Cakir, O. Irfan, & K. Cavdar, "An expert system approach for die and mold making operations," Robotics and Computer-Integrated Manufacturing, vol. 21, 2005, pp.175-183.

[viii] M. Jamaseb, S. Jafari, F. Montaseri, & M. Dadgar, "The use of Fuzzy expert system in robots decision making," IOP Conference Series: Materials Science and Engineering, 2014.

[ix] E. L. Fisher, "An AI-based methodology for factory design," AI Magazine, vol. 7, 1986, pp. 72.

[x] M. S. Fox, "Constraint-Directed Search," Carnegie-Mellon University, 1983.

[xi] G. E. Hayes, & H. G. Romig, "Modern quality control," Bruce, 1977.

[xii] O. İnan, D. Arslan, S. Taşdemir, & M. M. Özcan, "Application of fuzzy expert system approach on prediction of some quality characteristics of grape juice concentrate (Pekmez) after different heat treatments," Journal of food science and technology, vol. 48, 2011, pp.423-431.

[xiii] K. A. Jackson, D. H. Dubois, & C. A. Stallings, "An expert system application for network intrusion detection," 1991.

[xiv] P. W. James, T. J. Daniel, & R. Daniel, "The Machine That Changed the World: The Story of Lean Production," HarperCollins, 1991.

[xv] A. Jinidia,"Expert Systems remove repetitive tedious work for customer order entry," Industrial Engineering, vol. 22, 1990, pp. 31-53

[xvi] R. Kerr, "Knowledge-based Manufacturing Management: Applications of Artificial Intelligence to the Effective Management of Manufacturing Companies," Addison-Wesley Publishing Company, 1991.

[xvii] H. Kunz, T. Schaaf, "General and specific formalization approach for a Balanced Scorecard: An expert system with application in health care. Expert Systems with Applications, vol. 38, 2011, pp. 1947-1955

[xviii] S. L. Lauritzen, and D. J. Spiegelhalter, "Local computations with probabilities on graphical structures and their application to expert systems," Journal of the Royal Statistical Society. Series B (Methodological), 1988, pp. 157-224

[xix] C. S. Lee, and M. H. Wang, "A fuzzy expert system for diabetes decision support application. Systems, Man, and Cybernetics, Part B: Cybernetics," IEEE Transactions on, vol. 41, 2011, pp. 139-153

[xx] J. C. Chen, C. C. Wu, C. W. Chen, and K. H. Chen, "Flexible job shop scheduling with parallel machines using Genetic Algorithm and Grouping Genetic Algorithm," Expert Systems with Applications, vol. 39, 2012, pp. 10016-10021

[xxi] J. M. Mellichamp, and A. F. A. Wahab, "An expert system for FMS design," Simulation, vol. 48, 1987, pp. 201-208.

[xxii] D. Peng, X. Shi, and G. Li, "Expert System Application in Simulation Tutoring for Weapon Utilization," System Simulation and Scientific Computing. Springer, 2012

[xxiii] D. T. Pham, and E. Tacgin, "Grippex: a hybrid expert system for selecting robot gripper types," International Journal of Machine Tools and Manufacture, vol. 32, 1992, pp. 349-360.

[xxiv] V. Roshanaei, B. Vahdani, S. M. Mousavi, M. Mousakhani,and G. Zhang, "CAD/CAM system selection: a multi-component hybrid fuzzy MCDM model," Arabian Journal for Science and Engineering, vol. 38, 2013, pp. 2579-2594.

[xxv] R. Sahin, "A simulated annealing algorithm for solving the bi-objective facility layout problem," Expert Systems with Applications, vol. 38, 2011, pp. 4460-4465.

[xxvi] G. Tuzkaya, B. Gülsün, C. Kahraman, and D. Ozgen, "An integrated fuzzy multi-criteria decision making methodology for material handling equipment selection problem and an application," Expert Systems with Applications, vol. 37, 2853-2863, 2010, pp. 2853-2863

Section D
BASIC SCIENCES

Non-Standard Finite Difference Scheme for the Kinetics of Pentaerythritol Production Reactions

M. Basit[1], S. Riaz[2], M. Rafique[3], Q. A. Chaudhry[4], S Farid[5]

[1,2,4,5]*Department of Mathematics, UET Lahore, Pakistan*
[3]*Faculty of Engineering, University of Central Punjab Lahore, Pakistan*

Abstract- Pentaerythritol plays very crucial role in the preparation of many polyfunctionalized compounds such as explosives, dyes, paints and surface coatings. Estimation of numerical solutions of kinetics of pentaerythritol production reactions has been an important issue. The kinetic model of this reacting system has been converted into system of ordinary differential equations. In this paper, the obtained system of ordinary differential equations describing the kinetics of pentaerythritol has been solved numerically by using non-standard finite difference method and semi analytical scheme 'differential transform method'. Sometime experimental data is not easily available, for such case we have estimated solutions for reaction parameters using NSFD and DTM. Obtained results are approximately same as experimental data. Results obtained from these techniques have been compared with each other and also with the experimental data.

Keywords-Pentaerythritol, Polyfunctionalized, Differential Transform Method, Non Standard Finite Difference Method.

I. INTRODUCTION

Study of the system of differential equations has been the center of focus of many mathematicians. We have observed that in our daily life chemical reactions are long time process and we require too much time to get experimental results, and still chances of error do exist. In this case, to reduce the time estimation and error, we can develop the system of differential equations of chemical reactions and also construct the numerical schemes for getting experimental approximation. Real life problems can easily be modeled in mathematical form using differential equations. The systems of differential equations, obtained from the mathematical modeling of real world problems are some time so complex or the obtained system are so large that analytical methods are hard to apply, but we can approach the solutions of these systems numerically. Advancement in technology has made it much easier to solve big systems of differential equations numerically. In this paper, we will study the numerical approach to the solution of the system of differential equations, which is modeled for the reaction kinetics of pentaerythritol. Reaction kinetics of pentaerythritol is the study of chemical reactions of pentaerythritol [i]. Plastics, surface coatings, paints, dyes and explosives are made by using the pentaerythritol as an essential chemical. Confined publications are available on the reaction kinetics of pentaerythritol due to its complexity [ii-iv]. Aqueous alkaline mechanism of formaldehyde and acetaldehyde produces pentaerythritol, by-product of this reaction is methanol. Pentaerythritol is obtained from the resulted solution using crystallization process. In the first step of reactions, formaldehyde reacts with acetaldehyde to form pentaerythrose. Sodium hydroxide or calcium hydroxide is most commonly used base in this reaction. These chemical reactions are called cannizarro type chemical reactions, in which two aldehydes together give organic acid and alcohol. Pentaerythritol is achieved in the least reaction of the process when pentaerythrose reacts with formaldehyde in the presence of base [ii , iv].Chemical reactions to process pentaerythritol are modeled mathematically by using the corresponding system of ODEs, which are formed under the conditions applied to the reactions by using law of mass action [ii]. We will solve this system of ODEs numerically using non-standard finite difference (NSFD) method and semi analytic techniques differential transform method (DTM) in order to obtain the approximations for the concentration of Cm, Cn and Co. A most familiar method in numerical analysis is non-standard finite difference method to obtain numerical solutions, numerical schemes give the discrete model of differential equations [v-vi]. DTM is an important semi analytical scheme, to get the approximate solutions for ordinary differential equations [vii].

II. MATEIRAL AND METHODS

The most commonly known numerical method to solve ordinary differential equations (ODE) and partial differential equation (PDE), is standard finite difference (SFD) method. In this method finite difference scheme is applied on given differential equations to get algebraic equations which are rather easy to solve [v]. Mickens [viii], presented the idea of non-standard finite difference model by removing instabilities which were the shortcomings of standard finite difference scheme. Since this scheme has been introduced, many authors in [v,viii-ix] have presented the ideas of constructing numerically reliable schemes using the non- standard finite difference (NSFD)

modeling. Non-standard finite difference scheme is the finite difference scheme with the specification of following rules [v]:

a. Order of the derivatives in differential equation and discrete derivatives must be equal.
b. Discrete representations of the derivatives should consist of non-trivial denominator functions.
c. In general, non-linear terms should be replaced by non-local distinct representations.
d. Conditions that satisfy either or both the differential equaton and its solutions should also comply with the difference equation model and its solutions.

Aqueous alkaline medium of formaldehyde and acetaldehyde forms pentaerythritol, methanol is formed as a byproduct. The product is collected from mixture by the process of crystallization. In initial reaction, formaldehyde reacts with acetaldehyde in the presence of base, forming pantaerythrose. Mechanism of pentaerythritol reaction can be summarized in the following steps[x-xi]:

$$HCHO + 3CH_3CHO \xrightarrow{OH^-} (HOCH_2)_3CCHO \quad (1)$$

$$HCHO + OH^- + (HOCH_2)_3CCHO \xrightarrow{K_1} (HOCH_2)_4 + HCOO^- \quad (2)$$

$$2HCHO + OH^- \xrightarrow{k_2} CH_3OH + HCOO^- \quad (3)$$

Equation "(2)" shows condensation reaction that is comparatively fast. Before the formation of pentaerythritol, condensation reaction carried out at low temperature to form pentaerythrose from acetaldehyde. When we increase the temperature in the reactor, only cannizarro reactions takes place. By running a batch process in these reaction steps, we can easily estimate the kinetic parameters in refer to "(1)-(3)".We represent the concentration of HCHO,OH and by and respectively, resulting in the form of following set of ordinary differential equations via law of mass action [iv,xi],

$$\frac{dC_m}{dt} = - k_1 C_m C_n^2 C_o - 2k_2 C_m^2 C_n \quad (4)$$

$$\frac{dC_n}{dt} = - k_1 C_m C_n C_o - 2k_2 C_m^2 C_n \quad (5)$$

$$\frac{dC_o}{dt} = - k_1 C_m C_n C_o \quad (6)$$

We will apply non-standard finite difference scheme to approximate the solution of this system of ODEs. After applying our proposed NSFD scheme, the above system of differential equations refer to "(4)", "(5)", "(6)" can be written as the following set of algebraic equations.

$$C_m(n+1) = \frac{C_m(n)}{1 + hk_1 C_n(n) C_o(n) + 2hk_2 C_m(n) C_n(n)} \quad (7)$$

$$C_n(n+1) = \frac{C_m(n)}{1 + hk_1 C_n(n) C_o(n) + 2hk_2 C_m(n) C_n(n)} \quad (8)$$

$$C_o(n+1) = \frac{C_m(n)}{1 + hk_1 C_n(n) C_o(n)} \quad (9)$$

Solutions obtained for the concentration of formaldehyde, base and pentaerythrose. The rate constant k_1 and k_2 for this system has been taken from the experimental data [iii].

III. Resuls and Discussions

The reaction kinetics in the making of pentaerythritol represents the aldol condensation reactions which follows the production of pentaerythritose. Condensation reactions are relatively fast, than cannizarro reactions that produce pentaerythritose [iv,xi]. Rate constant expressions, k_1 and k_2, were used to express cannizarro reactions [iv]. Numerical solution obtained using NSFD and analytic solution obtained by semi analytical scheme DTM are compared with the experimental data in Table I.The results obtained by applying NSFD on the system of ODEs, Thus the comparison of two methods was made and was represented in Fig. 1-3. Table I shows the estimated error between experimental results, NSFD and DTM of the solution obtained for concentration of formaldehyde, base and pentaerythrose which is denoted by Em, En and Eo respectively.

The Table I shows that the error between experimental results, NSFD and DTM results, the above table shows that numerical scheme NSFD gives good approximation to experimental results. The first absolute column shows errors estimations of Cm, Cn and Co between experimental results and the approximated values obtained from NSFD scheme. Similarly the second column shows the error estimations of Cm, Cn and Co between experimental results and DTM results. From these results we can see that the numerical technique NSFD gave better results and is closer to experimental results, whereas the DTM, which is a semi analytical scheme, first shows good agreements with the experimental data approximately up to 50 seconds, after that it started diverging. The comparison of the experimental results with both numerical and semi analytical techniques are shown by graphs in Fig. 1-3. The Fig. 4-6 shows the error between numerical scheme NSFD and semi analytic scheme DTM, from these graphs it is shown that NSFD a numerical scheme is much better than the semi analytic scheme DTM.

TABLE I
SHOWING ERROR BETWEEN EXPERIMENTAL RESULTS, SEMI ANALYTICAL SCHEME AND NUMERICAL SCHEME.

	|Experimental - NSFD|			**|Experimental - DTM|**		
Time(s)	**E_m**	**E_n**	**E_o**	**E_m**	**E_n**	**E_o**
0	0.0000E+00	0.0000E+00	0.0000E+00	0.0000E+00	0.0000E+00	9.0000E+00
50	5.7000E+00	2.1500E+00	3.0000E-01	1.7200E+00	5.3000E+00	9.6000E-01
100	3.6000E+00	3.6900E+00	2.1000E+00	1.5860E+01	2.4110E+01	2.8880E+01
150	8.2300E+00	6.1000E-01	1.3940E+01	3.9270E+01	3.4630E+01	2.8470E+01
200	3.4000E-01	9.1100E+00	3.6100E+00	7.6570E+01	8.5210E+01	6.7140E+01
250	8.3700E+00	3.1800E+00	1.5300E+00	1.0416E+02	9.7910E+01	9.1320E+01
300	6.7100E+00	1.2580E+01	6.9500E+00	1.1425E+02	1.1786E+02	1.0733E+02
350	6.4600E+00	1.2720E+01	1.8000E-01	1.1969E+02	1.2223E+02	1.0439E+02
400	1.0230E+01	1.0600E+00	3.5100E+00	1.2486E+02	1.1036E+02	9.9820E+01
450	1.2130E+01	8.5600E+00	9.1000E-01	1.2562E+02	1.1488E+02	9.8420E+01
500	7.8500E+00	6.1100E+00	1.4360E+01	1.1902E+02	1.0803E+02	1.0794E+02
550	1.0950E+01	3.8100E+00	4.5800E+00	1.1960E+02	1.0091E+02	8.2530E+01
600	5.7000E-01	9.8800E+00	7.9600E+00	1.0702E+02	1.0237E+02	7.2590E+01
650	2.2400E+00	9.1000E+00	2.2130E+01	1.0719E+02	9.7450E+01	5.2060E+01
700	1.0740E+01	5.9400E+00	7.8500E+00	1.1507E+02	9.0810E+01	6.0380E+01
750	3.6900E+00	1.7560E+01	2.3100E+00	1.0827E+02	9.9620E+01	6.0470E+01
800	4.4100E+00	1.2130E+01	7.8200E+00	1.1004E+02	9.1970E+01	6.5580E+01
850	8.5200E+00	4.3600E+00	9.0100E+00	9.8890E+01	8.4590E+01	4.4100E+01
900	1.9700E+00	1.1200E+01	4.3100E+00	1.0799E+02	8.8490E+01	4.4580E+01
950	6.3000E-01	1.1740E+01	8.4600E+00	1.1386E+02	8.8600E+01	3.6590E+01
1000	8.4800E+00	8.9600E+00	1.1830E+01	1.2555E+02	8.5860E+01	2.9710E+01
∑Error	1.22E+02	1.54E+02	1.34E+02	1.87E+03	1.75E+03	1.29E+03
Total Error	4.10E+02			4.91E+03		

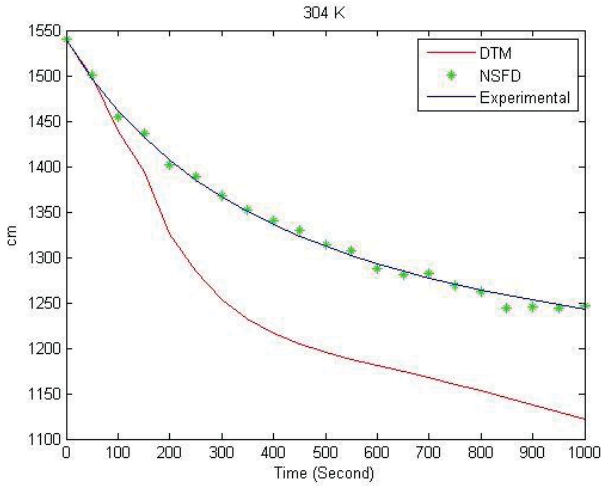

Fig. 1. Comparison between NSFD,RK4 and Experimental results for C_m.

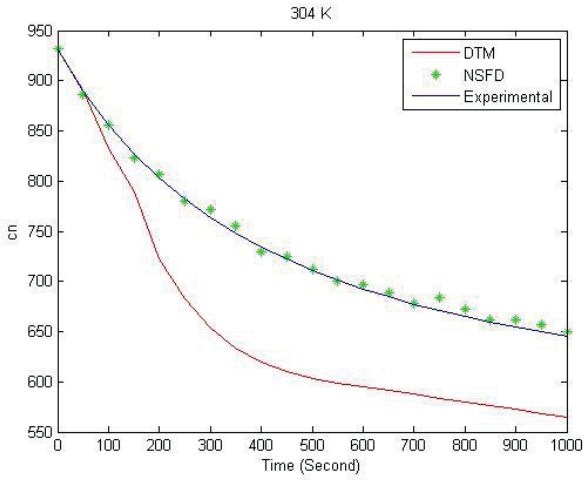

Fig. 2. Comparison between NSFD,RK4 and Experimental results for C_n.

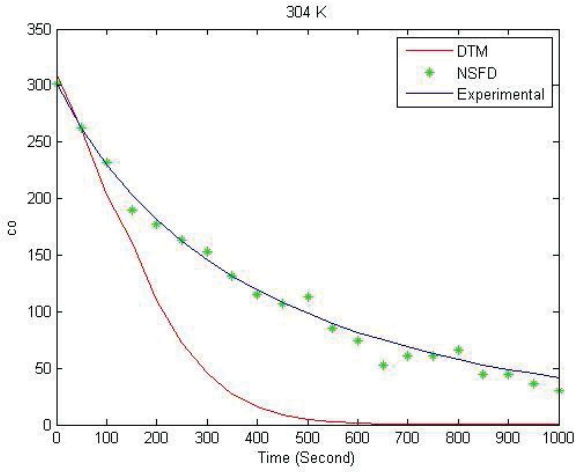

Fig. 3. Comparison between NSFD,RK4 and Experimental results for C_o.

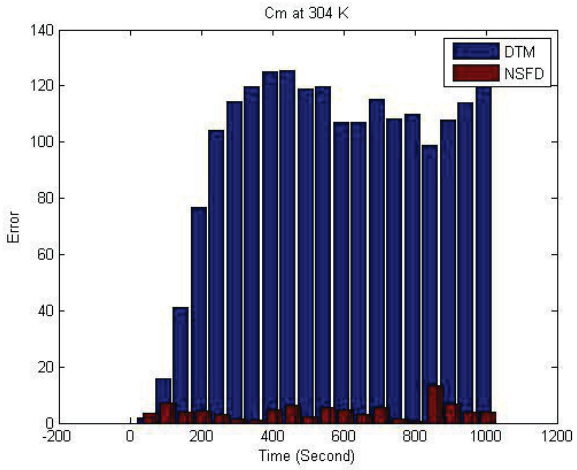

Fig. 4. Estimated error between NSFD and RK4

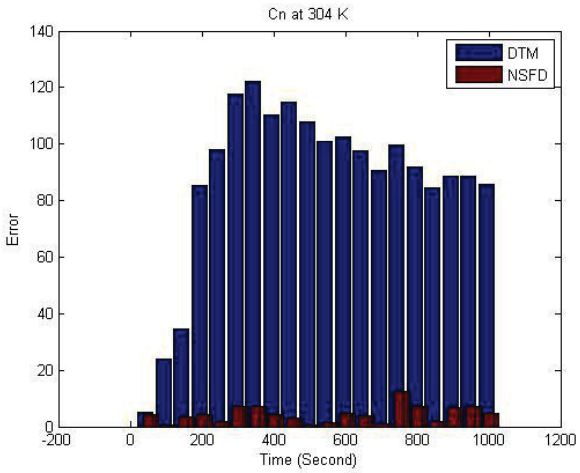

Fig. 5. Estimated error between NSFD and RK4

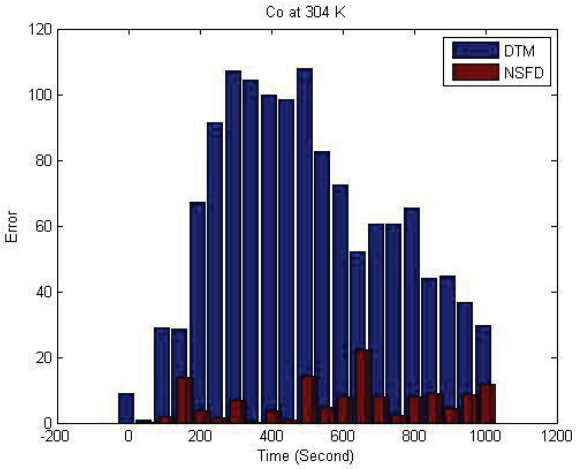

Fig. 6. Estimated error between NSFD and RK4.

IV. Conclusion

Pentaerythritol is the major product of all cannizarro type reactions. These chemical reactions are converted into system of differential equations of ODEs, modeled for the concentration of formaldehyde (Cm), concentration of base (Cn) and concentration of pentaerythrose (Co). We solved the obtained system of ODEs using NSFD, a numerical technique and DTM, a semi analytical technique to find out the rate of change of concentrations of Cm, Cn and Co with respect to time. We observed from the graphs and Table, that our proposed NSFD scheme is in good agreement to the experimental data. Whereas the DTM, which is a semi analytical technique converges for very short interval of time after that it started diverging. This work shows the validity and great potential of the non-standard finite difference method for solving the system of non-linear differential equations. We conclude that whenever a chemical process take a long time or it is not feasible to perform the experiments, we can approximate the rate of change of concentrations of the chemicals involved in the chemical reactions using our proposed scheme.

References

[i] Kenneth h, A. Connors "Chemical Kinetics. The study of Reaction Rate In solution" *VCH Publishers, Inc* 1990.

[ii] M. S. Peters, C. R. Cupit "Kinetics Of pentaerythritol-Production Reactions Chemical Engineering Division" University of Illinios, Urbana, Illinios U. S. A. nos "57-67", Received 11 July 1958, Available online 28 September 2001.

[iii] Barth R. H., J. E.snow., and E. H wood; "Paper presented at amer. chem soc" *North Jersey Section Meeting-in-Miniature* 8th January,

1951.

[iv] Wawzonek S. and D. A. J Rees; "Amer. Chem. Soc"1948 70 2433.

[v] Comsol AB Stockholm (2010) Comsol Reaction Engineering lab Model Library, version 1.5, no's 246, (September 2008)

[vi] Peter M. Manning and Gray F. Margrave "CREWES" *Research Report Volume* 18(2006).

[vii] Ibijola, E. A and Obayomi, "A. A. derivation of new non-standard finite difference schemes for non autonomous ordinary differential equation"

[viii] F. Mirzaee "Applied Mathematical sciences", vol. 5,2011 no 70 (3465-3472)

[ix] E. A. Ibijola, and J. Sunday (2010). "A comparative study of standard and exact Finite Difference Schemes for Numerical Solution of ODEs" *Emanating from the Radioactive decay of Substances. Australian Jornal of basic and Applied Science*,4(4): 624-632.

[x] R. E. Mickens, "Exact solutions to a finite difference model of a reaction-advection equation: Implications of numerical analysis" *Numerical methods for Partial Differenial Equations, no* 313-325, (1989).

[xi] R. E. Mickens, "Advances in the Applications of Non-Standard Finite Difference Schemes" *Clark Atlanta University, nos* 1-7, (2005)

[xii] R. Angeulov and J. M. S. Lubma (2003). "Nonstandard Finite Difference method by nonlocal approximation" *Mathematics and Computers in simulations*6:465-475.

Non-Standard Finite Difference Modeling for Transmission Dynamics of Dengue Fever

M. Rafiq[1], M. O. Ahmad[2]

[1]Mathematics Department, University of Engineering &Technology Lahore, Pakistan
[2]Mathematics Department, University of Lahore, Pakistan
[1]rafiq.piam@gmail.com

Abstract-Mathematical models have been widely used in various areas of infectious disease epidemiology. In this paper, the transmission dynamics of a vector borne infectious disease "Dengue Fever" has been analyzed numerically. An unconditionally convergent numerical scheme has been constructed for the model for Dengue Fever and numerical experiments are performed for different values of discretization parameter '*l*'. Results are compared with well-known numerical method i.e. Runge-Kutta method of order four (RK4). Unlike Rk4 which fails for large time steps, the developed scheme gives results that converged to true steady states for any time step used.

Keywords:Dengue Fever, Infectious Diseases, Transmission Dynamics, Runge-Kutta method of order 4,NSFD, Convergence

I. Introduction

Infectious diseases play a vital role in population dynamics and are responsible for ¼ of all human deaths [I- ii].Being the second largest cause of debilitation and premature death to large portions of the human population, infectious diseases lead to serious social-economic concerns [iii-v].

An infectious disease due to dengue virus is dengue fever. Dengue fever is estimated to have an effect on more than one hundred million people in over 100 countries of the world, so it has become a grand public health issue [vi]. This virus contains four serotypes known as DEN-1, DEN-2, DEN-3 and DEN-4. All of the four serotypes occur in many areas of Asian and European countries. Biting of an infected female Aedes mosquito to a human caused the transmission of these viruses to the human. Since the mosquito breed in water, so dengue fever mainly occurs in municipal and semi municipal areas around the world [x].

The following is the variety of illness of dengue ranges from gentle infection to brutal fatal infection.

- Dengue Fever (DF)
- Dengue Hemorrhagic Fever (DHF)
- Dengue Shock Syndrome (DSS).

If a person is infected by one serotype, it gives permanent protection to him against that serotype only. The person is still temporarily or partially secured from other three viruses. The person nowbecomes more favorable to brutal fatal infection and may catch other three viruses within few months [xi].

II. Mathematical Model

A. Assumptions

- Constant population of both human and mosquito.
- Infection by one DEN virus gives lifelong protection from that virus only but an object become more susceptible to other three viruses, this leads to omit the recovered compartment.
- First assumption leads to third assumption taking the birth rate of human and mosquito population equal to their death rate.

B. Parameters used in the Model

S_H = Number of susceptible human population

I_H = Number of infected human population

S_V = Number of susceptible mosquito population

I_V = Number of infected mosquito population

$A = \mu_V N_V$ = The recruitment rate of mosquito population

m = The number of other animals that the mosquitos can feed on

N_H = Number of human population

N_V = Number of mosqito population

b = Biting rate of mosquitos

μ_V = Death rate of mosquitos

r_H = Recovery rate of human population

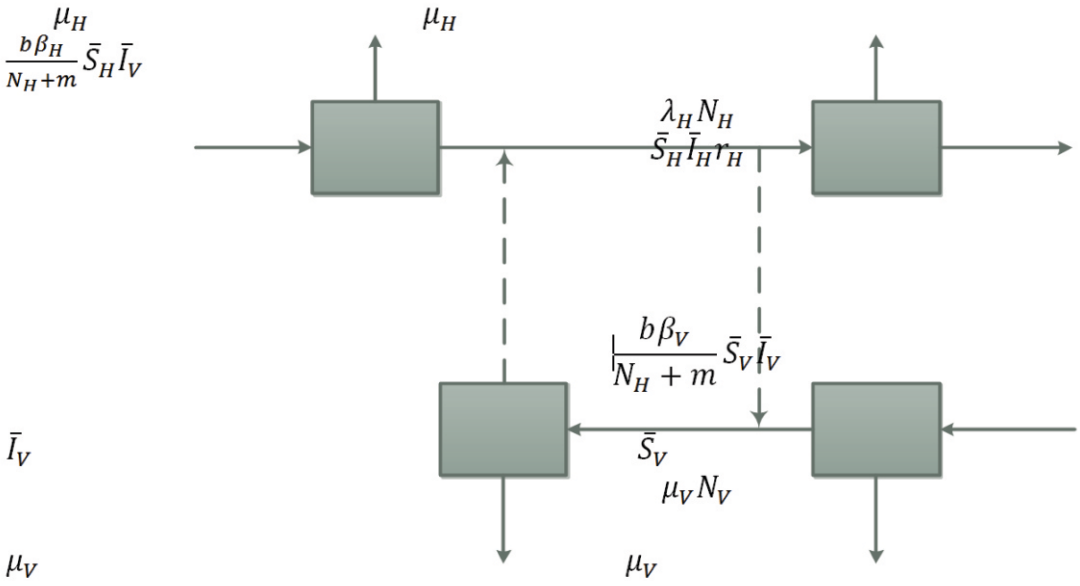

Fig. 1. shows the compartmental diagram of transmission of dengue disease [x].

There are two compartments for each human population and mosquito population described below,

- Susceptible human compartment ($\bar{S}_H$)
- Infected human compartment($\bar{I}_H$)
- Susceptible mosquito compartment ($\bar{S}_V$)
- Infected mosquito compartment ($\bar{I}_V$)

The flow chart above leads to the following differential equations with the consideration of given assumptions[x].

$$\begin{aligned}
\frac{d\bar{S}_H}{dt} &= \lambda_H N_H - \frac{b\beta_H}{N_H + m}\bar{S}_H\bar{I}_V - \mu_H\bar{S}_H \\
\frac{d\bar{I}_H}{dt} &= \frac{b\beta_H}{N_H + m}\bar{S}_H\bar{I}_V - (\mu_H + r_H)\bar{I}_H \\
\frac{d\bar{S}_V}{dt} &= A - \frac{b\beta_V}{N_H + m}\bar{S}_V\bar{I}_V - \mu_V\bar{S}_V \\
\frac{d\bar{I}_V}{dt} &= \frac{b\beta_V}{N_H + m}\bar{S}_V\bar{I}_V - \mu_V\bar{I}_V
\end{aligned} \quad (1)$$

With two conditions: $N_H = \bar{S}_H + \bar{I}_H, N_V = \bar{S}_V + \bar{I}_V$
Mosquito population is taken to be constant so the third equation can be omitted $\bar{S}_V = N_V - \bar{I}_V$. With the omission of third equation we are left with only three variables as $\bar{S}_H, \bar{I}_H, \bar{I}_V$.
Normalizing the model will lead new variables define as $S_H = \frac{\bar{S}_H}{N_H}$, $I_H = \frac{\bar{I}_H}{N_H}, S_V = \frac{\bar{S}_V}{N_V} = \frac{\bar{S}_V}{A/\mu_V}$

$$I_V = \frac{\bar{I}_V}{N_V} = \frac{\bar{I}_V}{A/\mu_V}$$

As death rate = birth rate, so $\lambda_H = \mu_H, \lambda_V = \mu_V$

As $A = \lambda_V N_V = \mu_V N_V$ or $N_V = \frac{A}{\mu_V}$

Utilizing all the information Eq. 1 will reduce to Eq. 2 as:

$$\begin{aligned}
\frac{dS_H}{dt} &= \mu_H(1 - S_H) - \frac{Ab\beta_H}{\mu_V(N_H + m)}S_H I_V \\
\frac{dI_H}{dt} &= \frac{Ab\beta_H}{\mu_V(N_H + m)}S_H I_V - (\mu_H + r_H)I_H \\
\frac{dI_V}{dt} &= \frac{b\beta_V N_H}{N_H + m}(1 - I_V)I_H - \mu_V I_V
\end{aligned} \quad (2)$$

2.3 Equilibrium Points

Equilibrium points are of two types described below.

A. Disease Free equilibrium (DFE)

When the disease will no longer persist within a population; there will be no infected vector and human, so the total population is considered as susceptible. Thus we have
$I_H = 0, I_V = 0$ *and* $S_H = 1$. Thus point when the disease will die out is $E_0(1, 0, 0)$.

$$(S_H^*, I_H^*, I_V^*) = \left(\frac{\beta + M}{\beta + MR_0}, \frac{R_0 - 1}{\beta + MR_0}, \frac{\beta[R_0 - 1]}{R_0[M + \beta]}\right)$$

Where

$$M = \frac{\mu_H + r_H}{\mu_H}, \beta = \frac{b\beta_V N_H}{\mu_V(N_H + m)}, R_0 = \frac{Ab^2\beta_H\beta_V N_H}{\mu_V^2(\mu_H + r_H)(N_H + m)^2}$$

III. NUMERICAL MODEL

In order to construct numerical model, time ($t \geq 0$) will be taken at the points $t_n = nl$ for $n = 0, 1, 2, 3, \ldots \ldots$ where l is taken as step size of time and is constant. Solution of Eq. 2 at the point t_n are $S_H(t_n)$, $I_H(t_n), I_V(t_n)$.

In numerical method, the solution at the same point t_n will be denoted by S_H^n, I_H^n, I_V^n respectively

First we make approximation to $\frac{dS_H}{dt}$, $\frac{dI_H}{dt}$ and $\frac{dI_V}{dt}$ using first order forward differences [vii]:

$$\frac{dS_H(t)}{dt} = \frac{1}{l}[S_H(t+l) - S_H(t)] + O(l) \text{ as } l \to 0 \text{ and } t = t_n$$

$$\frac{dI_H(t)}{dt} = \frac{1}{l}[I_H(t+l) - I_H(t)] + O(l) \text{ as } l \to 0 \text{ and } t = t_n$$

$$\frac{dI_V(t)}{dt} = \frac{1}{l}[I_V(t+l) - S_V(t)] + O(l) \text{ as } l \to 0 \text{ and } t = t_n$$

Using these approximations to the derivatives and non-local approximations [viii, ix]for non-linear terms, system (2) can be written as:

$$\frac{1}{l}(S_H^{n+1} - S_H^n) = \mu_H(1 - S_H^{n+1}) - \frac{Ab\beta_H}{\mu_V(N_H+m)} S_H^{n+1} I_V^n$$

$$\frac{1}{l}(I_H^{n+1} - I_H^n) = \frac{Ab\beta_H}{\mu_V(N_H+m)} S_H^{n+1} I_V^n - (\mu_H + r_H) I_H^{n+1}$$

$$\frac{1}{l}(I_V^{n+1} - I_V^n) = \frac{b\beta_V N_H}{N_H+m}(1 - I_V^{n+1}) I_H^{n+1} - \mu_V I_V^{n+1}$$

Solving the above equations for $\frac{dS_H}{dt}$, $\frac{dI_H}{dt}$ and $\frac{dI_V}{dt}$ we have:

$$S_H^{n+1} = \frac{(\mu_H\, l + S_H^n)}{\left(1 + \mu_H\, l + \frac{Abl\beta_H}{\mu_V(N_H+m)} I_V^n\right)} \quad (3)$$

$$I_H^{n+1} = \frac{\left[\frac{Abl\beta_H}{\mu_V(N_H+m)} S_H^{n+1} I_V^n + I_H^n\right]}{(1 + l\mu_H + lr_H)} \quad (4)$$

$$I_V^{n+1} = \frac{\left(\frac{bl\beta_V N_H}{N_H+m} I_H^{n+1} + I_V^n\right)}{\left(1 + \frac{bl\beta_V N_H}{N_H+m} I_H^{n+1} + l\mu_V\right)} \quad (5)$$

The discrete system given by Eq. (3) and (5) is the proposed Non-Standard Finite Difference (NSFD) scheme for the continuous model (2).

IV. Convergence Analysis

In this section we shall discuss the convergence of proposed numerical model. Let us consider

$$F_1(S_H, I_H, I_V) = \frac{(\mu_H\, l + S_H)}{\left(1 + \mu_H\, l + \frac{Abl\beta_H}{\mu_V(N_H+m)} I_V\right)}, F_2(S_H, I_H, I_V) = \frac{\left[\frac{Abl\beta_H}{\mu_V(N_H+m)} S_H I_V + I_H\right]}{(1 + l\mu_H + lr_H)}$$

$$F_3(S_H, I_H, I_V) = \frac{\left(\frac{bl\beta_V N_H}{N_H+m} I_H + I_V\right)}{\left(1 + \frac{bl\beta_V N_H}{N_H+m} I_H + l\mu_V\right)}$$

The Jacobian for this system is:

$$J(S_H, I_H, I_V) = \begin{bmatrix} \frac{\partial F_1}{\partial S_H} & \frac{\partial F_1}{\partial I_H} & \frac{\partial F_1}{\partial I_V} \\ \frac{\partial F_2}{\partial S_H} & \frac{\partial F_2}{\partial I_H} & \frac{\partial F_2}{\partial I_V} \\ \frac{\partial F_3}{\partial S_H} & \frac{\partial F_3}{\partial I_H} & \frac{\partial F_3}{\partial I_V} \end{bmatrix}$$

The numerical scheme (3)-(5) will converge to a fixed point of the system if and only if absolute value of each eigenvalue of the jacobian matrix is less than unity at that point i.e $|\lambda_i| < 1, i = 1,2,3.$

The Jacobian matrixat disease free equilibrium point $(S_H, I_H, I_V) = (1,0,0)$ is given by:

$$J(1,0,0) = \begin{bmatrix} \frac{1}{1+l\mu_H} & 0 & -\frac{Abl\beta_H}{\mu_V(1+l\mu_H)(N_H+m)} \\ 0 & \frac{1}{1+l\mu_H+lr_H} & \frac{Abl\beta_H}{\mu_V(1+l\mu_H+lr_H)(N_H+m)} \\ 0 & \frac{bl\beta_V N_H}{(1+l\mu_V)(N_H+m)} & \frac{1}{1+l\mu_V} \end{bmatrix}$$

$\lambda_1 = \frac{1}{1+l\mu_H} < 1.$ The remaining two eigenvalues are given by the matrix:

$$J^* = \begin{bmatrix} \frac{1}{1+l\mu_H+lr_H} & \frac{Abl\beta_H}{\mu_V(1+l\mu_H+lr_H)(N_H+m)} \\ \frac{bl\beta_V N_H}{(1+l\mu_V)(N_H+m)} & \frac{1}{1+l\mu_V} \end{bmatrix}$$

To calculate the eigenvalues of J^* we will use the following lemma:

A. Lemma:[2] *For the quadratic equation* $\lambda^2 - \lambda A + B = 0$ *both roots satisfy* $|\lambda_i| < 1, i = 1,2$ *if and only if the following conditions are satisfied:*

1. $1 - A + B > 0$
2. $1 + A + B > 0$
3. $B < 1$

Let us define $A = TraceJ^*, B = DetJ^*$.Therefore

$$A = \frac{2 + l(\mu_H + r_H + \mu_V)}{(1+l\mu_V)(1+l\mu_H+lr_H)} > 0$$

$$B = \frac{1}{(1+l\mu_V)(1+l\mu_H+lr_H)} - \frac{Ab^2 l^2 \beta_H \beta_V N_H}{\mu_V(1+l\mu_V)(1+l\mu_H+lr_H)(N_H+m)^2}$$

$$B = \frac{1 - R_0 l^2 \mu_V(\mu_H + r_H)}{(1+l\mu_V)(1+l\mu_H+lr_H)} < 1 \text{ if } R_0 < 1$$

$$\Rightarrow B < 1 \quad (6i)$$

$$1 + A + B = 1 + \frac{2 + l(\mu_H + r_H + \mu_V)}{(1+l\mu_V)(1+l\mu_H+lr_H)}$$

$$+\frac{1-R_0 l^2\mu_V(\mu_H+r_H)}{(1+l\mu_V)(1+l\mu_H+lr_H)}$$
$$=\frac{4+2l(\mu_H+r_H+\mu_V)+l^2\mu_V(\mu_H+r_H)[1-R_0]}{(1+l\mu_V)(1+l\mu_H+lr_H)}>0 \text{if } R_0<1$$
$$\Rightarrow 1-A+B>0 \quad (6ii)$$

Now for

$$1-A+B=1-\frac{2+l(\mu_H+r_H+\mu_V)}{(1+l\mu_V)(1+l\mu_H+lr_H)}$$
$$+\frac{1-R_0 l^2\mu_V(\mu_H+r_H)}{(1+l\mu_V)(1+l\mu_H+lr_H)}$$
$$=\frac{l^2\mu_V(\mu_H+r_H)[1-R_0]}{(1+l\mu_V)(1+l\mu_H+lr_H)}>0 \text{if } R_0<1$$
$$\Rightarrow 1-A+B>0 \quad (6iii)$$

From (*6i*), (*6ii*) *and* (*6iii*) we see that the conditions for the above Lemma hold. Then the absolute value of both eigenvalues of J^* is less than 1, for every value of the step size *'l'*, when $R_0 < 1$. Therefore the proposed NSFD scheme (3)-(5) will converge unconditionally from any starting values S_H^0, I_H^0 *and* I_V^0 to the disease free equilibrium point whenever $R_0 < 1$, for any $l > 0$.

V. Numerical Experiments

Numerical experiments are performed using values of parameters given in Table I[x]:

TABLE I

Parameters	Values
A	400(DFE)
A	5000(EE)
μ_V	$0.2500\ day^{-1}$
μ_H	$\frac{1}{60\times 365}\ day^{-1}$
r_H	$0.1428\ day^{-1}$
β_H	0.7500
β_V	1.0000
N_H	10,000
m	0
b	$0.5000\ day^{-1}$

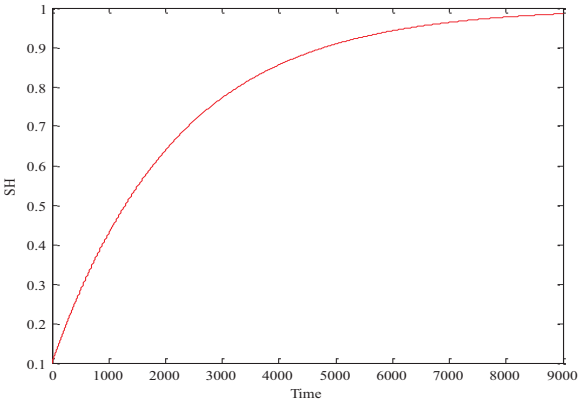

Fig. 2.1 Susceptible Human Fraction-DFE

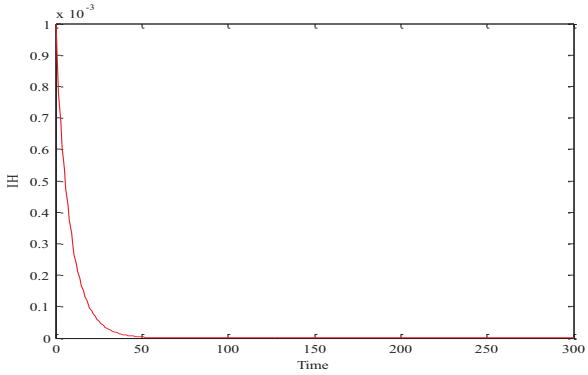

Fig. 2.2 Infected Human Fraction-DFE

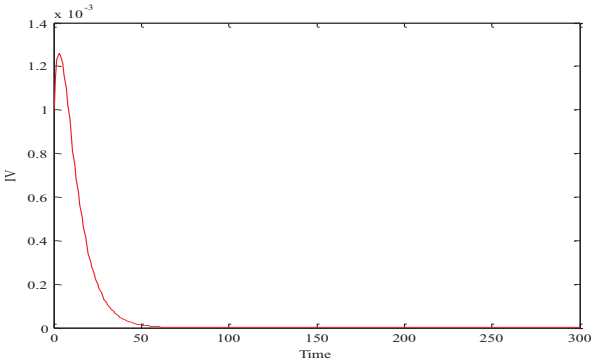

Fig. 2.3 Infected Vector Fraction-DFE

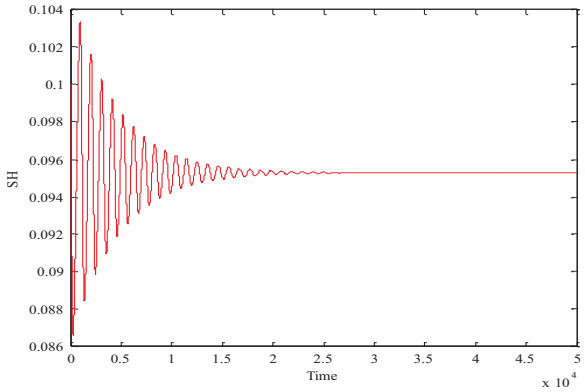

Fig. 2.4 Susceptible Human Fraction-EE

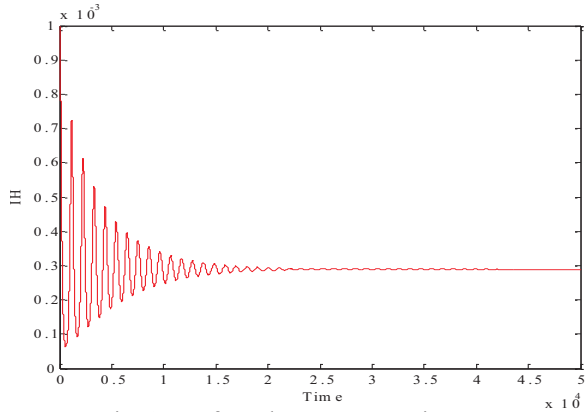

Fig. 2.5 Infected Human Fraction-EE

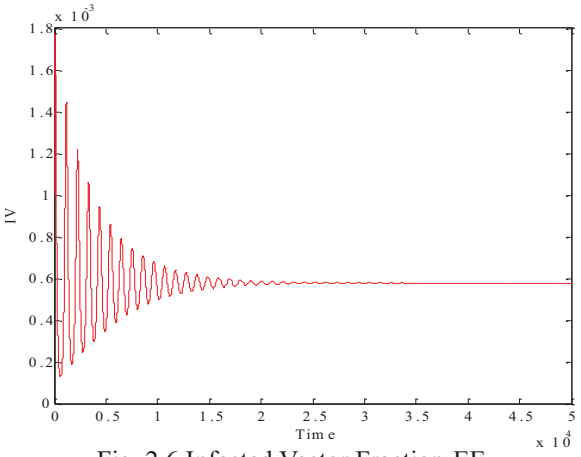

Fig. 2.6 Infected Vector Fraction-EE

I. Results and Discussion

A Non-Standard Finite Difference (NSFD) numerical model has been constructed for the continuous model and numerical experiments are performed for different values of discretizationparameter *l*. Results are compared with well known numerical method i.e. Runge-Kutta method of order four (RK4).Observations are listed in Table II.

TABLE II

	RK-4	NSFD
1	Convergence	Convergence
10	Divergence(method failed)	Convergence
100	Divergence	Convergence
1000	Divergence	Convergence

Table II shows that the Rk4 method converge for a small value of parameter *l* and it diverges for the large values but proposed NSFD scheme will remain convergent even for a very large value of discretization parameter i.e. $l = 1000$.

VII. Conclusions

An unconditionally convergent numerical scheme has been developed for the transmission dynamics of Dengue Fever. Unlike Rk4 which fails for large time steps, the developed scheme gives results that converged to true steady states for any time step used. The scheme is numerically stable, dynamically consistent and shows a good agreement with analytic results produced in [x].

References

[i] R. M. Anderson, R. M. May,"Infectious diseases of Humans", Oxford University Press, 1991.

[ii] F. Brauer, C. Castillo-Shavez,"Mathematical models in population biology and epidemiology", Texts in Applied Mathematics 40, (New York: Springer-Verlag), 2001.

[iii]. J. D. David Earn, "Mathematical Epidemiology of Infectious Diseases",S/Park City Mathematics Series(American Mathematical Society). vol.14,pp.151-186, 2009.

[iv] D. J. Gubler, "Dengue and Dengue Haemorrhagic Fever",Clinical Microbiology Review, vol.11,pp. 450-496,1998.

[v] J. J. Holland, "Models of Infectious Diseases"Stanford Spring Workshop in Formal Demography,2008.

[vi] R. E. Kongnuy, Naowanich, P. Pongsumpun. "Analysis of a dengue disease transmission model with clinical diagnosis in Thailand", International Journal of Mathematical Models and Methods in Applied Sciences, vol. 5, no. 3, pp. 594-601,2011.

[vii] N. Surapol, S. Rajabhat. "Dynamical Model for Determining Human Susceptibility to Dengue Fever",American Journal of Applied Sciences, vol. 8, no.11, pp. 1101-1106,2011.

[viii] World Health Organization. "Dengue Haemorrhagic fever: Diagnosis treatment and control", Geneva, 1997.

[ix] J. D. Lambert,"Numerical Methods for Ordinary Differential Systems: The Initial Value Problem", Wiley, Chichester, England, 1991.

[x] R. E. Mickens, "Dynamical consistency: a fundamental principle for constructing nonstandard finite difference schemes for differential equations",Journal of difference equations and Applications, vol.13, no.4, pp.645-654, 2005.

Technical Journal
Website: www.uettaxila.edu.pk.
University of Engineering and Technology, Taxila-Pakistan

Researchers and Academia are invited to submit the research articles to Technical Journal of UET Taxila. It is a peer reviewed, broad-based open access journal. It covers all areas of engineering sciences and engineering management.

Technical Journal is a quarterly publication of UET Taxila recognized by HEC in "Y" category. It is published regularly with a key objective to provide the visionary wisdom to academia and researchers to disseminate novel knowledge and technology for the benefit of society. Technical Journal is indexed by well recognized international database such as PASTIC Science Abstracts, AGRIS Data Base, ProQuest Products, EBSCO Data Bases, Library of Congress and various other nineteen (19) HEC approved abstracting and indexing agencies.

For enquiries, submissions of articles or any other information please visit our website http://web.uettaxila.edu.pk/techjournal/index.html or contact the Editorial Office on the following number: +92-51-9047298
e-mail: technical.journal@uettaxila.edu.pk

Submission of paper remains open round the year. Researchers and Academia can submit their papers at any time which they deem fit. Presently there are no charges for publication of research paper in Technical Journal.

It will be highly appreciated if the information is forwarded to interested colleagues from Pakistan as well as abroad.

Looking forward to receiving the research papers on behalf of Technical Journal Editorial Office.

Prof. Dr. Abdul Razzaq Ghumman
Chief Editor
Technical Journal,
UET, Taxila

Instruction for authors for publishing in Technical Journal UET Taxila

General

Papers may be submitted any time throughout the year. After receipt of paper it will be sent to concerned referees, at least one from a technology advanced countries. Papers reviewed and declared fit for publication will be published in the coming issue. The journal is quarterly publication, having four issues annually. A soft copy of paper must be submitted through online submission system by using the following link:-
http://tj.uettaxila.edu.pk/index.php/technical-journal/about/submissions
Authors are required to read the following carefully for writing a paper.

Manuscript Preparation

Text should be type-written with M.S word, Times New Roman Font size 10, at single space and with margins as 1 inch top,1 inch left, 0.5 inch right, and 1 inch bottom, on an A-4 size paper. The manuscript should be compiled in following order:-

Title Page

The Title page should contain:

- Paper title
- Author names and affiliations
- Postal and email addresses
- Telephone/Cell and fax numbers
- One author should be identified as the Corresponding Author

Abstract

An abstract up to maximum of 200 words should be written in the start of paper. The abstract should give a clear indication of the objectives, scope, methods, results and conclusions.

Keywords

Include at least five keywords (Title Case) in a separate line at the end of the abstract.

Body of the Paper

Body of the paper may include introduction and literature review, materials and methods, modeling/experimentation, results-discussions and conclusions etc.

- Define abbreviations and acronyms the first time they are used in the text, even after they have already been defined in the abstract. Do not use abbreviations in the title unless they are Unavoidable.
- Use zero before decimal places: "0.24" not ".24".
- Avoid contractions; for example, write "do not" instead of "don't."
- If you are using *Word,* use either the Microsoft Equation Editor or the *MathType* add-on (http://www.mathtype.com) for equations in your paper (Insert | Object | Create New | Microsoft Equation *or* Math Type Equation).

Number equations consecutively with equation numbers in parentheses flush with the right margin, as in (1). Refer to "(1)," not "Eq. (1)" or "equation (1)," except at the beginning of a sentence: "Equation (1) is ... ."

- Symbols used in the equations must be defined before or immediately after it appears.
- Use SI units only.

Originality

Only original contributions to Engineering, Science and Management literature should be submitted for publication. It should incorporate substantial information not previously published.

Length

Research paper should be consisting of 5-8 pages as per specifications given above.

Accuracy

All the technical, scientific and mathematical information contained in the paper should be checked with great care.

Figures

All figures should be at least 300 dpi in JPG format. It is to be also ensured that lines are thick enough to be reproduced conveniently after size reduction at the stage of composing. All figures (graphs, line drawings, photographs, etc.) should be numbered consecutively and have a caption consisting of the figure number and a brief title or description of the figure. This number should be used when referring to the figure in the text. Figure may be referenced within the text as "Fig. 1" etc.

Tables

Tables should be typed in a separate file using M.S. Word 'table' option. All tables should be numbered in Roman numerals consecutively. Tables should have a caption in Upper Case, must be centered and in 8 pt. consisting of the table number and brief title. This number should be used when referring to the table in text. Table should be inserted as part of the text as close as possible to its first reference.
When referencing your figures and tables within your paper, use the abbreviation "Fig." Even at the beginning of a sentence. Do not abbreviate "Table."

Acknowledgments
All individuals or institutions not mentioned elsewhere in the work who have made an important contribution should be acknowledged.

References
Reference may be cited with number in square brackets, e.g. "the scheme is discussed in [iii]". Multiple references are each numbered with in bracket. e.g. the scheme is discussed in [iv-vii]. Do not use "Ref." or "reference" except at the beginning of a sentence: "Reference [xi] illustrates... ."

Please do not use automatic endnotes in Word, rather, type the reference list at the end of the paper using the "References" style. Reference list/bibliography and in text references, both will be cited in roman alphabet. "Within text citations must be in chronological order in the first appearance. The subsequent appearance(s) of the same may be random as per need of the paper."

Note: For template of paper please visit our journal's page:
http://web.uettaxila.edu.pk/techjournal/index.html

Check List

<table>
<tr><th>Sr. No.</th><th>Description</th><th>Yes/No</th></tr>
<tr><td>1</td><td>Undertaking signed by all authors that the research paper has not been submitted to any other journal for publishing and submitted research work is their own original contribution is required as per following format.
<table>
<tr><td colspan="4">Paper Titled:</td></tr>
<tr><td colspan="4">Authorship and Contribution Declaration</td></tr>
<tr><td>Sr.#</td><td>Author-s Full Name</td><td>Contribution to Paper</td><td>Author-s Signature</td></tr>
<tr><td>1</td><td>Mr./Dr./Prof. Alpha (Main/principal Author)</td><td>Proposed topic, basic study Design, methodology and manuscript writing</td><td></td></tr>
<tr><td>2</td><td>Mr./Dr./Prof. Bravo(2nd Author)</td><td>Data Collection, statistical analysis and interpretation of results etc.</td><td></td></tr>
<tr><td>3</td><td>Mr./Dr./Prof. Charlie (3rd Author)</td><td>Literature review & Referencing, and quality insurer</td><td></td></tr>
<tr><td>⋮</td><td>⋮</td><td>⋮</td><td></td></tr>
</table></td><td></td></tr>
<tr><td>2</td><td>Pictures are placed on paper at proper places and separate pictures in JPEG format are provided in a separate file with their caption as well.</td><td></td></tr>
<tr><td>3</td><td>Technical Journal UET Taxila follow IEEE format. Please submit your paper according to required format i.e. double column, tables and figures captions & numbers, indentation and particularly in-text citation and bibliography according to IEEE format.</td><td></td></tr>
<tr><td>4</td><td>"Time New Roman" font shall be used in legends, captions of Figures, Graphs and Tables etc.</td><td></td></tr>
<tr><td>5</td><td>Complete contact information of the corresponding author:-.
Name:_____, Designation:_____
Institute Name:_____, Email:_____
Cell:_____, Ph No. and Fax (if any)_____</td><td></td></tr>
<tr><td>6</td><td>Main area of Research paper e.g. Electrical, Mechanical etc. shall be mentioned</td><td></td></tr>
<tr><td colspan="3">Note: Ensure that all requirements have been met before submitting the paper
http://tj.uettaxila.edu.pk/index.php/technical-journal/about/submissions For any query please visit:
http://web.uettaxila.edu.pk/techJournal/index.html</td></tr>
</table>

EDITORIAL OFFICE: Correspondences should be made on the following address:
Asif Ali General Editor, Technical Journal Editorial Office
Central Library, University of Engineering and Technology (UET) Taxila, Pakistan
Tel**:** +92 (51) 9047298 Email**:**technical.journal@uettaxila.edu.pk